



David Taylor Research Center

Bethesda, MD 20084-5000

DTRC-91/004 September 1991

Ship Hydromechanics Department
Research and Development Report

AD-A241 076



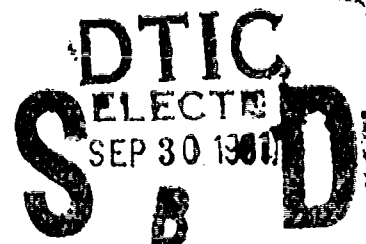
Comparative Accuracy of Numerical Kelvin Wake Code Predictions - "Wake-Off"

by

William T. Lindenmuth

Toby J. Ratcliffe

Arthur M. Reed



91-12009



Approved for public release; distribution is unlimited.

DTRC-91/004 Comparative Accuracy of Numerical Kelvin Wake Code Predictions - "Wake-Off"

91 9 30 181

MAJOR DTRC TECHNICAL COMPONENTS

CODE 011 DIRECTOR OF TECHNOLOGY, PLANS AND ASSESSMENT

12 SYSTEMS DEPARTMENT

14 SHIP ELECTROMAGNETIC SIGNATURES DEPARTMENT

15 SHIP HYDROMECHANICS DEPARTMENT

17 SHIP STRUCTURES AND PROTECTION DEPARTMENT

19 SHIP ACOUSTICS DEPARTMENT

27 PROPULSION AND AUXILIARY SYSTEMS DEPARTMENT

28 SHIP MATERIALS ENGINEERING DEPARTMENT

DTRC ISSUES THREE TYPES OF REPORTS:

1. **DTRC reports, a formal series**, contain information of permanent technical value. They carry a consecutive numerical identification regardless of their classification or the originating department.
2. **Departmental reports, a semiformal series**, contain information of a preliminary, temporary, or proprietary nature or of limited interest or significance. They carry a departmental alphanumeric identification.
3. **Technical memoranda, an informal series**, contain technical documentation of limited use and interest. They are primarily working papers intended for internal use. They carry an identifying number which indicates their type and the number of the originating department. Any distribution outside DTRC must be approved by the originating department on a case-by-case basis.

UNCLASSIFIED

SECURITY CLASSIFICATION OF THIS PAGE

REPORT DOCUMENTATION PAGE

1a. REPORT SECURITY CLASSIFICATION UNCLASSIFIED			1b. RESTRICTIVE MARKINGS	
2a. SECURITY CLASSIFICATION AUTHORITY			3. DISTRIBUTION/AVAILABILITY OF REPORT Approved for public release; distribution is unlimited.	
2b. DECLASSIFICATION/DOWNGRADING SCHEDULE				
4. PERFORMING ORGANIZATION REPORT NUMBER(S) DTRC-91/004			5. MONITORING ORGANIZATION REPORT NUMBER(S)	
6a. NAME OF PERFORMING ORGANIZATION David Taylor Research Center		6b. OFFICE SYMBOL (If applicable) Code 1552		7a. NAME OF MONITORING ORGANIZATION
6c. ADDRESS (City, State, and ZIP Code) Bethesda, MD 20084-5000			7b. ADDRESS (City, State, and ZIP Code)	
8a. NAME OF FUNDING/SPONSORING ORGANIZATION Office of Naval Technology, ONT21		8b. OFFICE SYMBOL (If applicable)		9. PROCUREMENT INSTRUMENT IDENTIFICATION NUMBER
8c. ADDRESS (City, State, and ZIP Code) 800 N. Quincy Street Arlington, VA 22217			10. SOURCE OF FUNDING NUMBERS	
			PROGRAM ELEMENT NO. 62121N	PROJECT NO. RH21C12
			TASK NO. 1	WORK UNIT ACCESSION NO. DN178067
11. TITLE (Include Security Classification) Comparative Accuracy of Numerical Kelvin Wake Code Predictions - "Wake-Off"				
12. PERSONAL AUTHOR(S) Lindenmuth, William T., Toby J. Ratcliffe, and Arthur M. Reed				
13a. TYPE OF REPORT Final		13b. TIME COVERED FROM _____ TO _____		14. DATE OF REPORT (YEAR, MONTH, DAY) 1991, September
15. PAGE COUNT 275				
16. SUPPLEMENTARY NOTATION				
17. COSATI CODES			18. SUBJECT TERMS (Continue on reverse if necessary and identify by block number) Analytical Wake Predictions Kelvin Wake Predictions Numerical Kelvin Wake Predictions	
FIELD	GROUP	SUB-GROUP		
19. ABSTRACT (Continue on reverse if necessary and identify by block number) Wave patterns predicted by several numerical codes were evaluated by comparing them with data from model basin experiments on two ship hulls at three Froude numbers each. In general, the codes all underpredict the amplitude of divergent waves springing from the ships' bow. High wave number detail is also lacking in the vicinity of the bow wave cusp line compared to model free-surface wave patterns. Conversely, the codes tend to overpredict the amplitudes of wave close to the ships' stern and in the transverse wave system behind. The codes are ranked according to how closely they simulate the empirical results. Within the ranking, adjacent codes give similar wave predictions and the rank might be interchanged for a few Froude number cases. Higher ranked codes gave consistently better predictions than the lower ranked codes. Problems for the lower ranked codes included: excessive wave damping such that waves are attenuated near the edges of the computational domain; reflections appear at the outer boundaries; high frequency "noise" exists beyond the 19-deg envelope of the spreading wave train; and wave energy has been severely underpredicted. (Continued on reverse side)				
20. DISTRIBUTION/AVAILABILITY OF ABSTRACT <input type="checkbox"/> UNCLASSIFIED/UNLIMITED <input checked="" type="checkbox"/> SAME AS RPT <input type="checkbox"/> DTIC USERS			21. ABSTRACT SECURITY CLASSIFICATION UNCLASSIFIED	
22a. NAME OF RESPONSIBLE INDIVIDUAL Toby J. Ratcliffe			22b. TELEPHONE (Include Area Code) (301) 227-1756	22c. OFFICE SYMBOL Code 1552

Block 19 (Continued)

Standardized graphic representations of the numerical and experimental data are included in the appendixes.

The predictions were made "blind," without prior knowledge of the specific experimental results. In view of the inherent difficulties including nonlinear wave breaking and real fluid effects (present in the experiments), the agreement achieved by the better codes is encouraging.

CONTENTS

	Page
Abstract	1
Administrative Information	1
Introduction	1
Physical Model Characteristics	2
Analytical Models	4
Data Formats	5
Evaluation Process	7
Results	7
General Observations	7
Specific Comparisons and Rankings	8
Discussion	10
Conclusions	11
Appendix A. Specifications for Wake-Off Competition	13
Appendix B. Experimental Results	23
Appendix C. FARWAV Predictions	41
Appendix D. NK-2 Predictions	65
Appendix E. DOCTORS N-K Predictions	93
Appendix F. SWIFT Predictions	107
Appendix G. NKSHIP Predictions	127
Appendix H. FLOPAN Predictions	135
Appendix I. XYZFS Predictions	147
Appendix J. Proprietary Code Predictions	175
Appendix K. SWIMFS Prediction	189
Appendix L. SAIC Slender-Ship Predictions Submitted After Wake-off	205
Appendix M. FLOPAN Predictions Submitted After Wake-off	233
Appendix N. XYZFS Predictions Submitted After Wake-off	237
References	257



Accession For	
NTIS GRA&I	<input checked="checked" type="checkbox"/>
DTIC TAB	<input type="checkbox"/>
Unannounced	<input type="checkbox"/>
Justification	
By	
Distribution/	
Availability Codes	
Dist	Avail and/or Special
A-1	

FIGURES

	Page
1. Typical panel scheme for Model 3531	3
2. Typical panel scheme for Model 5415	3
3. Measured wave spectrum for the ATF QUAPAW and Model 3531	12
A.1. Graphics format sample	15
B.1. Experimental wave contour for Model 5415 at $F_n = 0.25$	24
B.2. Experimental wave cut for Model 5415 at $F_n = 0.25$	25
B.3. Experimental wave spectrum for Model 5415 at $F_n = 0.25$	26
B.4. Experimental wave contours for Model 5415 at $F_n = 0.2755$	27
B.5. Experimental wave cut for Model 5415 at $F_n = 0.2755$	28
B.6. Experimental wave spectrum for Model 5415 at $F_n = 0.2755$	29
B.7. Experimental wave contours for Model 5415 at $F_n = 0.4136$	30
B.8. Experimental wave cut for Model 5415 at $F_n = 0.4136$	31
B.9. Experimental wave spectrum for Model 5415 at $F_n = 0.4136$	32
B.10. Experimental wave contours for QUAPAW at $F_n = 0.2131$	33
B.11. Experimental wave cut for QUAPAW at $F_n = 0.2131$	34
B.12. Experimental wave spectrum for QUAPAW at $F_n = 0.2131$	35
B.13. Experimental wave cut for QUAPAW at $F_n = 0.25$	36
B.14. Experimental wave spectrum for QUAPAW at $F_n = 0.25$	37
B.15. Experimental wave contours for QUAPAW at $F_n = 0.3197$	38
B.16. Experimental wave cut for QUAPAW at $F_n = 0.3197$	39
B.17. Experimental wave spectrum for QUAPAW at $F_n = 0.3197$	40
C.1. FARWAV prediction of wave contours for Model 5415 at $F_n = 0.25$	46
C.2. FARWAV prediction of wave cut for Model 5415 at $F_n = 0.25$	47
C.3. FARWAV prediction of wave spectrum for Model 5415 at $F_n = 0.25$	48
C.4. FARWAV prediction of wave contours for Model 5415 at $F_n = 0.2755$	49
C.5. FARWAV prediction of wave cut for Model 541 at $F_n = 0.2755$	50
C.6. FARWAV prediction of wave spectrum for Model 5415 at $F_n = 0.2755$	51

FIGURES (Continued)

	Page
C.7. FARWAV prediction of wave contours for Model 5415 at $F_n = 0.4136$	52
C.8. FARWAV prediction of wave cut for Model 5415 at $F_n = 0.4136$	53
C.9. FARWAV prediction of wave spectrum for Model 5415 at $F_n = 0.4136$	54
C.10. FARWAV prediction of wave contours for QUAPAW at $F_n = 0.2131$	55
C.11. FARWAV prediction of wave cut for QUAPAW at $F_n = 0.2131$	56
C.12. FARWAV prediction of wave spectrum for QUAPAW at $F_n = 0.2131$	57
C.13. FARWAV prediction of wave contours for QUAPAW at $F_n = 0.25$	58
C.14. FARWAV prediction of wave cut for QUAPAW at $F_n = 0.25$	59
C.15. FARWAV prediction of wave spectrum for QUAPAW at $F_n = 0.25$	60
C.16. FARWAV prediction of wave contours for QUAPAW at $F_n = 0.3197$	61
C.17. FARWAV prediction of wave cut for QUAPAW at $F_n = 0.3197$	62
C.18. FARWAV prediction of wave spectrum for QUAPAW at $F_n = 0.3197$	63
D.1. NK-2 prediction of wave contours ($-0.5 < 2x/LWL < 4$) for Model 5415 at $F_n = 0.25$	69
D.2. NK-2 prediction of wave contours ($4 < 2x/LWL < 8$) for Model 5415 at $F_n = 0.25$	70
D.3. NK-2 prediction of wave cut for Model 5415 at $F_n = 0.25$	71
D.4. NK-2 prediction of wave spectrum for Model 5415 at $F_n = 0.25$	72
D.5. NK-2 prediction of wave contours ($-0.5 < 2x/LWL < 4$) for Model 5415 at $F_n = 0.2755$	73
D.6. NK-2 prediction of wave contours ($4 < 2x/LWL < 8$) for Model 5415 at $F_n = 0.2755$	74
D.7. NK-2 prediction of wave cut for Model 5415 at $F_n = 0.2755$	75
D.8. NK-2 prediction of wave spectrum for Model 5415 at $F_n = 0.2755$	76

FIGURES (Continued)

	Page
D.9. NK-2 prediction of wave contours ($-0.5 < 2x/LWL < 4$) for Model 5415 at $F_n = 0.4136$	77
D.10. NK-2 prediction of wave contours ($4 < 2x/LWL < 8$) for Model 5415 at $F_n = 0.4136$	78
D.11. NK-2 prediction of wave cut for Model 5415 at $F_n = 0.4136$	79
D.12. NK-2 prediction of wave spectrum for Model 5415 at $F_n = 0.4136$	80
D.13. NK-2 prediction of wave contours ($-0.5 < 2x/LWL < 4$) for QUAPAW at $F_n = 0.2131$	81
D.14. NK-2 prediction of wave contours ($4 < 2x/LWL < 8$) for QUAPAW at $F_n = 0.2131$	82
D.15. NK-2 prediction of wave cut for QUAPAW at $F_n = 0.2131$	83
D.16. NK-2 prediction of wave spectrum for QUAPAW at $F_n = 0.2131$	84
D.17. NK-2 prediction of wave contours ($-0.5 < 2x/LWL < 4$) for QUAPAW at $F_n = 0.25$	85
D.18. NK-2 prediction of wave contours ($4 < 2x/LWL < 8$) for QUAPAW at $F_n = 0.25$	86
D.19. NK-2 prediction of wave cut for QUAPAW at $F_n = 0.25$	87
D.20. NK-2 prediction of wave spectrum for QUAPAW at $F_n = 0.25$	88
D.21. NK-2 prediction of wave contours ($-0.5 < 2x/LWL < 4$) for QUAPAW at $F_n = 0.3197$	89
D.22. NK-2 prediction of wave contours ($4 < 2x/LWL < 8$) for QUAPAW at $F_n = 0.3197$	90
D.23. NK-2 prediction of wave cut for QUAPAW at $F_n = 0.3197$	91
D.24. NK-2 prediction of wave spectrum for QUAPAW at $F_n = 0.3197$	92
E.1. DOCTORS N-K prediction of wave contours ($-0.5 < 2x/LWL < 4$) for QUAPAW at $F_n = 0.2131$	95
E.2. DOCTORS N-K prediction of wave contours ($4 < 2x/LWL < 8$) for QUAPAW at $F_n = 0.2131$	96
E.3. DOCTORS N-K prediction of wave cut for QUAPAW at $F_n = 0.2131$	97
E.4. DOCTORS N-K prediction of wave spectrum for QUAPAW at $F_n = 0.2131$	98

FIGURES (Continued)

	Page
E.5. DOCTORS N-K prediction of wave contours ($-0.5 < 2x/LWL < 4$) for QUAPAW at $F_n = 0.25$	99
E.6. DOCTORS N-K prediction of wave contours ($4 < 2x/LWL < 8$) for QUAPAW at $F_n = 0.25$	100
E.7. DOCTORS N-K prediction of wave cut for QUAPAW at $F_n = 0.25$	101
E.8. DOCTORS N-K prediction of wave spectrum for QUAPAW at $F_n = 0.25$	102
E.9. DOCTORS N-K prediction of wave contours ($-0.5 < 2x/LWL < 4$) for QUAPAW at $F_n = 0.3197$	103
E.10. DOCTORS N-K prediction of wave contours ($4 < 2x/LWL < 8$) for QUAPAW at $F_n = 0.3197$	104
E.11. DOCTORS N-K prediction of wave cut for QUAPAW at $F_n = 0.3197$	105
E.12. DOCTORS N-K prediction of wave spectrum for QUAPAW at $F_n = 0.3197$	106
F.1. SWIFT prediction of wave contours ($-0.5 < 2x/LWL < 4$) for Model 5415 at $F_n = 0.25$	108
F.2. SWIFT prediction of wave contours ($4 < 2x/LWL < 8$) for Model 5415 at $F_n = 0.25$	109
F.3. SWIFT prediction of wave cut for Model 5415 at $F_n = 0.25$	110
F.4. SWIFT prediction of wave contours ($-0.5 < 2x/LWL < 4$) for Model 5415 at $F_n = 0.2755$	111
F.5. SWIFT prediction of wave contours ($4 < 2x/LWL < 8$) for Model 5415 at $F_n = 0.2755$	112
F.6. SWIFT prediction of wave cut for Model 5415 at $F_n = 0.2755$	113
F.7. SWIFT prediction of wave contours ($-0.5 < 2x/LWL < 4$) for Model 5415 at $F_n = 0.4136$	114
F.8. SWIFT prediction of wave contours ($4 < 2x/LWL < 8$) for Model 5415 at $F_n = 0.4136$	115
F.9. SWIFT prediction of wave cut for Model 5415 at $F_n = 0.4136$	116
F.10. SWIFT prediction of wave contours ($-0.5 < 2x/LWL < 4$) for QUAPAW at $F_n = 0.2131$	117
F.11. SWIFT prediction of wave contours ($4 < 2x/LWL < 8$) for QUAPAW at $F_n = 0.2131$	118
F.12. SWIFT prediction of wave cut for QUAPAW at $F_n = 0.2131$	119

FIGURES (Continued)

	Page
F.13. SWIFT prediction of wave contours ($-0.5 < 2x/LWL < 4$) for QUAPAW at $F_n = 0.25$	120
F.14. SWIFT prediction of wave contours ($4 < 2x/LWL < 8$) for QUAPAW at $F_n = 0.25$	121
F.15. SWIFT prediction of wave cut for QUAPAW at $F_n = 0.25$	122
F.16. SWIFT prediction of wave contours ($-0.5 < 2x/LWL < 4$) for QUAPAW at $F_n = 0.3197$	123
F.17. SWIFT prediction of wave contours ($4 < 2x/LWL < 8$) for QUAPAW at $F_n = 0.3197$	124
F.18. SWIFT prediction of wave cut for QUAPAW at $F_n = 0.3197$	125
G.1. NKSHIP prediction of wave contours for QUAPAW at $F_n = 0.3197$	130
G.2. NKSHIP prediction of wave cut for QUAPAW at $F_n = 0.3197$	131
G.3. NKSHIP prediction of wave profiles along QUAPAW hull at $F_n = 0.2131$	132
G.4. NKSHIP prediction of wave profiles along QUAPAW hull at $F_n = 0.25$	133
G.5. NKSHIP prediction of wave profiles along QUAPAW hull at $F_n = 0.3197$	134
H.1. FLOPAN half-plane panel model of QUAPAW	136
H.2. FLOPAN prediction of wave contours for QUAPAW at $F_n = 0.2131$	137
H.3. FLOPAN prediction of wave cut for QUAPAW at $F_n = 0.2131$	138
H.4. FLOPAN prediction of wave contours for QUAPAW at $F_n = 0.25$	139
H.5. FLOPAN prediction of wave cut for QUAPAW at $F_n = 0.25$	140
H.6. FLOPAN prediction of wave contours for QUAPAW at $F_n = 0.3197$	141
H.7. FLOPAN prediction of wave cut for QUAPAW at $F_n = 0.3197$	142
H.8. FLOPAN prediction of wave profile along QUAPAW hull at $F_n = 0.2131$	143
H.9. FLOPAN prediction of wave profile along QUAPAW hull at $F_n = 0.25$	144
H.10. FLOPAN prediction of wave profile along QUAPAW hull at $F_n = 0.3197$	145
I.1. XYZFS prediction of wave contour for Model 5415 at $F_n = 0.25$	150

FIGURES (Continued)

	Page
I.2. XYZFS prediction of wave cut for Model 5415 at $F_n = 0.25$	152
I.3. XYZFS prediction of wave spectrum for Model 5415 at $F_n = 0.25$	153
I.4. XYZFS prediction of wave contour for Model 5415 at $F_n = 0.2755$	154
I.5. XYZFS prediction of wave cut for Model 5415 at $F_n = 0.2755$	156
I.6. XYZFS prediction of wave spectrum for Model 5415 at $F_n = 0.2755$	157
I.7. XYZFS prediction of wave contour for Model 5415 at $F_n = 0.4136$	158
I.8. XYZFS prediction of wave cut for Model 5415 at $F_n = 0.4136$	160
I.9. XYZFS prediction of wave spectrum for Model 5415 at $F_n = 0.4136$	161
I.10. XYZFS prediction of wave contour for QUAPAW at $F_n = 0.2131$	162
I.11. XYZFS prediction of wave cut for QUAPAW at $F_n = 0.2131$	164
I.12. XYZFS prediction of wave spectrum for QUAPAW at $F_n = 0.2131$	165
I.13. XYZFS prediction of wave contour for QUAPAW at $F_n = 0.25$	166
I.14. XYZFS prediction of wave cut for QUAPAW at $F_n = 0.25$	168
I.15. XYZFS prediction of wave spectrum for QUAPAW at $F_n = 0.25$	169
I.16. XYZFS prediction of wave contour for QUAPAW at $F_n = 0.3197$	170
I.17. XYZFS prediction of wave cut for QUAPAW at $F_n = 0.3197$	172
I.18. XYZFS prediction of wave spectrum for QUAPAW at $F_n = 0.3197$	173
J.1. Proprietary Code prediction of wave contour for QUAPAW at $F_n = 0.2131$	177
J.2. Proprietary Code prediction of wave cut for QUAPAW at $F_n = 0.2131$	179
J.3. Proprietary Code prediction of wave spectrum for QUAPAW at $F_n = 0.2131$	180
J.4. Proprietary Code prediction of wave contour for QUAPAW at $F_n = 0.25$	181
J.5. Proprietary Code prediction of wave cut for QUAPAW at $F_n = 0.25$	183

FIGURES (Continued)

	Page
J.6. Proprietary Code prediction of wave spectrum for QUAPAW at $F_n = 0.25$	184
J.7. Proprietary Code prediction of wave contour for QUAPAW at $F_n = 0.3197$	185
J.8. Proprietary Code prediction of wave cut for QUAPAW at $F_n = 0.3197$	187
J.9. Proprietary Code prediction of wave spectrum for QUAPAW at $F_n = 0.3197$	188
K.1. SWIMFS prediction of wave contour for QUAPAW at $F_n = 0.2131$	192
K.2. SWIMFS prediction of wave cut for QUAPAW at $F_n = 0.2131$	194
K.3. SWIMFS prediction of wave spectrum for QUAPAW at $F_n = 0.2131$	195
K.4. SWIMFS prediction of wave contour for QUAPAW at $F_n = 0.25$	196
K.5. SWIMFS prediction of wave cut for QUAPAW at $F_n = 0.25$	198
K.6. SWIMFS prediction of wave spectrum for QUAPAW at $F_n = 0.25$	199
K.7. SWIMFS prediction of wave contour for QUAPAW at $F_n = 0.3197$	200
K.8. SWIMFS prediction of wave cut for QUAPAW at $F_n = 0.3197$	202
K.9. SWIMFS prediction of wave spectrum for QUAPAW at $F_n = 0.3197$	203
L.1. Post wake-off SAIC slender-ship prediction of wave contours ($-0.5 < 2x/LWL < 4$) for Model 5415 at $F_n = 0.25$	206
L.2. Post wake-off SAIC slender-ship prediction of wave contours ($4 < 2x/LWL < 8$) for Model 5415 at $F_n = 0.25$	207
L.3. Post wake-off SAIC slender-ship prediction of wave cut for Model 5415 at $F_n = 0.25$	208
L.4. Post wake-off SAIC slender-ship prediction of wave spectrum for Model 5415 $F_n =$ at 0.25	209
L.5. Post wake-off SAIC slender-ship prediction of wave contours ($-0.5 < 2x/LWL < 4$) for Model 5415 at $F_n = 0.2755$	210
L.6. Post wake-off SAIC slender-ship prediction of wave contours ($4 < 2x/LWL < 8$) for Model 5415 at $F_n = 0.2755$	211
L.7. Post wake-off SAIC slender-ship prediction of wave cut for Model 5415 at $F_n = 0.2755$	212
L.8. Post wake-off SAIC slender-ship prediction of wave spectrum for Model 5415 at $F_n = 0.2755$	213
L.9. Post wake-off SAIC slender-ship prediction of wave contours ($-0.5 < 2x/LWL < 4$) for Model 5415 at $F_n = 0.4136$	214

FIGURES (Continued)

	Page
L.10. Post wake-off SAIC slender-ship prediction of wave contours ($4 < 2x/LWL < 8$) for Model 5415 at $F_n = 0.4136$	215
L.11. Post wake-off SAIC slender-ship prediction of wave cut for Model 5415 at $F_n = 0.4136$	216
L.12. Post wake-off SAIC slender-ship prediction of wave spectrum for Model 5415 at $F_n = 0.4136$	217
L.13. Post wake-off SAIC slender-ship prediction of wave contours ($-0.5 < 2x/LWL < 4$) for QUAPAW at $F_n = 0.2131$	218
L.14. Post wake-off SAIC slender-ship prediction of wave contours ($4 < 2x/LWL < 8$) for QUAPAW at $F_n = 0.2131$	219
L.15. Post wake-off SAIC slender-ship prediction of wave cut for QUAPAW at $F_n = 0.2131$	220
L.16. Post wake-off SAIC slender-ship prediction of wave spectrum for QUAPAW at $F_n = 0.2131$	221
L.17. Post wake-off SAIC slender-ship prediction of wave contours ($-0.5 < 2x/LWL < 4$) for QUAPAW at $F_n = 0.25$	222
L.18. Post wake-off SAIC slender-ship prediction of wave contours ($4 < 2x/LWL < 8$) for QUAPAW at $F_n = 0.25$	223
L.19. Post wake-off SAIC slender-ship prediction of wave cut for QUAPAW at $F_n = 0.25$	224
L.20. Post wake-off SAIC slender-ship prediction of wave spectrum for QUAPAW at $F_n = 0.25$	225
L.21. Post wake-off SAIC slender-ship prediction of wave contours ($-0.5 < 2x/LWL < 4$) for QUAPAW at $F_n = 0.3197$	226
L.22. Post wake-off SAIC slender-ship prediction of wave contours ($4 < 2x/LWL < 8$) for QUAPAW at $F_n = 0.3197$	227
L.23. Post wake-off SAIC slender-ship prediction of wave cut for QUAPAW at $F_n = 0.3197$	228
L.24. Post wake-off SAIC slender-ship prediction of wave spectrum for QUAPAW at $F_n = 0.3197$	229
M.1. Post wake-off FLOPAN prediction of QUAPAW at $F_n = 0.3197$ using blended 3/4/5 point upwind formula	234
M.2. Post wake-off FLOPAN prediction of QUAPAW at $F_n = 0.3197$ using blended 4/5 point upwind formula	235
M.3. Post wake-off FLOPAN prediction of QUAPAW at $F_n = 0.3197$ using blended 5 point upwind formula	236

FIGURES (Continued)

	Page
N.1. Post wake-off XYZFS prediction of wave contours for Model 5415 at $F_n = 0.25$	238
N.2. Post wake-off XYZFS prediction of wave cut for Model 5415 at $F_n = 0.25$	239
N.3. Post wake-off XYZFS prediction of wave spectrum for Model 5415 at $F_n = 0.25$	240
N.4. Post wake-off XYZFS prediction of wave contours for Model 5415 at $F_n = 0.2755$	241
N.5. Post wake-off XYZFS prediction of wave cut for Model 5415 at $F_n = 0.2755$	242
N.6. Post wake-off XYZFS prediction of wave spectrum for Model 5415 at $F_n = 0.2755$	243
N.7. Post wake-off XYZFS prediction of wave contours for Model 5415 at $F_n = 0.4136$	244
N.8. Post wake-off XYZFS prediction of wave cut for Model 5415 at $F_n = 0.4136$	245
N.9. Post wake-off XYZFS prediction of wave spectrum for Model 5415 at $F_n = 0.4136$	246
N.10. Post wake-off XYZFS prediction of wave contours for QUAPAW at $F_n = 0.2131$	247
N.11. Post wake-off XYZFS prediction of wave cut for QUAPAW at $F_n = 0.2131$	248
N.12. Post wake-off XYZFS prediction of wave spectrum for QUAPAW at $F_n = 0.2131$	249
N.13. Post wake-off XYZFS prediction of wave contours ($-0.5 < 2x/LWL < 4$) for QUAPAW at $F_n = 0.25$	250
N.14. Post wake-off XYZFS prediction of wave cut for QUAPAW at $F_n = 0.25$	251
N.15. Post wake-off XYZFS prediction of wave spectrum for QUAPAW at $F_n = 0.25$	252
N.16. Post wake-off XYZFS prediction of wave contours for QUAPAW at $F_n = 0.3197$	253
N.17. Post wake-off XYZFS prediction of wave cut for QUAPAW at $F_n = 0.3197$	254

FIGURES (Continued)

	Page
N.18. Post wake-off XYZFS prediction of wave spectrum for QUAPAW at $F_n = 0.3197$	255
N.19. XYZFS prediction of QUAPAW wave spectrum compared to full scale and model scale experimental measurements	256

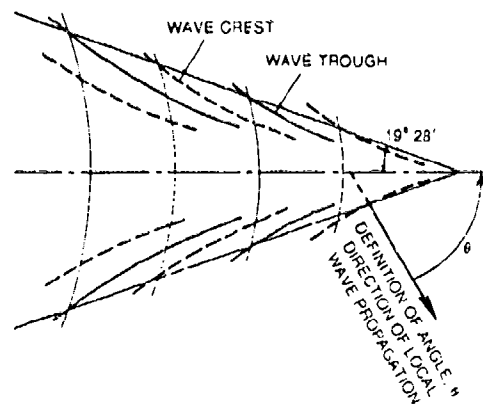
TABLES

1. Computer programs based on Havelock source potential	4
2. Computer programs based on Rankine source potential	4
3. Relative wave amplitudes	8
4. Code ranking by category	9
5. Wave pattern resistance coefficient predictions	11
A.1. Model experimental conditions	14
L.1. Summary of Kelvin wake computations performed by SAIC in conjunction with the wake-off	230

NOMENCLATURE

Dimension
(L = length and T = time, LT^{-1})

AP	Aft perpendicular	
DBW	Diverging bow wave	
DSW	Diverging stern wave	
E	Amplitude of the free wave spectra	
F	Sine component of the free wave spectra	
F_n	Froude number, $U/(g \text{ LWL})^{1/2}$, $K_o \times \text{LWL} = 1/F_n^2$	
FP	Forward perpendicular	
G	Cosine component of the free wave spectra	
K_o	Fundamental wave number (g/U^2)	L^{-1}
LWL	Length at waterline	L
TW	Transverse wave	
U	Free stream velocity	LT^{-1}
X	Longitudinal coordinate (origin at FP)	L
Y	Transverse coordinate	L
Z	Vertical coordinate	L
g	Gravitational constant	LT^{-2}
u	Circular wave number induced in y direction ($\sec \theta \tan \theta$)	
w	Circular wave number induced in x direction ($\sec \theta$)	
h	Wave elevation	L
q	Direction of wave propagation	
λ_o	Fundamental wave length ($2\pi/K_o$)	L
θ	Angle from which the transverse wave number is computed: defined as the angle between the direction of wave propagation and the direction in which the ship/model is travelling (see figure)	



ABSTRACT

Wave patterns predicted by several numerical codes were evaluated by comparing them with data from model basin experiments on two ship hulls at three Froude numbers each. In general, the codes all underpredict the amplitude of divergent waves springing from the ships' bow. High wave number detail is also lacking in the vicinity of the bow wave cusp line compared to model free-surface wave patterns. Conversely, the codes tend to overpredict the amplitudes of waves close to the ships' stern and in the transverse wave system behind.

The codes are ranked according to how closely they simulate the empirical results. Within the ranking, adjacent codes give similar wave predictions and the rank might be interchanged for a few Froude number cases. Higher ranked codes gave consistently better predictions than the lower ranked codes.

Problems for the lower ranked codes included: excessive wave damping such that waves are attenuated near the edges of the computational domain; reflections appear at the outer boundaries; high frequency "noise" exists beyond the nineteen-degree envelope of the spreading wave train; and wave energy has been severely underpredicted.

Standardized graphic representations of the numerical and experimental data are included in the appendixes.

The predictions were made "blind," without prior knowledge of the specific experimental results. In view of the inherent difficulties including nonlinear wave breaking and real fluid effects (present in the experiments), the agreement achieved by the better codes is encouraging.

ADMINISTRATIVE INFORMATION

This investigation was sponsored by the Chief of Naval Research, Office of Naval Technology, Code ON721, under the Surface Ship Technology Program (ND1A), Program Element 62121N, Acoustic and Wake Signature Project RH21C12, Task 1, Signature Reduction. The DTRC Work Unit numbers are 1506-710 and 1506-810.

INTRODUCTION

The rapid increase in the availability and power of digital computers has made it practical to solve the Neumann-Kelvin problem. Significant interest in the problem has led to three "International Workshops" on wave resistance in the last ten years. While the wave resistance problem is interesting and challenging, the closely related Kelvin wake problem is more exacting and has a critical application in modeling ship wake electromagnetic signatures, an important practical problem since the advent of satellite remote sensing of ship wakes which resulted from NASA's oceanographic SEASAT program in 1978. Wave phase relations are important regarding peak amplitude and slope, hence the occurrence of wave breaking. Furthermore, wave pattern prediction requires finer spatial resolution because short wave lengths have an integral role in radar cross section. Wave resistance prediction relies on an integrated quantity which is fairly insensitive to the high wave number end of the free wave spectrum or phase relations in wave space.

Several researchers have developed numerical codes that may have utility for predicting or evaluating the impact of hull design on surface ship-wake patterns regarding remote sensing from wave-wave interactions, wave breaking, white-water, etc. In general, these various codes have not been validated with regard to their overall power,

accuracy, suitability, etc. This study was performed to provide an initial validation, based simply on experimental model basin surface ship wave pattern data. The objective is to provide a rational basis for selecting the code(s) showing the greatest potential for further development as a useful design/evaluation tool and to set the course and framework for such a development effort.

Various researchers were invited to submit numerical predictions for comparative evaluation of their codes. The specifications for the competition are reproduced in Appendix A. The hull forms and Froude numbers were selected for specific cases that had extensive Kelvin wake data from previous DTRC model-scale, towing tank experiments. These data were not disclosed to the researchers; thus they were afforded a "blind" test for their code's predictive capability. Three Froude numbers for each of two nonpropelled ship models, DTRC Model 3531 (QUAPAW) and Model 5415, were selected for the "competition." Most invited entries considered only the QUAPAW model because they were unable to deal with the transom stern of Model 5415, a high speed destroyer-type hull. Standard formats were established for presenting the codes' predictions (see Appendix A) so that comparisons might be facilitated by overlaying transparencies based on the experimental results presented in Appendix B.

Three "referees" evaluated the entries independently and then met to achieve a consensus regarding the weaknesses and strengths of each entry. Areas of consideration included: wake realism, relative wave amplitudes, appropriate wave radiation and/or attenuation, and free-wave spectra.

The following sections discuss the ship hull characteristics, the analytical models, rationales for the data formats and comparative evaluation, results, and conclusions. The graphic empirical data and each numerical code entry are presented in individual appendices, in the order of their assessed proficiency.

PHYSICAL MODEL CHARACTERISTICS

The QUAPAW (ATF 110) is an ocean-going fleet tug represented by the 1/12th scale model, DTRC Model 3531, appended with a rudder. The model's waterline length is 16.25 ft, so the three Froude numbers, 0.2131, 0.25, and 0.3197 correspond to full-scale ship speeds of 10.0, 11.7, and 15.0 knots, respectively. The top ship speed is about 16 knots. This ship is of particular interest because full-scale data from the so-called "Georgia Straits" experiment,¹ are available for further validation.

DTRC Model 5415 represents a prototype twin screw, transom stern destroyer. This model is fitted with a large sonar dome. The waterline length of this model is 18.767 ft; thus the Froude numbers, 0.25, 0.2755, and 0.4136 correspond to ship speeds of 18.1, 20.0, and 30.0 knots, based on a 24.822 scale ratio. This model was appended with shafts, struts, and rudders.

The model experiments were conducted with freedom in pitch and heave so that the hull took on a trim condition when underway. The trim data were supplied to the numerical modellers so that wave patterns would be derived for the "as trimmed condition." Similarly, the "lines" for the two models were furnished in the form of ship panelization files, depicted graphically in Figs. 1 and 2 for the two ship model hulls. The numerical modellers were not restricted to a specific panelization scheme, however, and some used modified panels.

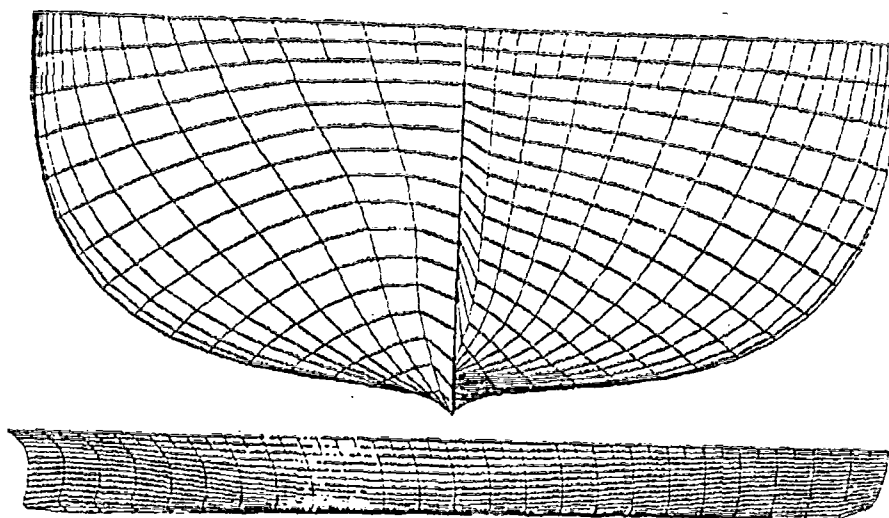


Fig. 1. Typical panel scheme for Model 3531.

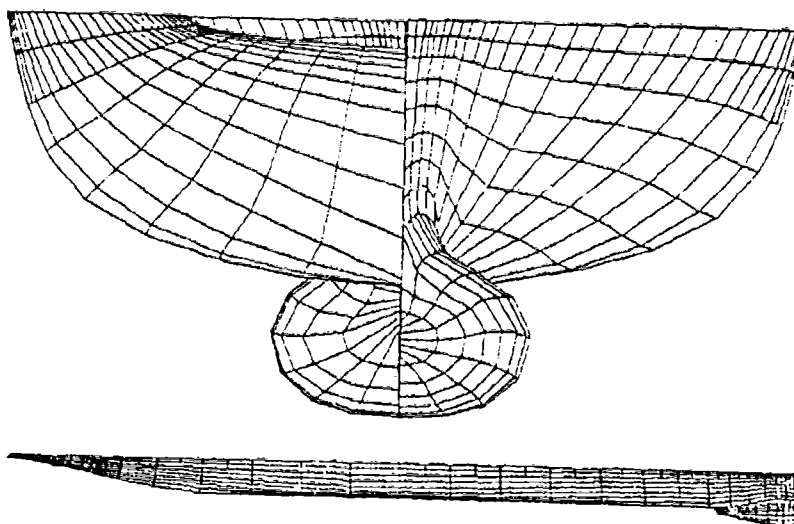


Fig. 2. Typical panel scheme for Model 5415.

ANALYTICAL MODELS

The predictive programs which were evaluated can be divided into two categories: those using Havelock sources, which automatically satisfy the linearized free-surface condition, distributed over the surface of the body; and those which use Rankine sources distributed over the body and the undisturbed free-surface. These latter methods are closely related to Dawson's pioneering approach² wherein singularities are distributed on the free surface (as well as on the hull surface) in such a fashion that they satisfy a linearized free surface condition.

The creators of five computer programs based on the Havelock source potential were asked to make Kelvin wake predictions. These authors, their employers, and their computer programs' names are given in Table 1. Creators of seven Rankine Source programs were also asked to make Kelvin wake predictions. A list of these authors, their employers, and the names of their computer programs are given in Table 2.

Table 1. Computer programs based on Havelock source potential.

Author	Employer	Program Name
R.F. Beck	University of Michigan	DOCTORS N- K ^{3,4}
F. Noblesse	DTRC	EPPAC1, FARWAV ⁵
T. Schmidt, J.V. Rattayya, and J.R. Brooks	Lockheed, Advanced Marine Systems	---
C.A. Scragg	SAIC, San Diego	NK- 2 ⁶
J. Telste	DTRC	SWIM, SWIMFS ⁷

Table 2. Computer programs based on Rankine source potential.

Author	Employer	Program Name
W. Cheng	DTRC	XYZFS ⁸
J. Dean (proprietary)	DTRC	---
Y.H. Kim and S.H. Kim	DTRC	SWIFT ⁹
L. Larsson	SSPA	---
B. Rosen	Self	FLOPAN ¹⁰
P. Schlavounos and J.N. Newman	MIT	NKSHIP ¹¹
K. Weems and C. Oliver	SAIC, Annapolis	---

On 12 and 13 January 1988, a workshop was held at DTRC to discuss and compare results of the Kelvin wake computations. A formal letter announcing the workshop was sent to each participant. The letter is reproduced in Appendix A. This workshop was attended by the various individuals who had made Kelvin wake computations, and additional corporate representatives from many of the organizations represented in the

computational effort. In addition, the workshop was held in conjunction with a meeting of the Society of Naval Architects and Marine Engineers (SNAME) Analytical ShipWave Relations (H-5) panel. The participation of the H-5 panel greatly broadened the attendance at the meeting, both in numbers of people and in technical breadth.

During the course of the workshop, the authors of the various codes discussed their prediction methods and our comparative evaluations of the codes were presented. Graphic representations of the various invited predictions are reproduced in Appendixes C - K along with written discussions that the authors prepared for the workshop in response to the "Wake-Off Questionnaire" and "Kelvin Wave Computations" (reproduced in Appendix A.)

Although it was hoped that Dr. Lars Larsson of SSPA and Chalmers University would be able to contribute to the computational effort, his travel commitments made it impossible for him to complete the computations within the time frame required. In addition, two of the programs (those of Schmidt, et al, and Weems and Oliver) were judged to need further development, and thus these computer programs are not included in the comparative evaluation.

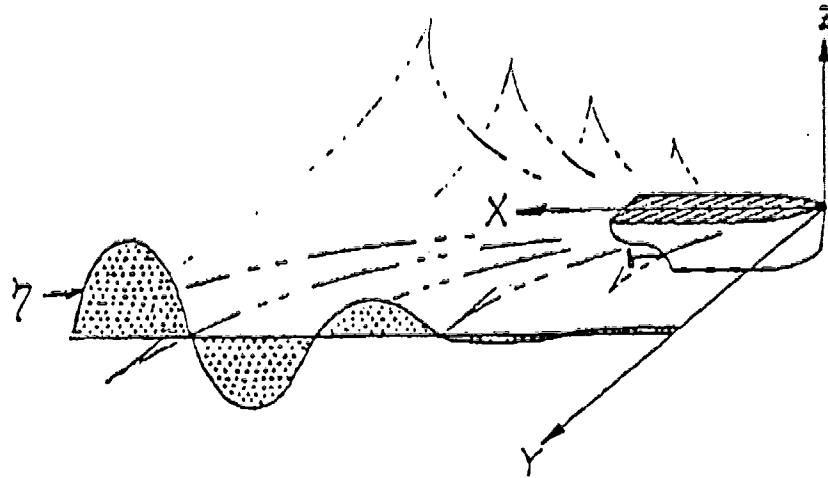
DATA FORMATS

Details of the formats that were specified for graphical data presentations are shown in Appendix A. Three types of plots were included: iso-elevation contours, longitudinal wave cuts, and free-wave spectra. Scales were selected based on the model test data ranges and more-or-less standard dimensionless parameters.

The most complete spatial representation of free-surface elevation are contour plots showing lines of iso-elevation at a specific interval; e.g., $0.01/K_0$, where K_0 is the fundamental wave number and $1/K_0 = 2h_0$ or twice the pressure head of the flow). The experimental contours, obtained from stereophotographic data, were all drawn with a 2% ($\Delta ZK_0 = 0.02$) interval as a compromise between too many confusing lines (smaller interval) and insufficient detail (larger interval).

Basic two-dimensional wave profiles, obtained with capacitance wave probes, are depicted in longitudinal cuts of the free surface elevation in a vertical plane parallel to the ship's longitudinal centerline. The transverse location for wave cuts is $Y = 0.324 \cdot \text{LWL}$ for Model 5415 and $Y = 0.373 \cdot \text{LWL}$ for Model 3531. The disturbed wave elevation (Z) and longitudinal coordinate (X) have been normalized by the fundamental wave number, i.e., $Z \cdot K_0$ and $X \cdot K_0$. The origin is abreast the ship's forward perpendicular, at the undisturbed free-surface, as sketched below. Note, the vertical scale is greatly magnified compared to the horizontal scale, so that the wave profiles have a very steep appearance. The range for the vertical scale was specified to be $\pm 0.1\%$, or $\pm 20\%$ of the fluid velocity head; experimental wave cut surface elevations were bounded by this range. The horizontal scale ranged from 0 to 100, so that roughly sixteen fundamental wavelengths, λ_0 , are contained in the graph ($\lambda_0 = 2\pi/K_0$).

In order to make a quantitative comparison between analytical predictions and experimental data it is important to quantify the uncertainties generated during the model experiment. Although there are a vast number of potential sources of inaccuracy only a few of the more important will be quantified here; model speed, model construction, model surface finish, and the repeatability of the capacitance probe data.



The speed of the model being towed on the carriage is measured using a toothed gear, which rotates along with one of the carriage drive wheels and triggers a magnetic pick-up with a pulsed output. The resultant precision error of the measurement of carriage speed is ± 0.001 ft/sec and the bias error associated with that is 0.005 ft/sec.

Both the models which were used as part of this study were of wooden construction which ensures a certain stability of shape over time. The model section shape contours are constant to within $\pm 1/16$ in. and the "waviness" is less than $1/32$ in. between ends of a 3-ft batten. Model 5415 was a newly constructed model, and thus the above tolerances apply, however Model 3531 was built in the 1940's and most probably has additional distortion enough to double the tolerances in section shape contours from that of a new model. The surface finish for both models is obtained using enamel paint applied to a high gloss smooth finish with roughness over the surface of no more than 60 – 100 micro-inches RMS.

In an effort to examine the repeatability of the capacitance probe response to waves produced by the model during a run, two repeat wave records from the same probe were compared. For two model speeds, 4.36 knots and 11.65 knots, these comparisons yielded a relative precision error (standard deviation) of 2 percent and 1.8 percent, respectively, referenced to the peak amplitude of the wave record. This error was obtained by calculating a standard deviation between two wave records using each of the 2000 data points in the record. A more detailed account of the uncertainties introduced in obtaining measurements of model wave heights is found in Reference 12.

Free wave spectra show the distribution of wave energy density amplitude and its two (Fourier) components as a function of the transverse wave number, u . Transverse wave energy is manifested in the very low wave number range and divergent waves correspond to the remaining wave numbers. Note, the three graphic representations for each data set are, in some sense, redundant—one can, in theory, derive each graph from either one of the other two.

EVALUATION PROCESS

The entries were evaluated independently by three referees (the authors), against standardized wake criteria agreed upon at the beginning of the evaluation process. They then met to compare their individual findings and achieve a consensus regarding the weakness and strength of each entry. Areas of consideration included: wake pattern realism (appropriate cusp wave angle, phase relationships, fine scale detail, and no unrealistic reflection planes); relative amplitudes of bow divergent, stern divergent and transverse waves; appropriate wave radiation trajectory and attenuation, and free wave spectra distributions with regard to amplitude and phase.

The findings are discussed in the following sections with tables of comparative wave amplitude and relative ranking. For completeness, the entries are all reproduced in appendixes, in the order of their closeness of fit to the experimental wave pattern wakes. For this assessment, no account was taken of the relative software documentation and user friendliness, nor of the hardware and CPU time.

RESULTS

The evaluations were based largely on graphic plot comparisons. The reader is invited to make his own set of clear "viewgraphs" from the experimental data representations in Appendix B. These can then be overlaid on corresponding numerical data plots to corroborate the results discussed below.

GENERAL OBSERVATIONS

There were some basic similarities between the results of many of the computer programs. In general, the agreement between prediction and measurement was better at the highest Froude number for each model. Other similarities were found in the bow and stern wave systems; the amplitude of the bow wave was consistently underpredicted and the amplitudes of the stern and transverse waves were overpredicted. Table 3 shows several comparisons, derived from wave cut graphs, for predicted wave amplitude divided by the corresponding experimental wave amplitude. This ratio is seen to be less than one for the peak value arising from the diverging bow wave (DBW) and greater than one for most peak diverging stern wave (DSW) predictions. The amplitude mismatch for the predictions made on diverging stern waves (and transverse wave trains) is decidedly worse for Model 3531 than for Model 5415.

The crest lines along the bow wave cusp line are predicted to have larger angles than shown experimentally. This may be caused by the transverse waves being overpredicted, while DBW is underpredicted.

Table 3. Relative wave amplitudes.

Table 3a. Model 5415.

CODE NAME	FROUDE NUMBER								
	0.25			0.2755			0.41360		
	DBW	DSW	TW	DBW	DSW	TW	DBW	DSW	TW
FARWAV	0.7	1.36	2.0	0.6	1.45	3.5	0.8	1.0	1.4
NK-2	0.2	1.45	3.0	0.33	1.80	3.0	0.67	1.26	1.4
SWIFT	0.2	0.64	—	0.25	0.62	—	0.45	0.80	—
XYZFS	0.16	0.05	—	0.13	0.06	—	0.45	0.73	—

Note: Values show the ratio of predicted wave amplitude to experimental wave amplitude. DBW: diverging bow wave, DSW: diverging stern wave, TW: transverse wave.

Table 3b. QUAPAW, Model 3531.

CODE NAME	FROUDE NUMBER								
	0.2131			0.25			0.3197		
	DBW	DSW	TW	DBW	DSW	TW	DBW	DSW	TW
FARWAV	0.86	2.7	4.0	0.80	6.2	5.0	1.0	1.8	2.0
NK-2	0.52	2.6	2.5	0.6	10	7.5	0.75	2.4	3.5
SWIFT	0.25	0.92	—	0.37	1.8	—	0.56	1.33	—
FLOPAN	0.36	0.35	—	0.47	2.2	—	0.71	0.89	—
XYZFS	0.14	0.16	0.05	0.45	0.88	2.5	0.32	1.26	1.8
Dean	0.11	0.05	0.20	0.18	0.16	1.7	0.38	0.44	2.5
SWIMFS	0.93	1.8	2.4	0.58	6.2	8	—	4	7

Note: Values show the ratio of predicted wave amplitude to experimental wave amplitude. DBW: diverging bow wave, DSW: diverging stern wave, TW: transverse wave.

A strong intermediate crest line is seen in the empirical wave patterns in the region between the diverging bow and stern wave systems. It may be emanating from the forward shoulder region of the hull. This feature is generally not seen in predicted wave patterns; it is an important feature because the local wave slope (and thus wave breaking) is affected by such pattern details. This feature is evident in the experimental wave cuts as an "extra" wave between the bow and stern divergent wave peaks.

Another weakness evident in the code predictions (except for FARWAV) was that wave amplitude is over-attenuated downstream, along the bow wave cusp line. The Rankine source programs generally had greater damping of waves diverging away from the ship. At the extreme, FLOPAN predictions showed no waves at the boundaries of the computational domain. Conversely, experimental transverse waves were attenuated more rapidly than predictions (and/or the classical analytical $R^{-1/2}$ dependence).

Experimental free-wave amplitude spectra exhibit more sharply defined nodes or null points; hence, wave phase relationships were incorrectly predicted numerically.

SPECIFIC COMPARISONS AND RANKINGS

Comparative rankings of the codes are enumerated in Table 4 for three categories: contour plots, wave cuts, and free-wave spectra. Some entries did not include one category of graph (e.g., spectra); they were judged solely by the categories submitted (wave cuts and contour plots), without prejudice.

Table 4. Code ranking by category.

Table 4a. Model 5415.

Contour Plot	Wave Cut	Spectra
1. FARWAV	1. FARWAV	1. FARWAV
2. NK-2	2. SWIFT	2. NK-2
3. SWIFT	3. NK-2	3. XYZFS
4. XYZFS	4. XYZFS	

Table 4b. QUAPAW, Model 3531.

Contour Plot	Wave Cut	Spectra
1. FARWAV, FLOPAN*	1. FARWAV	1. FARWAV
2. SWIFT, NKSHIP, NK-2, DOCTORS N-K	2. NK-2	2. DOCTORS N-K
3. Dean, SWIM, XYZFS	3. DOCTORS N-K	3. NK-2
	4. SWIFT, NKSHIP	4. SWIM, XYZFS
	5. XYZFS	5. Dean
	6. FLOPAN, Dean, SWIM	
*Note: FLOPAN predictions are superior very close to the hull, while FARWAV predictions are better for waves radiating away from the hull.		

Five of the computational results were significantly better than the others, those of: FARWAV, NK-2, DOCTORS N-K, SWIFT, and FLOPAN. FARWAV predictions were consistently superior for both models at all speeds and in the three evaluation categories. Wave cuts were very similar between FARWAV and NK-2 owing to similar mathematical representations of source potentials. However, spectra predicted by FARWAV compared more favorably to the experimentally determined results; the diverging waves did not decay as fast as those from the other Havelock source methods.

It is interesting to note that FARWAV used a more rudimentary slender-ship (zeroeth-order) approximation for the source distributions on the ship hull. Subsequent to the Wake-Off workshop, NK-2 was exercised with the slender-ship approximation

and the results, which essentially duplicated the FARWAV predictions, are included in Appendix L.

As stated previously, FLOPAN wave patterns died out much too rapidly. However, FLOPAN gave the best predictions of all for the details of the free-surface disturbance in the region of one ship's beam from the model. These predictions showed free-surface details (evident in experiments) which were, at best, hinted at by the predictions from the better of the other programs. Subsequent to the workshop, FLOPAN was rerun with two alternative finite differencing schemes that served to alleviate the wave attenuation problem and enhanced the detail, but with some signs of instability. These modified results are included in Appendix M.

The predictions by SWIFT were very similar to FLOPAN, with high attenuation at the boundaries of the computational domain. The wave patterns near the ship lacked some of the fine scale detail seen in FLOPAN's contour plots. NKSHIP predictions seem qualitatively similar to SWIFT's, but only a limited range was submitted so our finding is somewhat tentative in this case.

The remaining codes gave noticeably poorer quality results. XYZFS predictions for both models are marginally acceptable at the highest Froude numbers. XYZFS was rerun after the workshop with a revised surface panel distribution. Improved results are very similar to those from SWIFT, and are included in Appendix N.

Dean's results with the proprietary code exhibited unnatural growth in transverse waves downstream at low Froude numbers. SWIM/SWIMFS predictions appear to have problems with numerical resolution and waves propagating upstream.

DISCUSSION

Havelock source codes generally out performed Dawson/Rankine source codes. On the other hand, near-field results such as FLOPAN's may favor the Rankine source approach.

Wave profiles along the hull surface are readily available and would have been useful for comparing "very" near-field predictions. This output was overlooked when setting the ground rules for the competition (empirical wave profiles were unavailable as ground truth, however). Similarly, predicted wave pattern resistance, C_w , should have been requested in the specification. These data are shown in Table 5 for those cases where submitted by the invitees.

Table 5. Wave pattern resistance coefficient predictions. (Values shown are $C_w \times 1000$)

	Model 5415			Model 3531			
Code	$F_n =$	0.25	0.2755	0.4136	0.2131	0.25	0.3197
DOCTORS N-K					0.96	3.94	6.0
FLOPAN					0.21	0.62	3.5
NK-2		0.51	1.39	4.4	1.37	6.40	7.9
XYZFS		0.80	0.89	2.3	0.66	0.48	5.1
Experiment		0.37	0.46	2.4	0.21	0.40	1.8

Some of differences between experimental and predicted wave patterns can be attributed to real fluid or viscous effects. The experimental stern wave cusp line is noticeably offset outboard of the model compared to the predicted wave patterns. Some of differences between experimental and predicted wave patterns can be attributed to real fluid or viscous effects. The experimental stern wave cusp line is noticeably offset outboard of the model compared to the predicted wave patterns. The thick boundary layer at the stern is probably affecting the pattern here as well as contributing to the reduction in stern wave amplitudes.

Attenuation of the transverse waves may likewise be affected by the viscous wake trailing behind the experimental model. In this regard, viscous effects are exaggerated (by the low Reynolds number) in the experiments compared to full-scale ships.

Science Applications International Corp. (SAIC) has performed detailed analysis of full-scale wake data for the ATF QUAPAW.¹³ Figure 3 shows SAIC's (ship) free-wave amplitude spectrum compared with Model 3531 data for an unpropelled 15-knot case ($F_n = 0.32$). The full-scale data represent a 15.5-knot run; specific displacement and trim are unknown, but believed to be relatively near those used in the experiment. In view of the difficulties inherent in full-scale experimentation, the agreement seen for these two data sets is encouraging.

The codes generally assume that the ship hull is "wall sided" at the free-surface, i.e., the vertical gradient in the hull offsets is zero. This simplification may affect the predicted wave patterns.

CONCLUSIONS

One might have hoped for better results from the comparison of the experimental and computational results. The technical problems are difficult and wide ranging, but are not intractable. The work of Noblesse, Scragg, Beck, Kim, and Rosen indicate that there is a good chance for successfully predicting Kelvin wave fields, particularly if a method can be developed which can take advantage of the excellent near-field calculations of FLOPAN and the superior far-field capability of the Havelock source methods. The Wake-Off workshop helped to focus on the directions for future improvements.

The fact that Noblesse, Scragg, and Beck can produce results which are virtually identical when they use consistent approximations of the body boundary condition is certainly an encouraging finding. This is particularly true when one considers the large

amount of scatter in wave resistance calculations which were performed as recently as four or five years ago. It is to be expected that Noblesse, Scragg, and Beck would all predict similar wave resistance values; this implies an unprecedented degree of consistency in their solution to the Neumann-Kelvin problem. Although it should not be given too much significance, it is also encouraging that the phases of the humps and hollows of the free-wave spectra predicted by Noblesse, Scragg, and Beck are essentially in agreement with the experimental data, although the amplitude does not always agree. Less satisfactory results are obtained when the sine and cosine components of the free-wave spectra are compared with the model data.

Scragg's studies of the effects of smaller panels near the waterline show a disturbing divergence of the wave resistance due to the behavior of the waterline integral. This is caused by the fact that the source strengths on the panels near the free surface are approaching infinity as the panel size decreases; so, while the product of the source strength and the panel area remains bounded, the source strength in the waterline integral goes to infinity. This leads to anomalous results for the wave resistance and, obviously, for other quantities that may be less sensitive to the waterline integral than is the wave resistance. A close examination of the derivation of the waterline integral is probably warranted, as is exploring ways to evaluate the waterline integral without using the source strength on the free surface. Perhaps a method based purely on the wave potential would avoid these difficulties.

Additional work is still required to obtain an efficient, fast, and accurate evaluation of the Green's function of the Havelock source potential. Other technical areas needing further effort include: the proper treatment of non-wall-sidedness, the dependence of the solution on panelization or convergence, the effect of propulsion on the wave system, the proper boundary conditions to apply with a transom stern, and the inclusion of lifting components. An ultimate task would be the inclusion of the full nonlinear free-surface condition, at least near the ship.

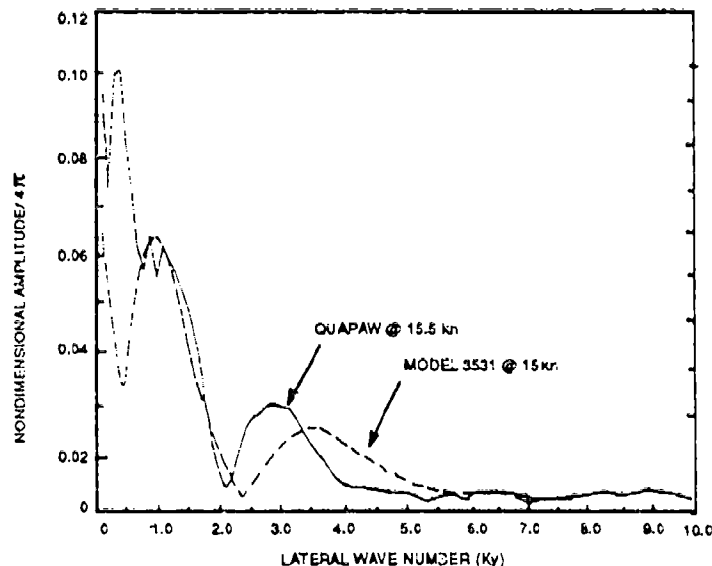


Fig. 3. Measured wave spectra for the ATF QUAPAW and Model 3531.

APPENDIX A
SPECIFICATIONS FOR WAKE-OFF COMPETITION

APPENDIX A **SPECIFICATIONS FOR WAKE-OFF COMPETITION**

TASK

Use your free-surface Kelvin Wake code to compute the free surface elevations in the near field of two models, one a high speed transom stern destroyer (Model 5415) and the other the QUAPAW (Model 3531). The calculations should produce the entire wave system in the area bounded by a cross-track line 0.1 ship length ahead of the bow and another cross-track line three ship lengths downstream from the stern. The calculations should be made for several values of Froude number for each model, as specified in Table A.1. The calculations should be presented as surface contours, as wave cuts parallel to the ship track, and as spectral representations of the wave cuts. The calculations should be presented for the parametric values shown in Fig. A.1.

Table A.1. Model experimental conditions.

Model 5415			
LWL = 18.787 ft $\lambda = 24.8220$			
V_k (knots)	F_n	Depth to Keel (ft)	
		at FP	at AP
0.0	0.0000	20.22	20.22
18.1	0.2500	21.00	20.30
20.0	0.2755	21.20	20.70
30.0	0.4136	20.00	23.60
Wave cut at $y/LWL = 6.083/18.767 = 0.324$			
Model 3531 (QUAPAW)			
LWL = 16.250 ft $\lambda = 12.000$			
V_k (knots)	F_n	Depth to Keel (ft)	
		at FP	at AP
0.0	0.0000	13.60	16.75
10.0	0.2131	13.87	17.28
11.7	0.2500	13.94	17.52
15.0	0.3197	14.43	18.42
Wave cut at $y/LWL = 6.060/16.250 = 0.373$			

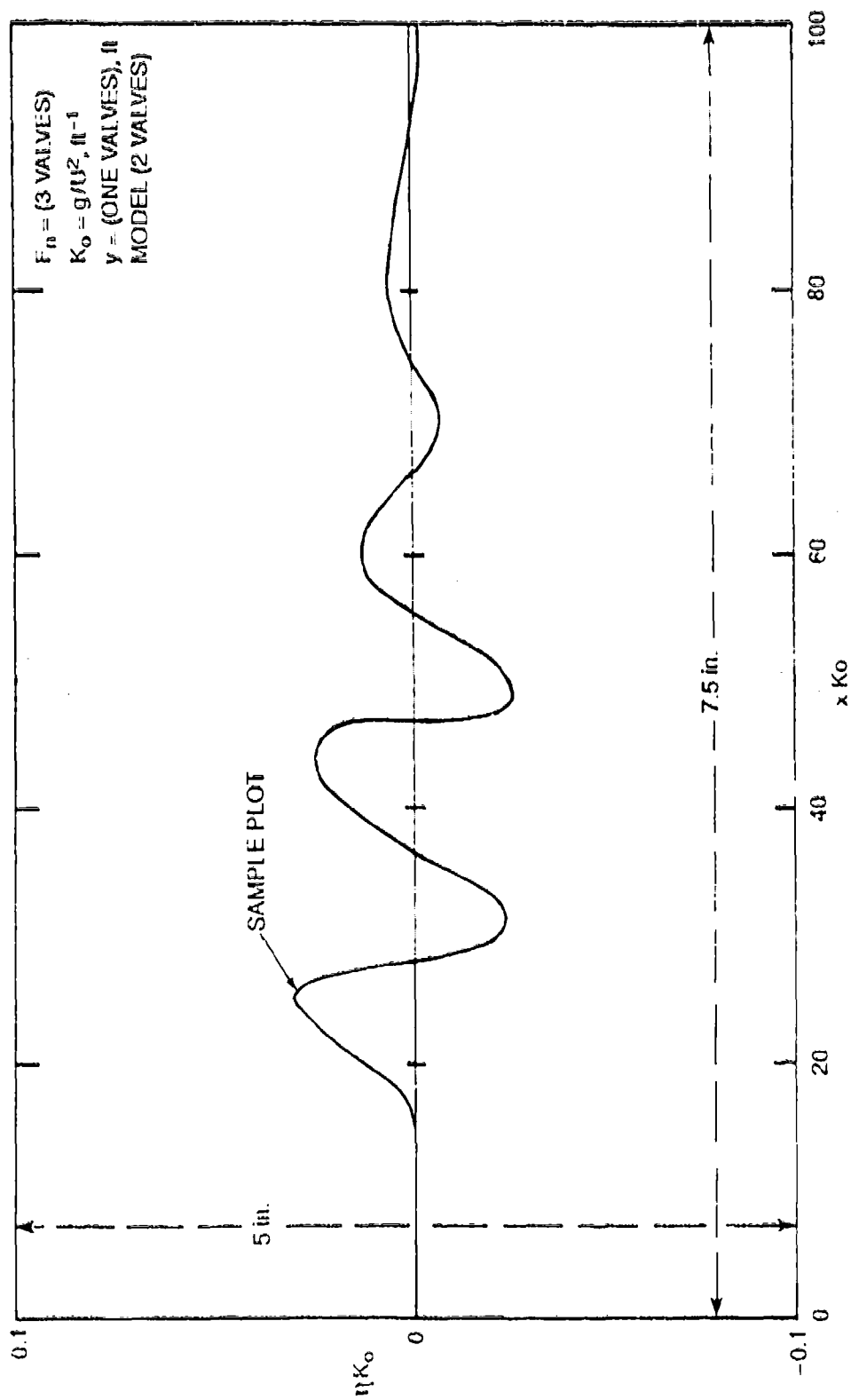
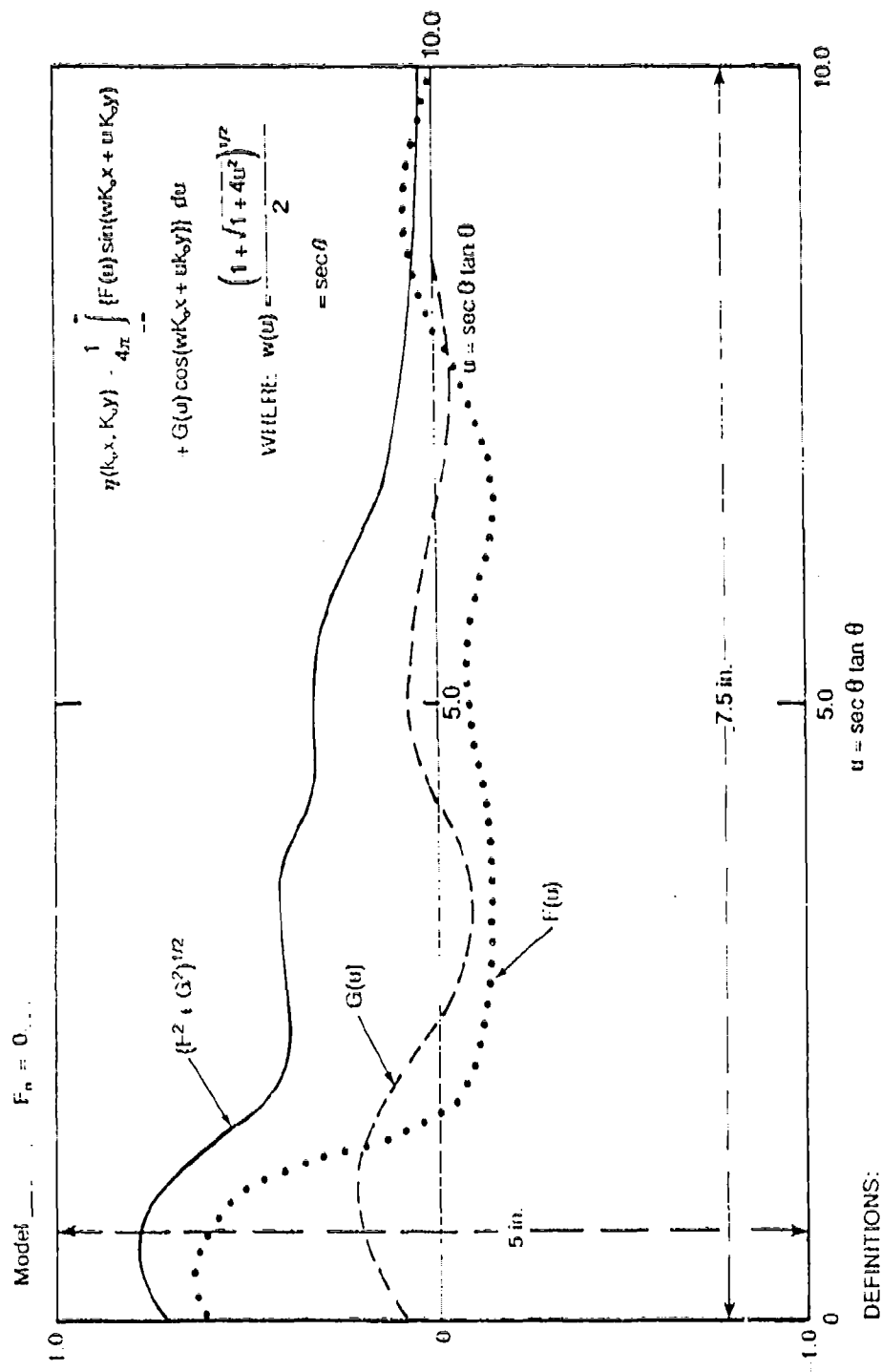


Fig. A.1a. Wave cut.

Fig. A.1. Graphics format sample.



$$F(u) = \frac{4\sqrt{w^2 - 1}}{(2w^2 - 1)} \times \{C(w, y) \sin(uy) + S(w, y) \cos(uy)\}$$

$$G(u) = \frac{4\sqrt{w^2 - 1}}{(2w^2 - 1)} \times \{C(w, y) \cos(uy) + S(w, y) \sin(uy)\}$$

$$C(w, y) + iS(w, y) = \int_{-\infty}^{\infty} \eta(x, y) \exp(iux) dx, \quad 0 \leq w < \infty$$

Fig A.1b. Free-wave spectra.

Fig. A.1. (Continued)

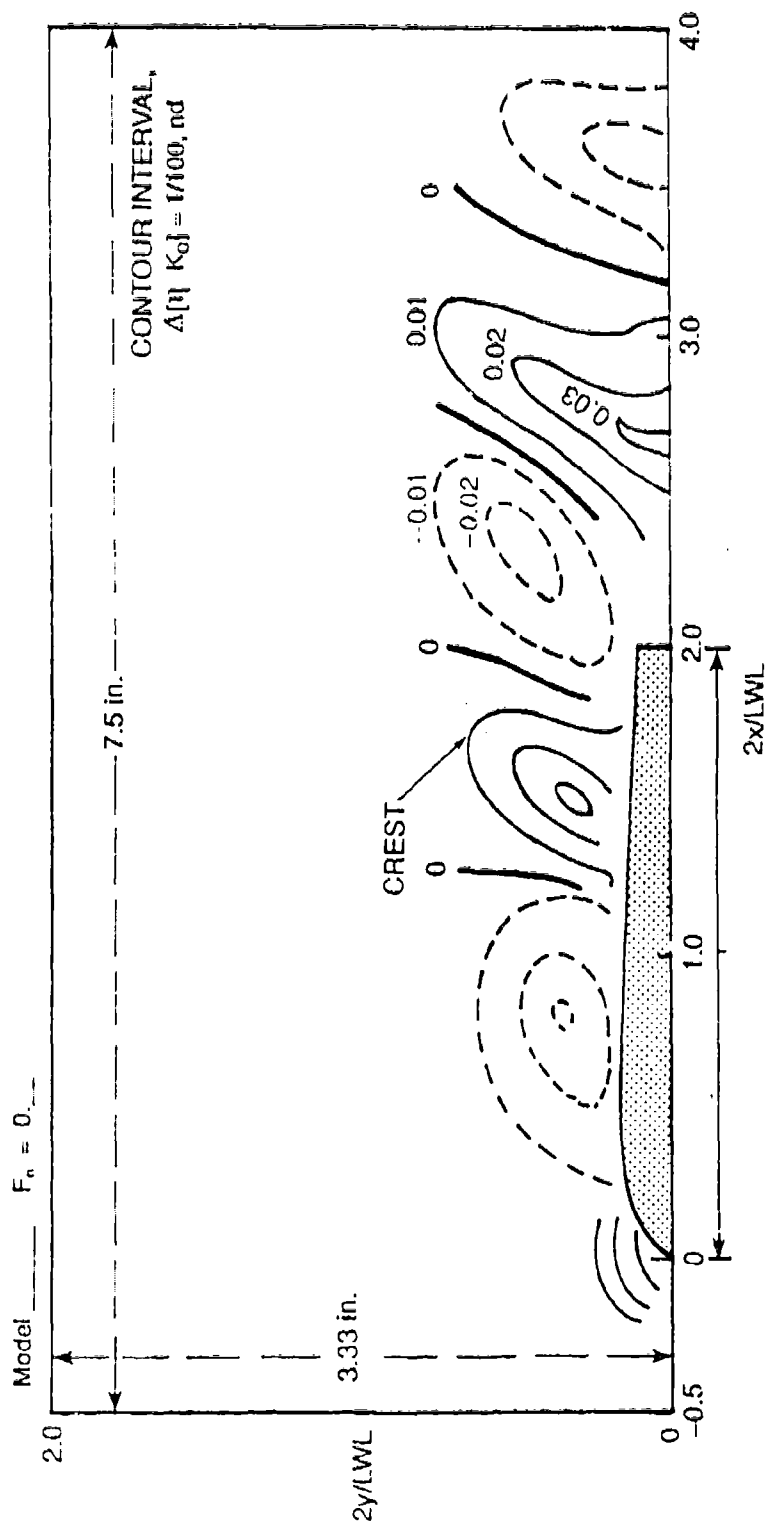


Fig. A.1c. Contour plots.

Fig. A.1. (Continued)

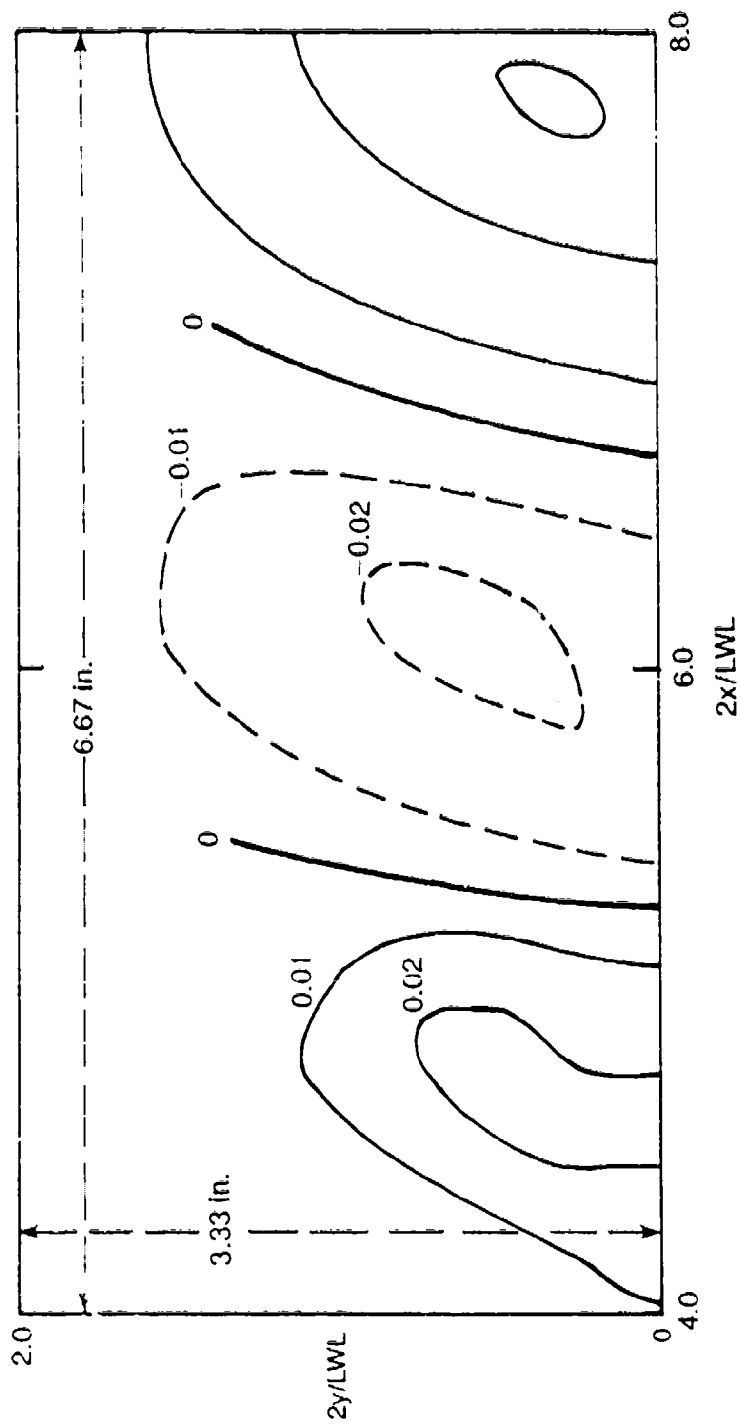


Fig. A.1c. (Continued)

Fig. A.1. (Continued)

OBJECTIVE

The results will be evaluated with a view toward using the code in the development of the Surface Ship Hydrodynamic Wake Reduction Code. The evaluation will include the following criteria:

1. For Accuracy,
 - Wave length
 - Elevation pattern
 - Wave cut spectra
 - Wave amplitude (local slope)
 - Peak amplitude
 - Minimum resolvable wave length
2. For Physical Code
 - User friendliness
 - Overall power
 - Efficiency — fast and easily modified input preparation
 - Flexibility for modifying geometry
 - Modular format
 - Adaptability to different computers
 - Ability to provide a graphical display
 - Ease in obtaining arbitrary wave cut spectra
 - Accommodation for nonlinear effects
 - Wide range of Froude numbers
3. For Documentation
 - Availability
 - Clarity

GEOMETRY

The geometry for paneling the hull is available; calculations should be done for the sinkage and trim conditions found in Table A.1.

FORMAT

The results are to be presented in graphical format as shown in Fig. A.1 so that comparisons between calculated and empirical data may be made easily and directly by overlaying the graphics. The data are to be normalized in the manner shown in Fig. A.1.



DEPARTMENT OF THE NAVY
DAVID W. TAYLOR NAVAL SHIP RESEARCH
AND DEVELOPMENT CENTER
HEADQUARTERS
BETHESDA, MARYLAND 20841-5000

ANNAPOLIS LABORATORY
ANNAPOLIS, MD 21403-6067
CARDEROCK LABORATORY
BETHESDA, MD 20864-1668

IN REPLY REFER TO:

9 Dec 1987

Dear

As you are aware from previous communications, we are planning to hold a two-day workshop to discuss the results of the comparative Kelvin wake calculations on 12 and 13 January 1988. You are invited to attend and participate in this workshop, which will also be a joint meeting with the SNAME H-5 ANALYTICAL SHIP WAVE RELATIONS PANEL.

The exact agenda of the meeting has not yet been prepared, however, the general outline is to have those participants who have prepared results for either the Qwapaw or DDG-51 make approximately a 30 minute presentation on the details of their computational method. It is to be assumed that all participants are familiar with the boundary value problem associated with the Kelvin wake problem for a ship in steady motion on a free surface, and the Havelock source and Rankine source methods for solving this problem. The experimental techniques and results will then be presented. This will be followed by presentations on what was learned in doing the computations and the specific difficulties which were encountered. This presentation will be optional for those who did calculations. Finally, the comparative evaluations of the computational results will be presented followed by a set of general conclusions.

For those individuals who have done comparative computations, it is asked that you present two or three viewgraphs at the beginning of your presentation which answer the questions that are attached as Enclosure (1). The purpose of these questions is to provide a uniform set of measures as to the maturity and sophistication of each of the codes. In your presentation of the details of your code, it is suggested that you include information on the Green's function used, the integration method over the panels, the method for satisfying the body and free surface boundary conditions and the general algorithm for the solution of the entire boundary value problem. You are encouraged to present any other information which you think will be relevant.

If at all possible, you are requested to provide us with hard copies of your presentation or at least those viewgraphs responding to Enclosure (1) approximately one week before the meeting.

It is our intention to provide those individuals whose codes are evaluated, with unique private identifiers so that only the best codes will be explicitly identified during the comparative evaluation. This is intended to avoid embarrassment to those individuals whose codes have significant deficiencies.

We look forward to seeing you on the 12th and 13th. If you have any questions, please feel free to contact me at 202-227-1450 which is my office number or 301-587-3270 at my home.

Sincerely,

Arthur M. Reed

WAKE-OFF QUESTIONNAIRE

In order to complete the Kelvin wake code evaluations, the committee is requesting all participants to supply answers to the following questions regarding the numerical code which was used as well as the resulting computations.

COMPUTATIONAL CODE

Name of Code?

How many lines of Coding?

How many subroutines?

What are the limitations on the number of panels which can be used?

Describe the status of the program documentation.

Does a user's manual exist?

What hardware could/has the Code run on? With what modifications?

Can the Wave Resistance Coefficient, C_w , be predicted?

Can/Does the Code include lift? Describe the difficulties of modifying the Code to include lift and/or nonlinearities.

Can/Does the Code include provision for a propulsor/actuator disc?

Are on-body and/or off-body streamlines calculated?

What kind of boundary conditions or numerical techniques are used to deal with the radiation condition?

Is the Code suitable for transom-stern type hull forms?

What experience level is necessary to prepare the input data, run the program, and display the results?

Describe the "user-friendliness" aspects of the Code.

KELVIN WAVE COMPUTATIONS

On what machine were the computations run?

How long (CPU time) did it take to run each case?

How involved, streamlined, and time consuming is the input data preparation process?

Was a check done for convergence during or after the computations?

How many panels were used (for each case/hull)?

What is the nature of the panel shape and distribution, and singularity distributions?

If C_w was calculated, please provide the predictions for each case.

THIS PAGE INTENTIONALLY LEFT BLANK

APPENDIX B
EXPERIMENTAL RESULTS

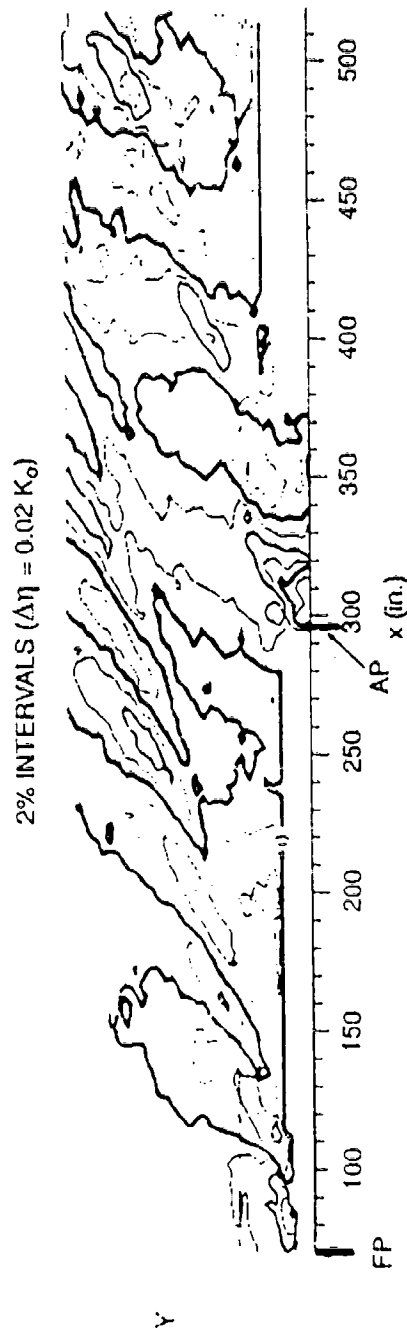


Fig. B.1. Experimental wave contour for Model 5415 at $F_n = 0.25$.

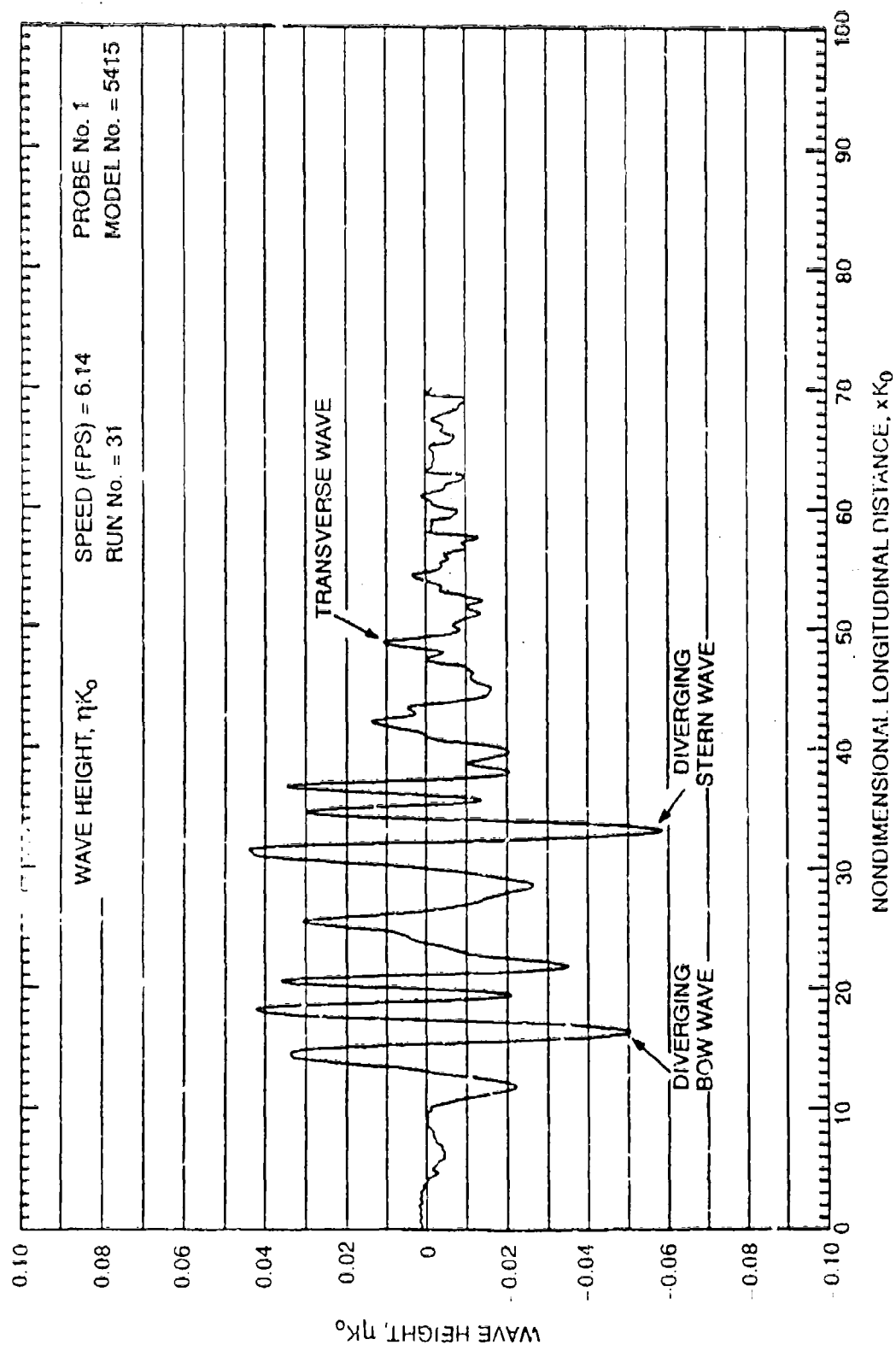


Fig. B.2. Experimental wave cut for Model 5415 at $F_n = 0.25$.

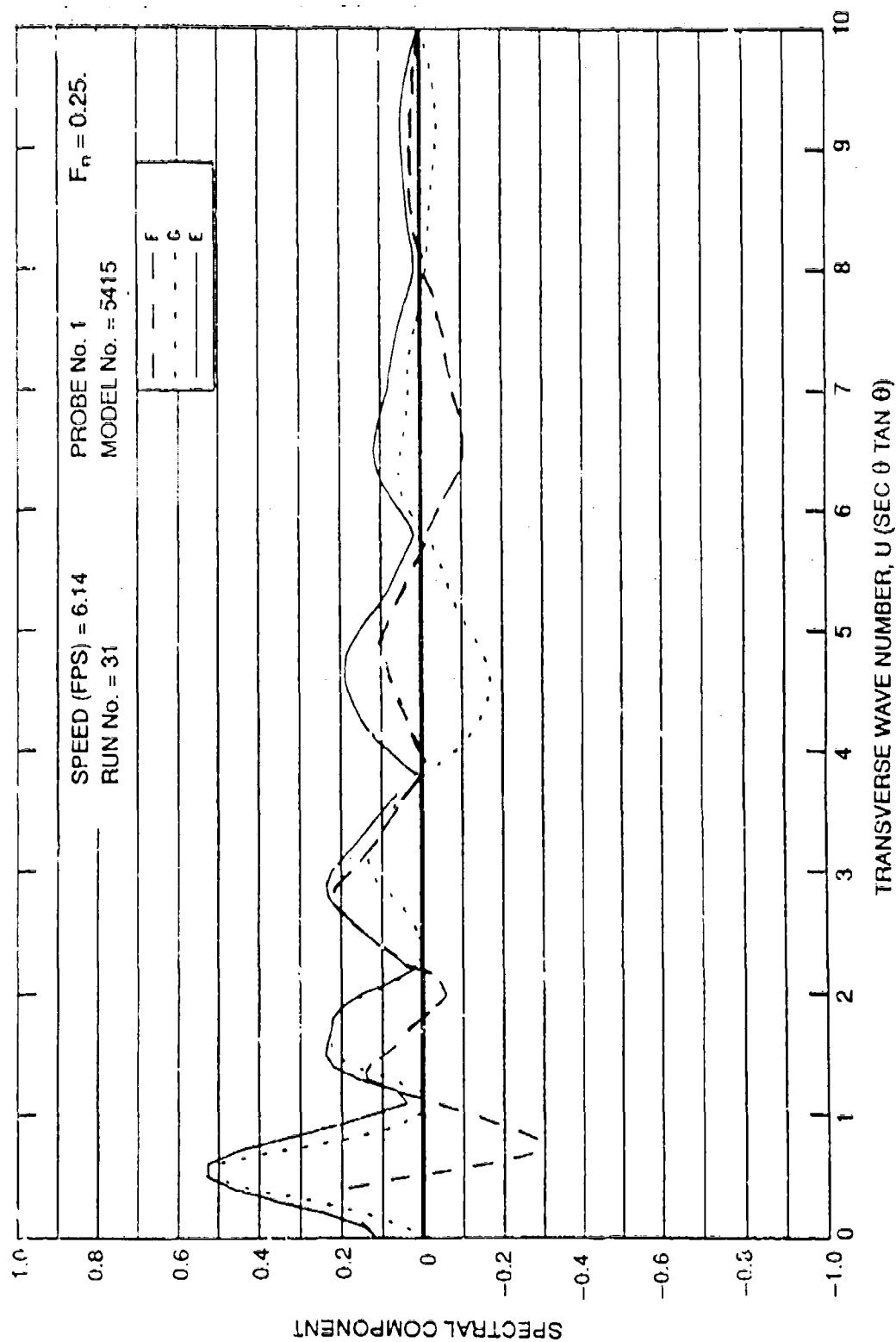


Fig. B.3. Experimental wave spectrum for Model 5415 at $F_n = 0.25$.

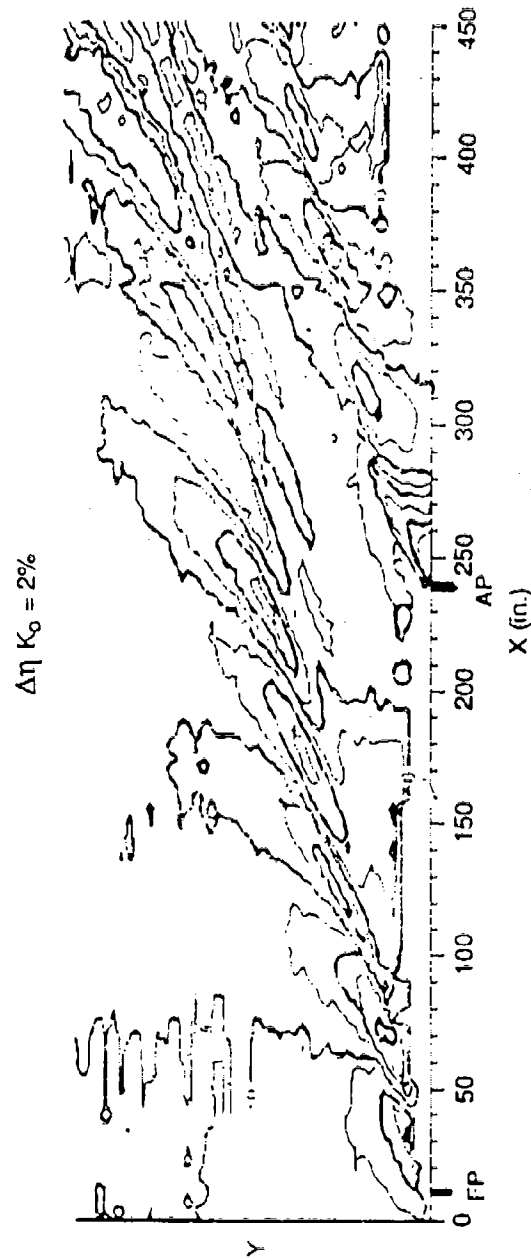


Fig. B.4. Experimental wave contours for Model 5415 at $F_n = 0.2755$.

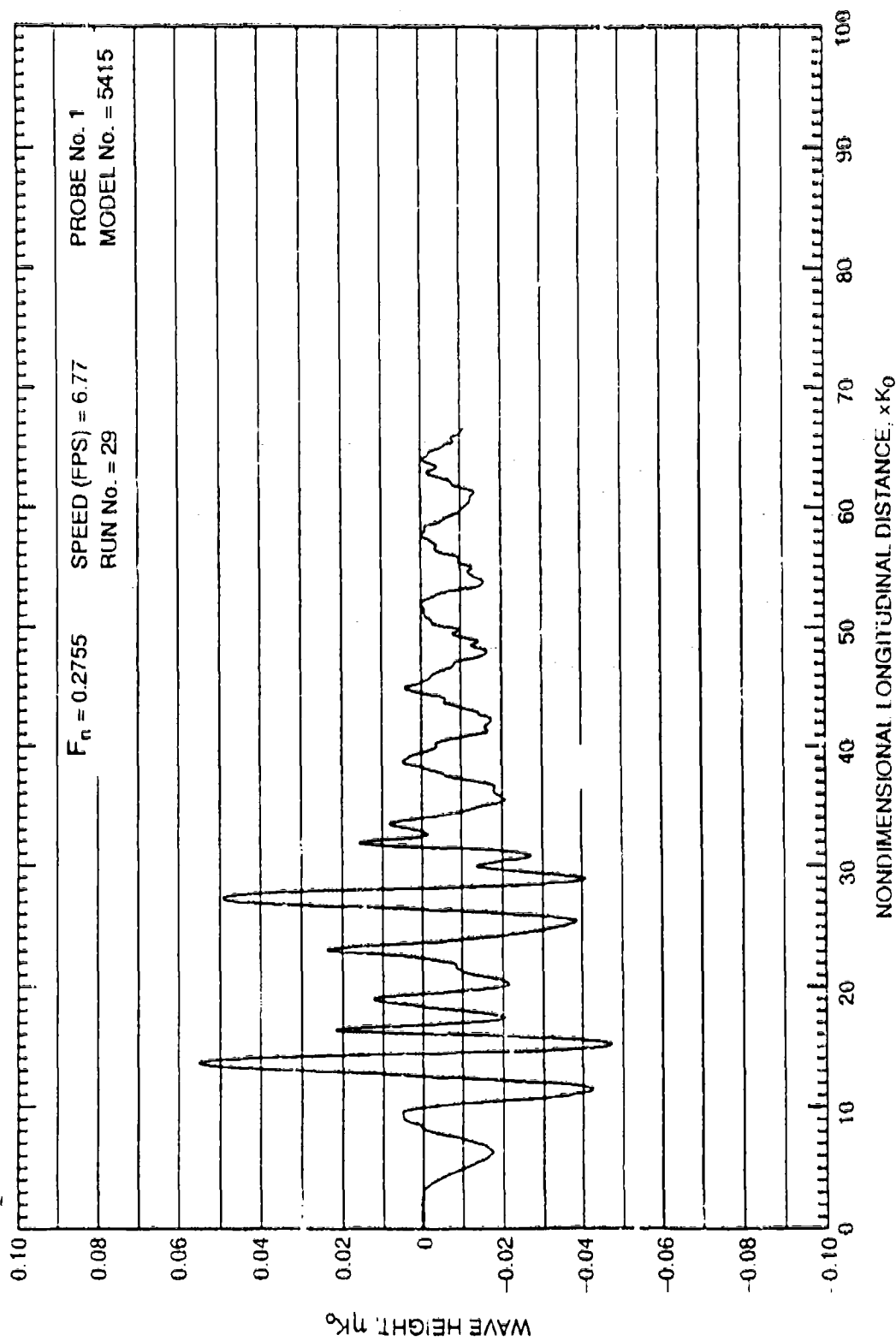


Fig. B.5. Experimental wave cut for Model 5415 at $F_n = 0.2755$.

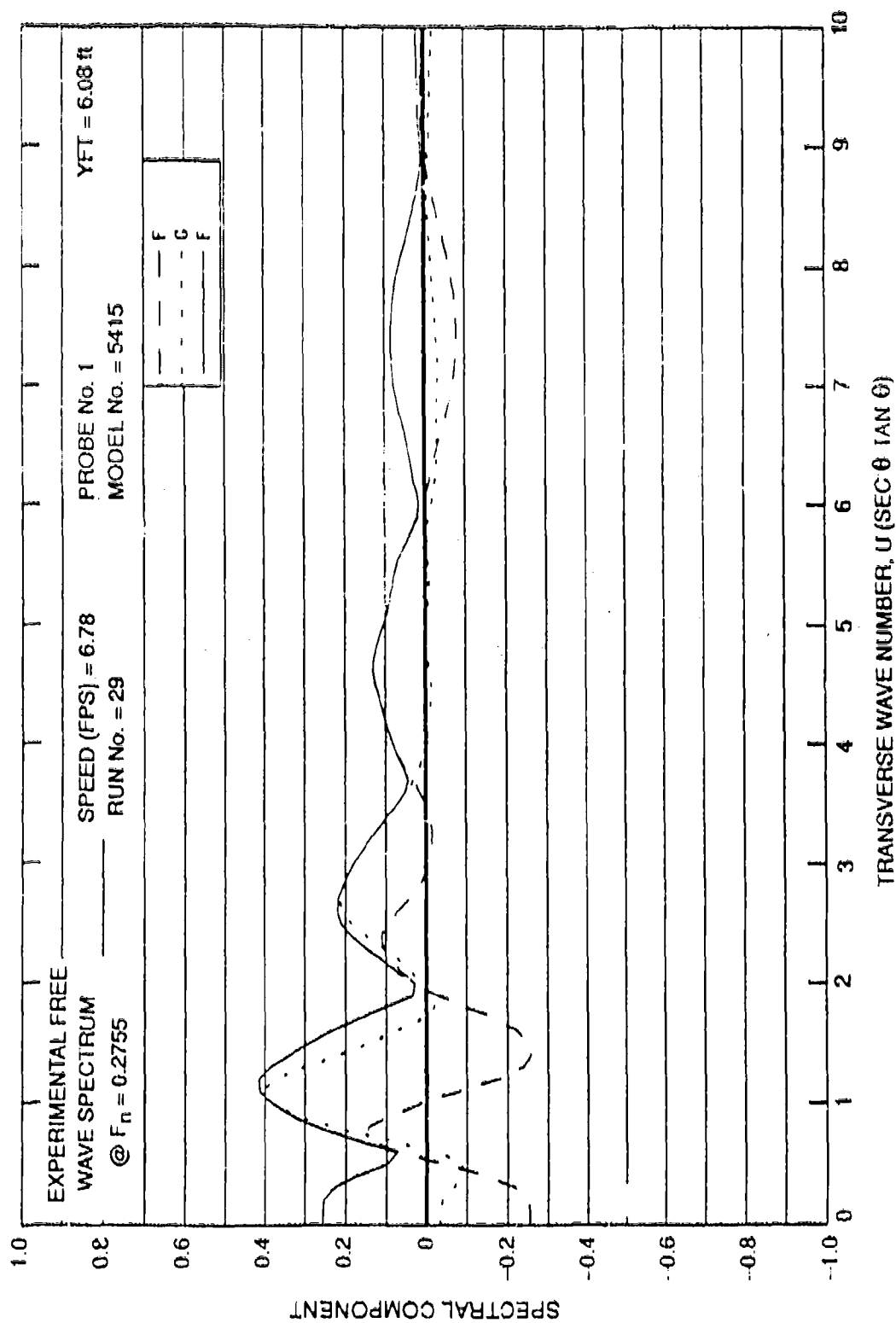


Fig. B.6. Experimental wave spectrum for Model 5415 at $F_n = 0.2755$.

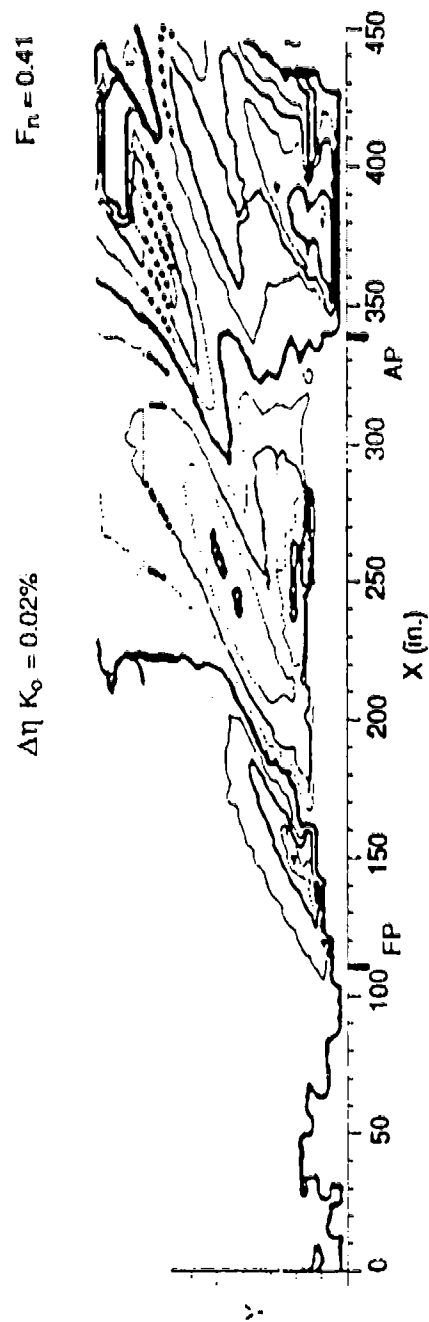


Fig. B.7. Experimental wave contours for Model 5415 at $F_n = 0.4136$.

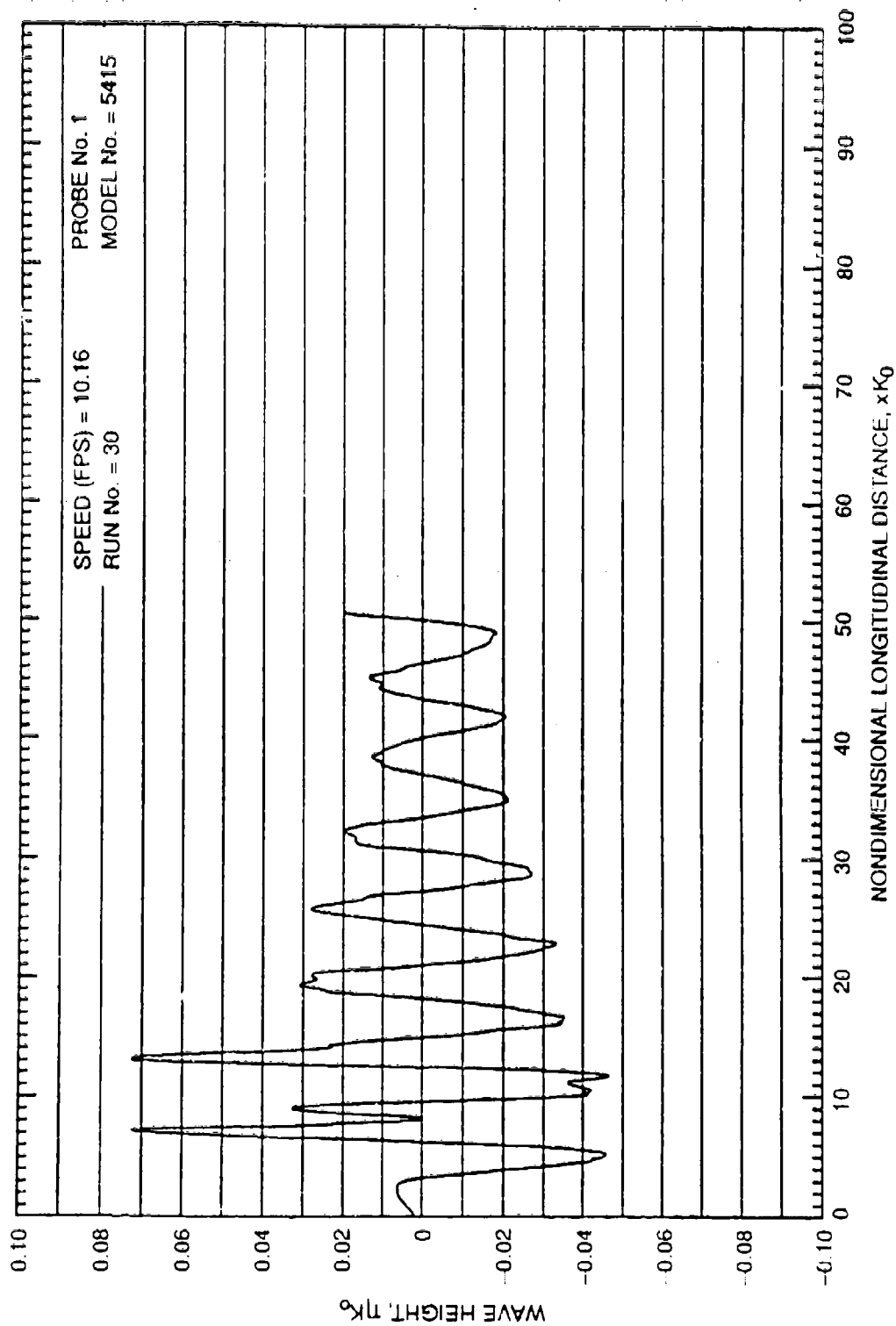


Fig. B.8. Experimental wave cut for Model 5415 at $F_n = 0.4136$.

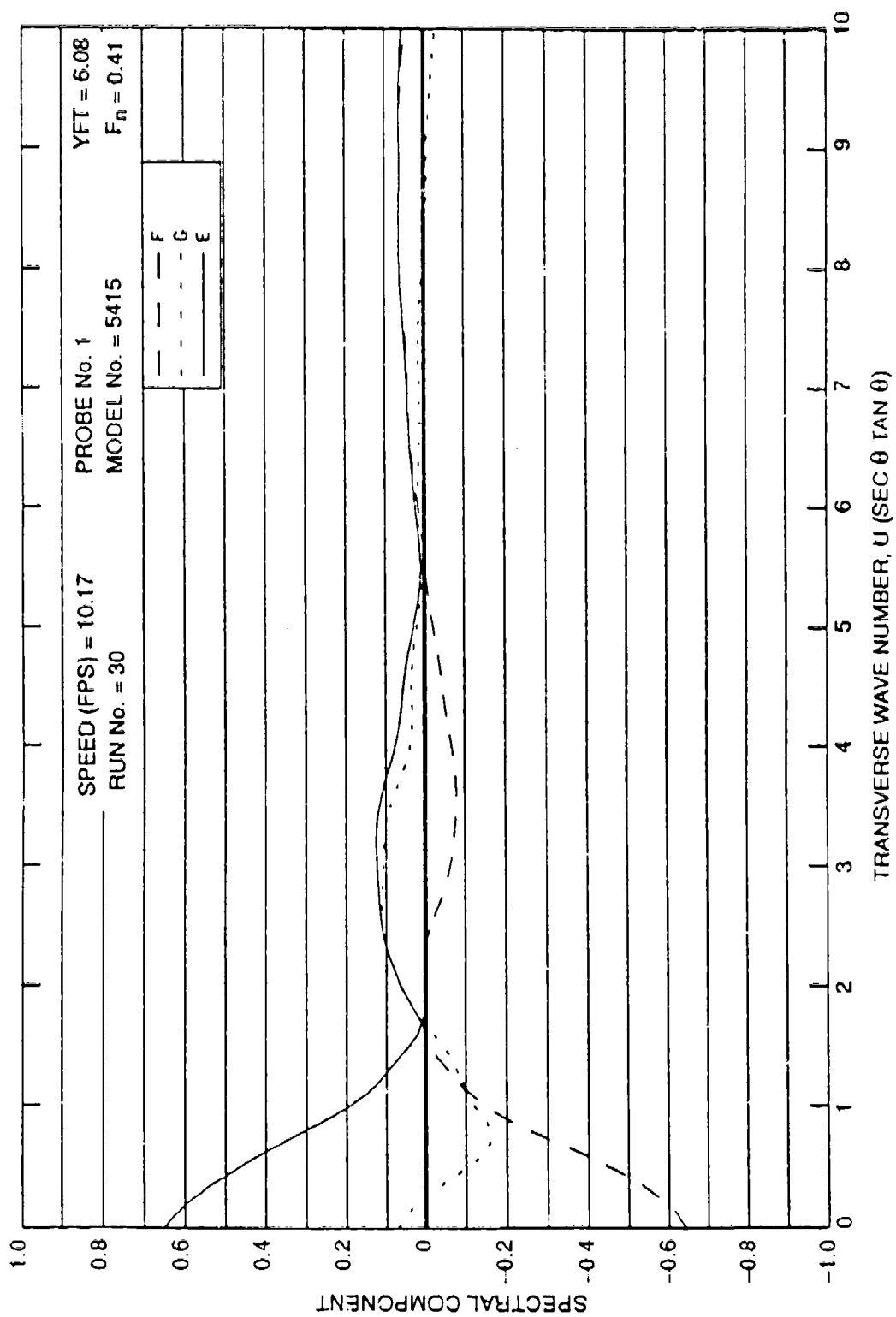


Fig. B.9. Experimental wave spectrum for Model 5415 at $F_n = 0.4136$.

FROUDE No. 0.213 MODEL No. = 3531

$\Delta\eta K_0 = 0.02\%$

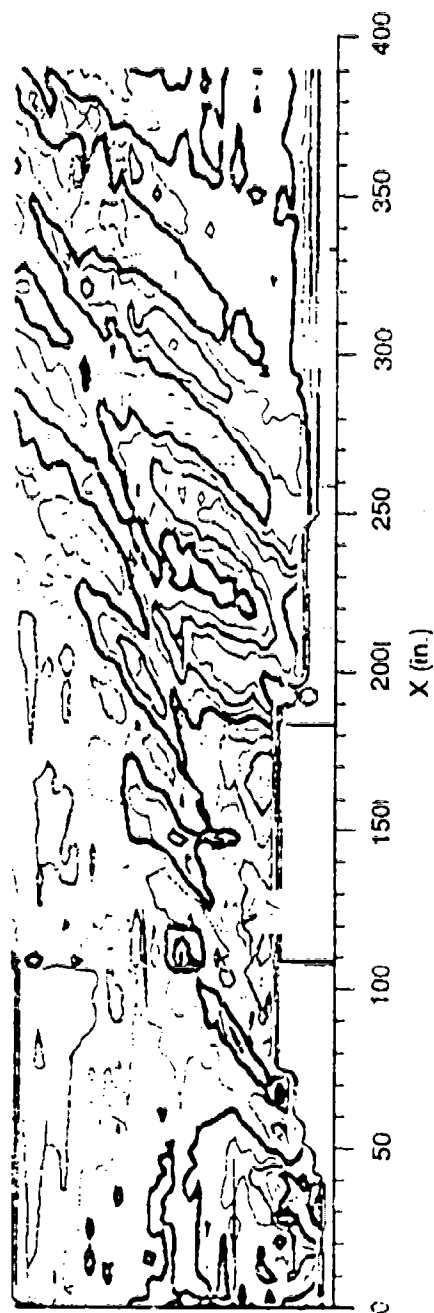


Fig. B.10. Experimental wave contours for QUAPAW at $F_n = 0.2131$.

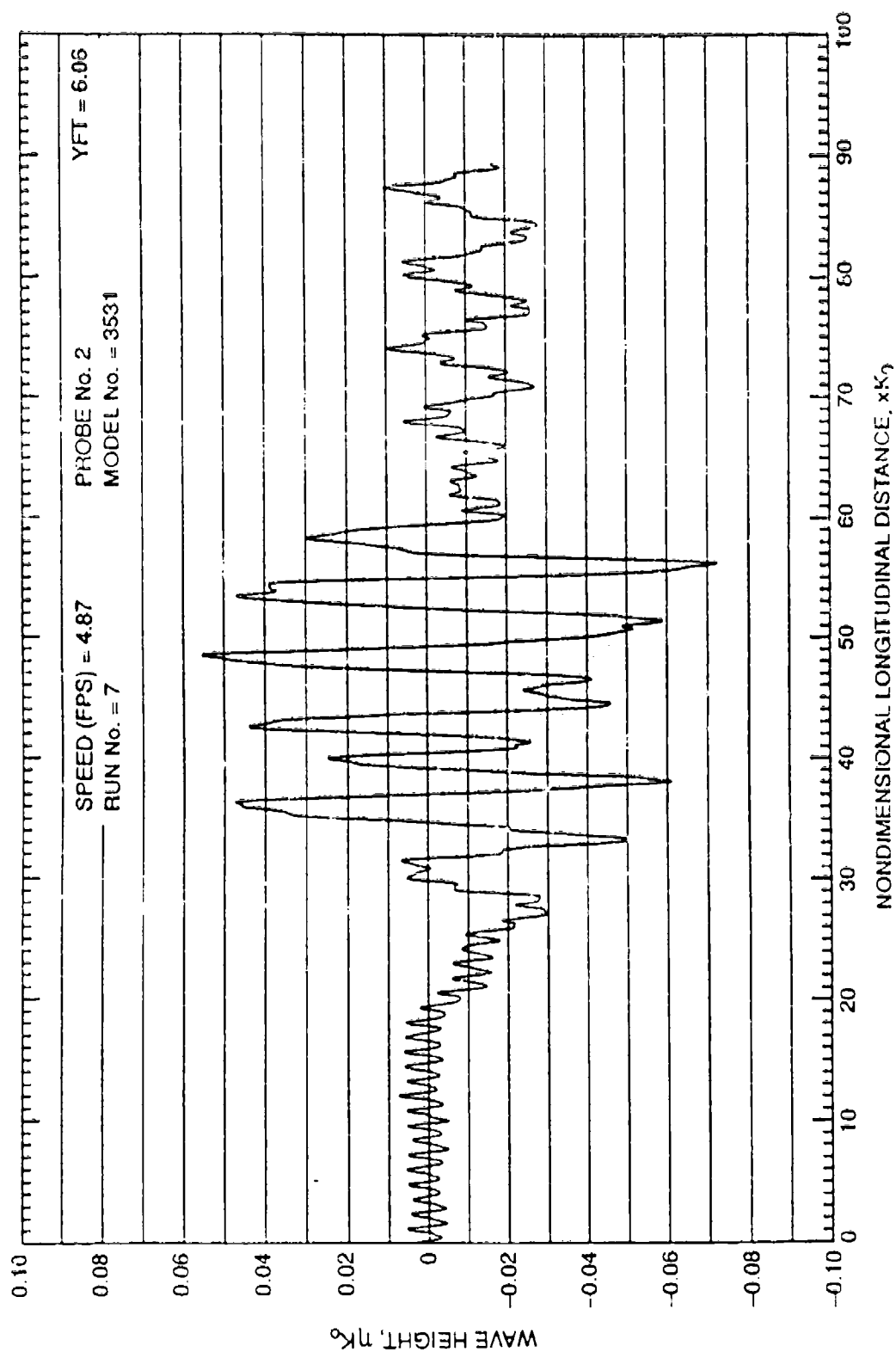


Fig. B.11. Experimental wave cut for QUAPAW at $F_n = 0.2131$

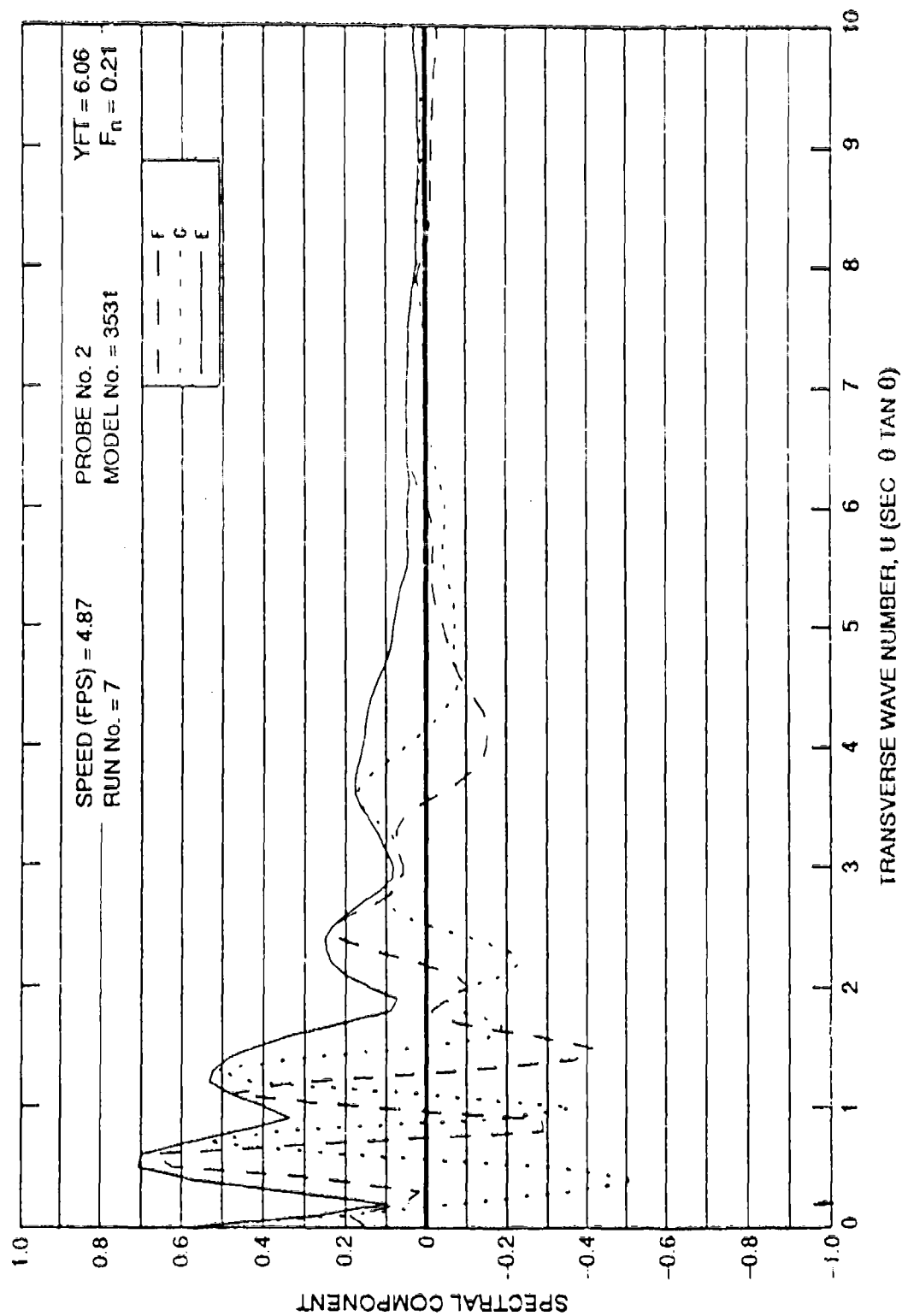


Fig. B.12. Experimental wave spectrum for QUAPAW at $F_n = 0.2131$.

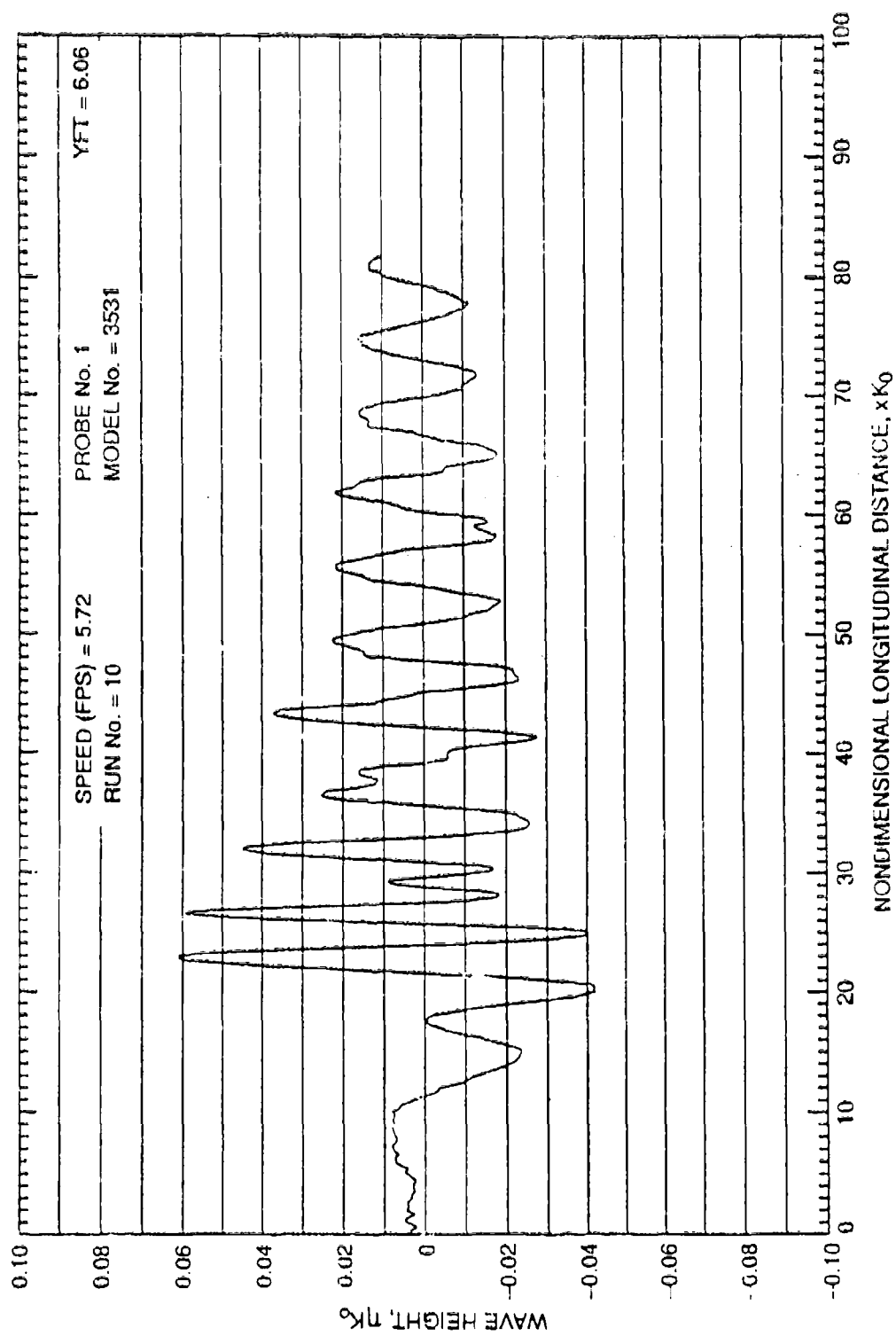


Fig. B.13. Experimental wave cut for QUAPAW at $F_n = 0.25$.

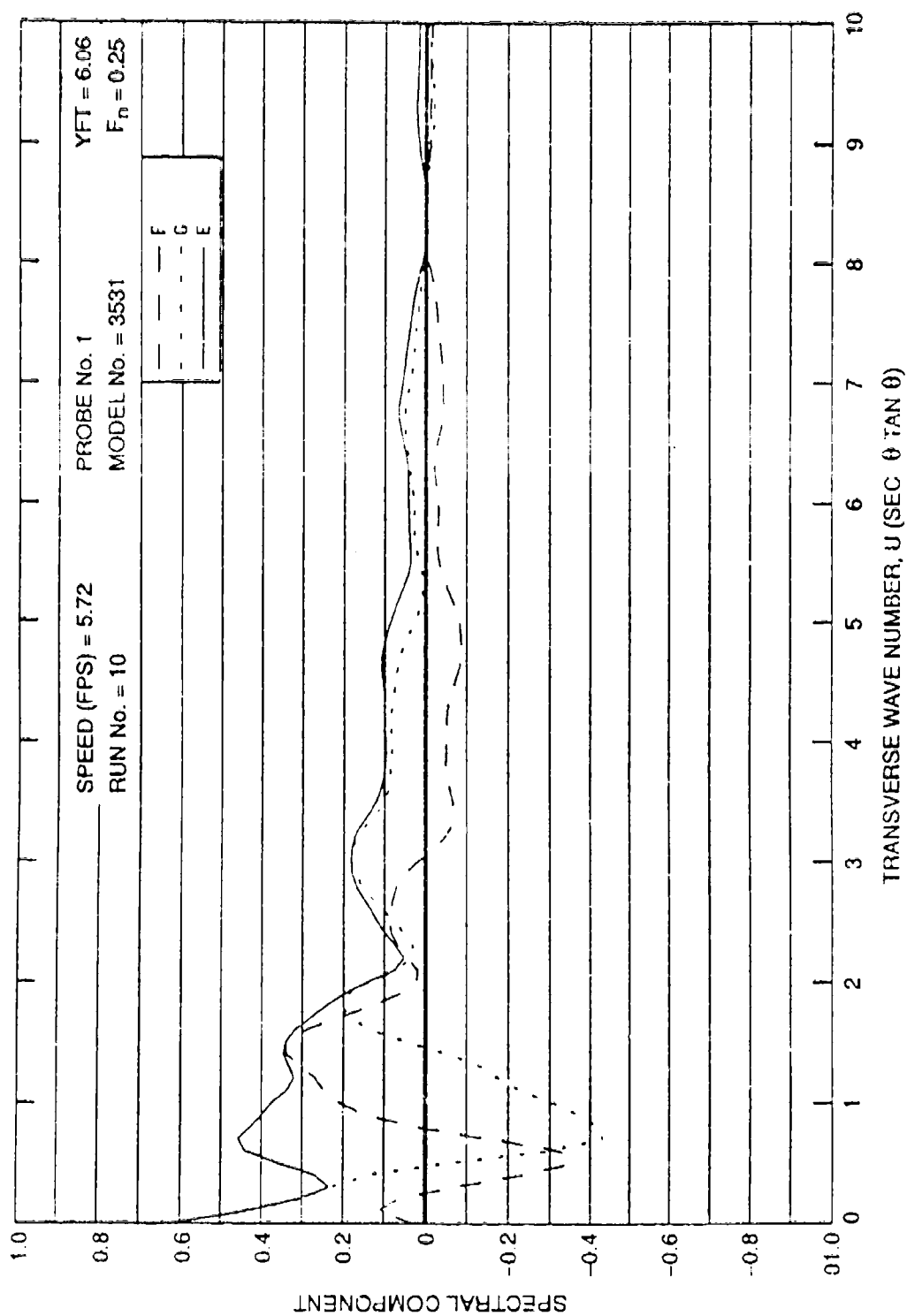


Fig. B.14. Experimental wave spectrum for QUAPAW at $F_n = 0.25$.

FROUDE No. 0.32 MODEL NO. 3531

$\Delta\eta K_0 = 0.02$

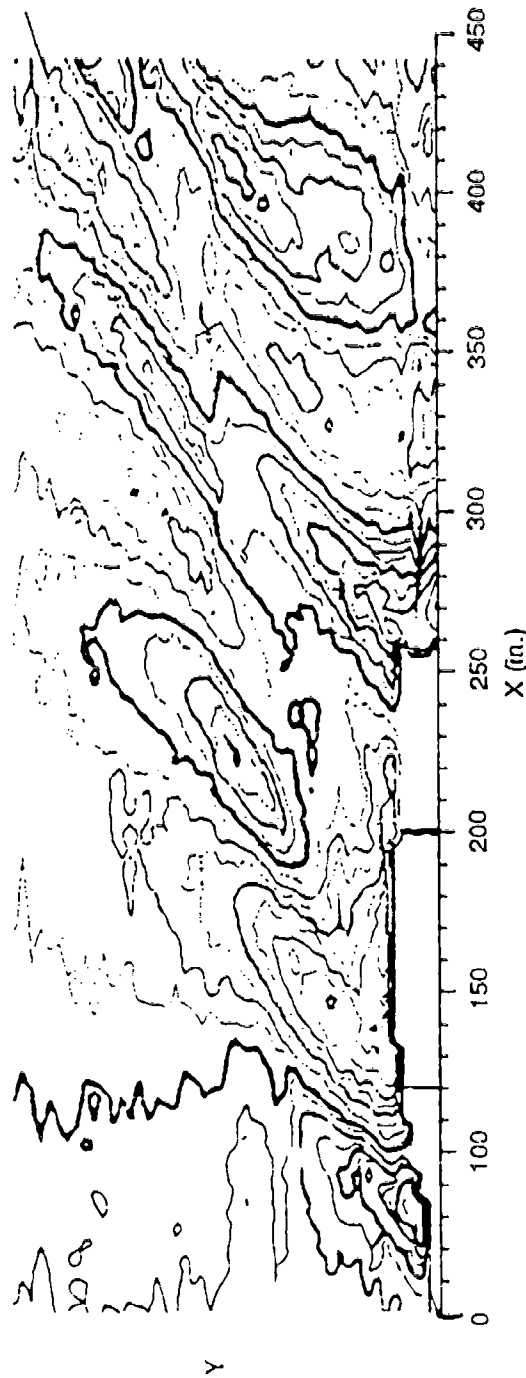


Fig. B.15. Experimental wave contours for QUAPAW at $F_r = 0.3197$.

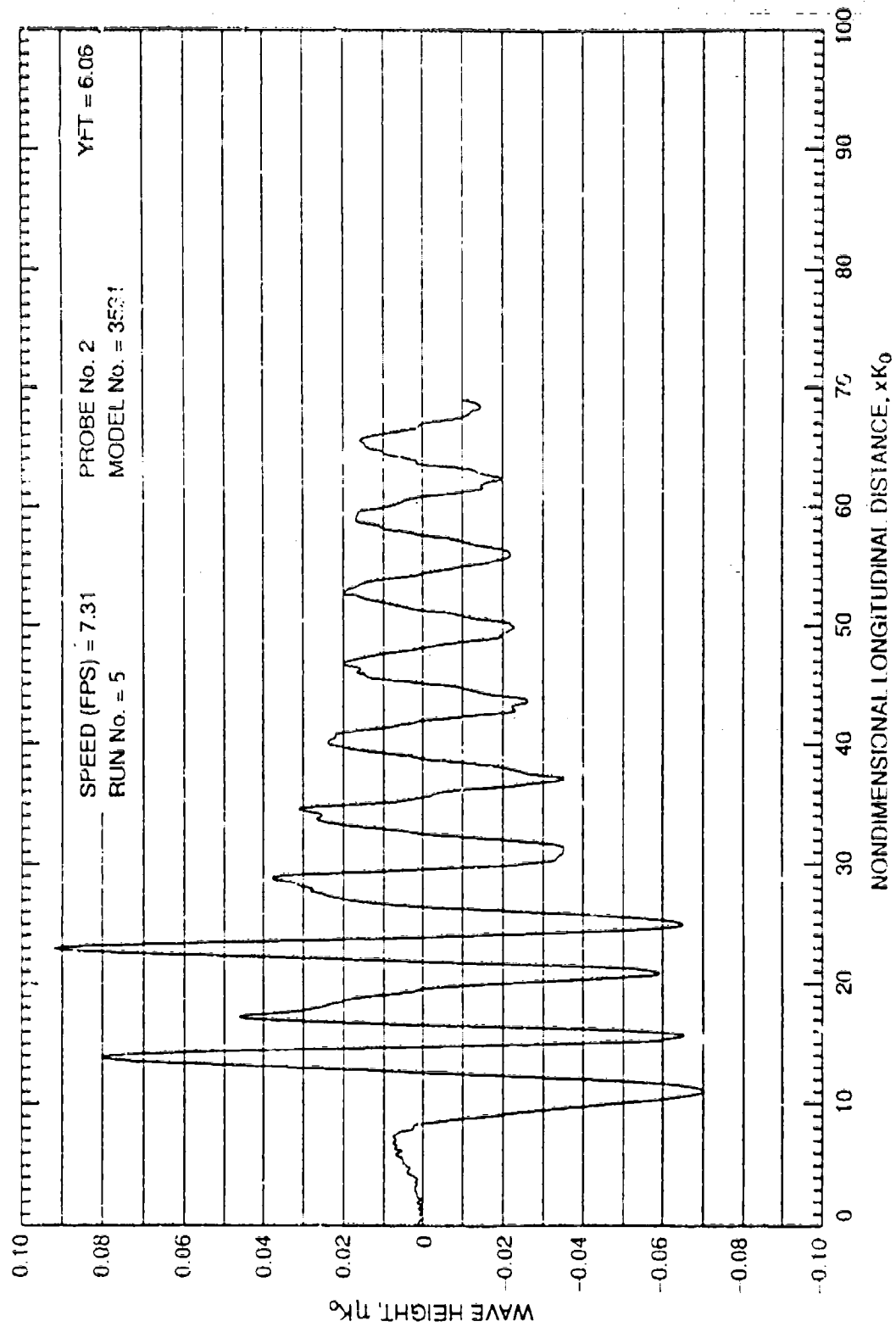


Fig. B.16. Experimental wave cut for QUAPAV at $F_n = 0.3197$.

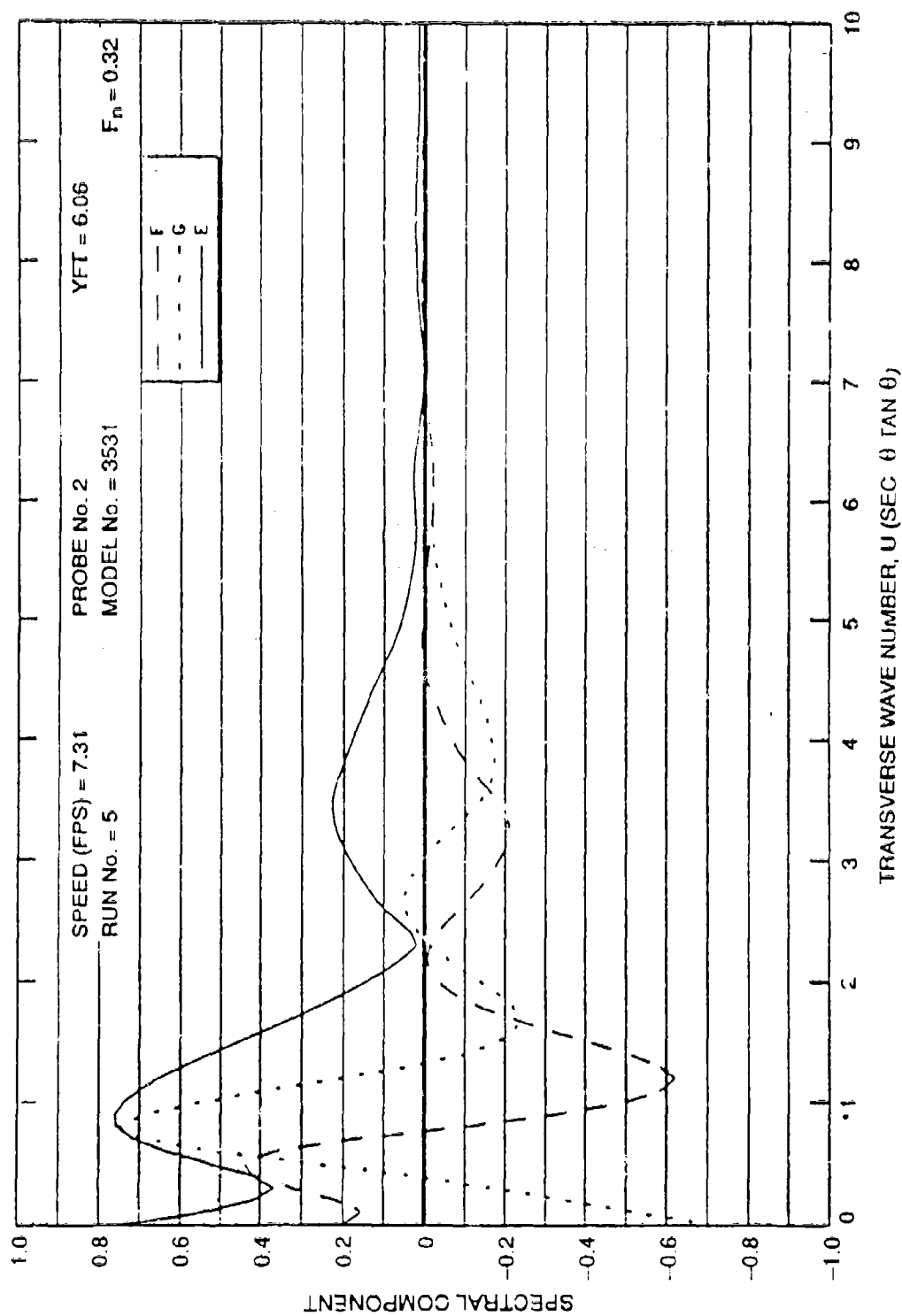


Fig. B.17. Experimental wave spectrum for QUA.PAW at $F_n = 0.3197$.

APPENDIX C
FARWAY PREDICTIONS

FARWAY PREDICTIONS

WAKE-OFF QUESTIONNAIRE

COMPUTATIONAL CODE

Name of Code? We have Two Codes, Named EPPAC1 and FARWAV.

EPPAC1 provides an approximate solution, defined explicitly in terms of the hull shape and the value of the Froude number, to the Neumann-Kelvin problem. This code predicts the flow, both on the mean wetted hull surface and at any prescribed points (including points in the far field) outside the ship, according to the so-called first-order slender-ship approximation presented by Noblesse in the Journal of Ship Research, Vol. 27, pp. 13-33 (1983). EPPAC1 can either be used alone (as was the case for the calculations we performed for the DDG51 and QUAPAW models), or it can be coupled with (more precisely: its predictions can be used as input to) the code FARWAV.

FARWAV computes the wave potential, at any prescribed point behind the ship stern, given the value of the Froude number, the hull shape and the value of the velocity potential on the mean-wetted hull surface. If the disturbance velocity potential is set equal to zero, the wave potential predicted by FARWAV is identical to that predicted by EPPAC1. FARWAV is based on the Neumann-Kelvin theoretical framework. This code can be coupled with ANY code, not just EPPAC1, that predicts the potential on the mean-wetted hull surface.

How Many Lines of Coding? How Many Subroutines?

EPPAC1 and FARWAV each consist of 35 subroutines totaling nearly 14,000 lines, a significant portion of which are comments. Of these 35 subroutines only 18, totaling 9,722 lines are actually responsible for the calculations. The remaining 17 subroutines of 4,275 lines are nearly evenly divided between pre-processing and post-processing. The pre-processing routines manipulate the information about the hull into the format required by EPPAC1. The post-processing routines combine the individual components of the potential and output them in a format ready for plotting.

Limitations on the Number of Panels which Can be Used?

Dimensions for the hull panels are currently set at 150 x 21, but these can be modified at will as there are NO limitations on the number of panels which can be used in these two codes. The current dimensions appear to be sufficient for most applications, based on the convergence tests we have performed.

Program Documentation?

The theory underlying the codes has been published. We are currently in the process of completing some detailed numerical studies designed to refine and finalize several numerical aspects of the codes. Most of these numerical studies will be completed in the very near future. We then intend to prepare a series of DTRC reports presenting a detailed account of the numerical aspects of the codes (e.g., methods used for evaluating the Green function and for integrating it over a panel) and comparisons of numerical results and experimental data. We expect that most of this work can be performed in 1988, although some particular points will still require further work; and that will be presented

when completed. We also expect that this detailed documentation of the numerical aspects of the codes can ultimately be published, at a Conference or in the Journal of Ship Research.

User Manual?

No user manual exists at this time, and we do not envision preparing one in the near future. The reason is that a number of modifications and refinements can and must be done. We therefore believe it would be most appropriate to complete the previously mentioned numerical studies and documentation reports first, and then to modify the codes in accordance with the results of the aforementioned studies and with the experience of using the codes, and finally to prepare a user's manual.

Hardware?

The codes have been run on APOLLO and MICROVAX micro-computers. They could presumably be run with very little modification on any virtual memory computer. Use on a computer with limited memory would require writing some variables to scratch files.

Wave Resistance?

The wave resistance coefficient can readily be evaluated in both EPPAC1 and FARWAV since these codes compute the wave amplitude function (also known as wave spectrum or Kochin function). A comparison between the wave resistance coefficients predicted by EPPAC1 and FARWAV and available experimental data for the Wigley hull held in fixed position (no sinkage or trim permitted) is attached to this questionnaire. The dashed line corresponds to the zeroth-order approximation to the wave-resistance, which is predicted by EPPAC1. The solid line was predicted by FARWAV, with EPPAC1 used as input, as thus corresponds to the first-order approximation. It is interesting that the amplitude of the humps and hollows in the resistance curve are considerably attenuated in the first approximation, in comparison to the zeroth approximation.

Lift, Nonlinearities, Propulsor Actuator Disk?

The codes include neither lift nor nonlinearities. Flow past lifting surfaces can of course be modeled with the Neumann-Kelvin theoretical framework, by including normal-dipole sheets and using the Kutta condition. This extension would entail substantial modifications of the codes, however.

Nonlinearities could be included in FARWAV, not in EPPAC1. The nonlinear terms in the free-surface boundary condition are modeled via an integral on the mean-free surface plane. The density of the free-surface source distribution representing the nonlinear effects could be evaluated by using EPPAC1, or some other near-field code. This approach could probably be implemented relatively easily, and would represent a fairly simple extension of the existing codes. However, extensive testing would probably be required to ascertain the accuracy of the calculations.

Provision for a propulsor/actuator disk could probably be included in the codes, at least in some approximate manner, by including a normal-dipole sheet.

Streamlines?

Streamlines are not calculated in the current version of EPPAC1. These calculations could however be included since $\nabla\phi$ can be evaluated everywhere.

Radiation Condition?

The radiation condition is satisfied automatically and exactly in these codes by means of the Green function, which only permits waves behind the singularity.

Transom-Stern Type Hull?

The codes can be used for transom-stern type hulls, by assuming the hull is extended smoothly into a closed wake, and by treating the transom-stern hull and its wake as a (modified) closed hull. To be sure, this approach is merely approximate and indeed probably fairly crude. A more refined potential-flow model for treating transom-stern ships should be formulated. We suspect that this would lead to modifications that might be included into FARWAV fairly easily.

Experience Required for Using the Code? User Friendliness?

The codes are pretty straightforward and could probably be used by any engineer with fairly little training. Nevertheless, the required input data could be simplified by modifying the codes somewhat. We would like to perform these modifications at some later time.

KELVIN WAKE COMPUTATIONS

Computer?

The reported calculations for the DDG51 and the QUAPAW models were performed on an APOLLO microcomputer, by using the code EPPAC1. The code FARWAV was not used for these calculations, because we were quite pressed to meet the deadline and had not had any time for validating FARWAV. Both EPPAC1 and FARWAV have since been run on a MICROVAX computer for another hull form (a Series 60 hull).

Computing Time?

The computing time used for computing the velocity potential on the hull surface and at the free surface with EPPAC1 on an APOLLO workstation was approximately 1 hour per Froude number. However, we regard this computing time as very excessive, and we have now devised improvements in several basic aspects of the code which we expect will reduce the computing time very significantly by a factor of four or better. Significant further improvements can still be made. We believe that we can have EPPAC1 and FARWAV run interactively on a microcomputer.

Input Data Preparation?

The codes require that the hull be approximated by means of a set of triangular panels, which is a fairly routine (although not trivial) task.

Convergence?

Checks for convergence were NOT directly performed for the DDG51 and the QUAPAW models, because of limited time. However, checks have been performed for

the Wigley hull and a Series 60 hull. These numerical studies on the effect of panel size (and other aspects influencing the accuracy of the calculations) led to conclusions and guidelines which were used in our calculations for the DDG51 and QUAPAW models.

Panelization?

EPPAC1 requires only a relatively small number of panels; typically 30 to 70 "framelines" by 15 to 18 "waterlines," depending on the Froude number and the hull form. FARWAV requires more panels, because the velocity potential varies more rapidly than the hull form (especially at low Froude numbers). However, we recently obtained a modified mathematical expression for evaluating the wave-amplitude function (Kochin function) which requires only the tangential velocity components (not the velocity potential) on the mean wetted hull surface as input (as well as the hull shape and the Froude number, of course). This fact, together with mathematical properties of the modified expression, lead us to expect that fewer panels will be required.

The hull is approximated by means of flat triangular panels, within which the velocity potential is assumed to vary linearly (in the modified version of FARWAV based upon the modified expression for the Kochin function noted previously, linear variation will be assumed for the tangential velocity components).

Wave Resistance?

The wave resistance of the DDG51 and QUAPAW models was not computed, because it was not required. This information could readily have been obtained since the wave-spectrum function was determined.

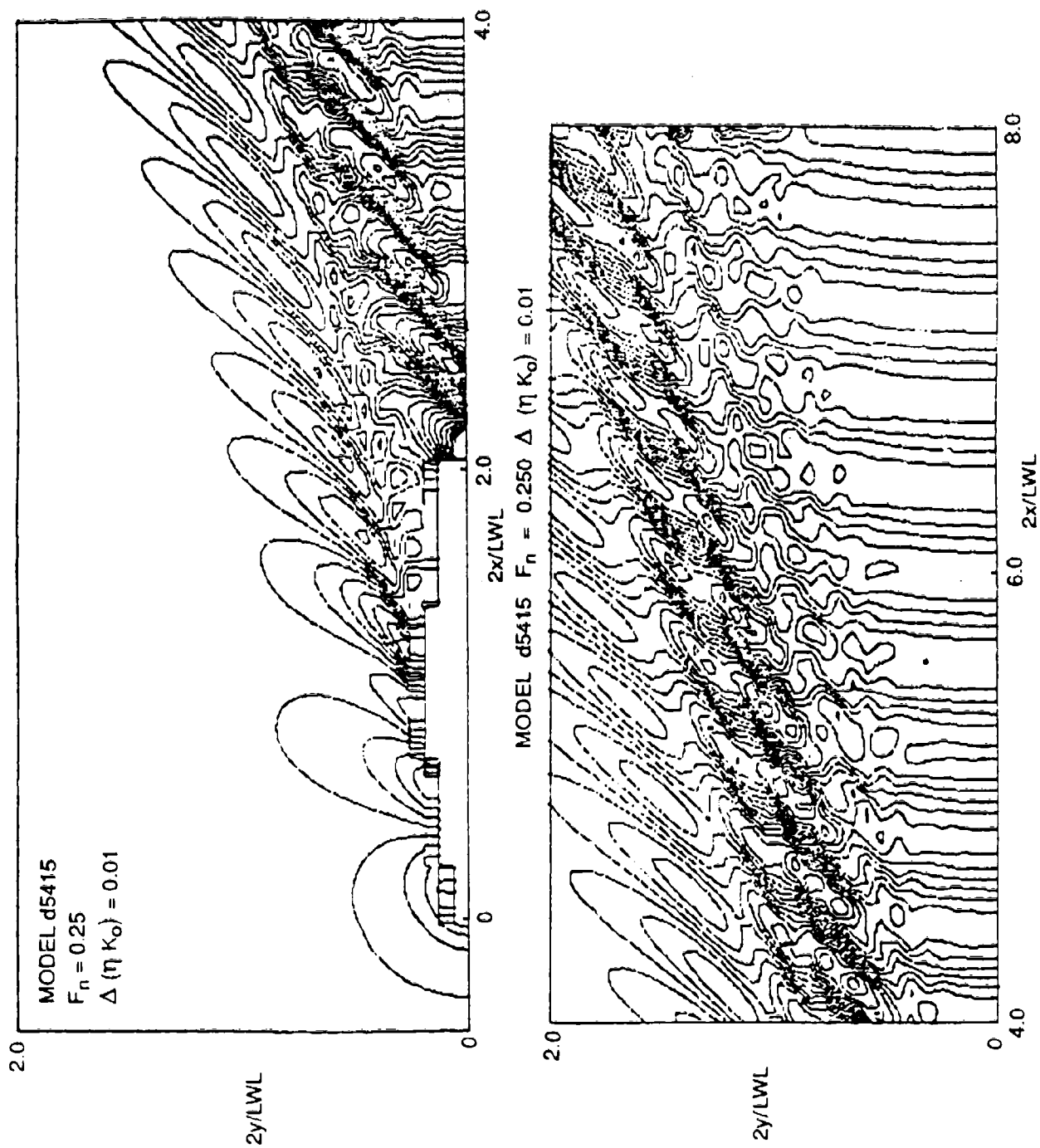


Fig. C.1. FARWAV prediction of wave contours for Model 5415 at $F_n = 0.25$.

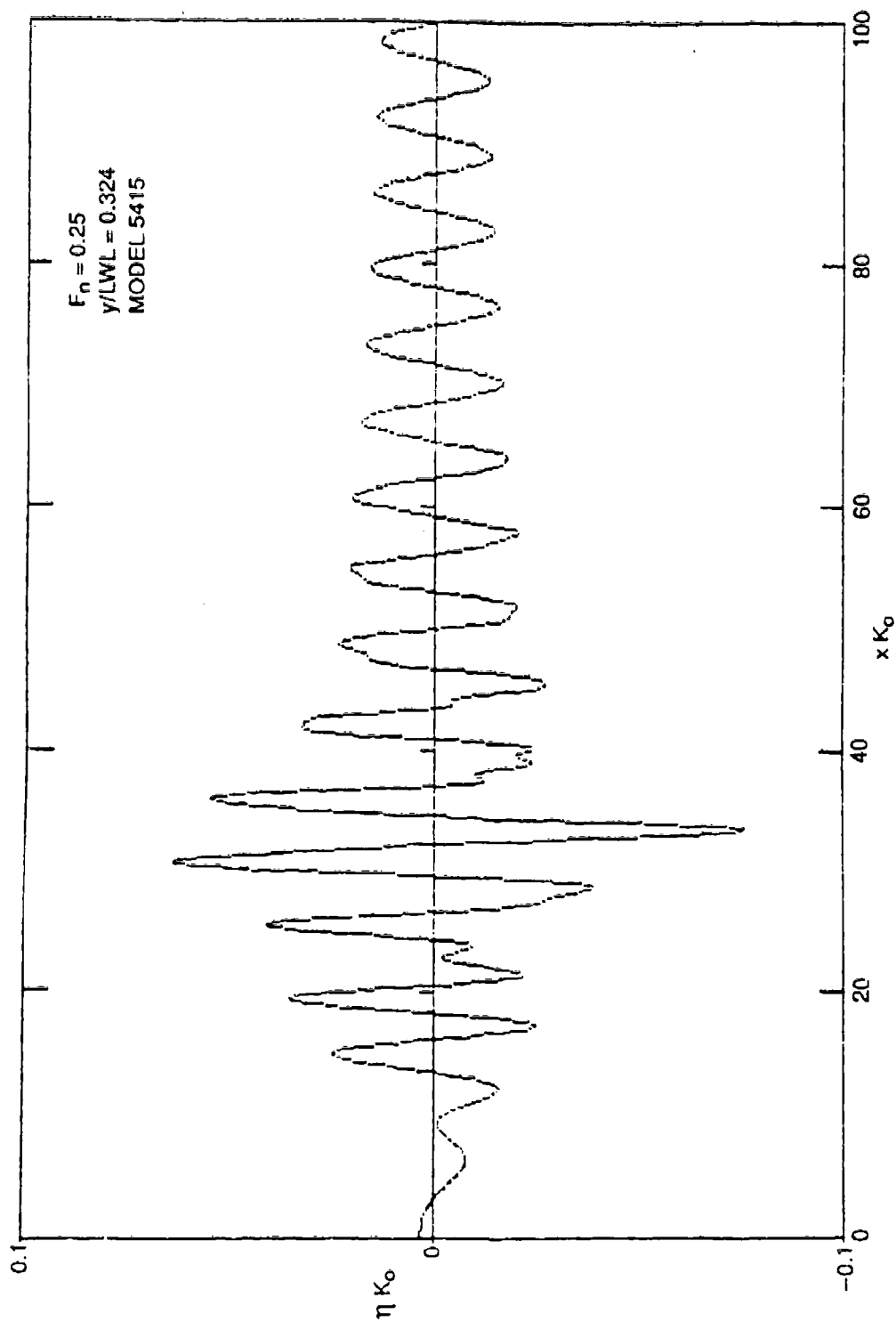


Fig. C.2. FARWAV prediction of wave cut for Model 5415 at $F_n = 0.25$.

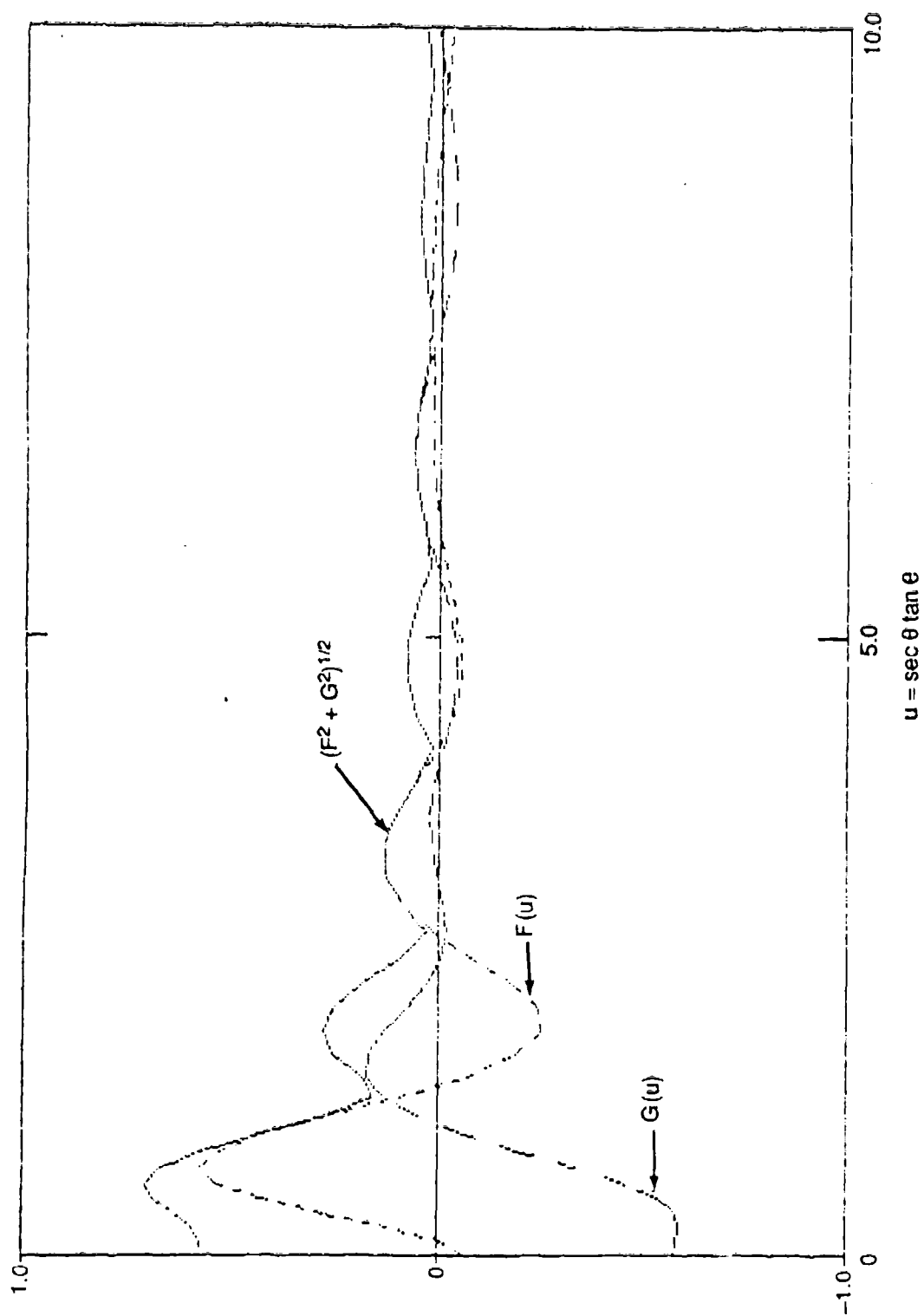


Fig. C.3. FARWAV prediction of wave spectrum for Model 5415 at $F_n = 0.25$.

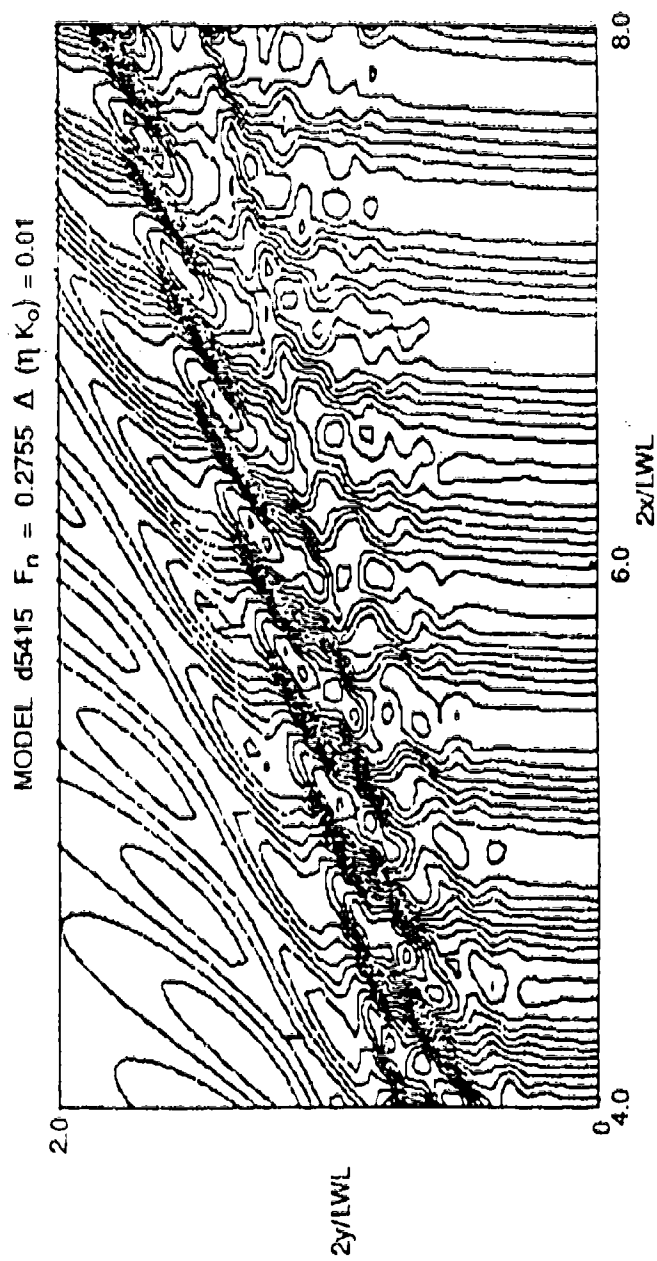
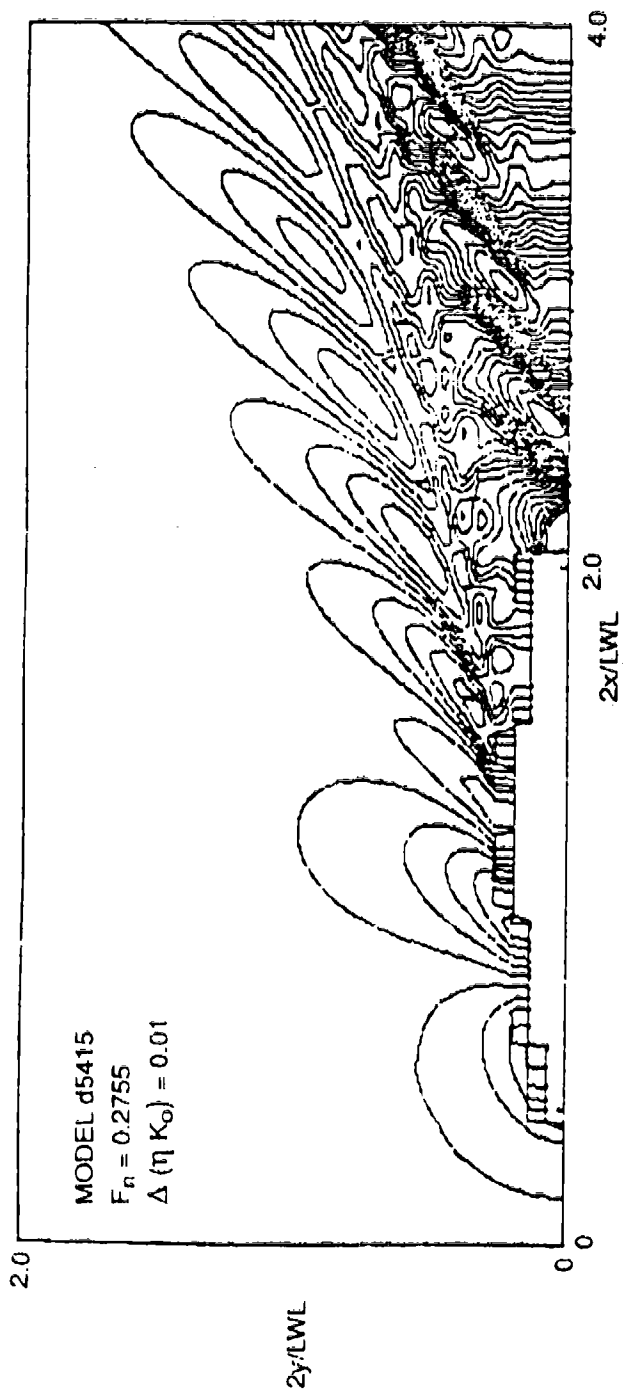


Fig. C.4. FARWAV prediction of wave contours for Model 5415 at $F_n = 0.2755$.

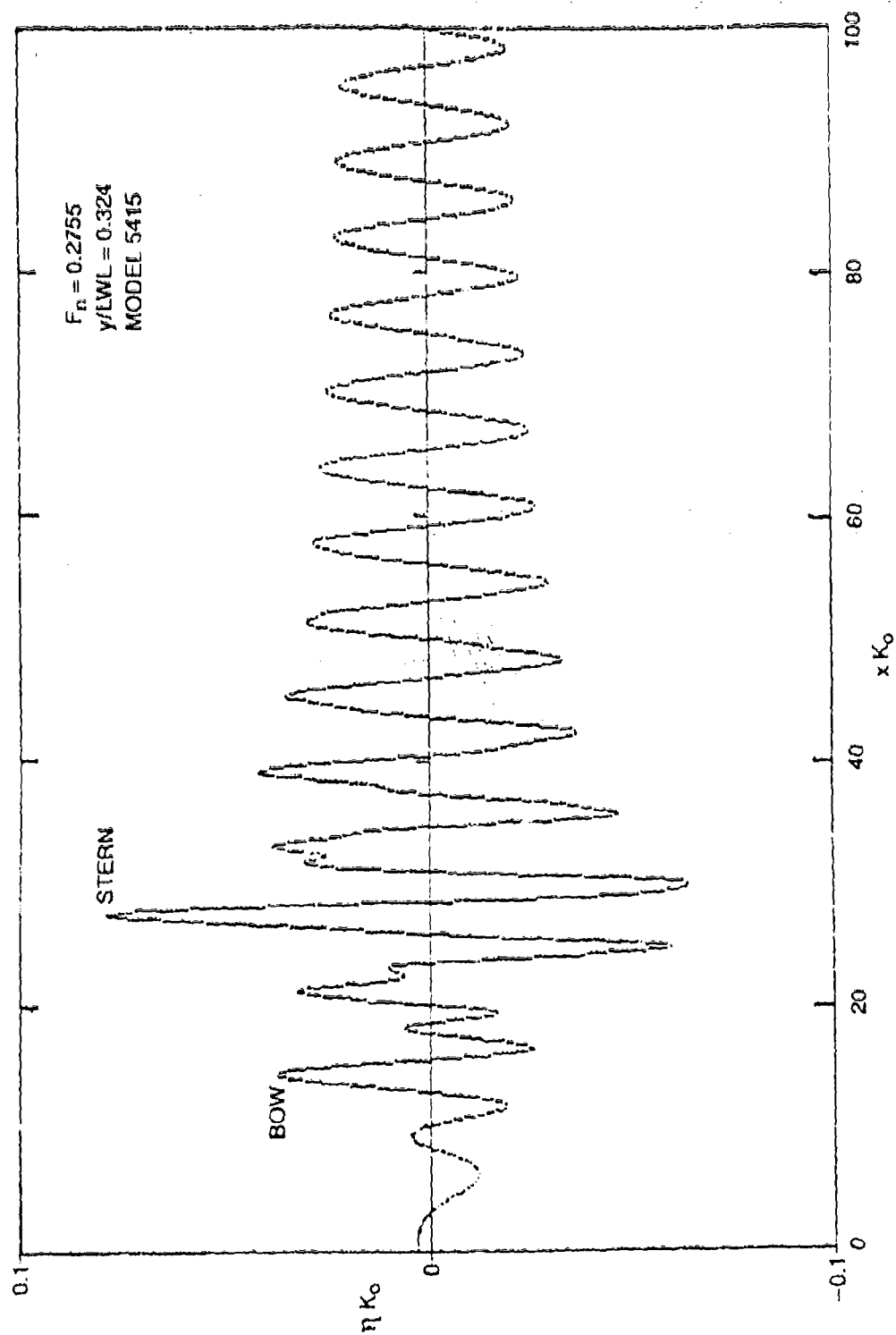


Fig. C.5. FARWAV prediction of wave cut for Model 5415 at $F_n = 0.2755$.

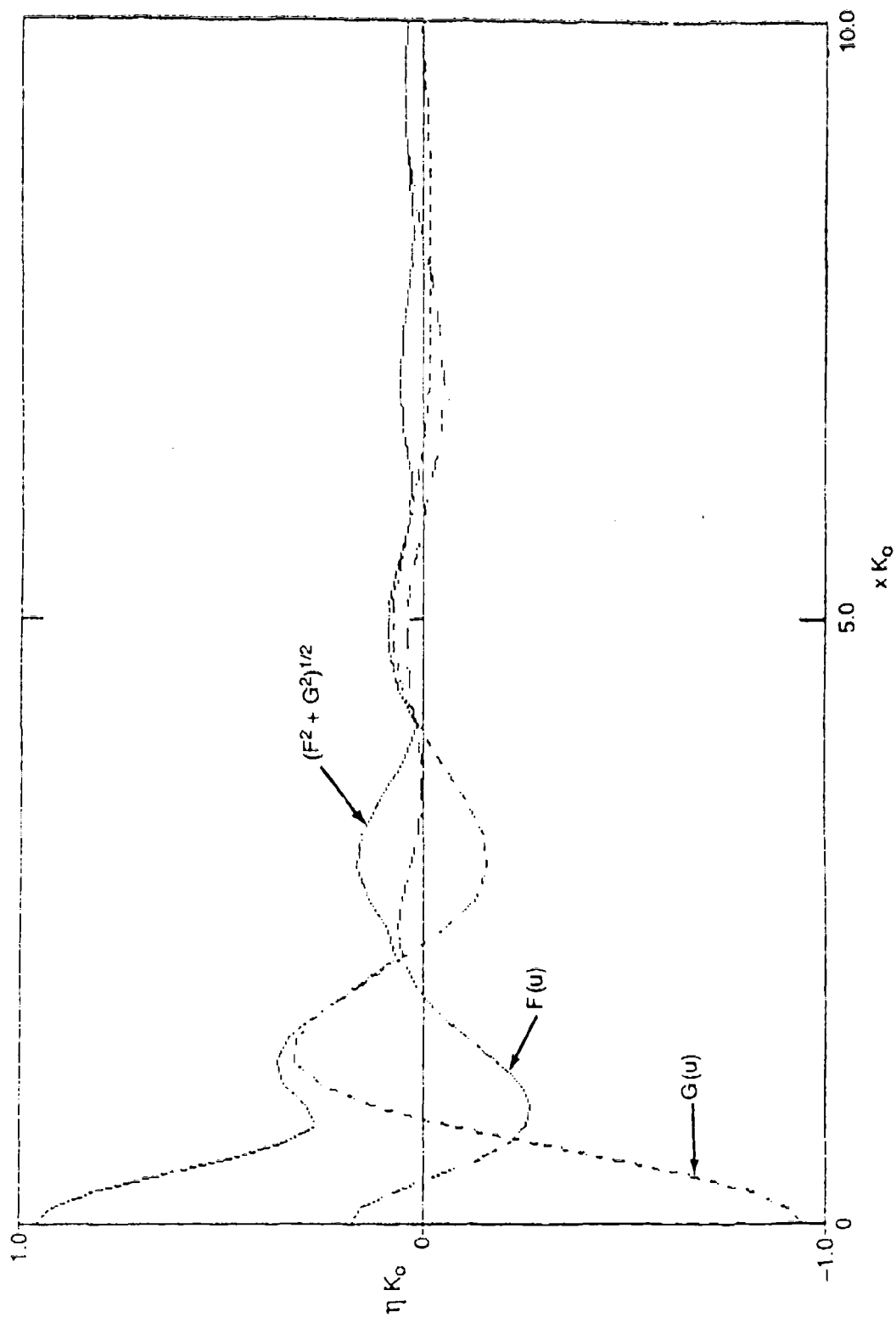
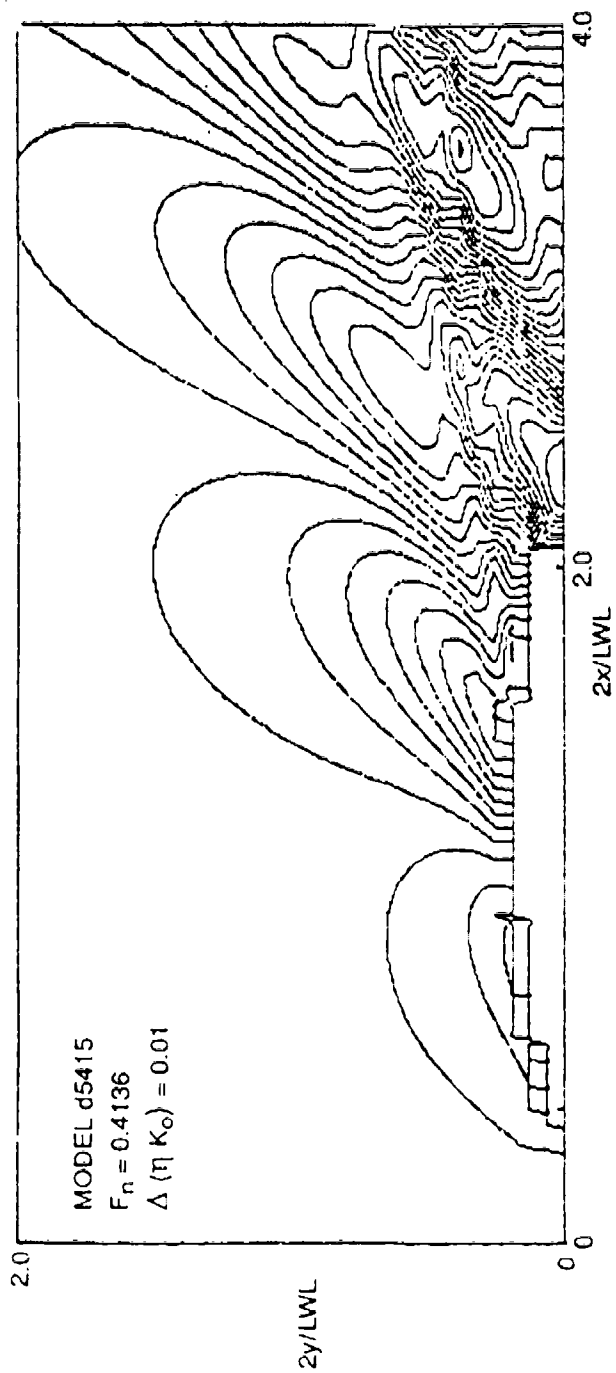


Fig. C.6. FARWAV prediction of wave spectrum for Model 5415 at $F_n = 0.2755$.



MODEL d5415 $F_n = 0.4136$ $\Delta(\eta K_o) = 0.01$

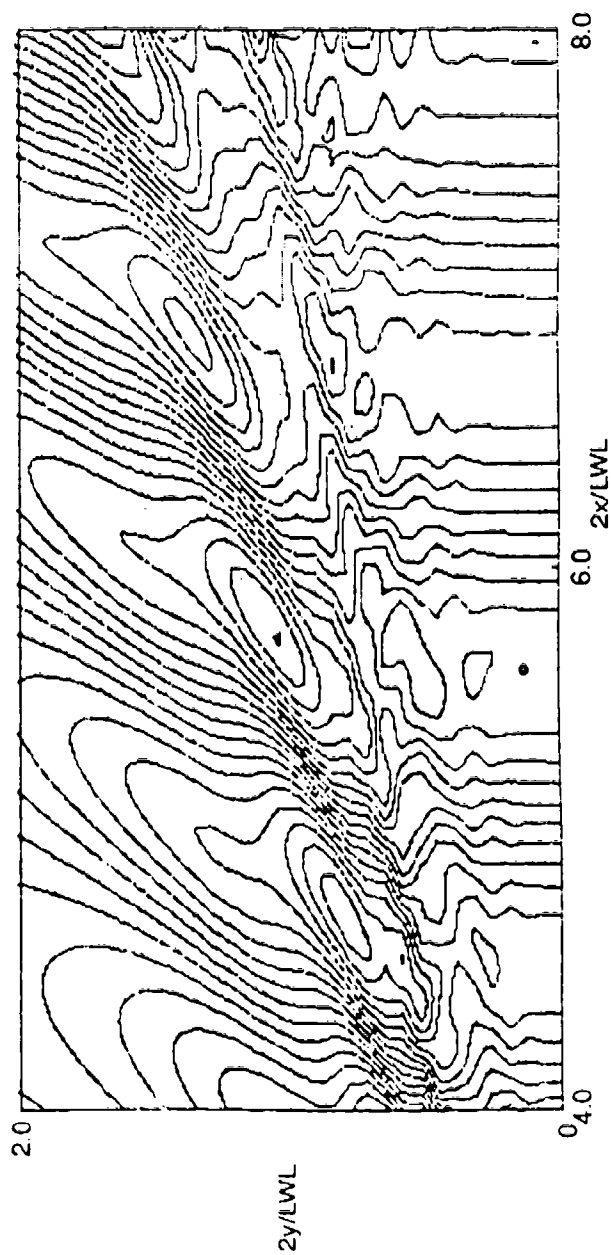


Fig. C.7. FARWAV prediction of wave contours for Model 5415 at $F_n = 0.4136$.

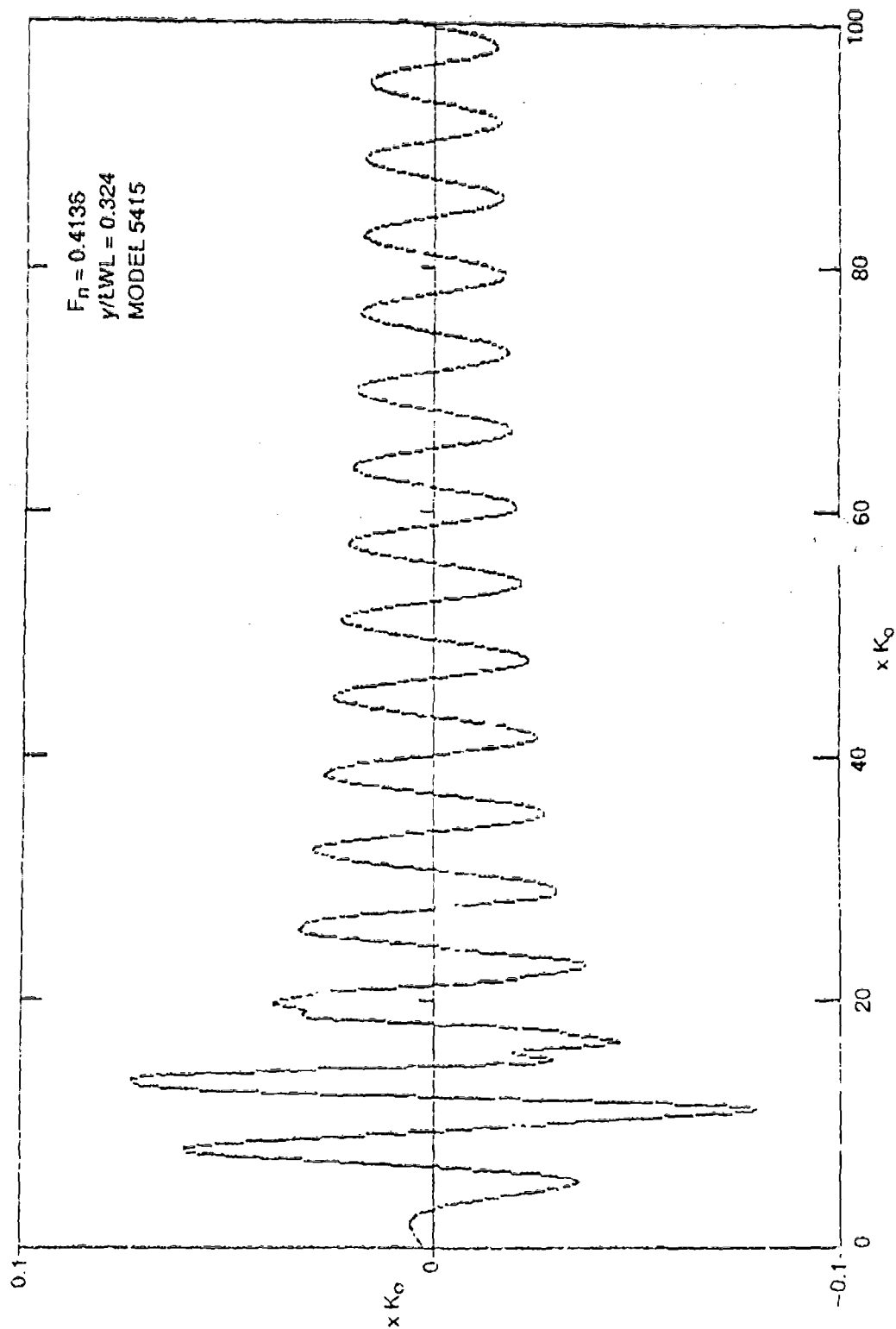


Fig. C.8. FARWAV prediction of wave cut for Model 5415 at $F_n = 0.4136$.

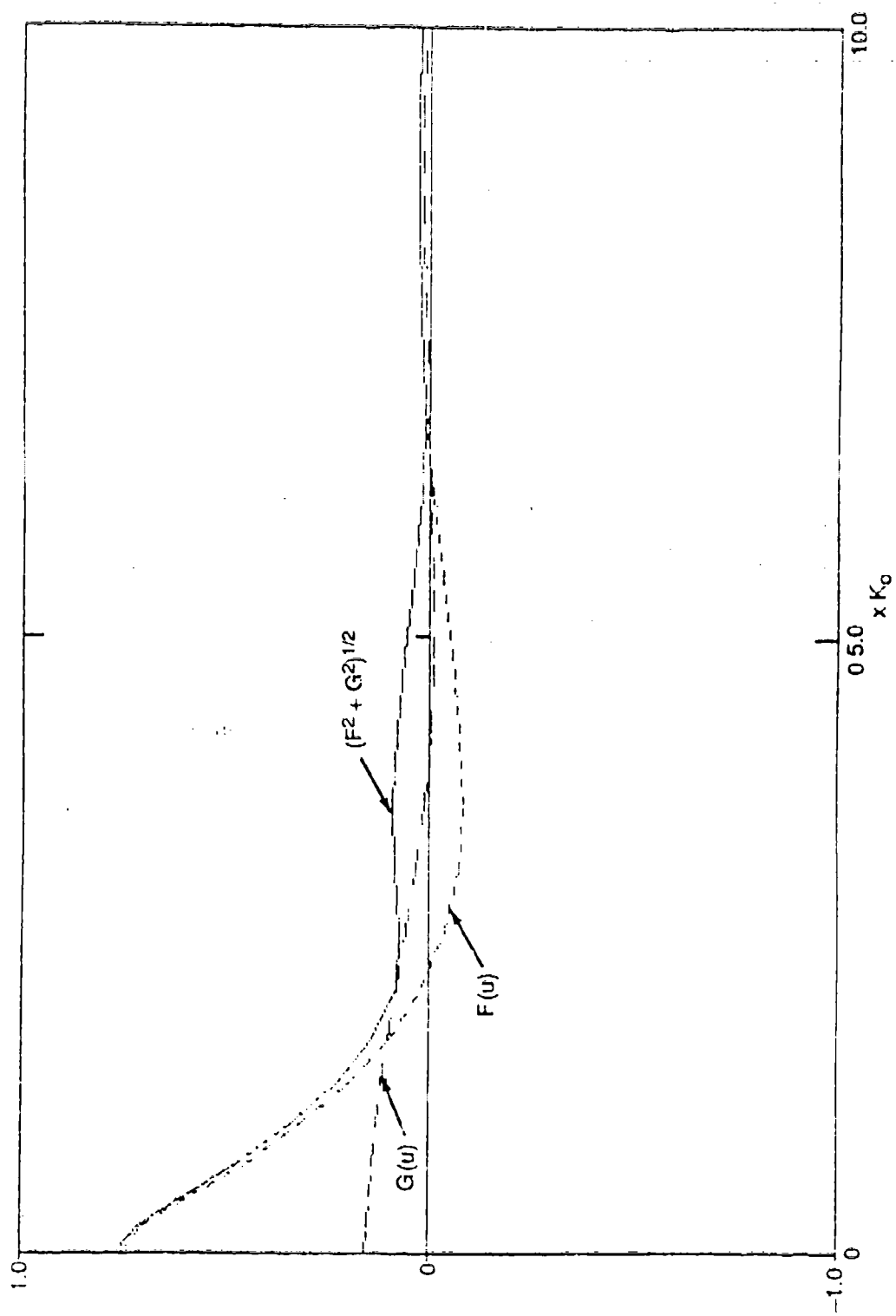


Fig. C.9. FARWAV prediction of wave spectrum for Model 5415 at $F_n = 0.4136$.

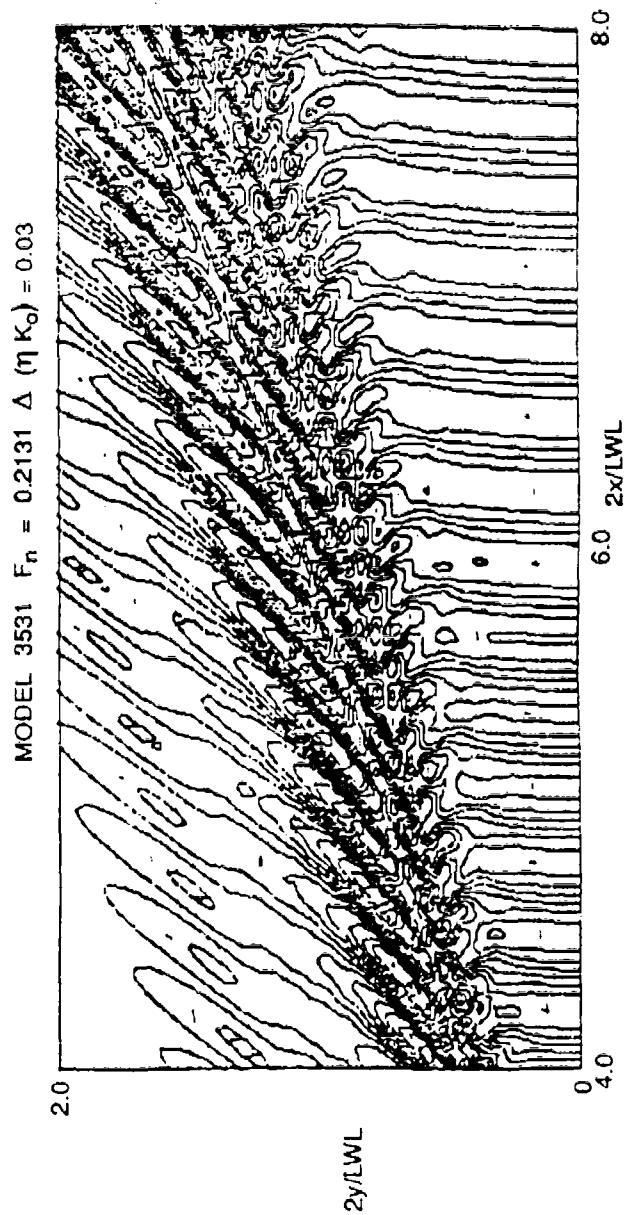
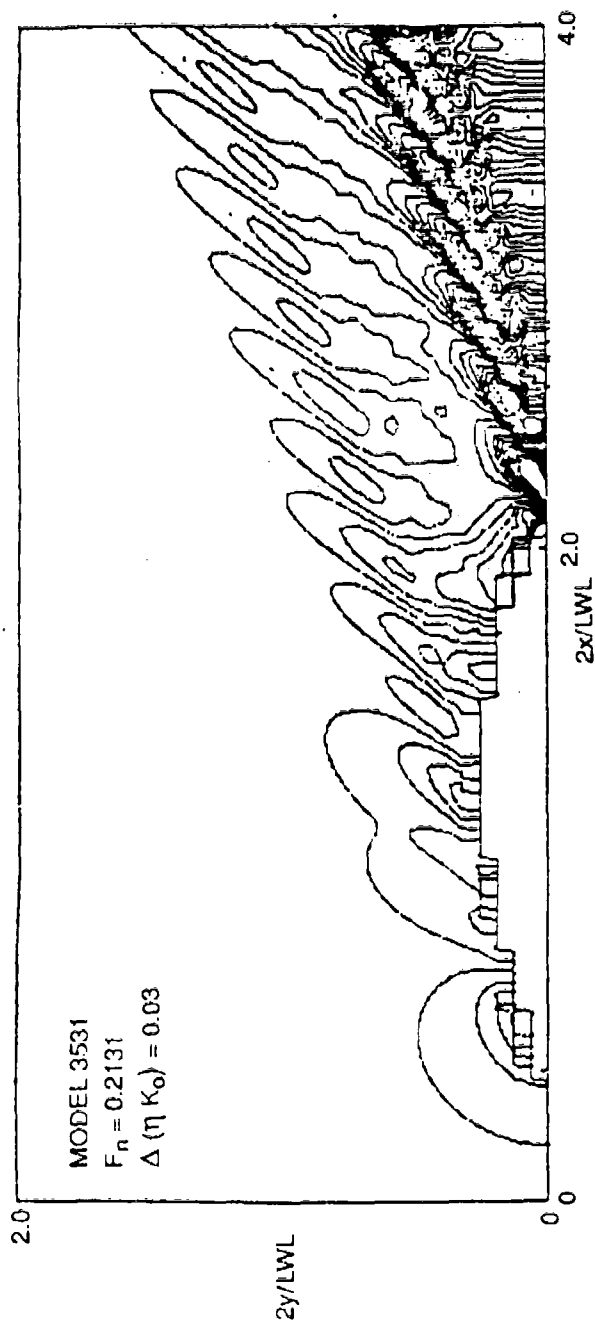


Fig. C.10. FARWAV prediction of wave contours for QUAPAW at $F_n = 0.2131$.

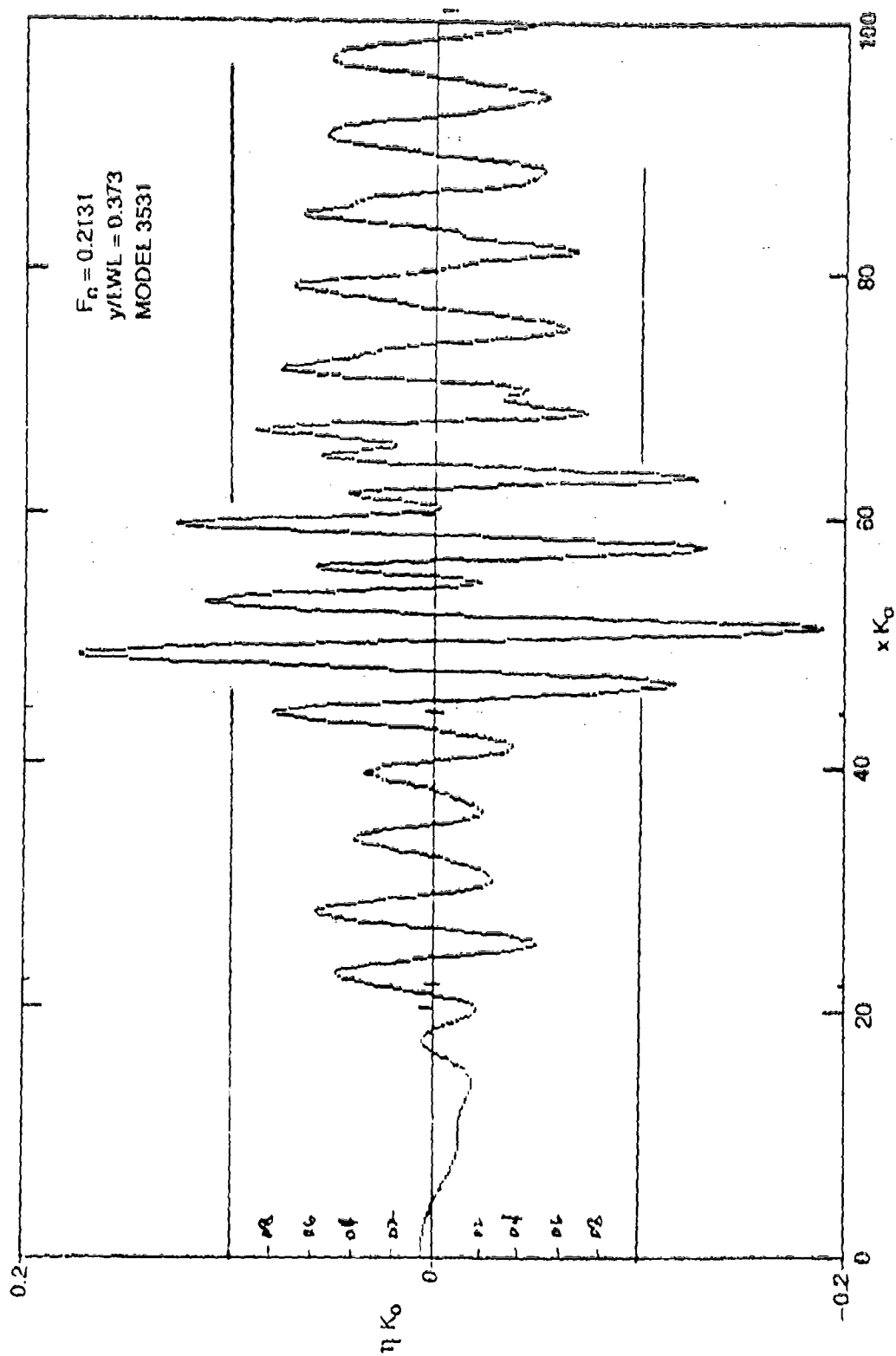


Fig. C.11. FARWAV prediction of wave cut for QUAPAW a .2131.

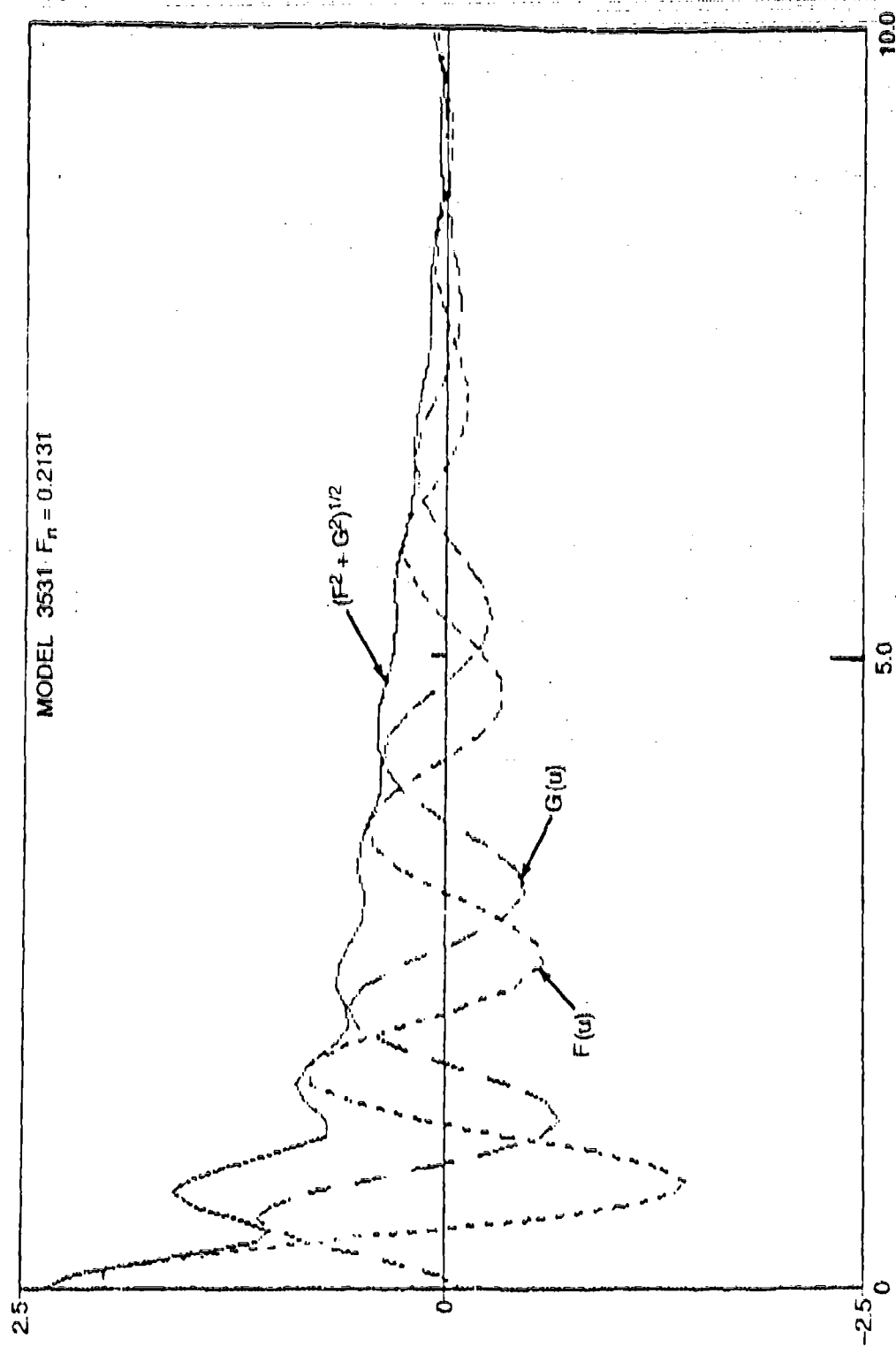


Fig. C-12. FARWAV prediction of wave spectrum for QUAPAW at $F_n = 0.2131$.

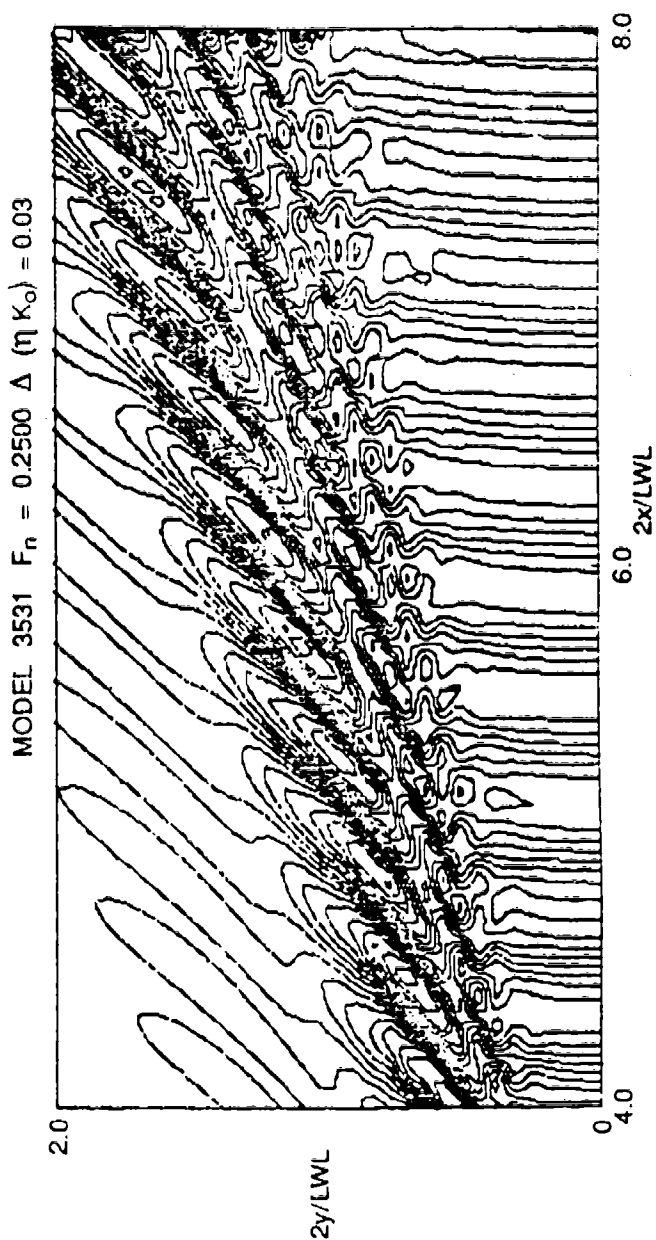
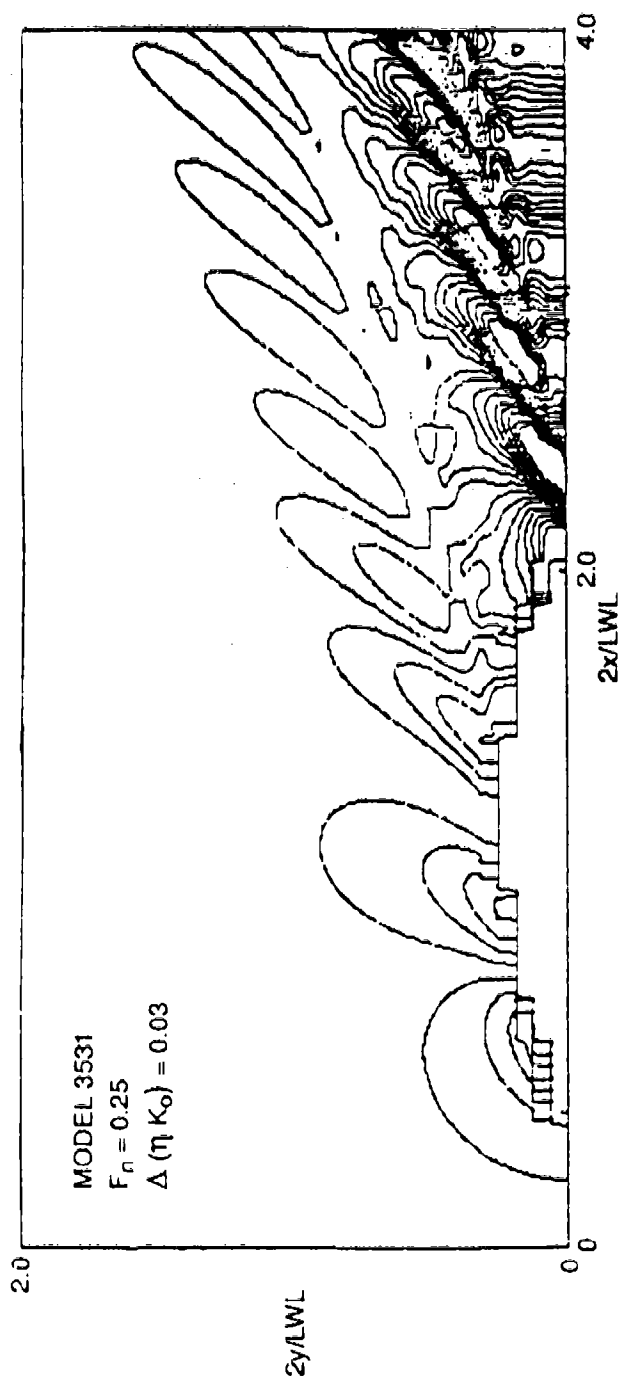


Fig. C.13. FARWAV prediction of wave contours for QUAPAW at $F_n = 0.25$.

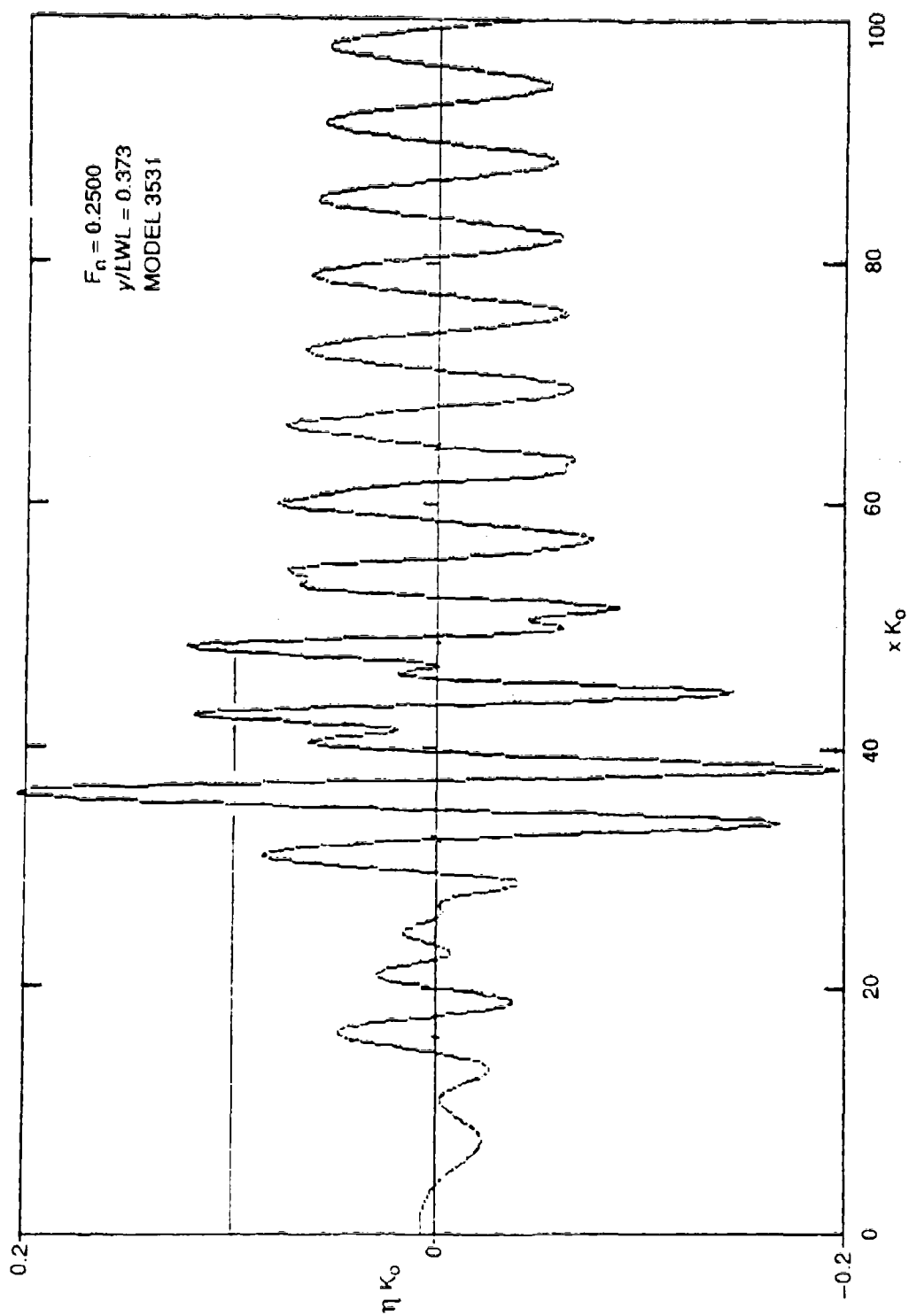


Fig. C.14. FARWAV prediction of wave cut for QUAPAW at $F_n = 0.250$.

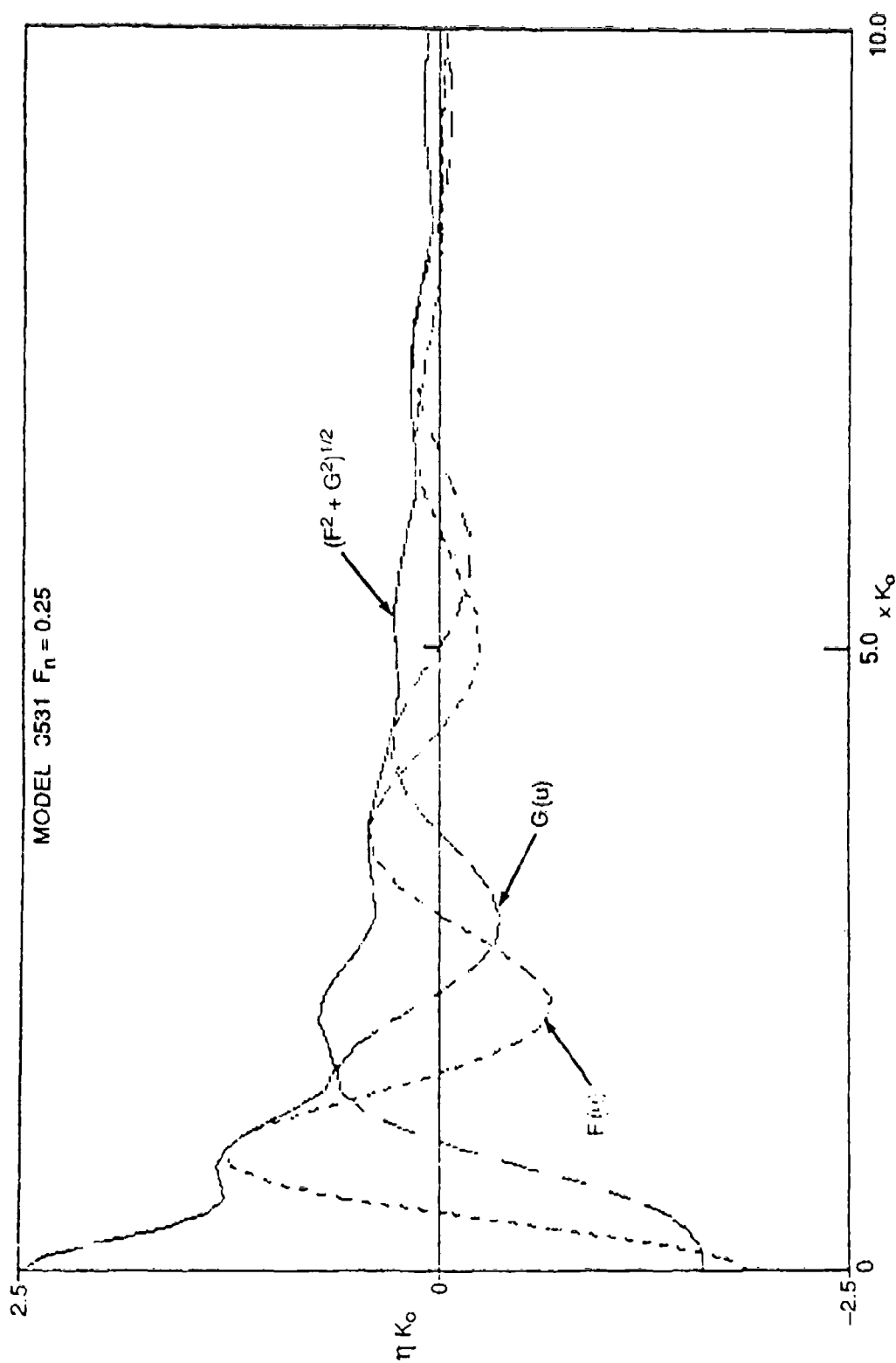


Fig. C.15. FARWAV prediction of wave spectrum for QUAPAW at $F_n = 0.25$.

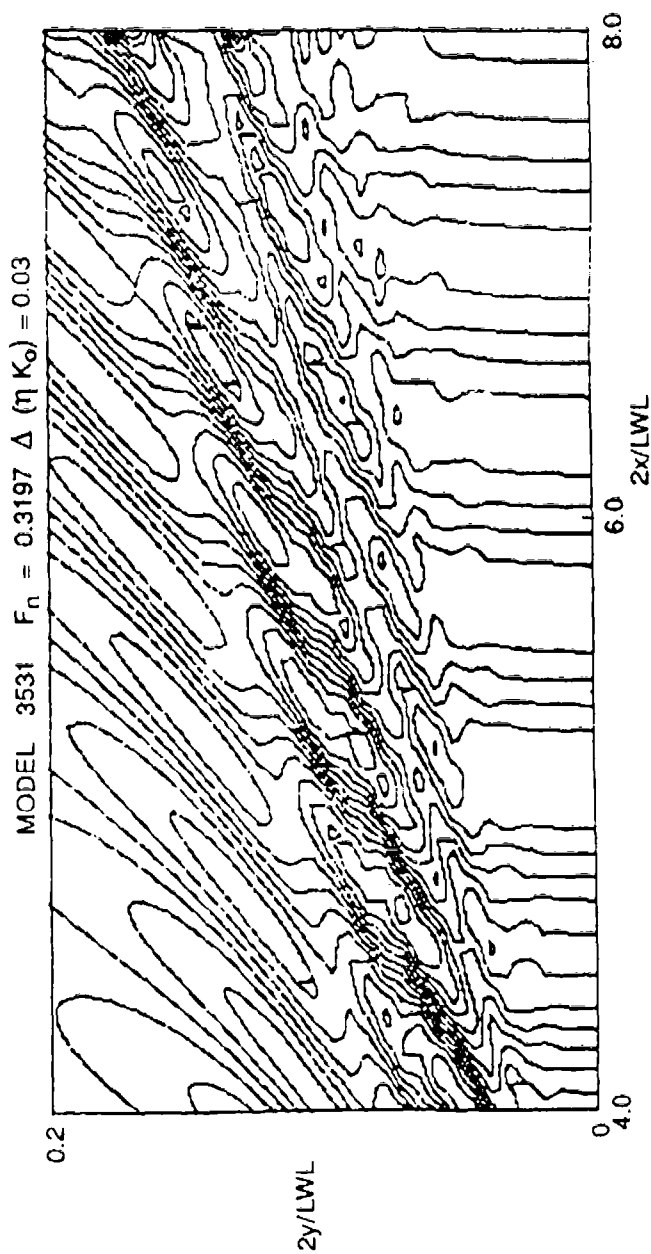
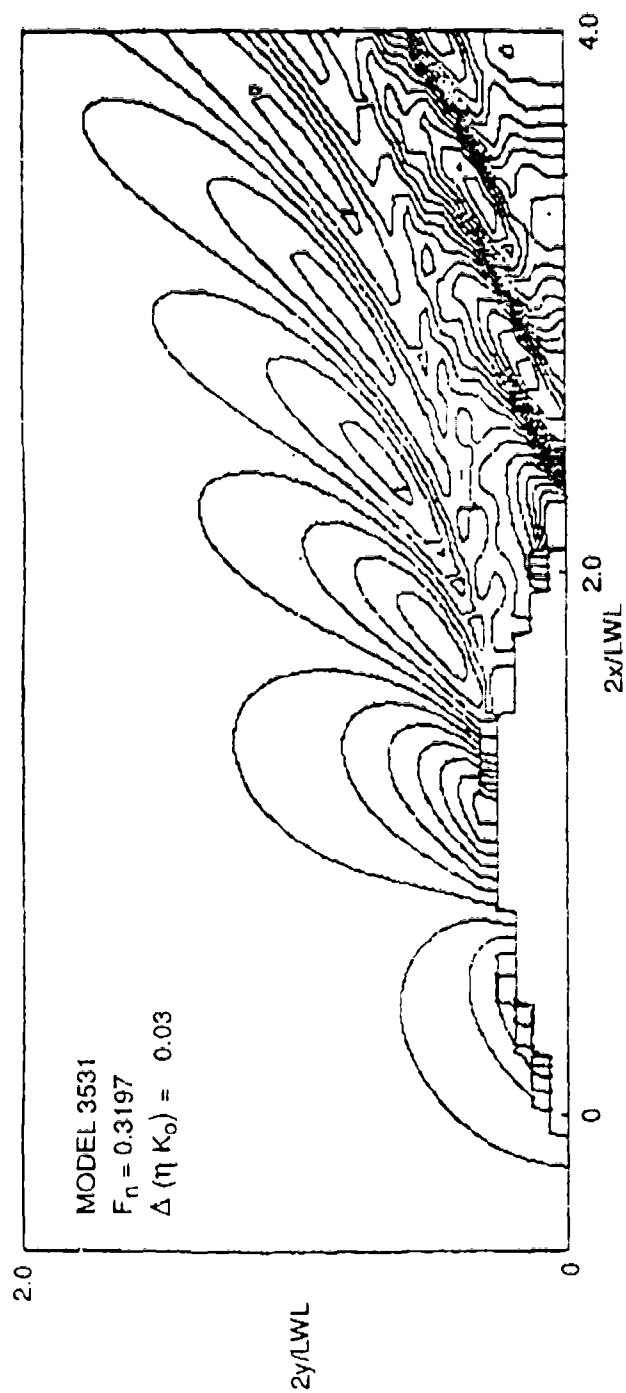


Fig. C.16. F ARWAV prediction of wave contours for QUAPAW at $F_n = 0.3197$.

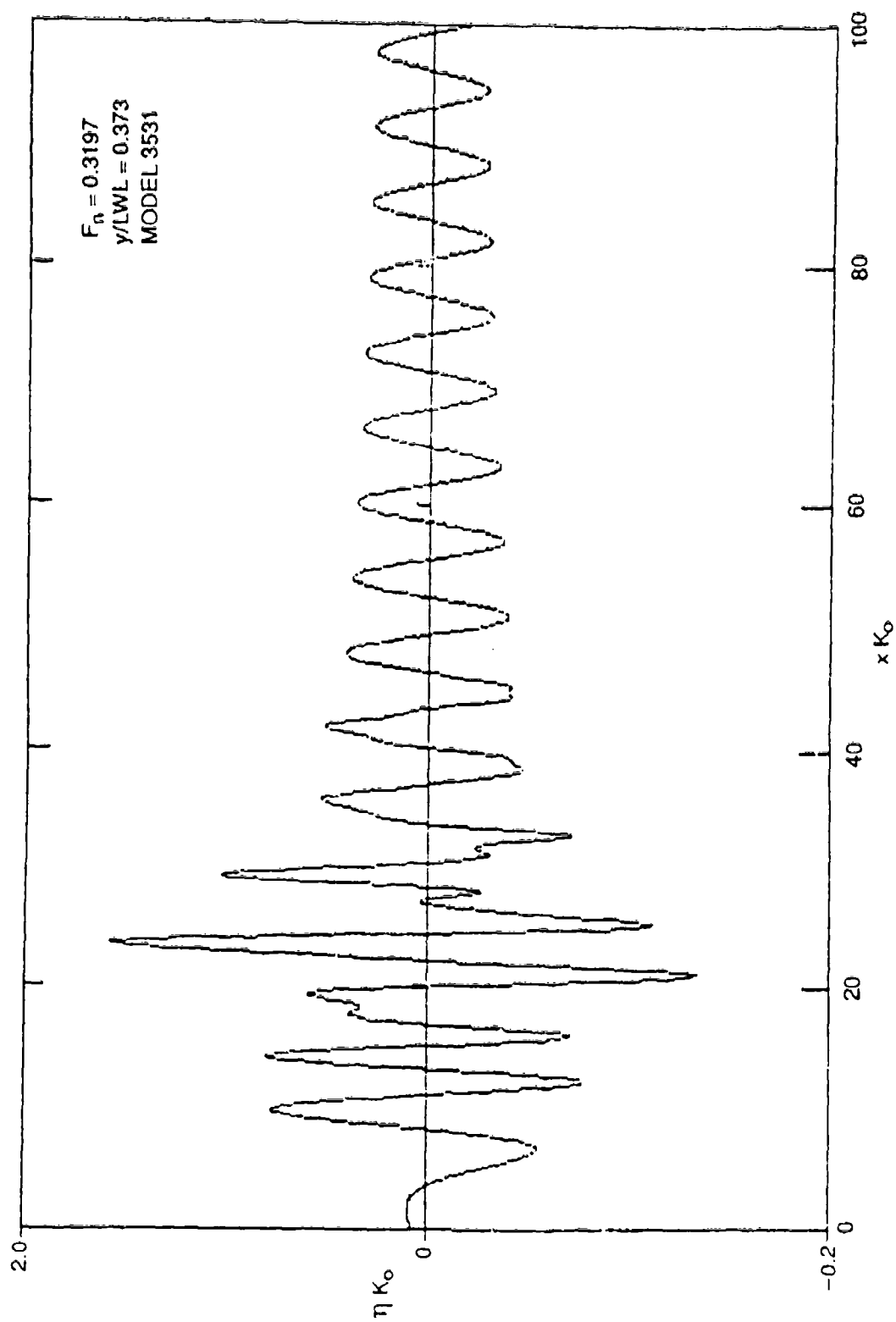


Fig. C.17. FARWAV prediction of wave cut for QUAPAW at $F_n = 0.3197$.

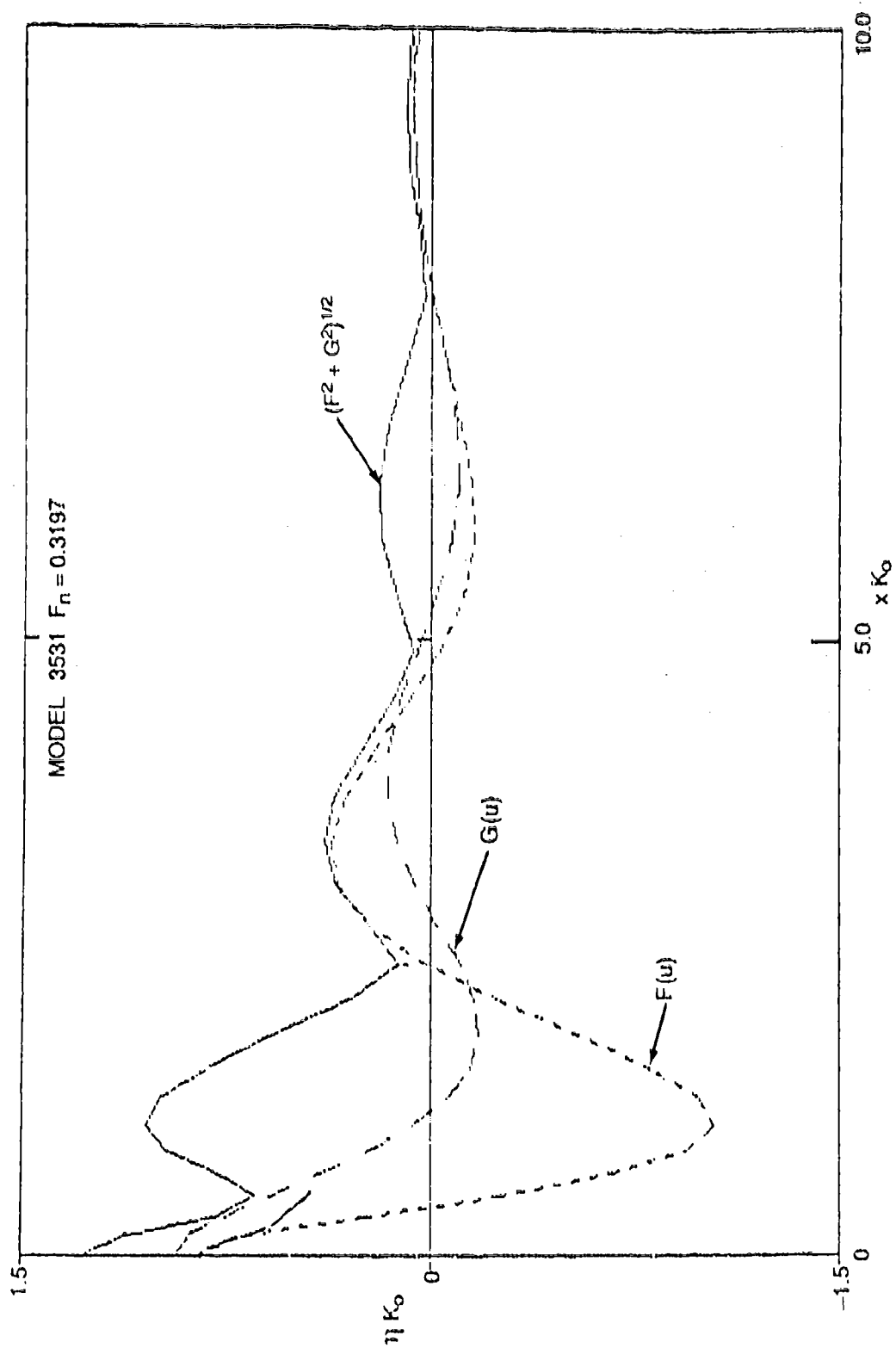
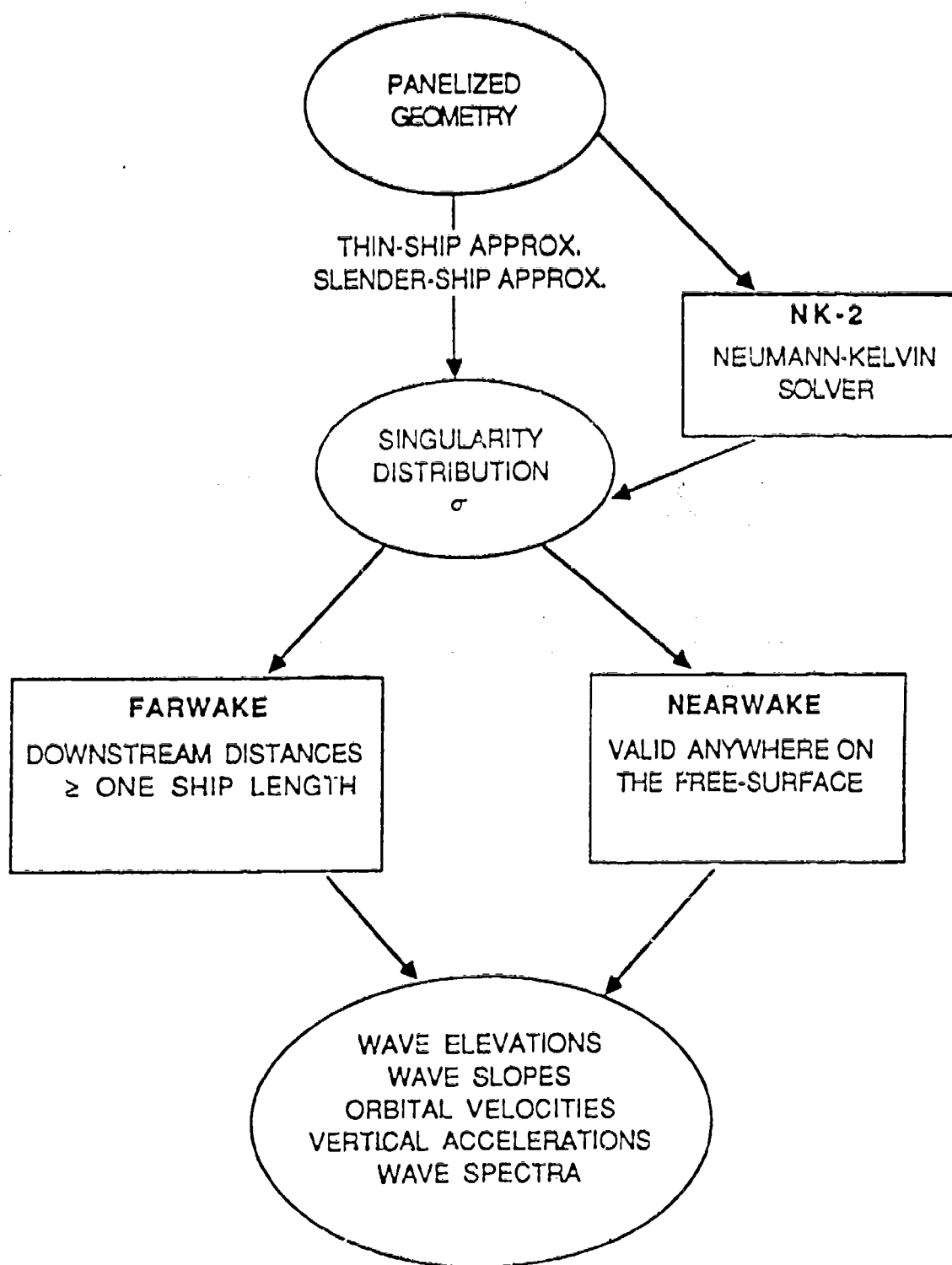


Fig. C.18. FARWAV prediction of wave spectrum for QJAPAW at $F_n = 0.3197$.

THIS PAGE INTENTIONALLY LEFT BLANK

APPENDIX D
NK-2 PREDICTIONS



COMPUTATIONAL CODES

<u>CODE NAME:</u>	<u>NK-2</u>	<u>NEAR-WAKE</u>	<u>FAR-WAKE</u>
Lines:	2350 (+ IMSL EQ. Solver)	1600	800
Subroutines:	46	23	12
Number of Panels:	Unlimited	Unlimited	Unlimited
Documentation:	Poor	Poor	Poor
User's Manual:	No	No	No
Hardware:	VAX 750 & 8650 CRAY X-MP	VAX 750 & 8650 CRAY X-MP	VAX 750 & 8650 CRAY X-MP
Cw:	No	No	Yes
Lift:	Yes	Yes	Yes
Actuator Disc:	No	No	No
Streamlines:	No	Yes	No
Facilitation Condition:	Havelock Source	Havelock Source	Havelock Source
Transom Steam:	?	?	?
Experience Level:	Moderate	High	Moderate
User Friendliness:	Moderate	Low	Moderate

KELVIN WAVE COMPUTATIONS

Code Name:	<u>NK-2</u>	<u>NEAR-WAKE</u>	<u>FAR-WAKE</u>
Machine:	VAX 8650	VAX 8650	VAX 8650

CPU Cost: \$52/hour (Night Batch Rate)

Seconds of CPU Time (Cost):

QUAPAW (432 Panels)

10.0 kts	1150 (\$17)	4200 (\$61)	100 (\$1)
11.7 kts	1200 (\$17)	1700 (\$25)	100 (\$1)
15.0 kts	1300 (\$19)	1600 (\$23)	100 (\$1)

Model 5415 (376 Panels)

18.1 kts	1300 (\$19)	4400 (\$64)	100 (\$1)
20.0 kts	1400 (\$20)	4400 (\$64)	100 (\$1)
30.0 kts	2700 (\$39)	4400 (\$64)	100 (\$1)

Input data Preparation: GEOPAN (SAIC panelization code)

Convergence: Will be discussed

Panels: Will be discussed

	<u>Fn</u>	<u>Cw</u>
QUAPAW	.213	1.37
S=9000	.250	6.40
	.320	7.92
Model 5415	.250	0.51
S=32200	.276	1.39
	.414	4.39

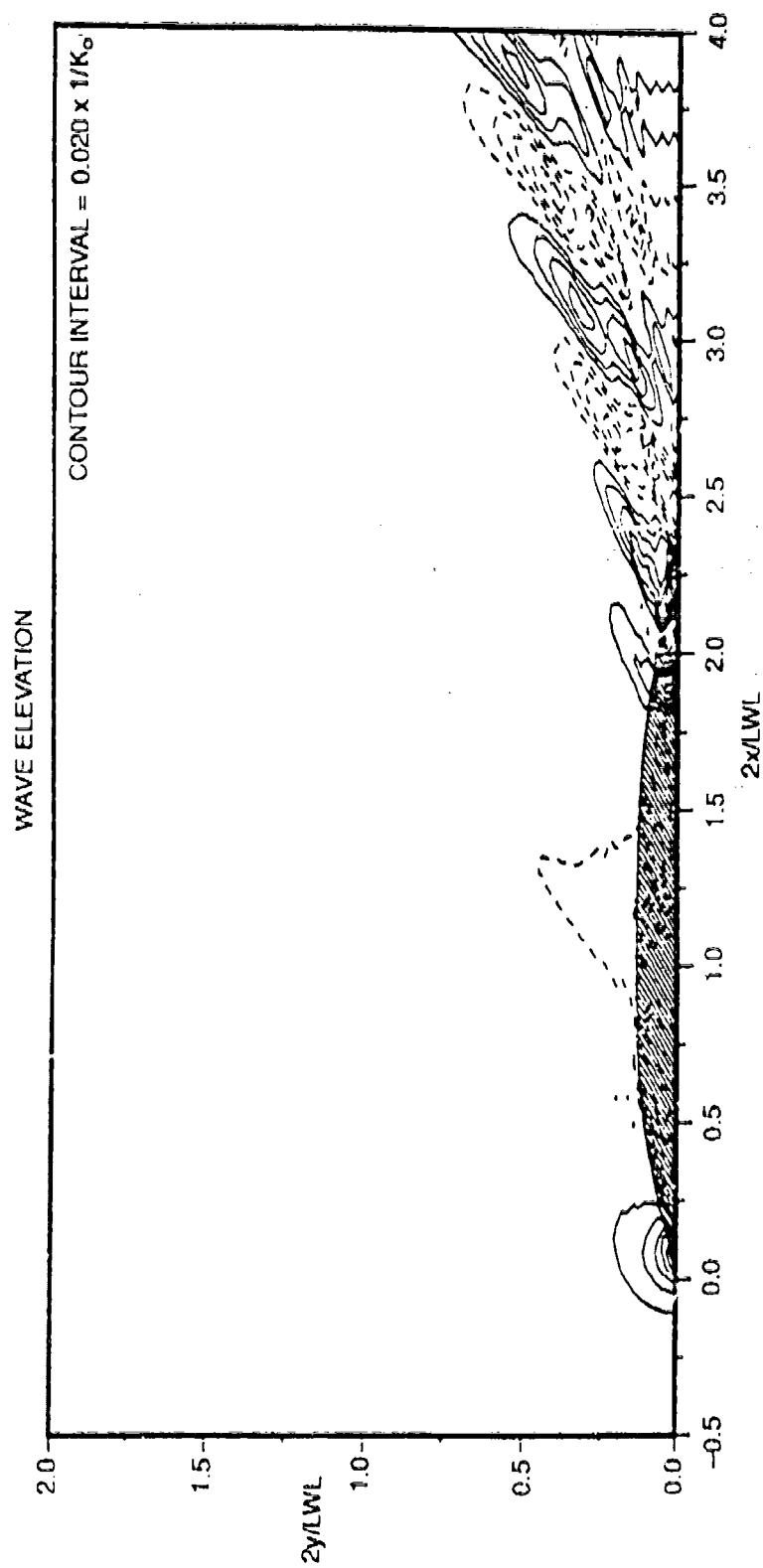


Fig. D.1. NK-2 prediction of wave contours ($-0.5 < 2x/LWL < 4$) for Model 5415 at $F_n = 0.25$.

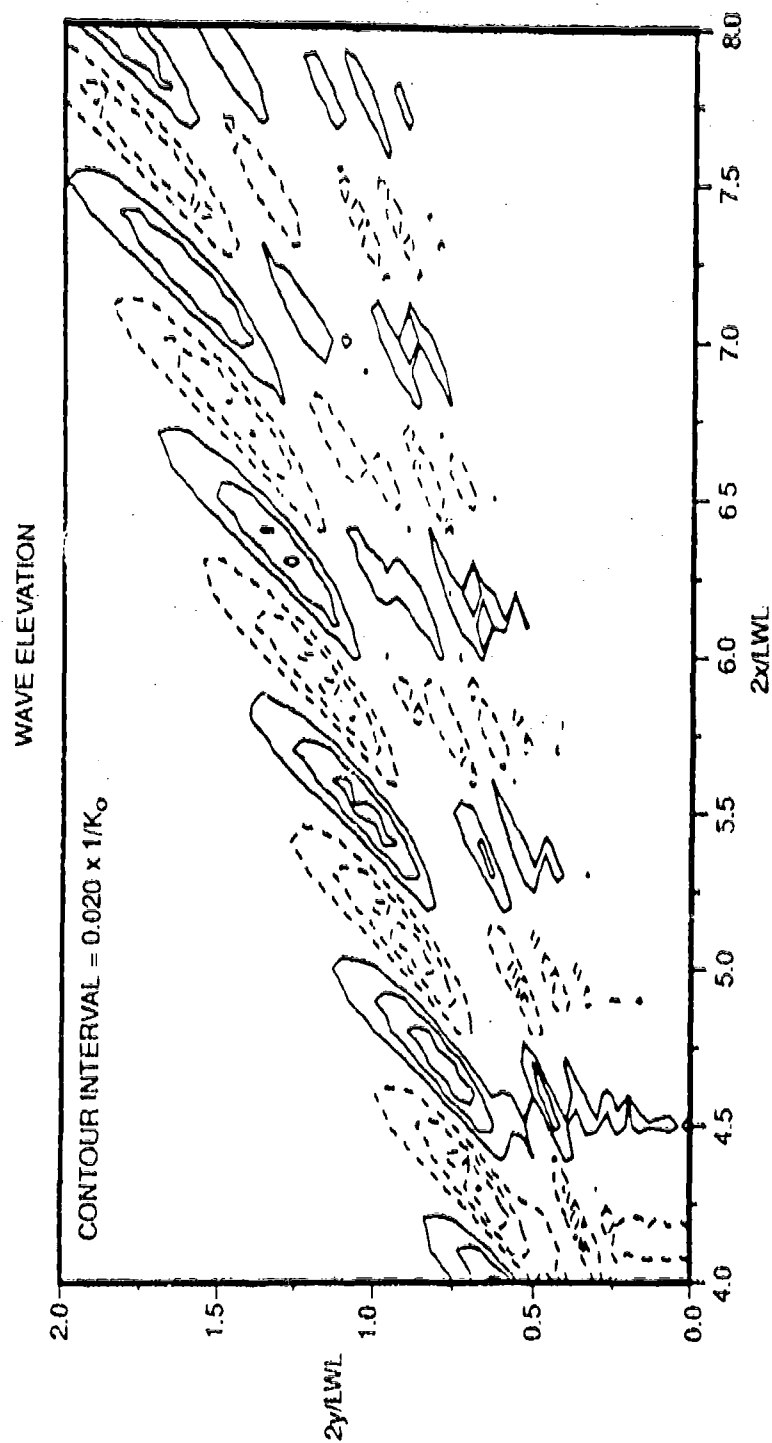


Fig. D.2. NK-2 prediction of wave contours ($4 < 2x/LWL < 8$) for Model 5415 at $F_n = 0.25$.

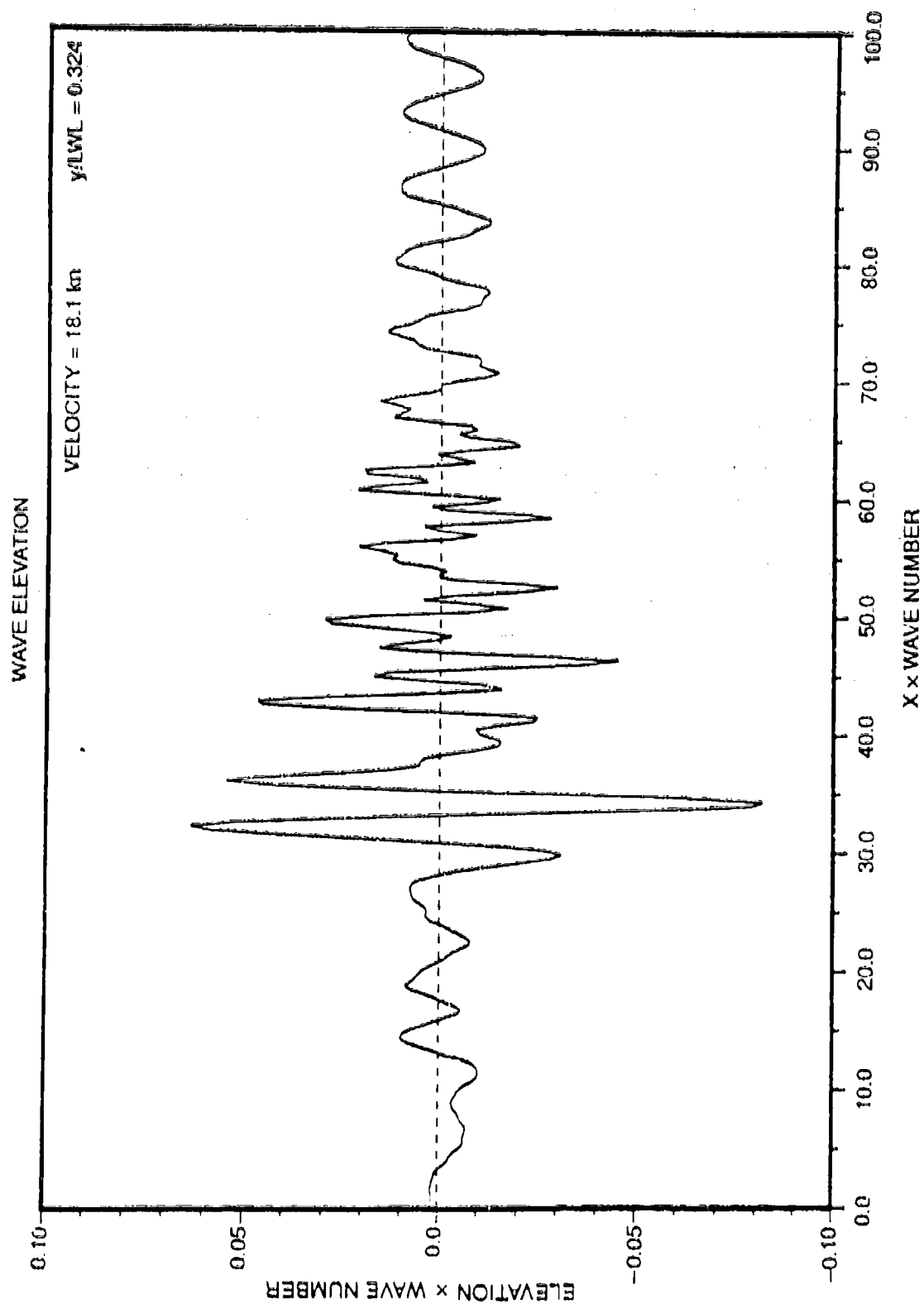


Fig. D.3. NK-2 prediction of wave cut for Model 5415 at $F_n = 0.25$.

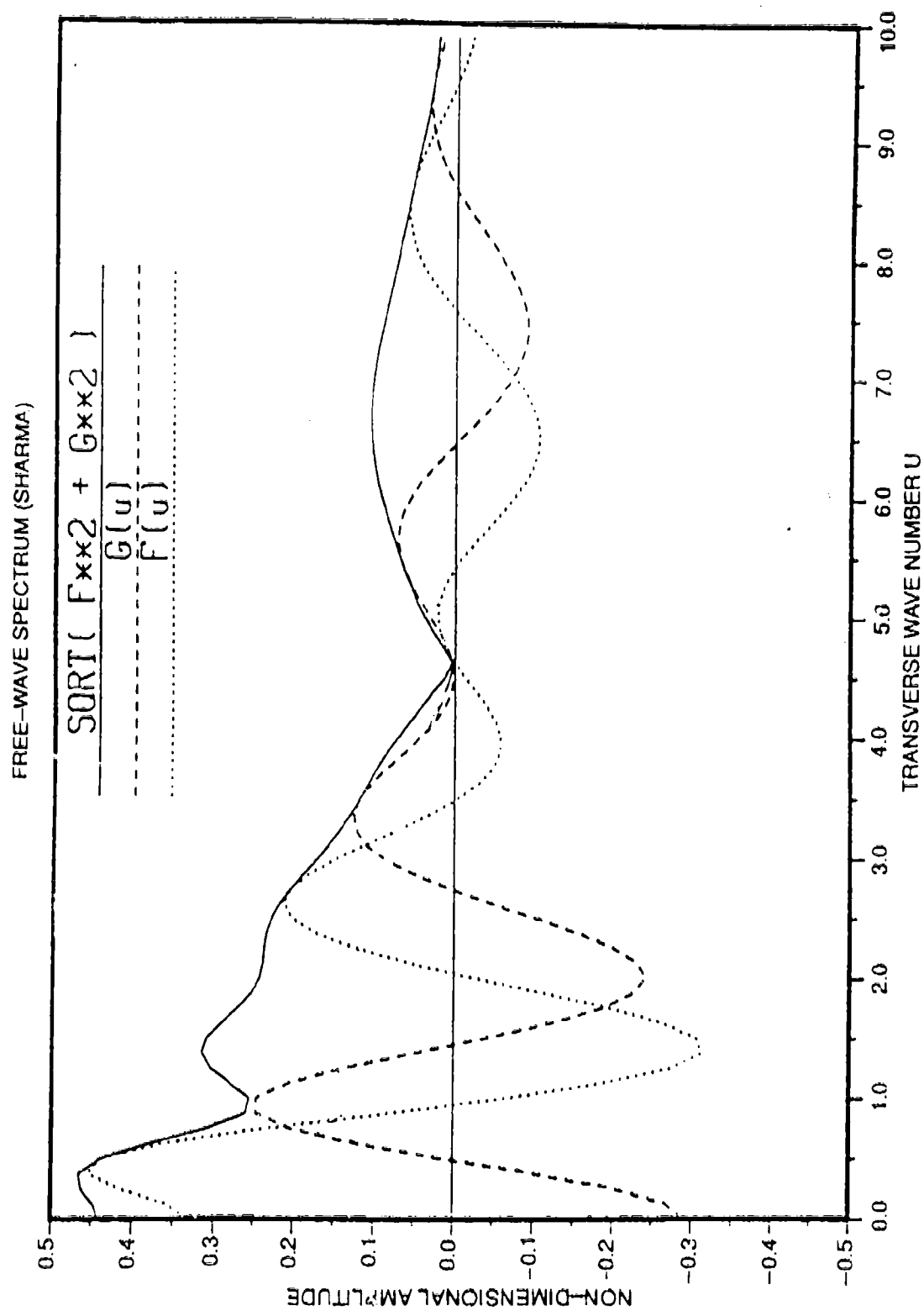


Fig. D.4. NK-2 prediction of wave spectrum for Model 5415 at $F_n = 0.25$.

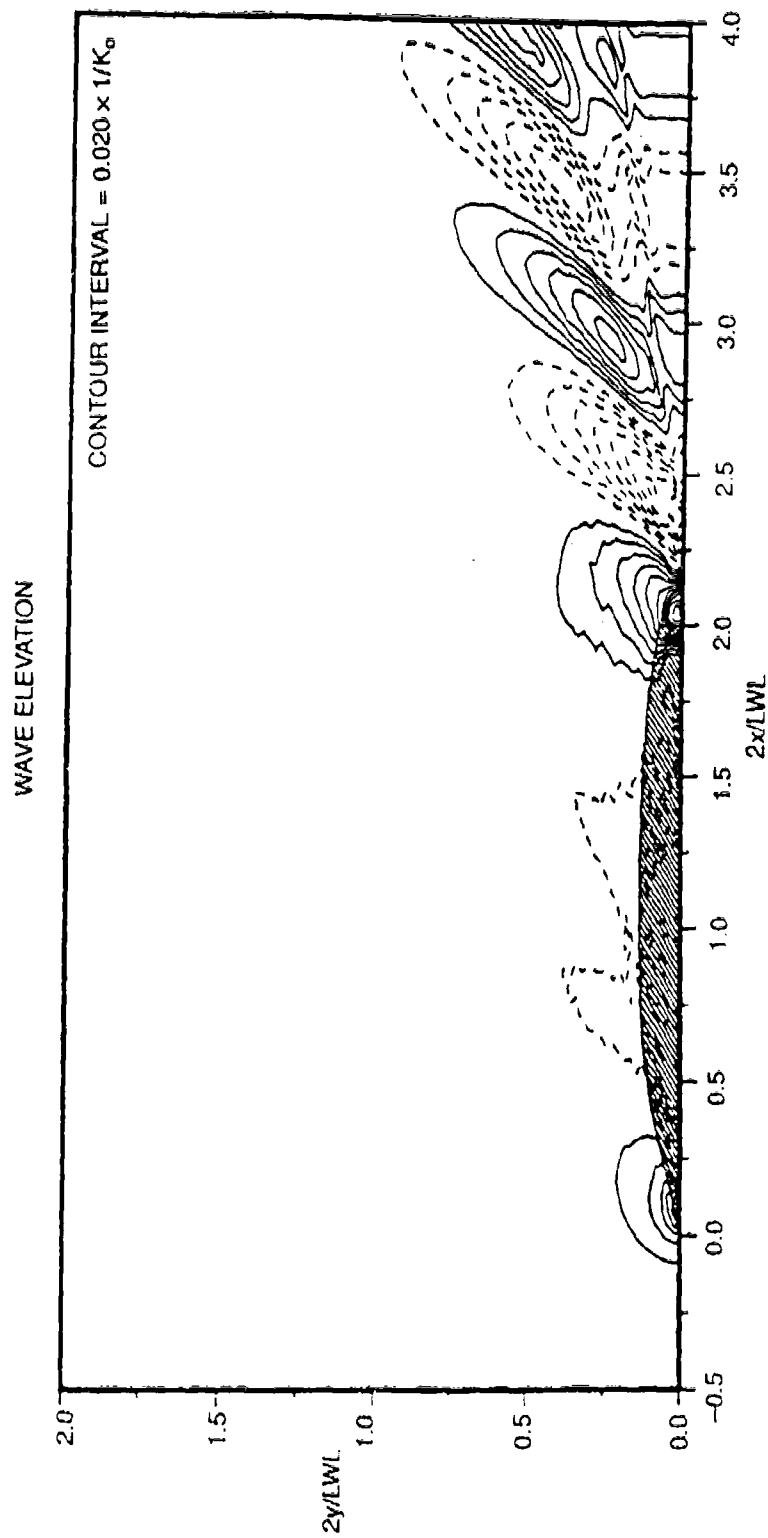


Fig. D 5. NK-2 prediction of wave contours ($-0.5 < 2x/LWL < 4$) for Model 5415 at $F_n = 0.2755$.

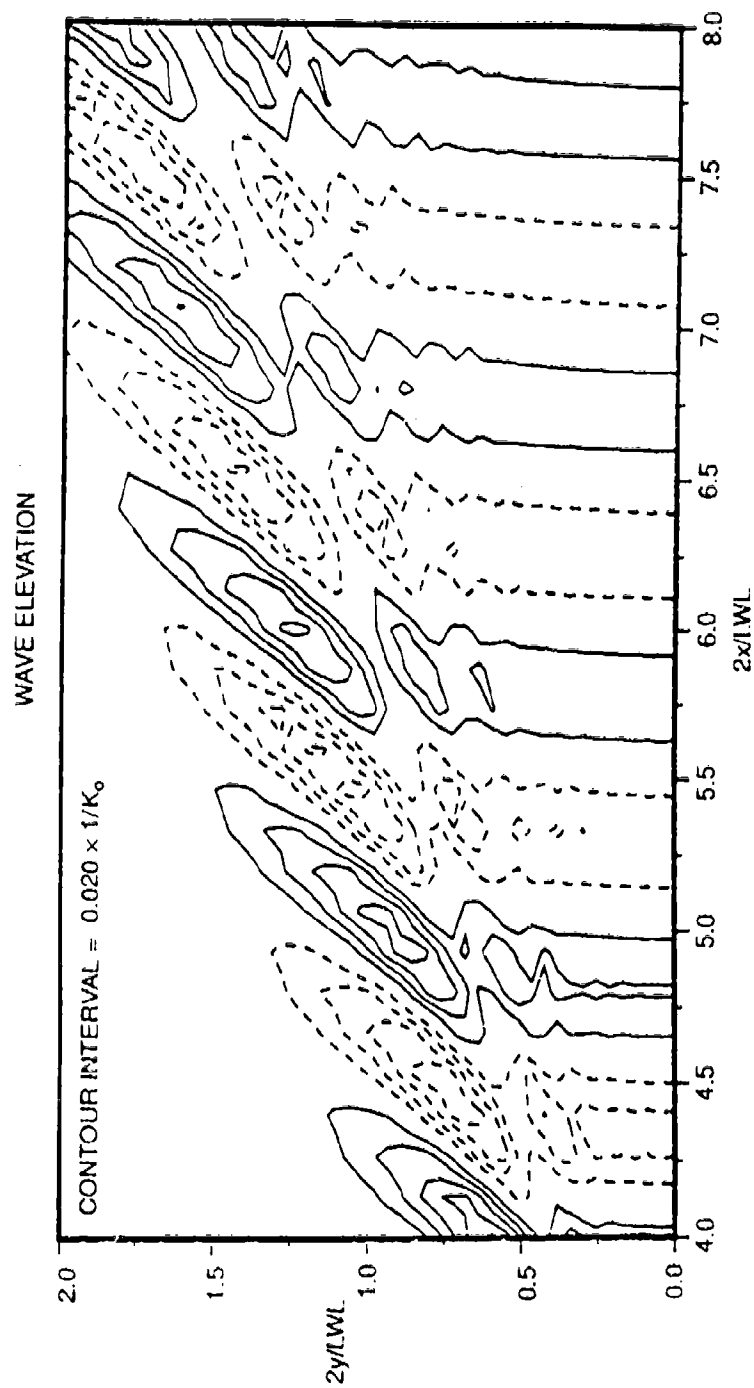


Fig. D.6. NK-2 prediction of wave contours ($4 < 2x/LWL < 8$) for Model 5415 at $F_n = 0.2755$.

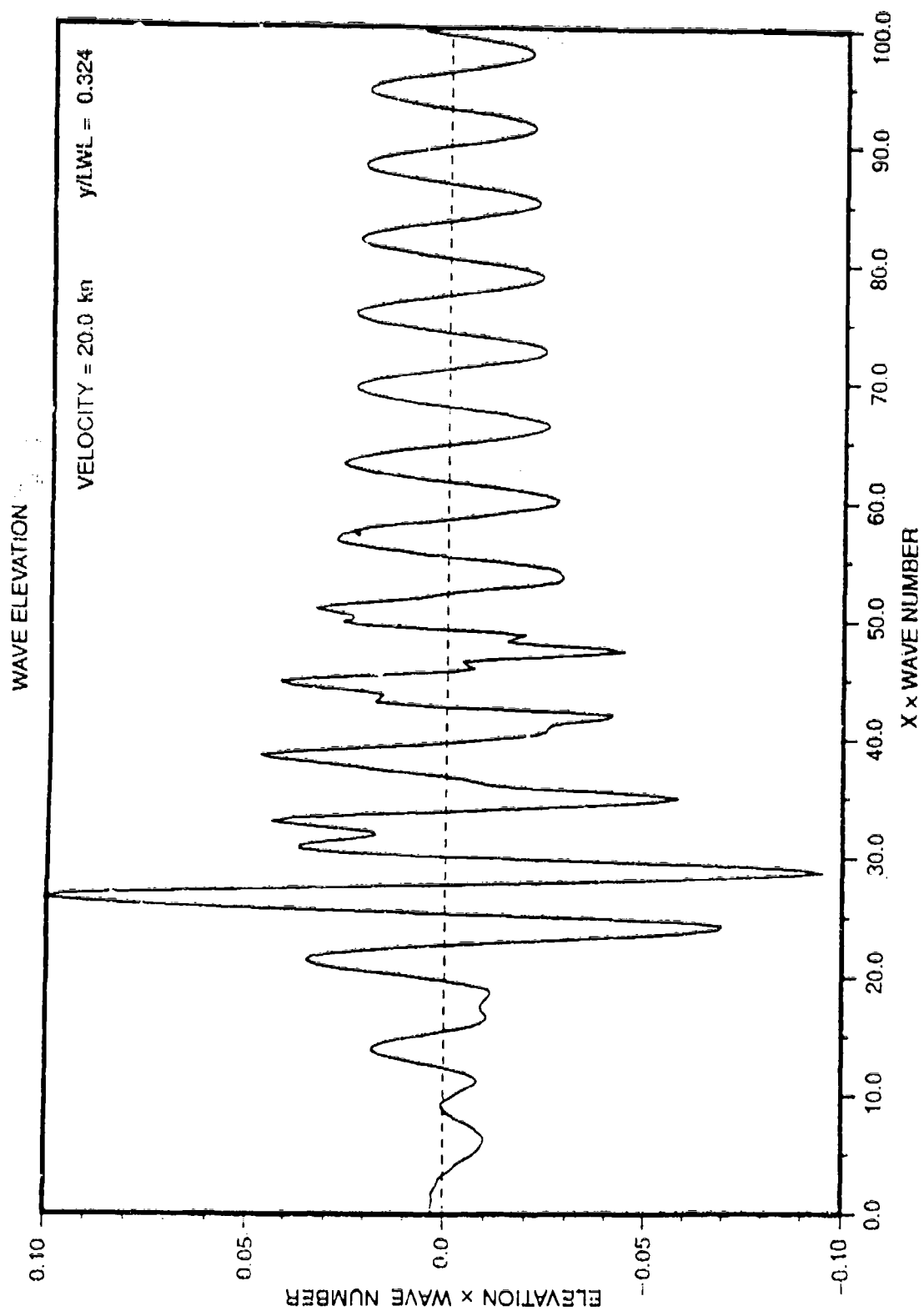


Fig. D.7. NK-2 prediction of wave cut for Model 5415 at $F_n = 0.2755$.

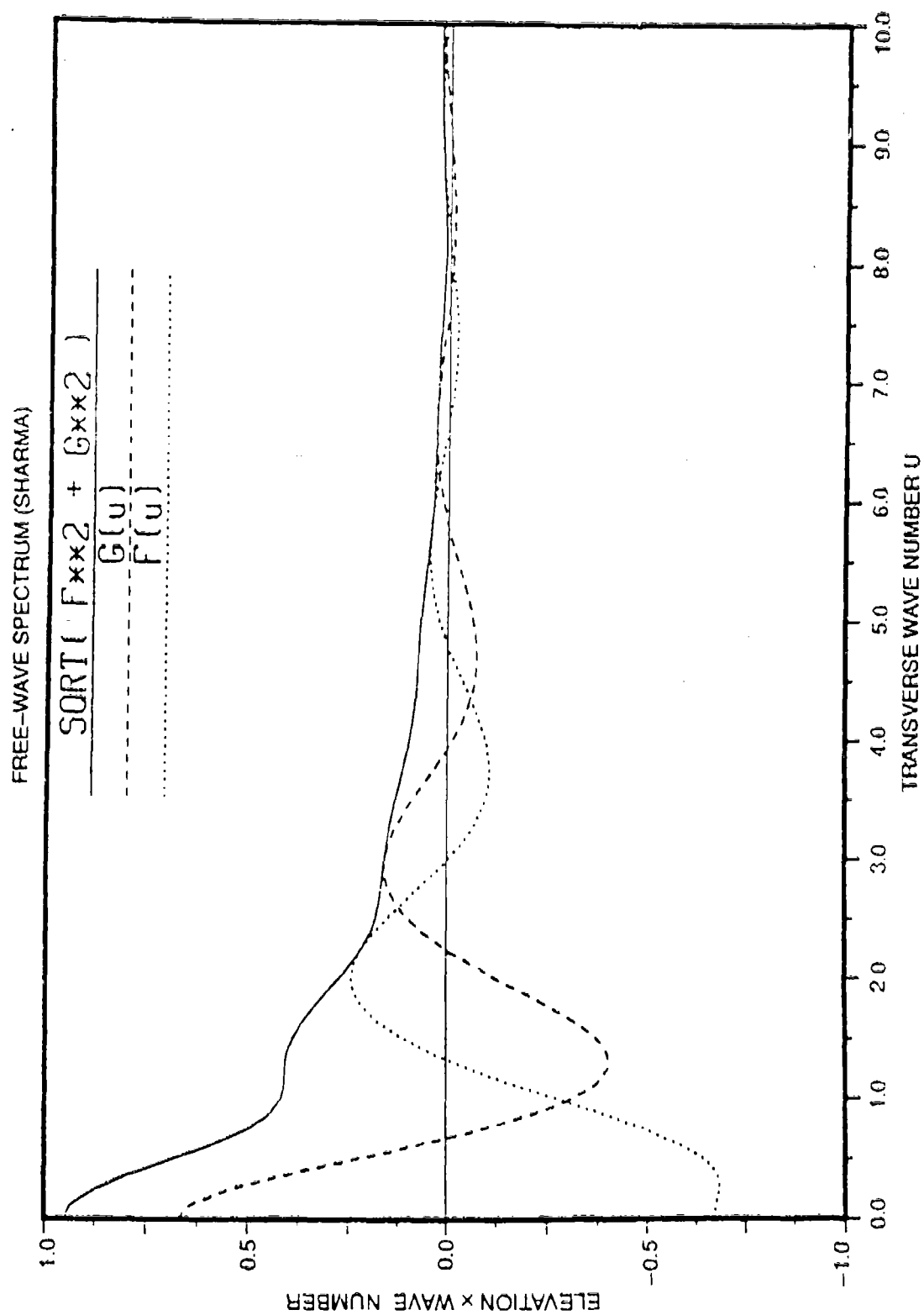


Fig. D.8. NK-2 prediction of wave spectrum for Model 5415 at $F_n = 0.2755$.

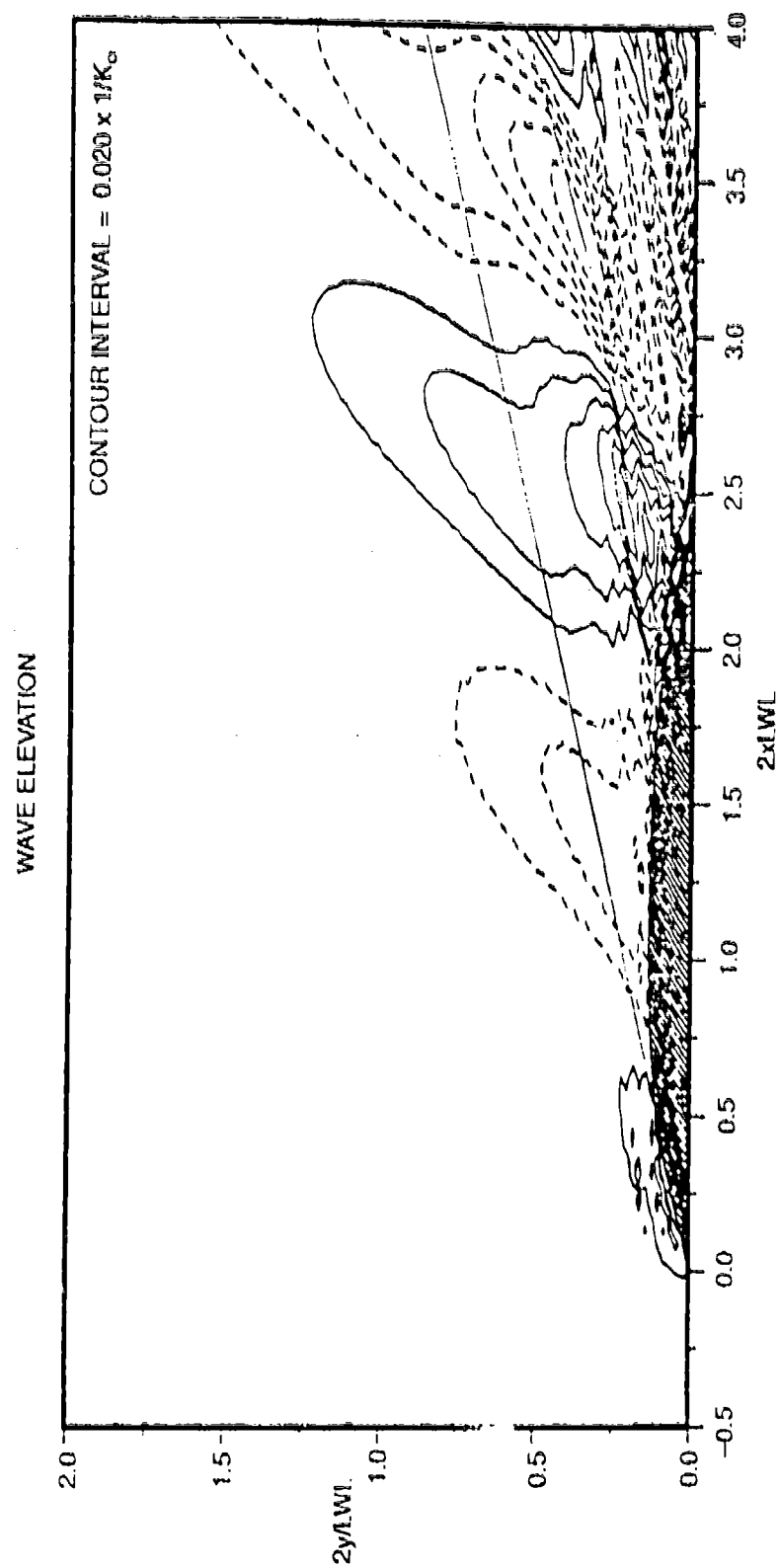


Fig. D.9. NK-2 prediction of wave contours ($-0.5 < 2y/LWL < 4$) for Model 5415 at $F_n = 0.4136$.

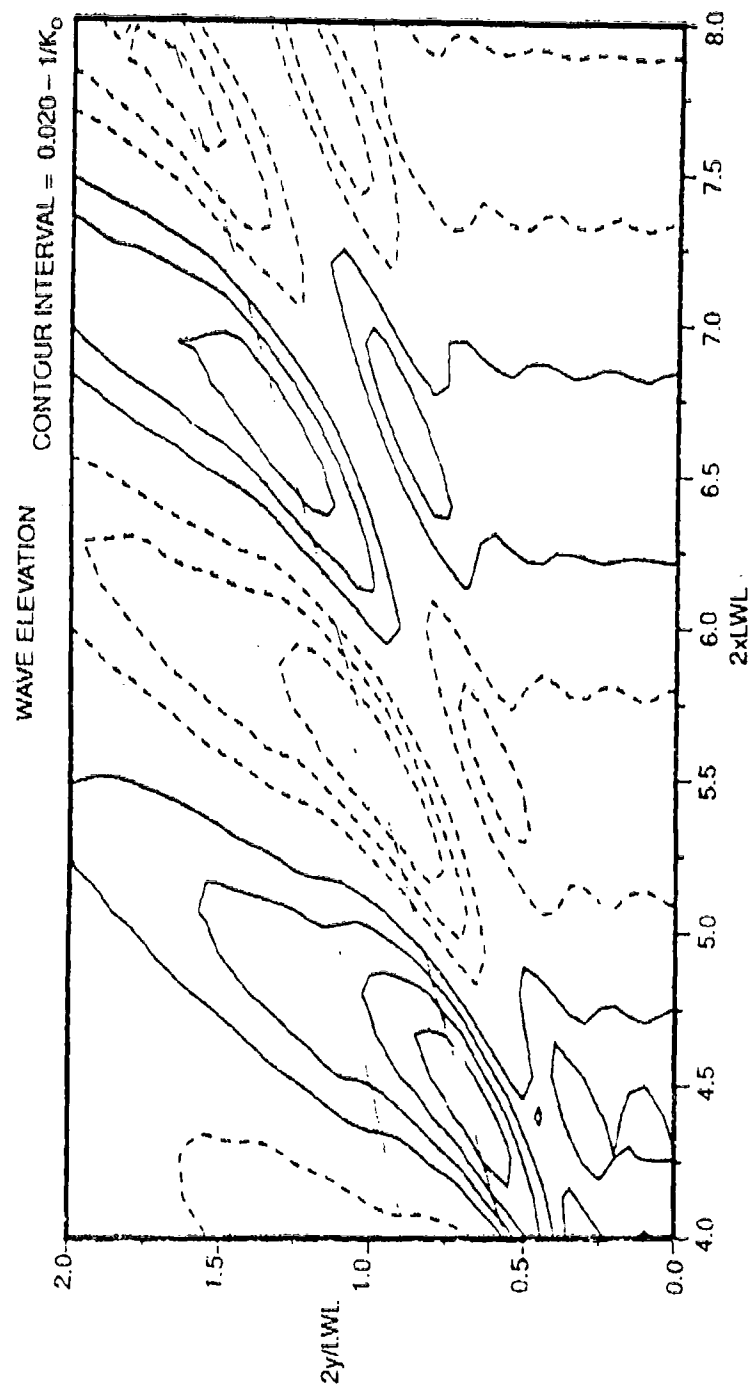


Fig. D.10. NK-2 prediction of wave contours ($4 < 2x/LWL < 8$) for Model 5415 at $F_n = 0.4136$.

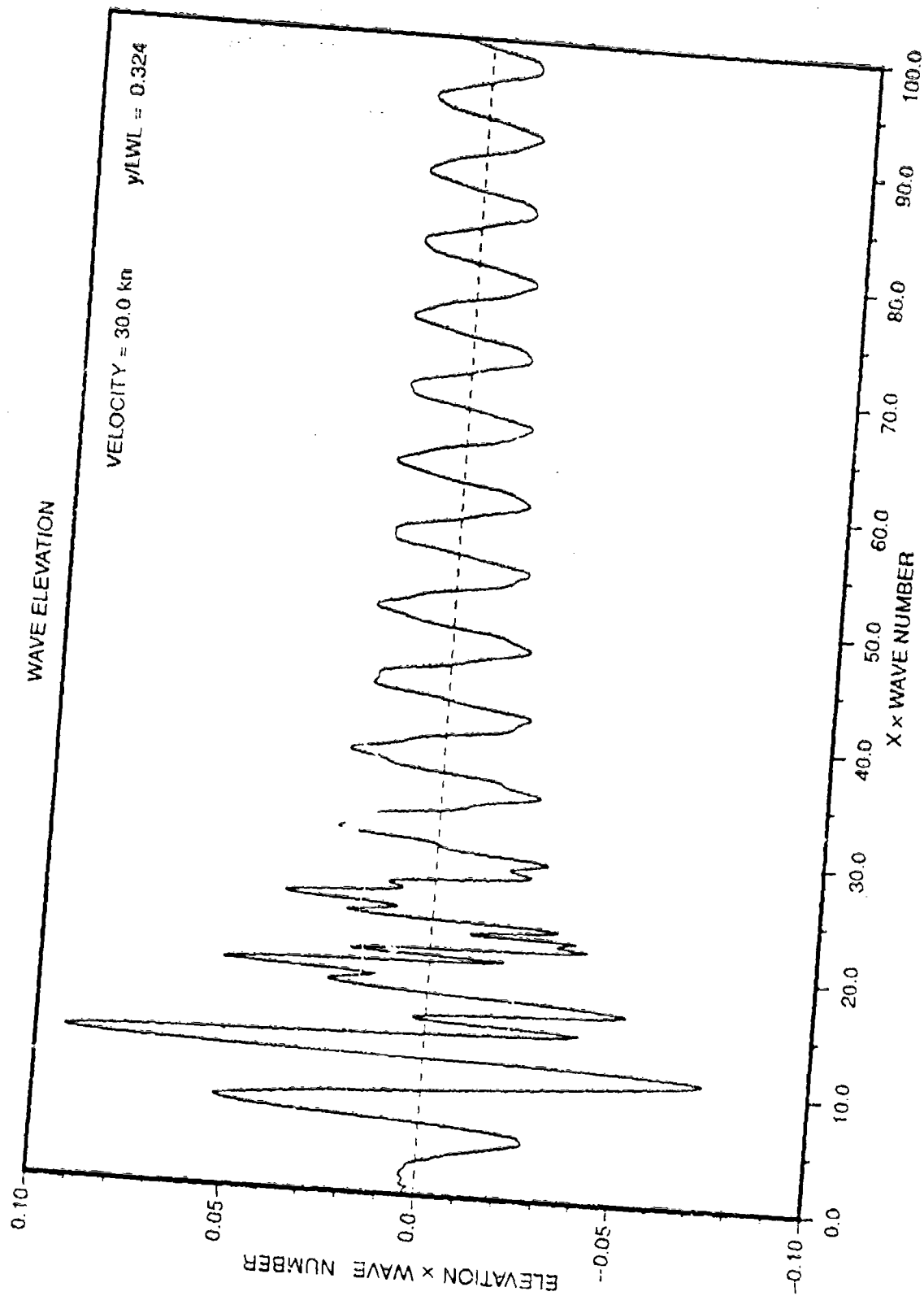


Fig. D.11. NK-2 prediction of wave cut for Model 5415 at $F_n = 0.4136$.

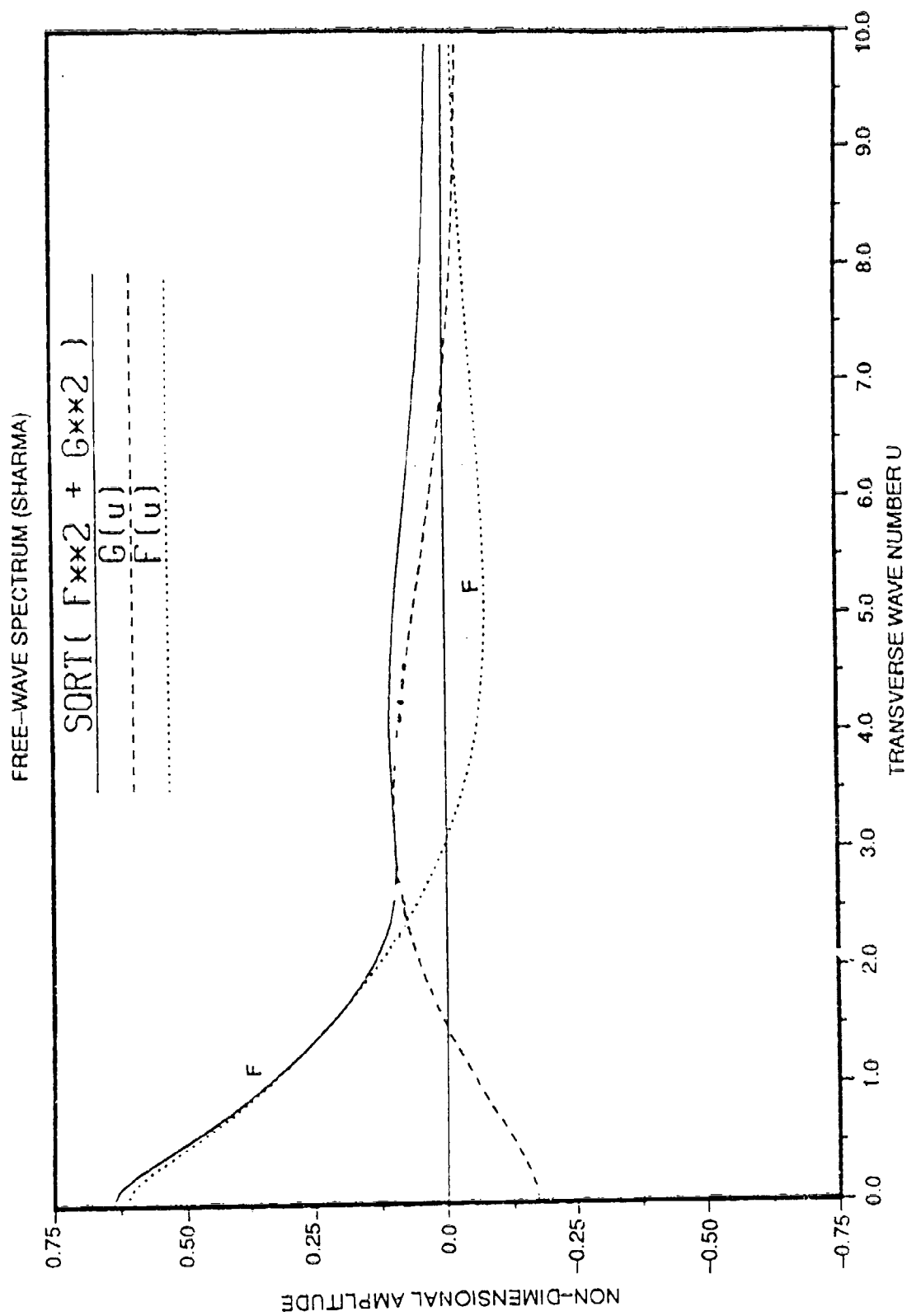


Fig. D.12. NK-2 prediction of wave spectrum for Model 5415 at $F_n = 0.4136$.

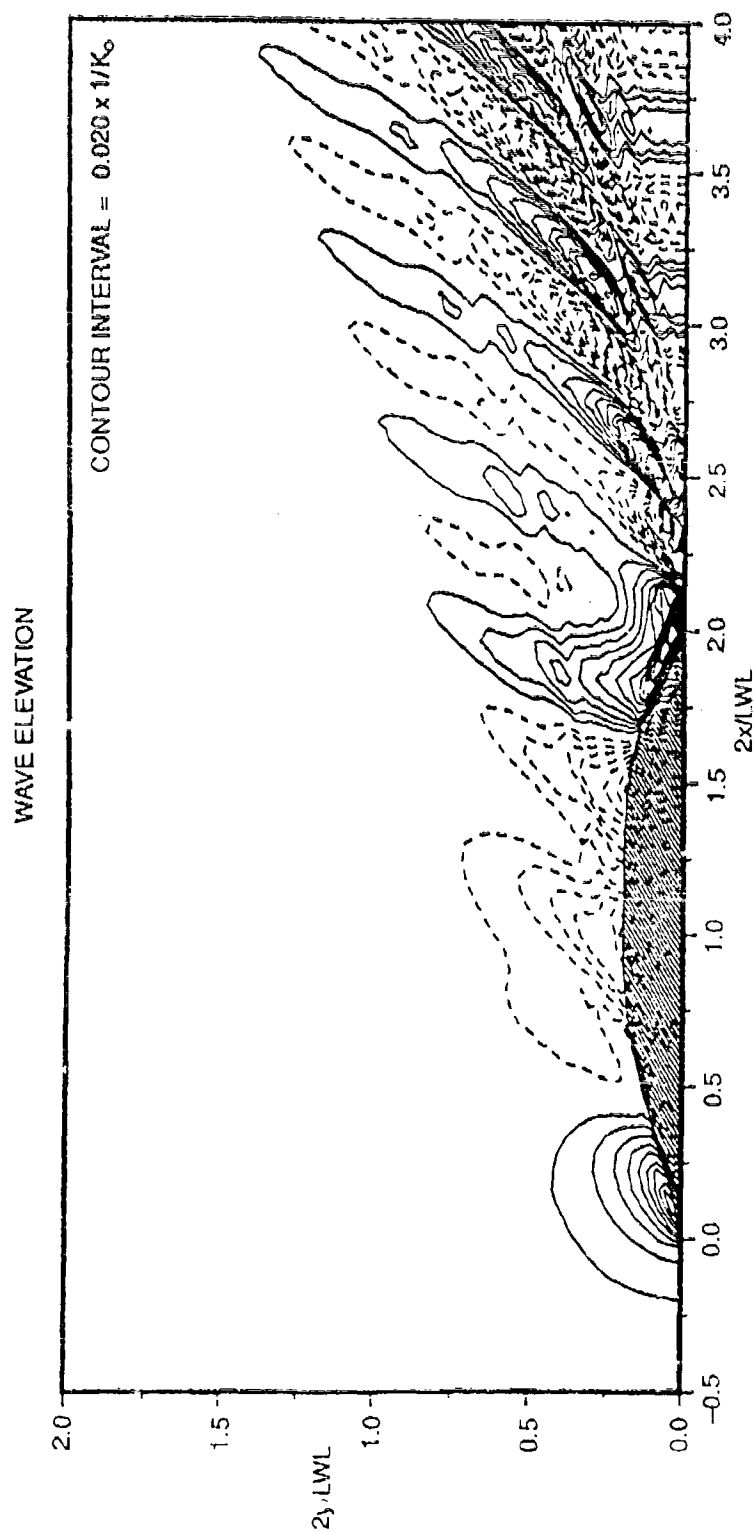


Fig. D.13. NK-2 prediction of wave contours ($-0.5 < 2x/LWL < 4$) for QUAPAW at $F_n = 0.2131$.

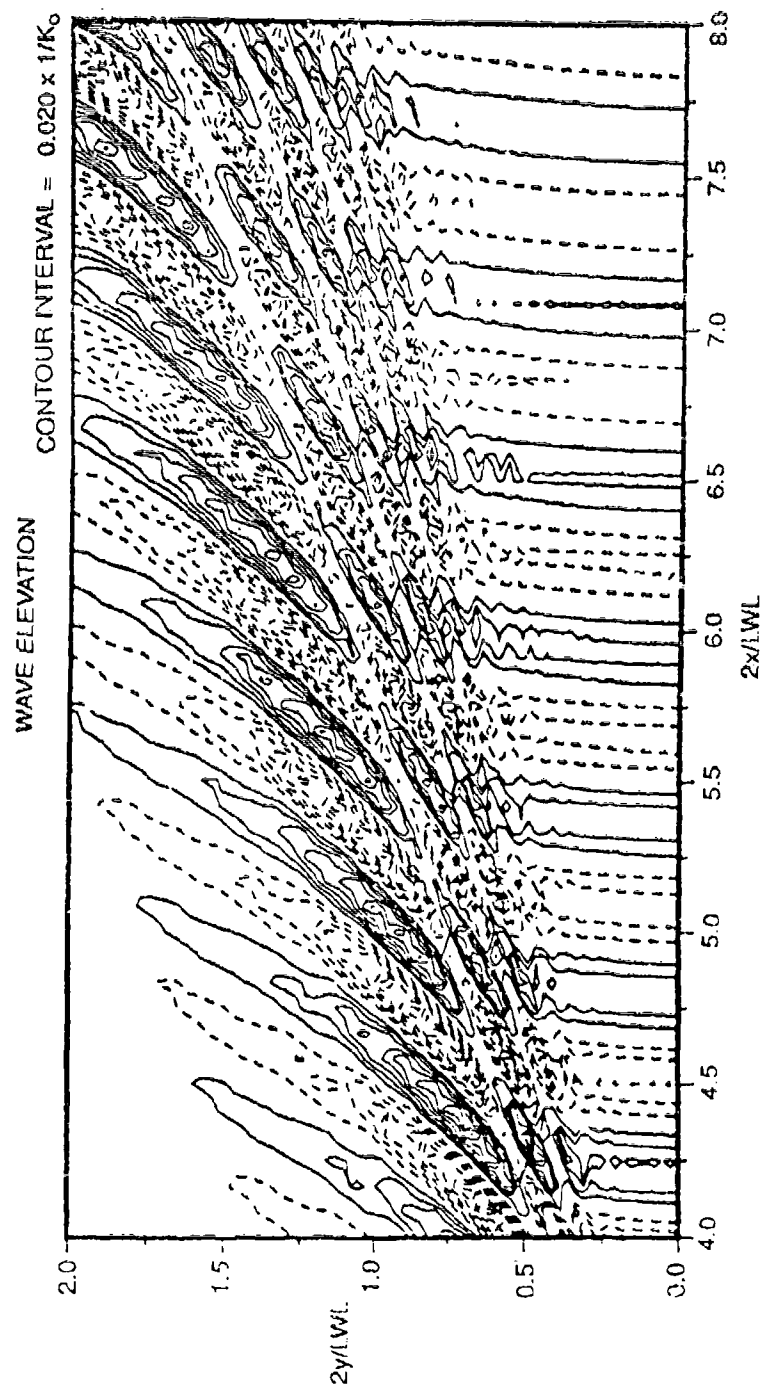


Fig. D.14. NK--2 prediction of wave contours ($4 < 2x/LWL < 8$) for QUAPAW at $F_n = 0.2131$.

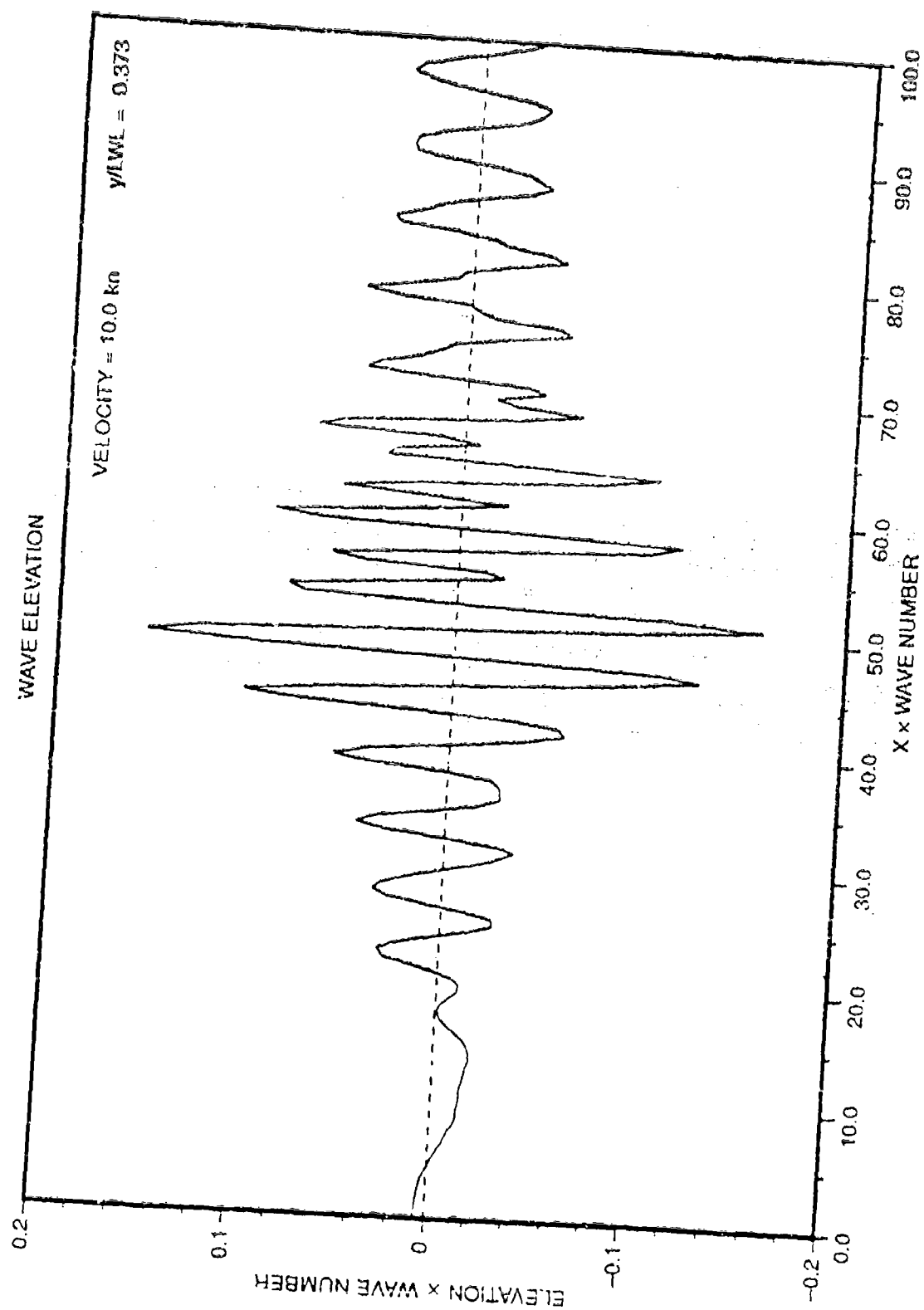


Fig. D.15. NK-2 prediction of wave cut for QUAPAW at $F_n = 0.2131$.

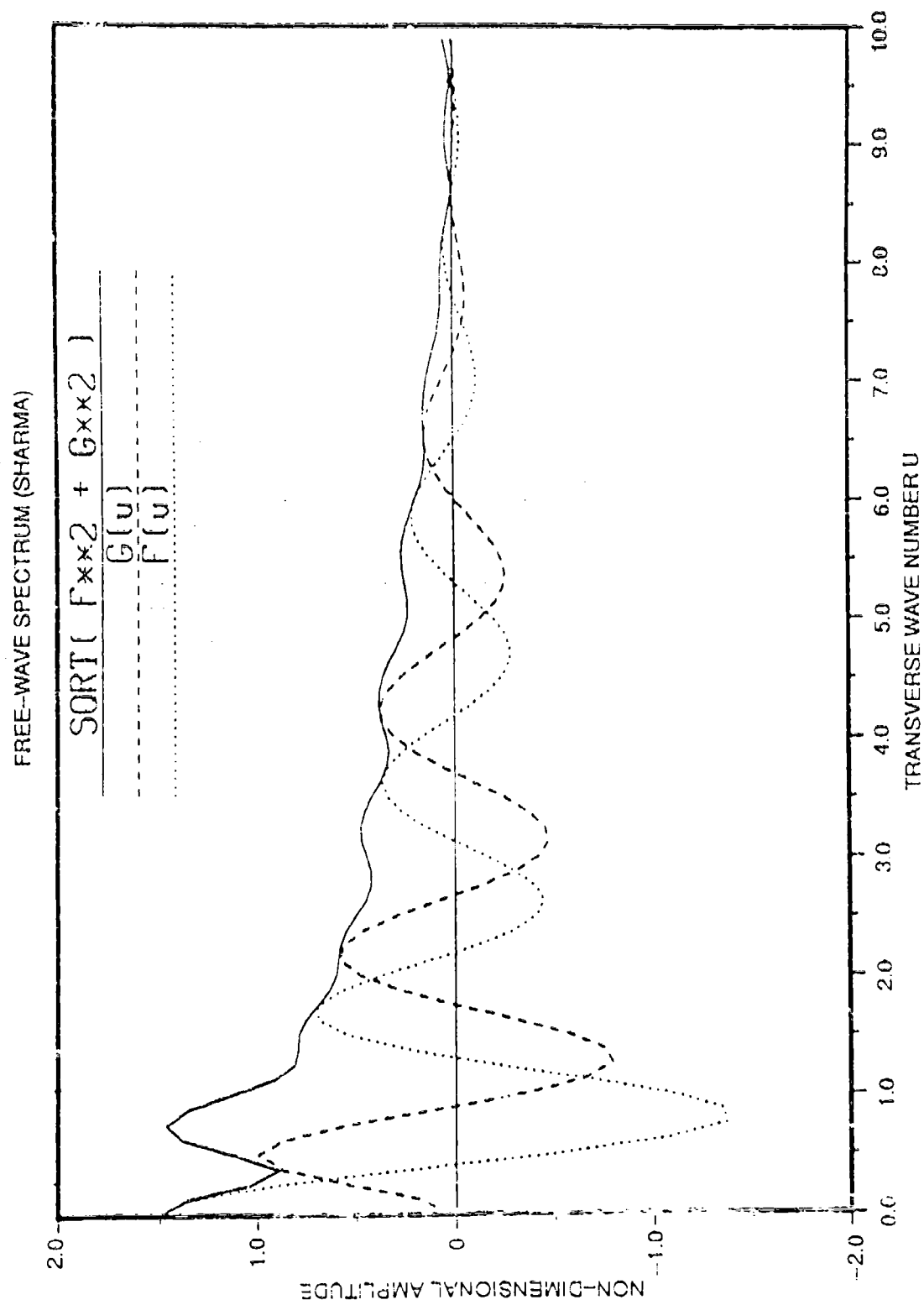


Fig. D.16. NK-2 prediction of wave spectrum for QUAPAW at $F_n = 0.2131$.

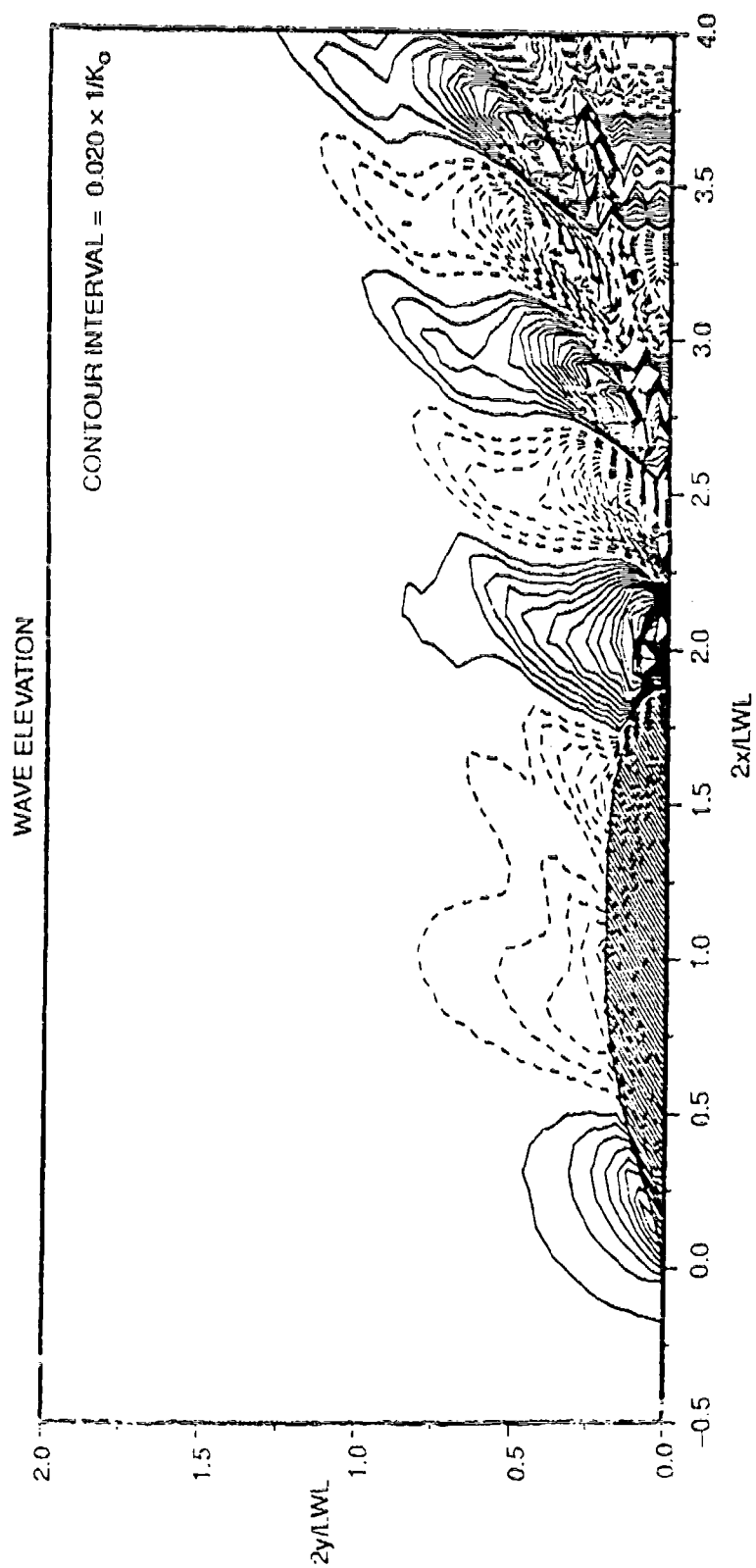


Fig. D.17. NK-2 prediction of wave contours ($-0.5 < 2x/LWL < 4$) for QUAPAW at $F_n = 0.25$.

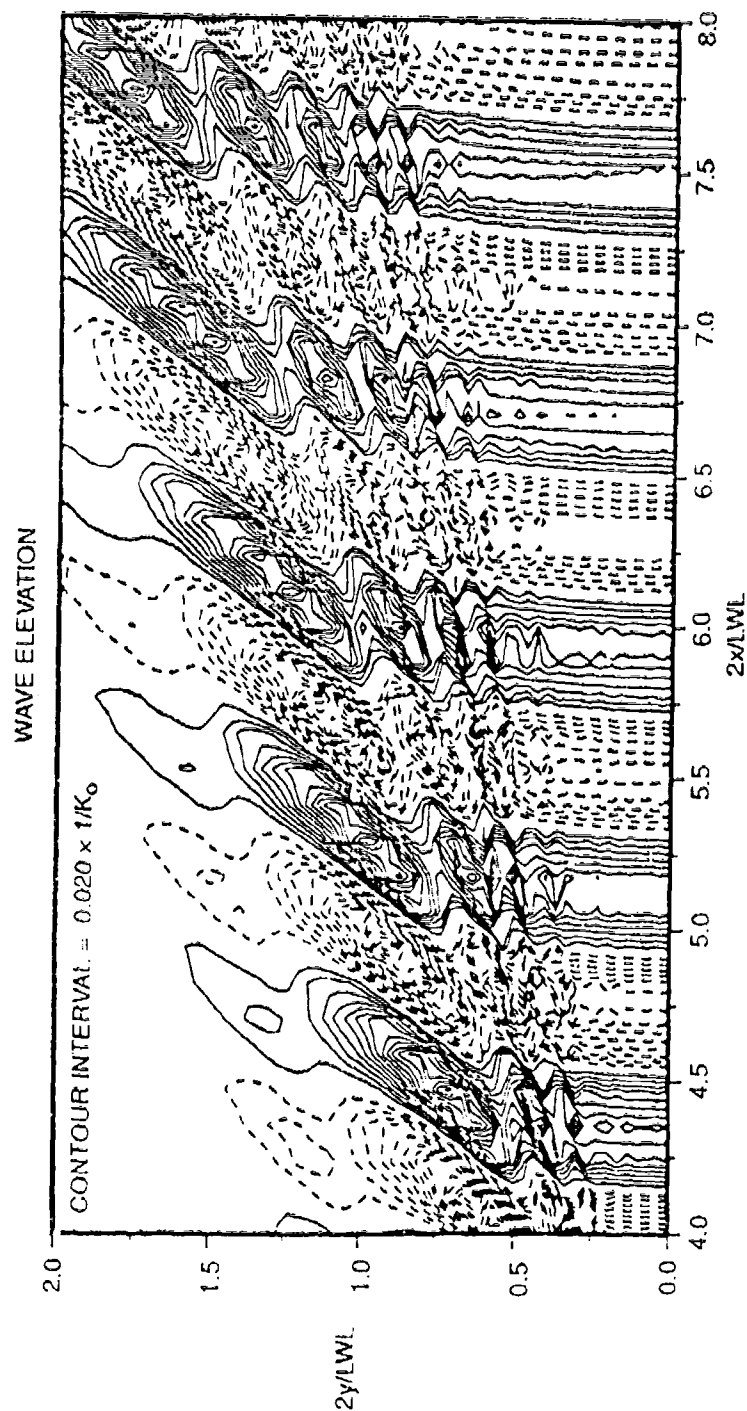


Fig. D.18. NK-2 prediction of wave contours ($4 < 2x/LWL < 8$) for QUAPAW at $F_n = 0.25$.

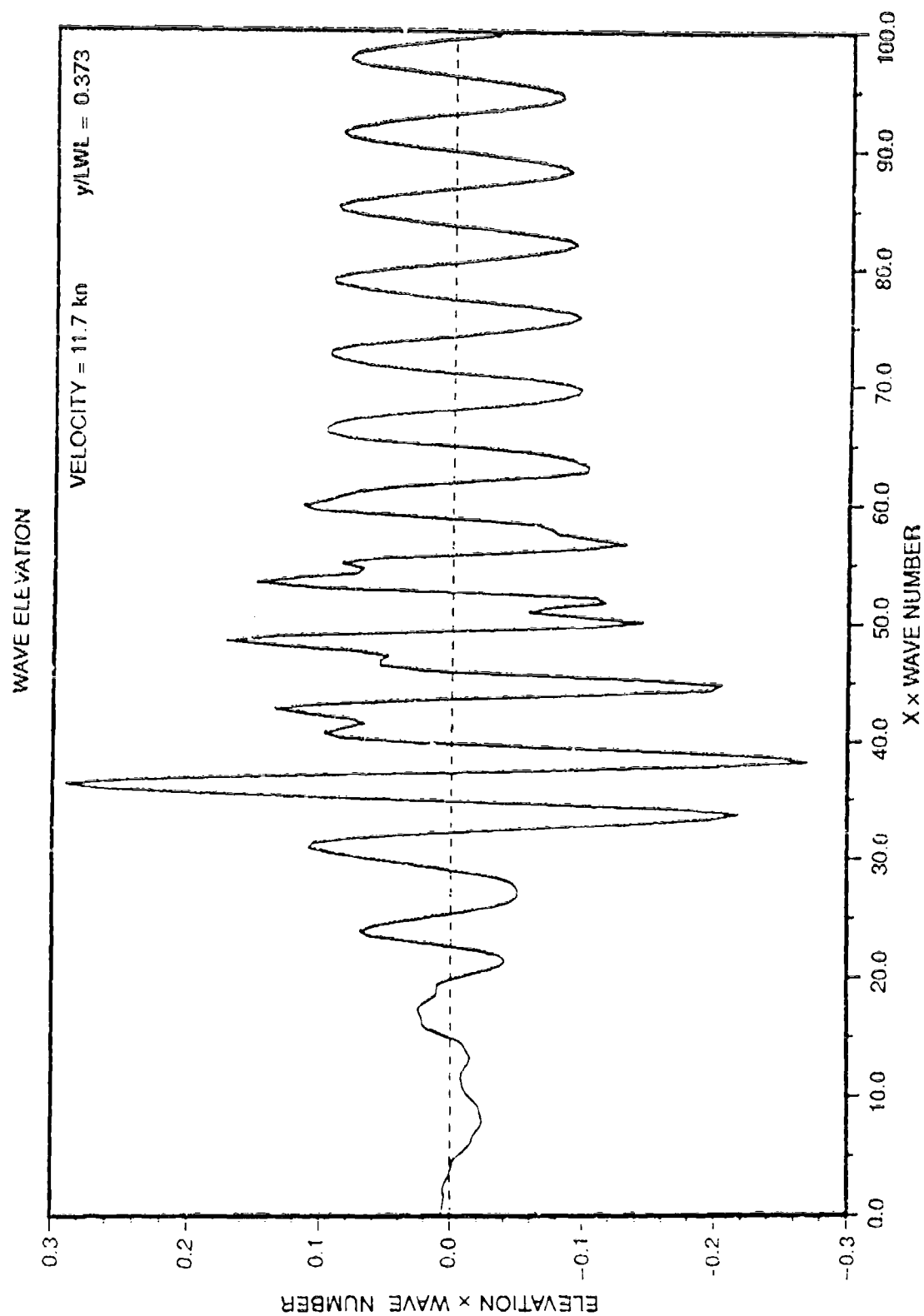


Fig. D.19. NK-2 prediction of wave cut for QUAPAW at $F_n = 0.25$.

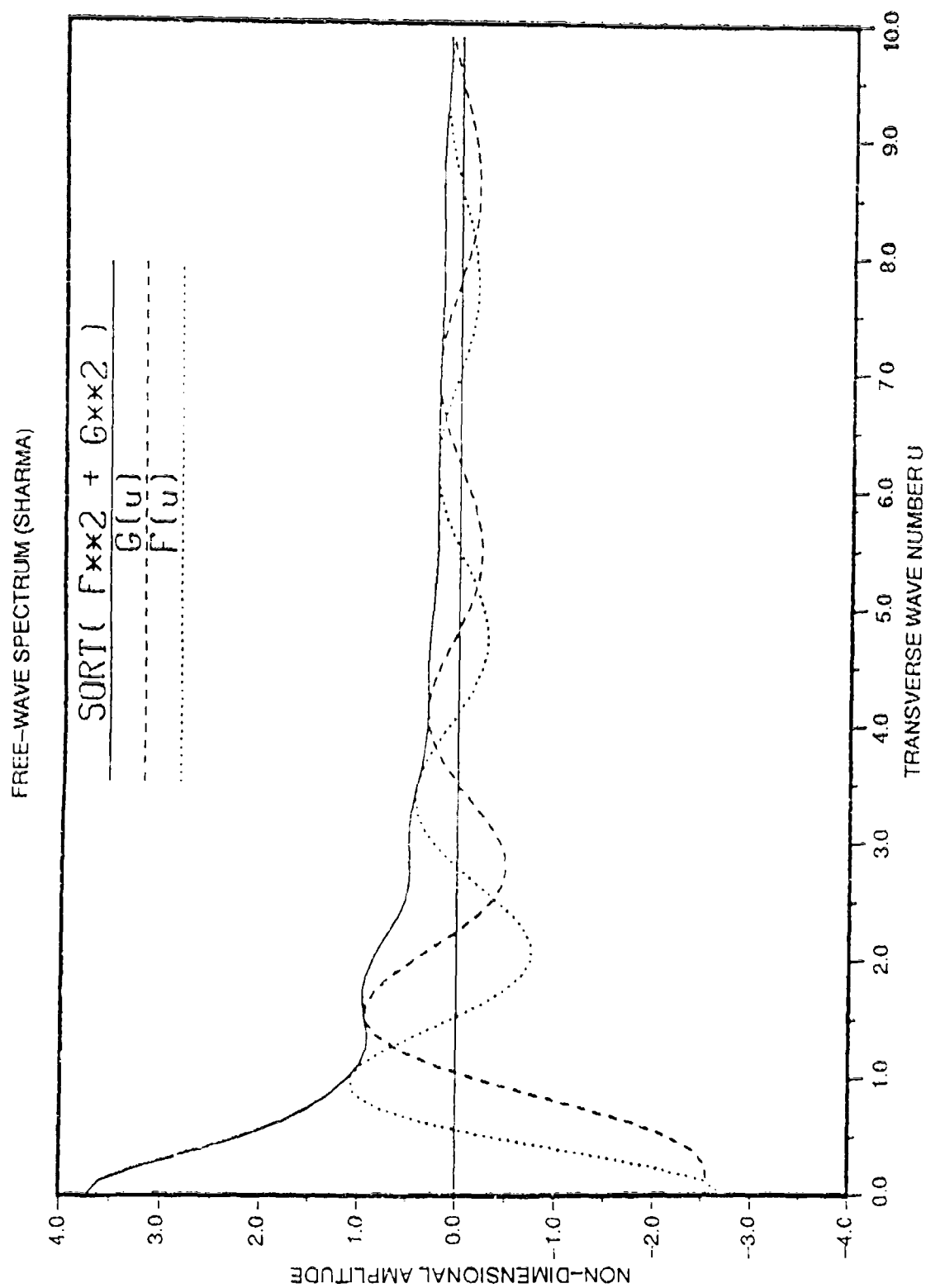


Fig. D.20. NK-2 prediction of wave spectrum for QUAPAW at $F_n = 0.25$.

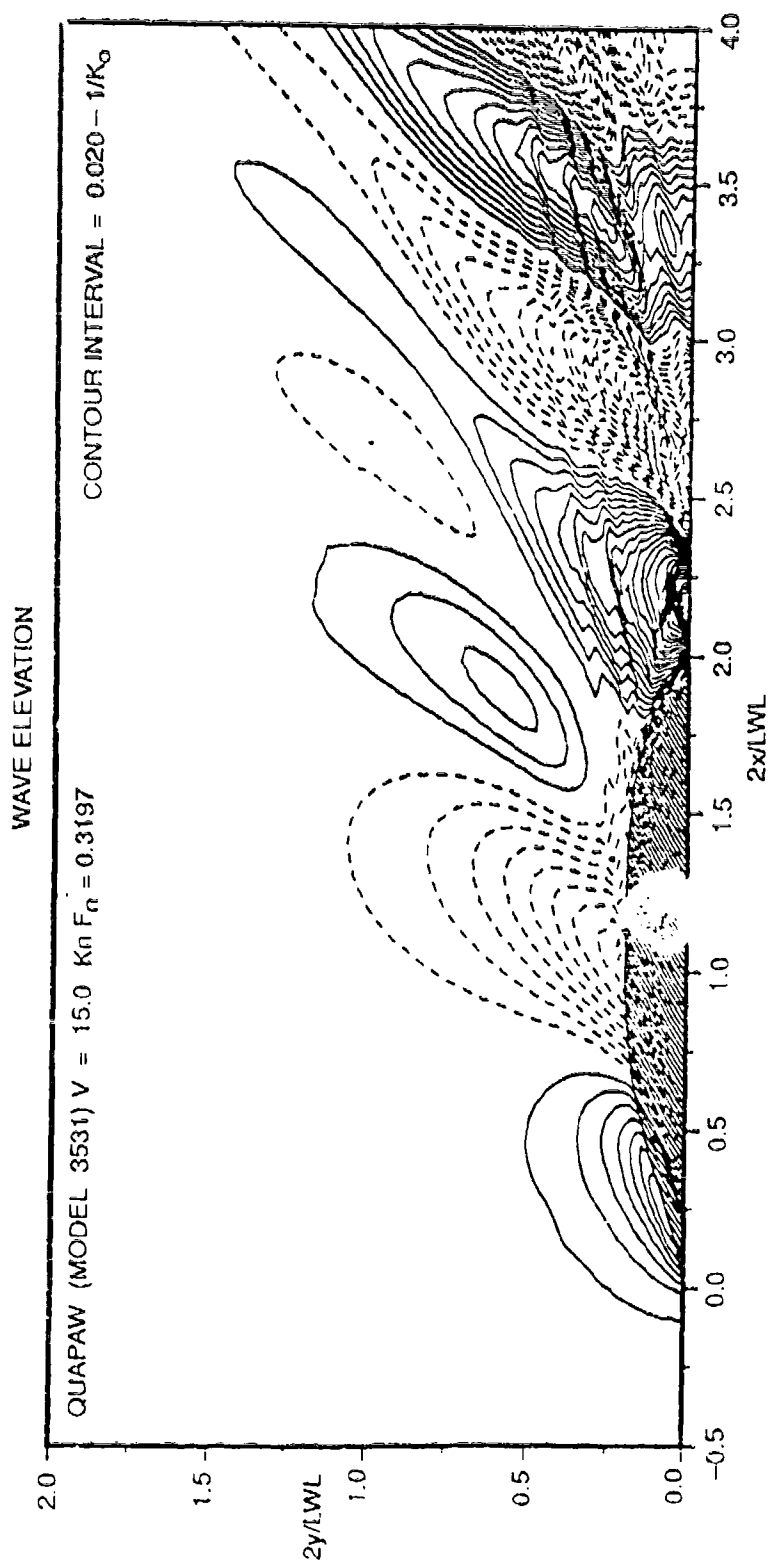


Fig. D.21. NK-2 prediction of wave contours ($-0.5 < 2x/LWL < 4$) for QUAPAW at $F_n = 0.3197$.

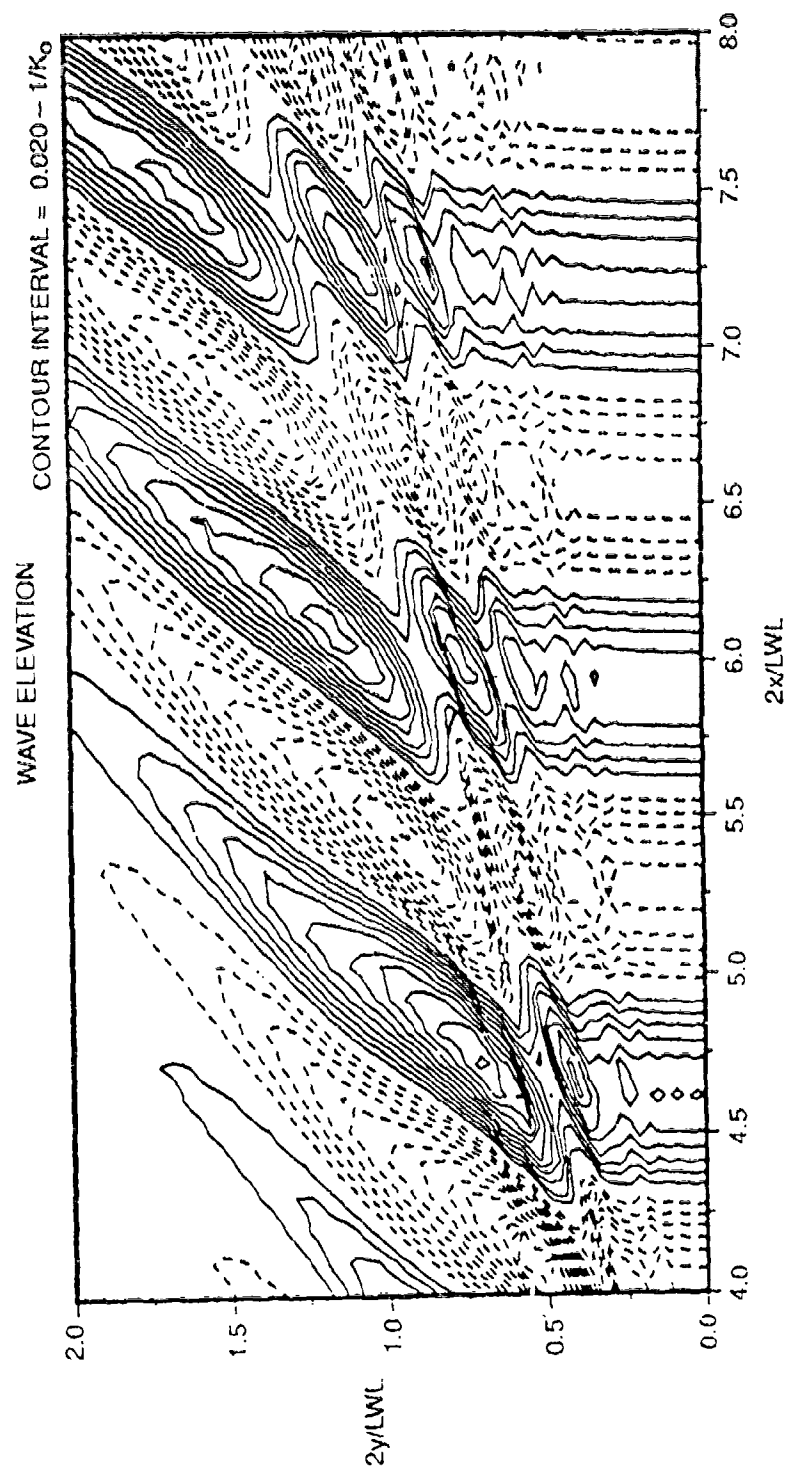


Fig. D.22. NK-2 prediction of wave contours ($4 < 2x/LWL < 8$) for QUAPAW at $F_n = 0.3197$.

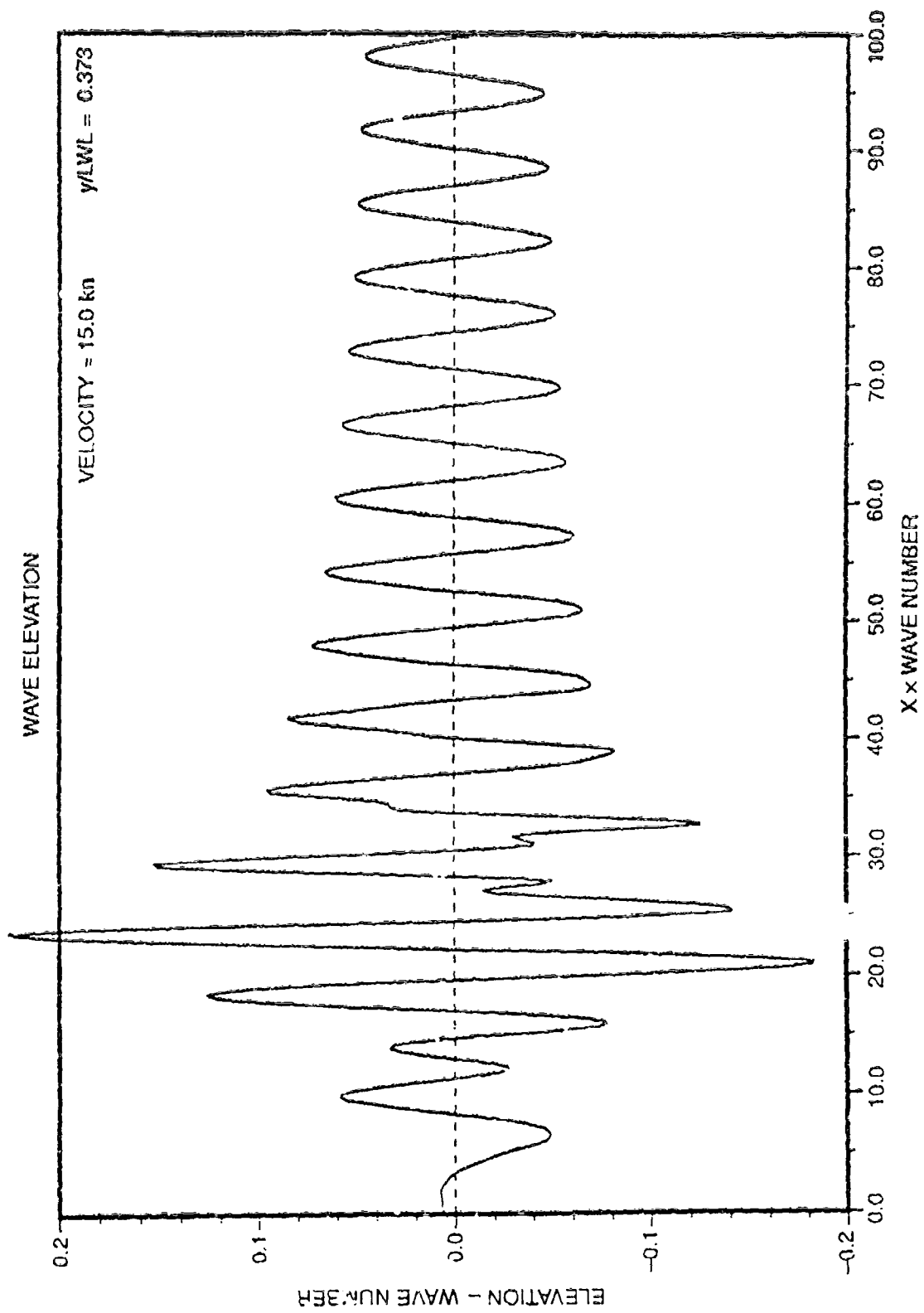


Fig. D.23. NK-2 prediction of wave cut for QUAPAV at $F_n = 0.3197$.

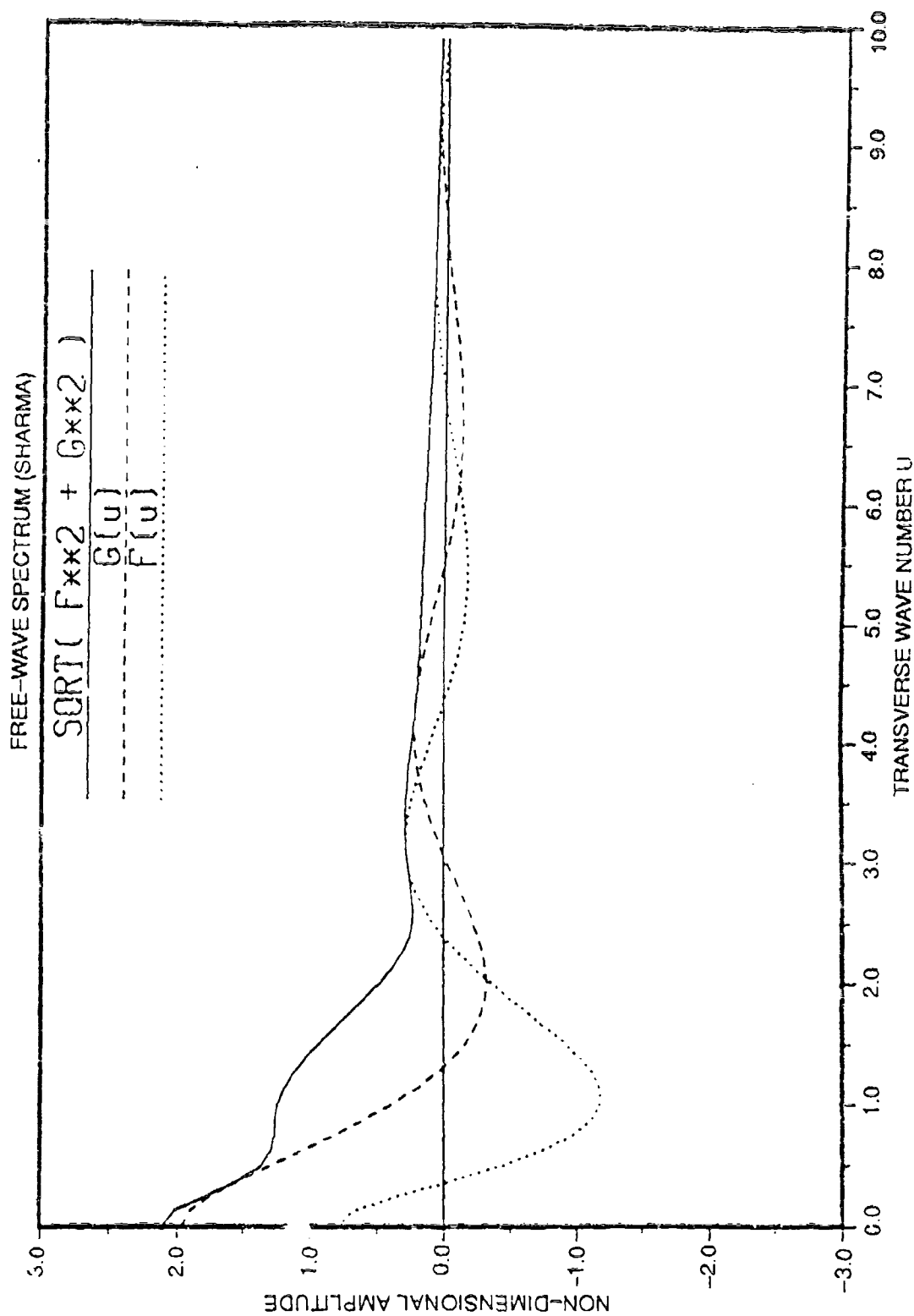


Fig. D.24. NK-2 prediction of wave spectrum for QUAPAW at $F_n = 0.3197$.

APPENDIX E
DOCTORS N-K PREDICTIONS

Program - DOCTORS.N-K

A Neumann-Kelvin code using
the source distribution technique

- 4000 lines of code
- 29 subroutines
- presently limited to 200 panels by dimensions statements
- no user's manual; but extensive program comments including input and output descriptions
- assumed P/S symmetry and no propulsor
- no streamlines are computed
- output is source strengths, sinkage force, trim moment, wave resistance, and free wave spectrum
- run on Apollo, IBM 3090, and CRAY

9

KELVIN WAVE COMPUTATIONS

- CRAY and Apollo
- on the CRAY DOCTORS.N-K took 10 minutes for 192 panels and 1 Froude number
- computation time for wave amplitude calculations depends heavily on integration scheme
- input data is in the form required by Hess and Smith
- a simple 15 line program changed paneling data sent by DTRC into DOCTORS.N-K input format
- 192 panels were used on the 1/2 hull in all cases
- quadrilateral panels with constant source strength are used
- convergence tests and wave resistance calculations were done

Program - WAVEAMP

A program to predict the wave amplitude at any point
using the source strengths and geometry
from DOCTORS.N-K

- 600 lines of code
- 3 subroutines
- no limitation on number of field points
- same restrictions as DOCTORS.N-K

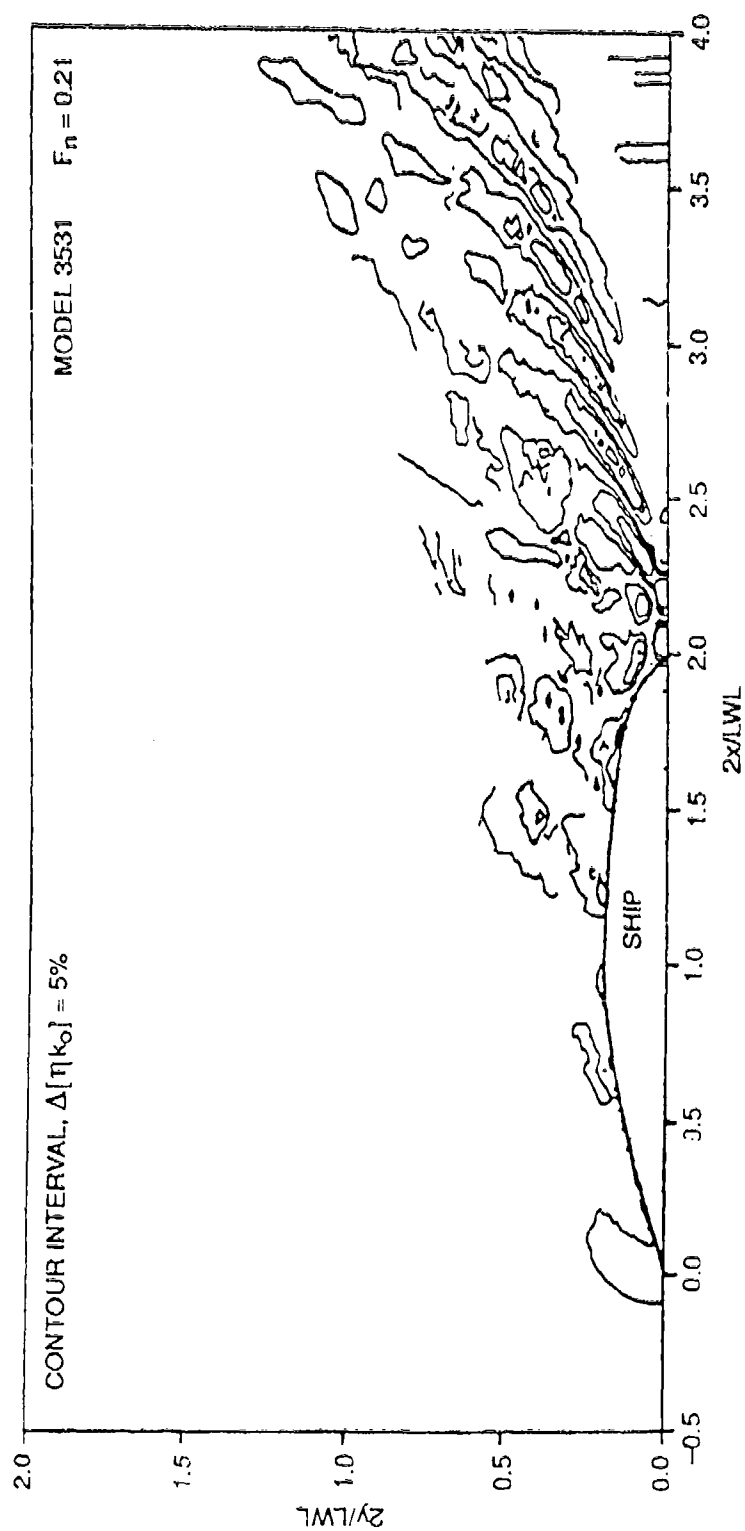


Fig. E.1. DOCTORS N-K prediction of wave contours ($-0.5 < 2x/LWL < 4$) for QUAPAW at $F_n = 0.2131$.

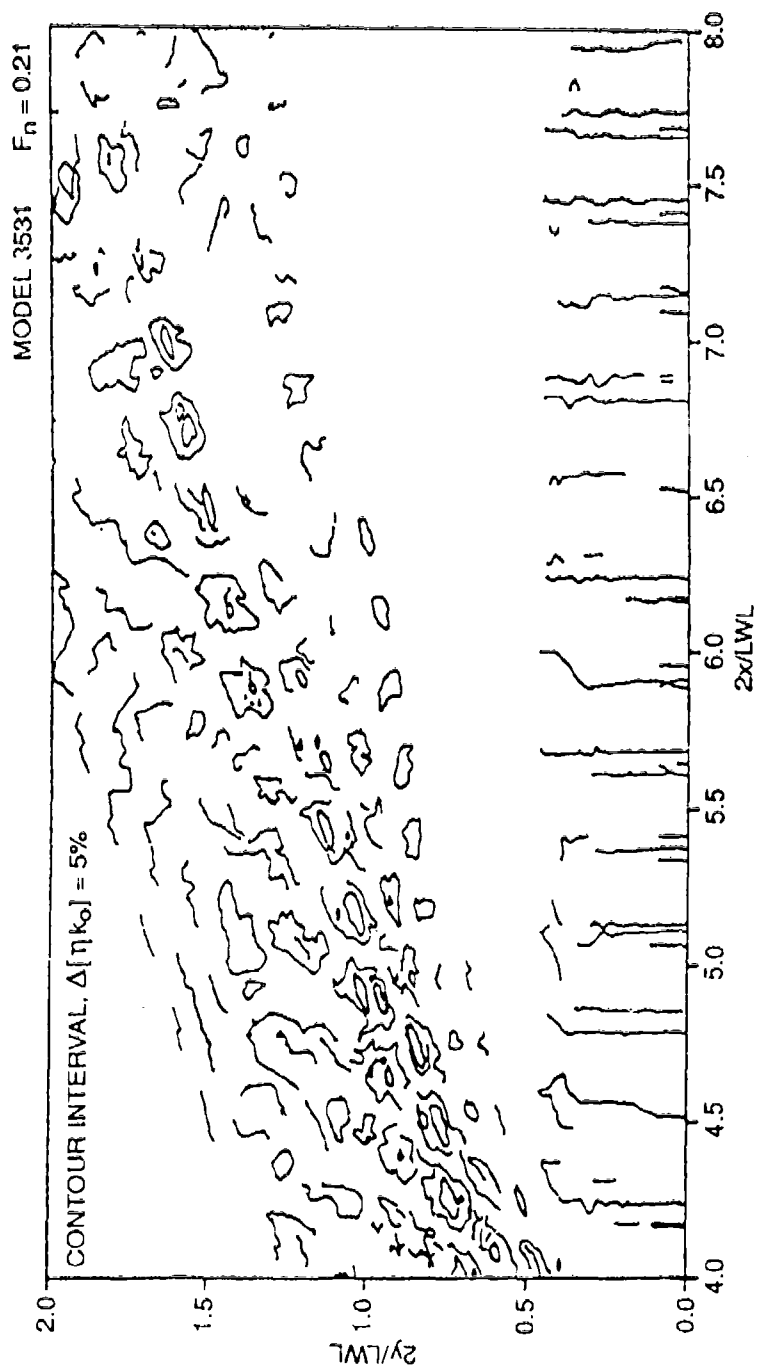


Fig. E.2. DOCTORS N-K prediction of wave contours ($4 < 2x/LWL < 8$) for QUAPAW at $F_n = 0.2131$.

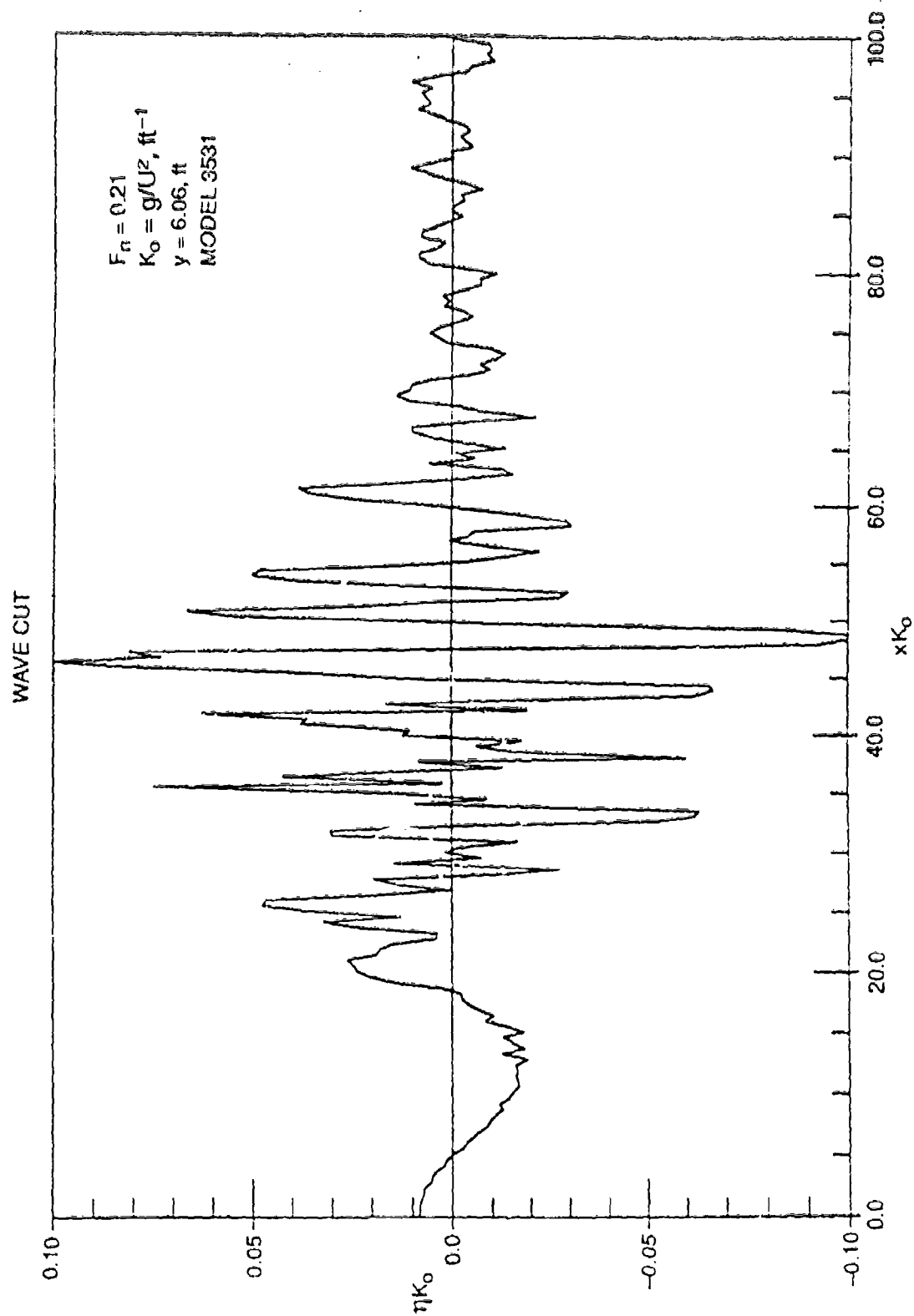


Fig. E.3. DOCTORS N-K prediction of wave contours for QUAPAW at $F_n = 0.2131$.

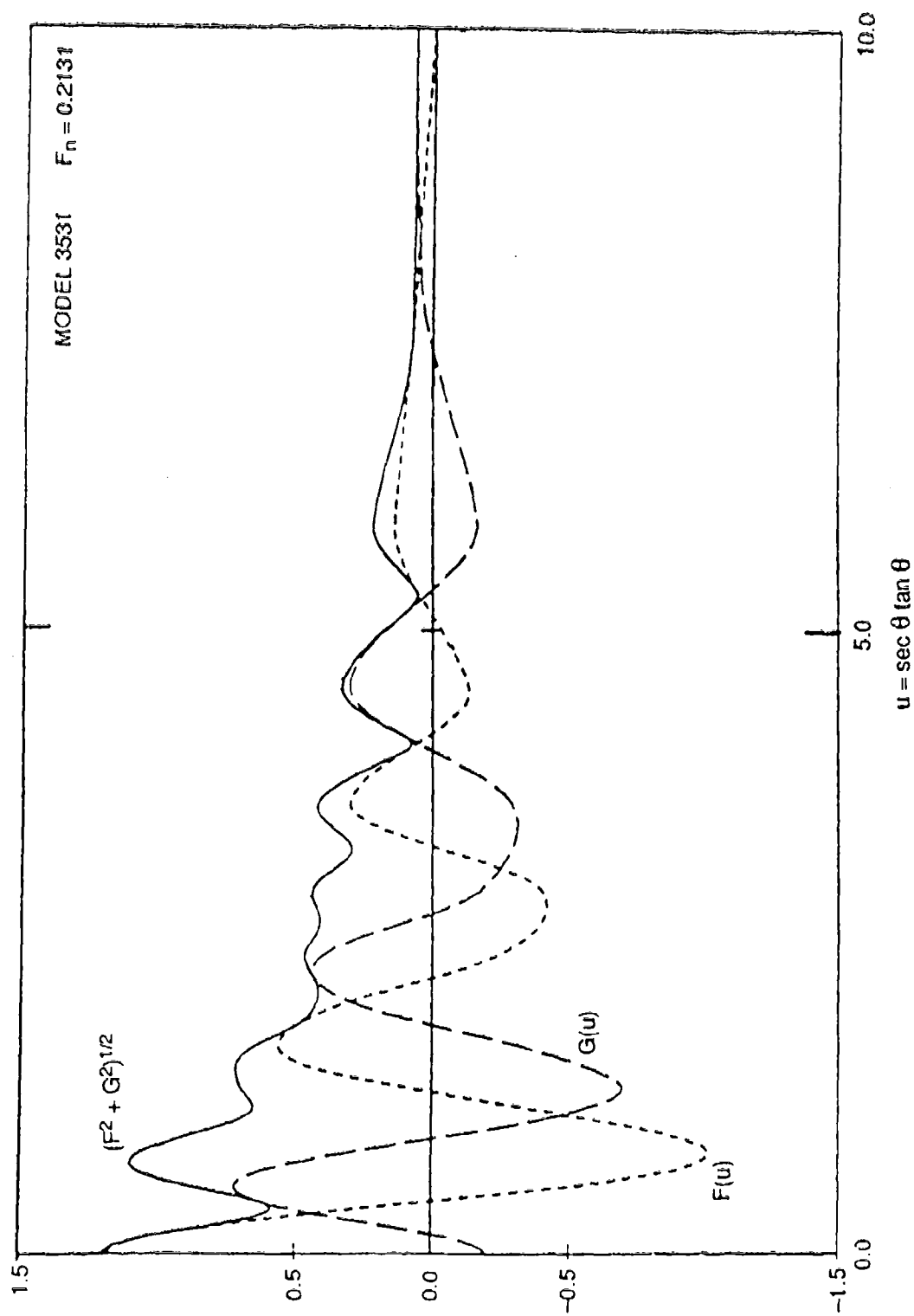


Fig. E.4. DOCTORS N-K prediction of wave spectrum for QUAPAW at $F_n = 0.2131$.

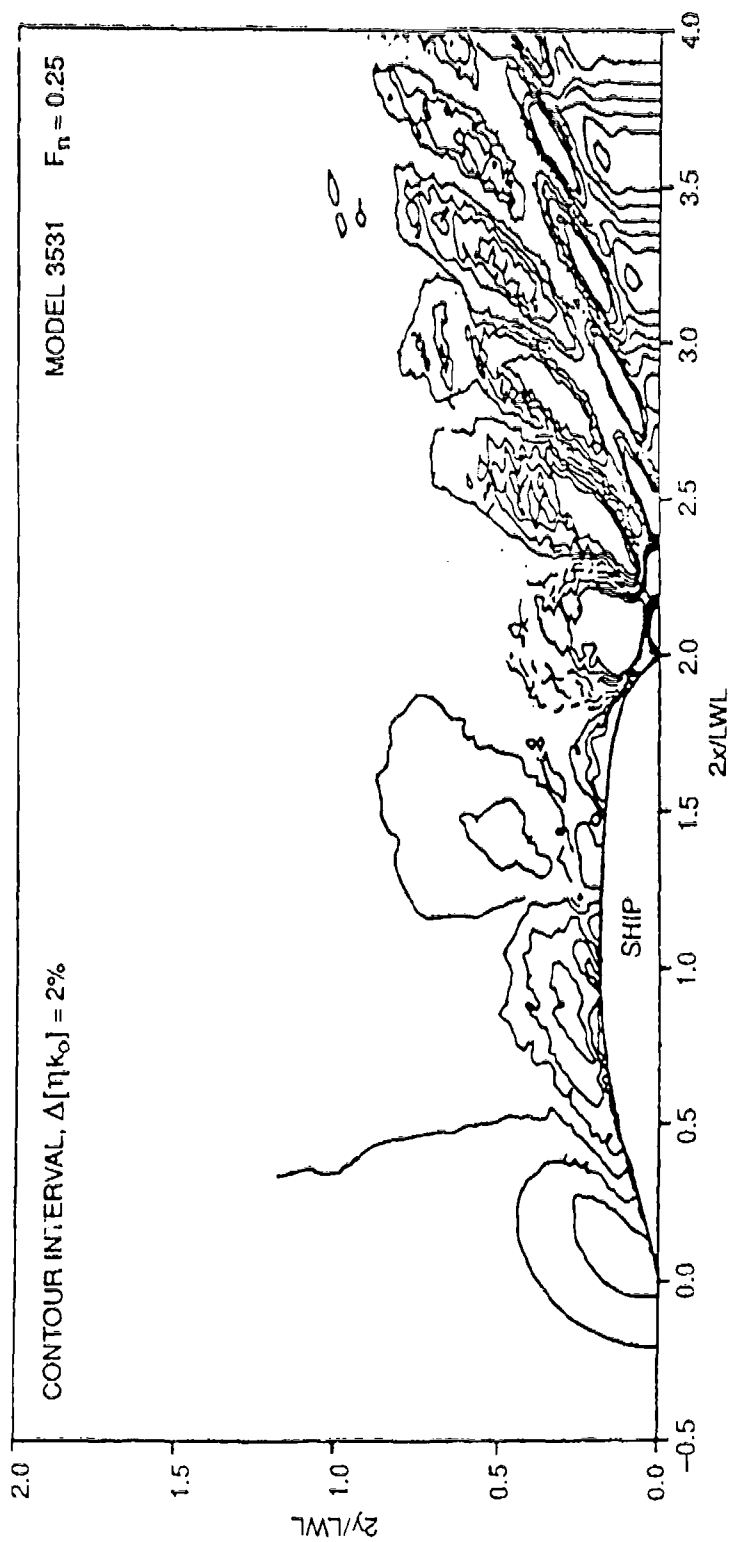


Fig. E.5. DOCTORS N-K prediction of wave contours ($-0.5 < 2x/LWL < 4$) for QUAPAW at $F_n = 0.25$.

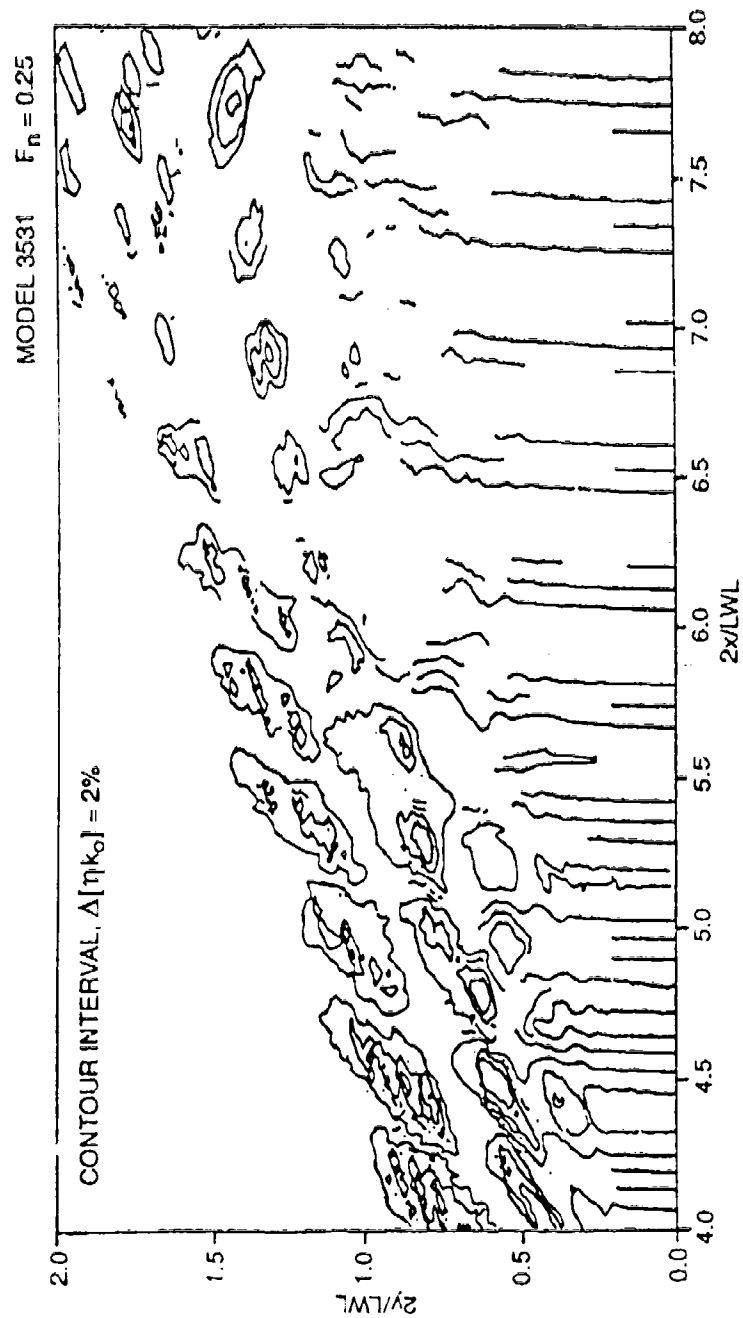


Fig. E.6. DOCTORS N-K prediction of wave contours ($4 < 2x/LWL < 8$) for QUAPAW at $F_n = 0.25$.

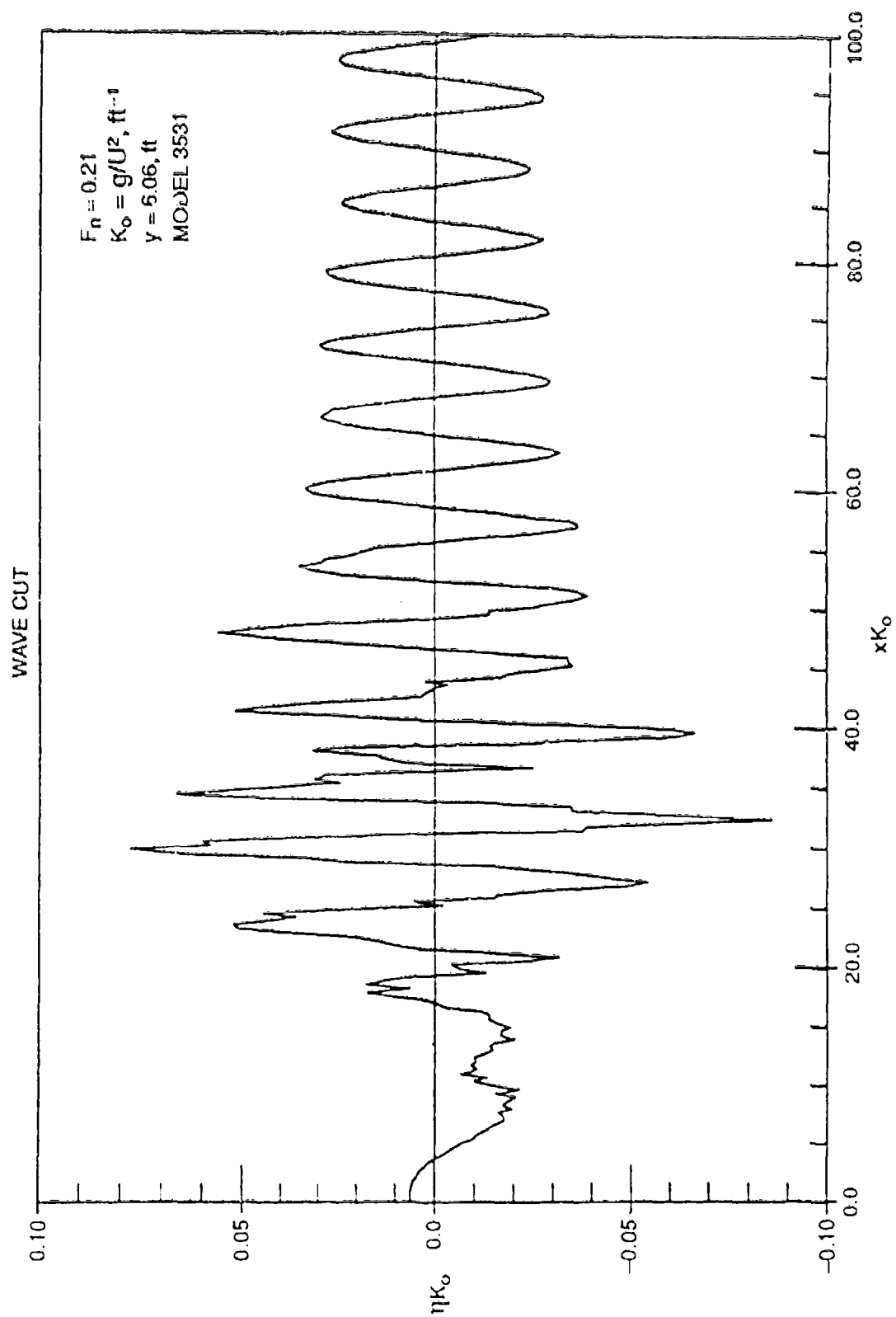


Fig. E.7. DOCTORS N-K prediction of wave contours for QUAPAW at $F_n = 0.25$.

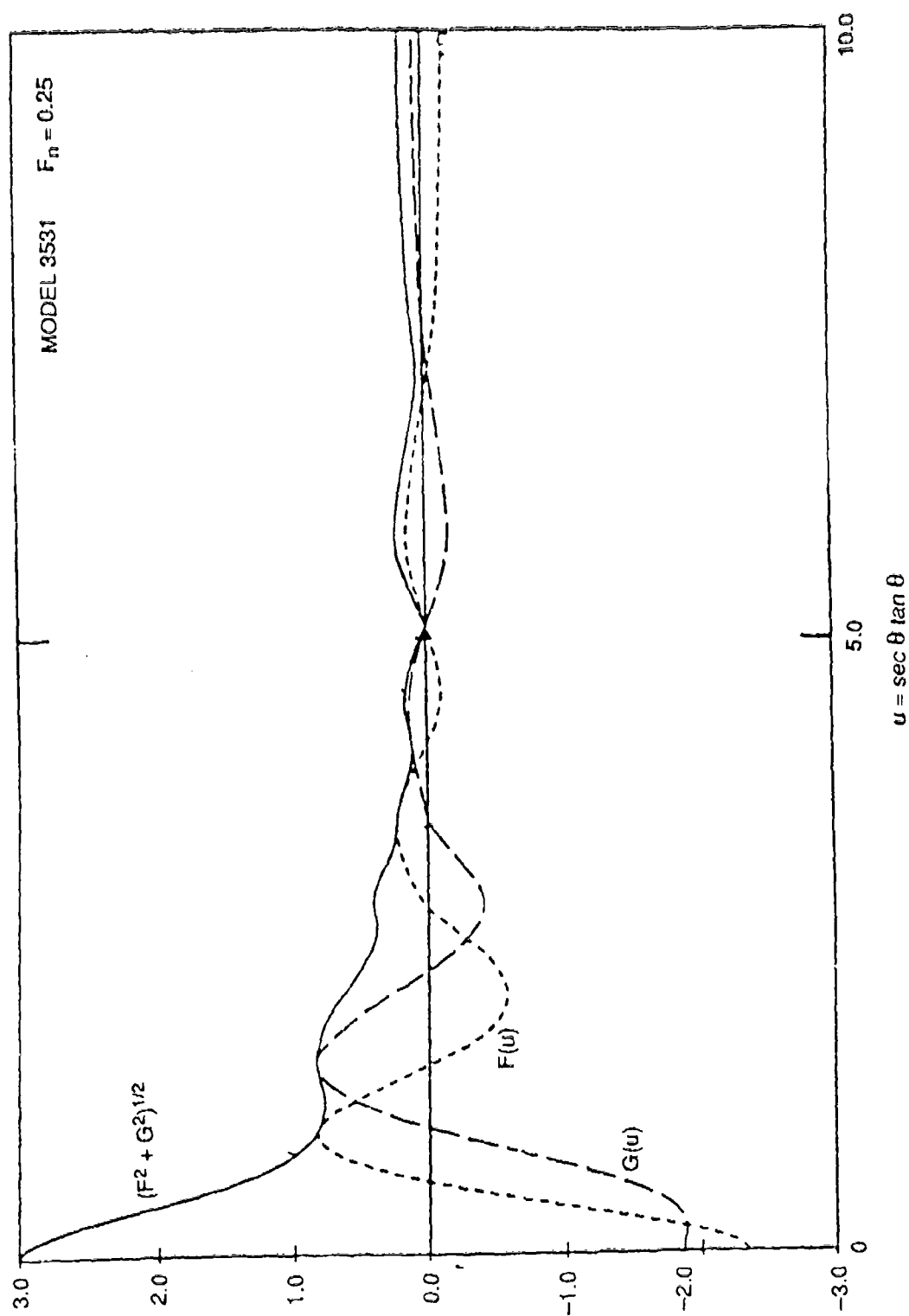


Fig. E.8. DOCTORS N-K prediction of wave spectrum for QUAPAW at $F_n = 0.25$.

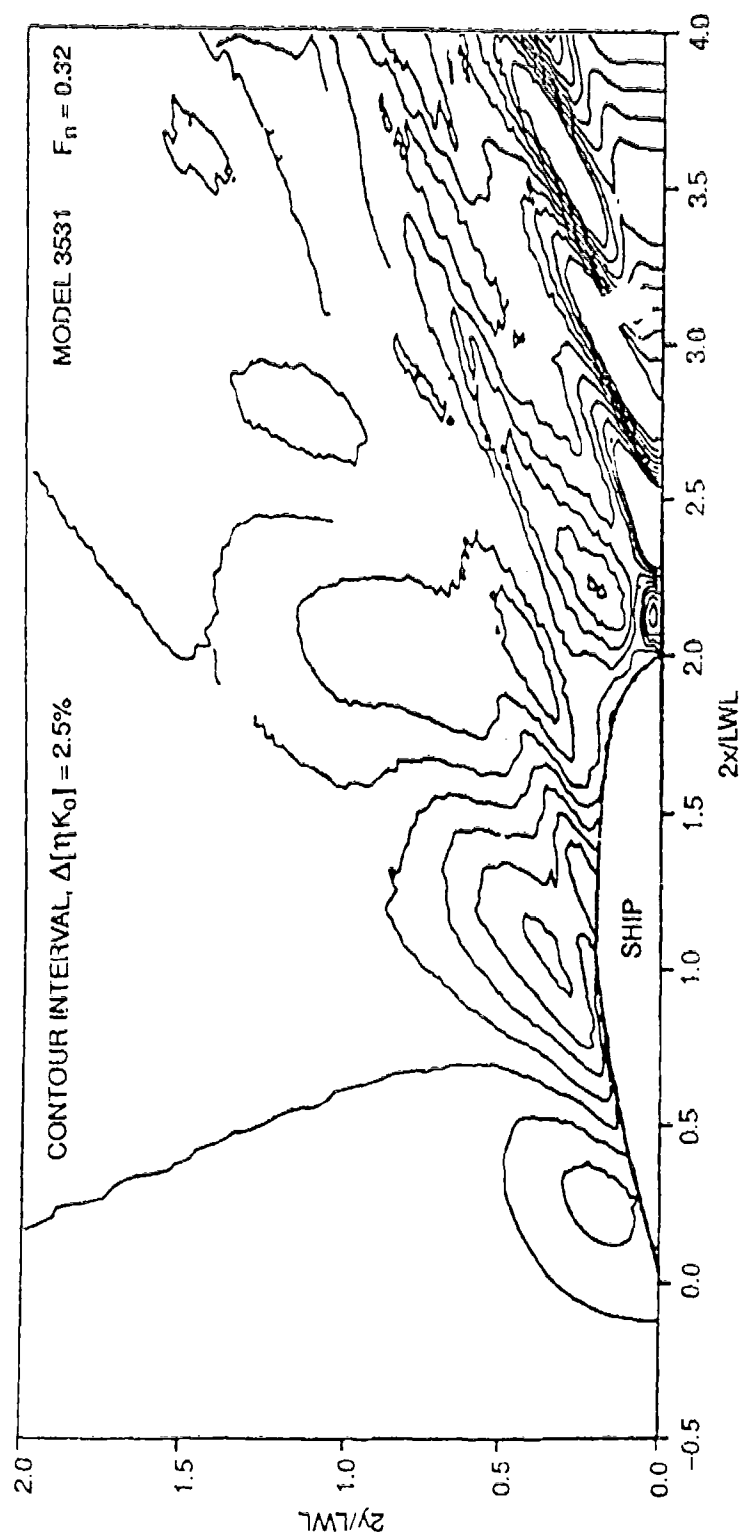


Fig. E.9. DOCTORS N-K prediction of wave contours ($-0.5 < 2x/LWL < 4$) for QUAPAW at $F_n = 0.3197$.

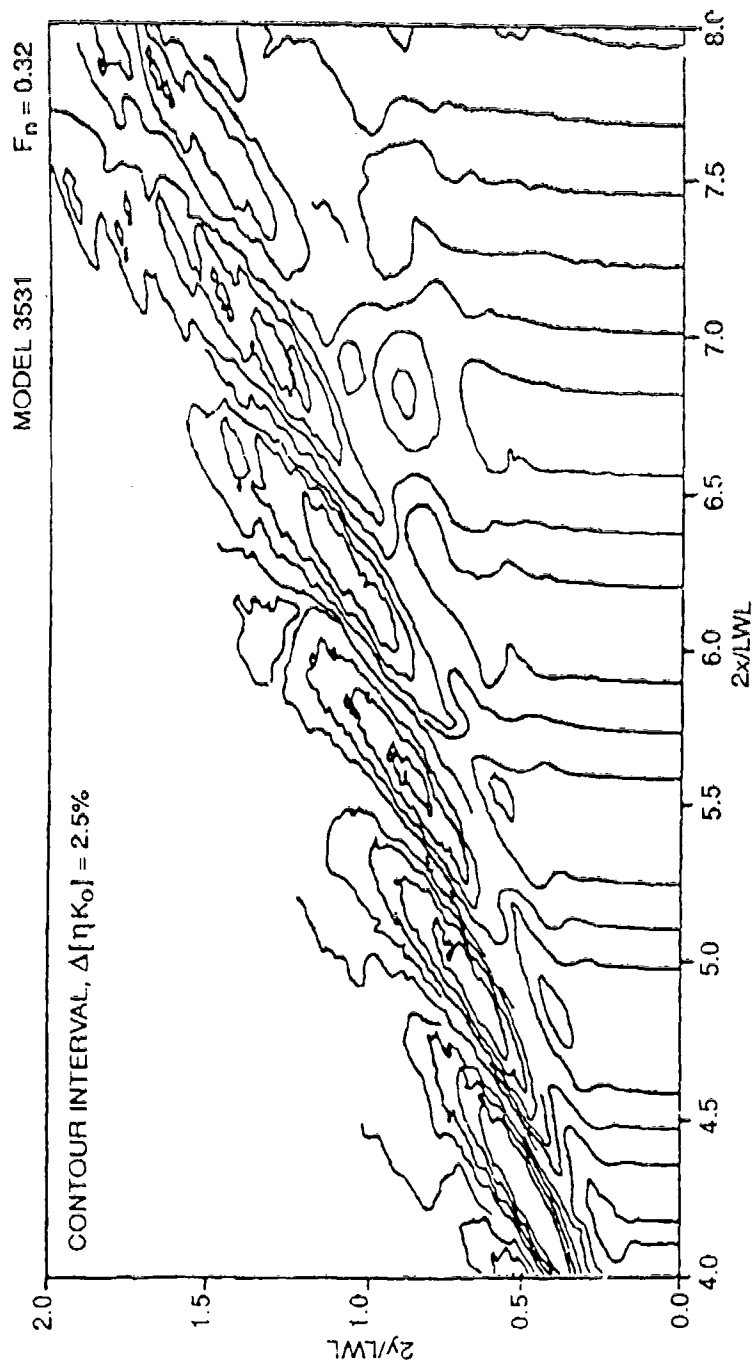


Fig. E.10. DOCTORS N-K prediction of wave contours ($4 < 2x/LWL < 8$) for QUAPAW at $F_n = 0.3197$.

WAVE CUT

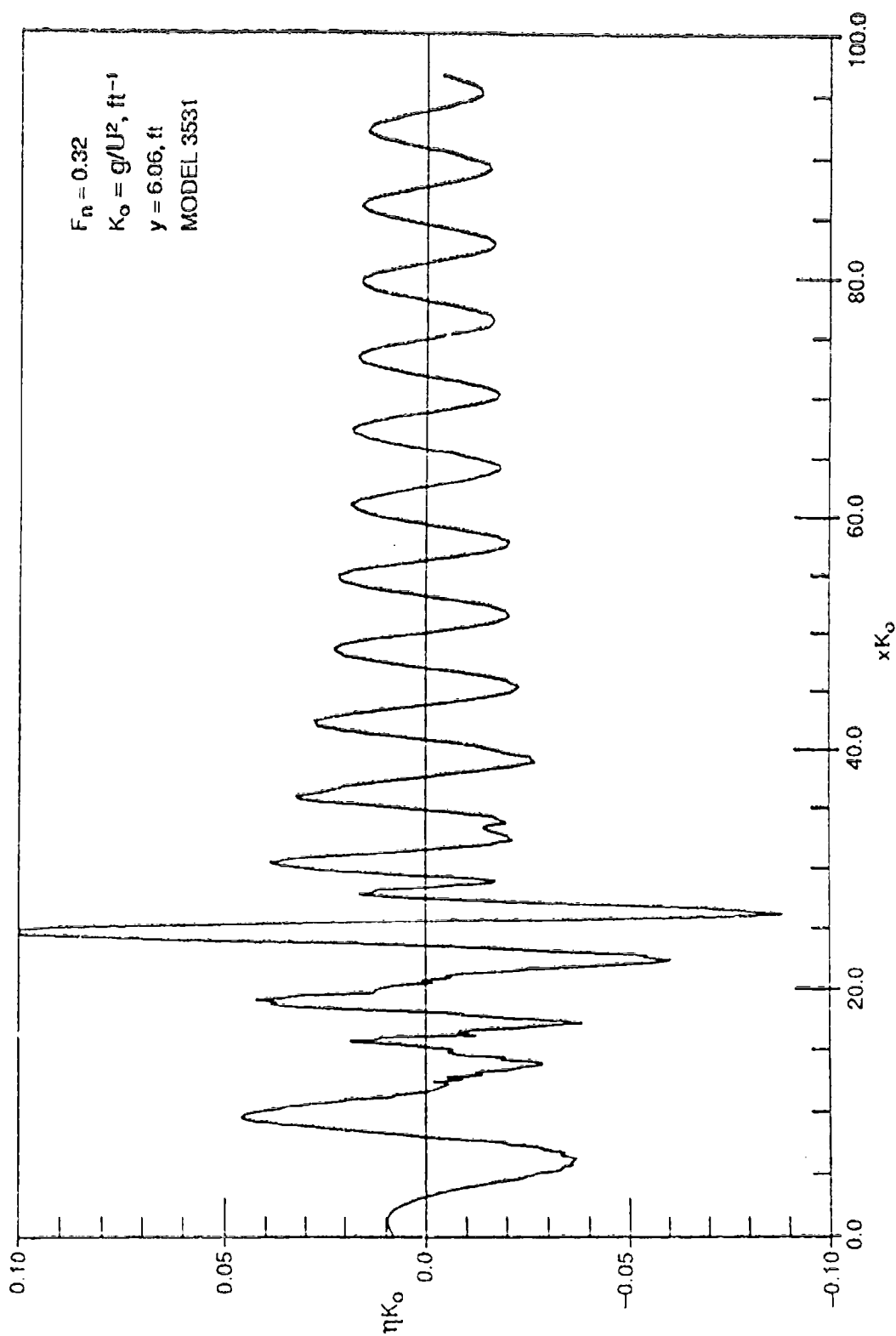


Fig. E.11. DOCTORS N-K prediction of wave contours for QUAPAW at $F_n = 0.3197$.

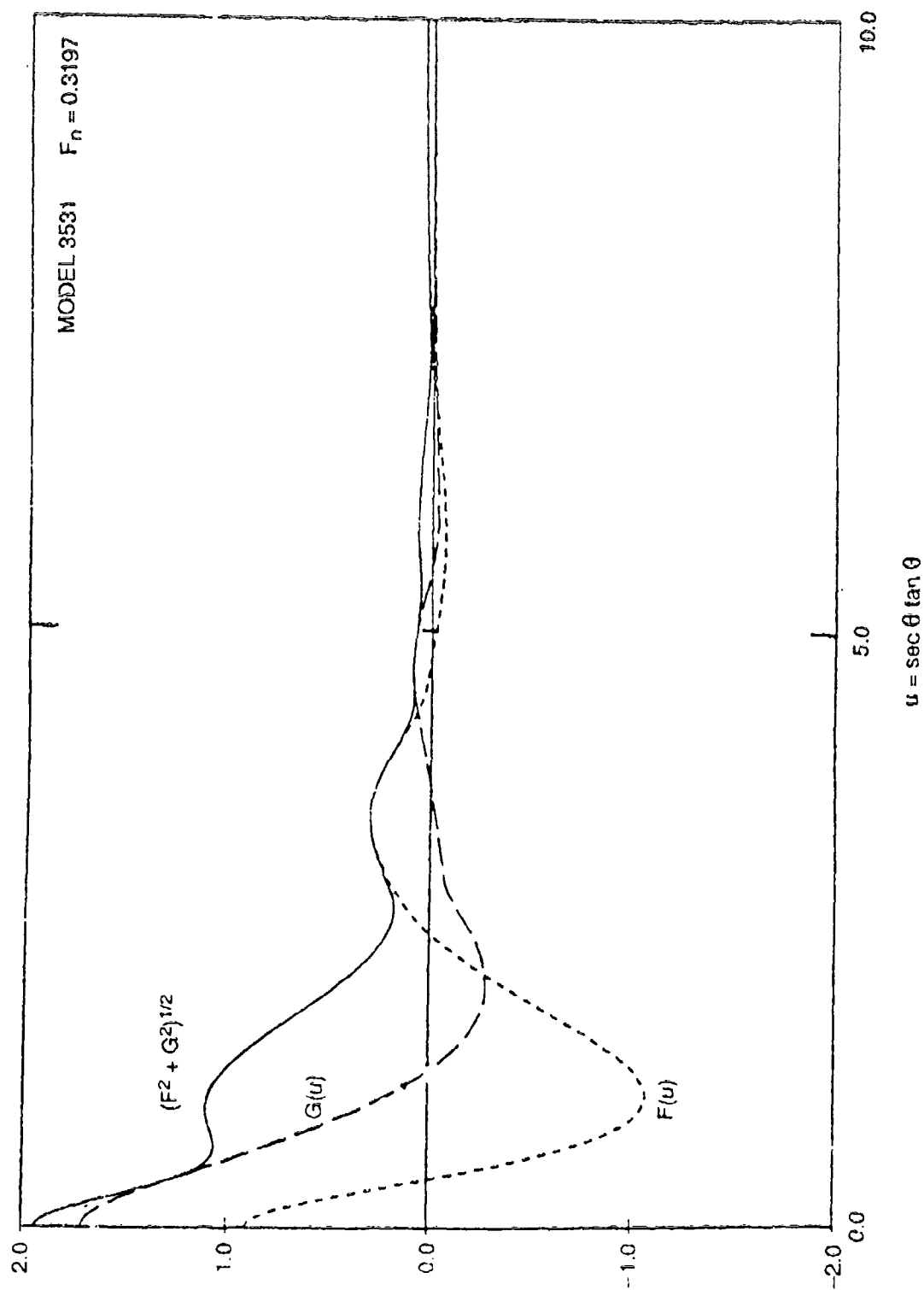


Fig. E.12. DOCTORS N-K prediction of wave spectrum for QUAPAW at $F_n = 0.3197$.

APPENDIX F
SWIFT PREDICTIONS

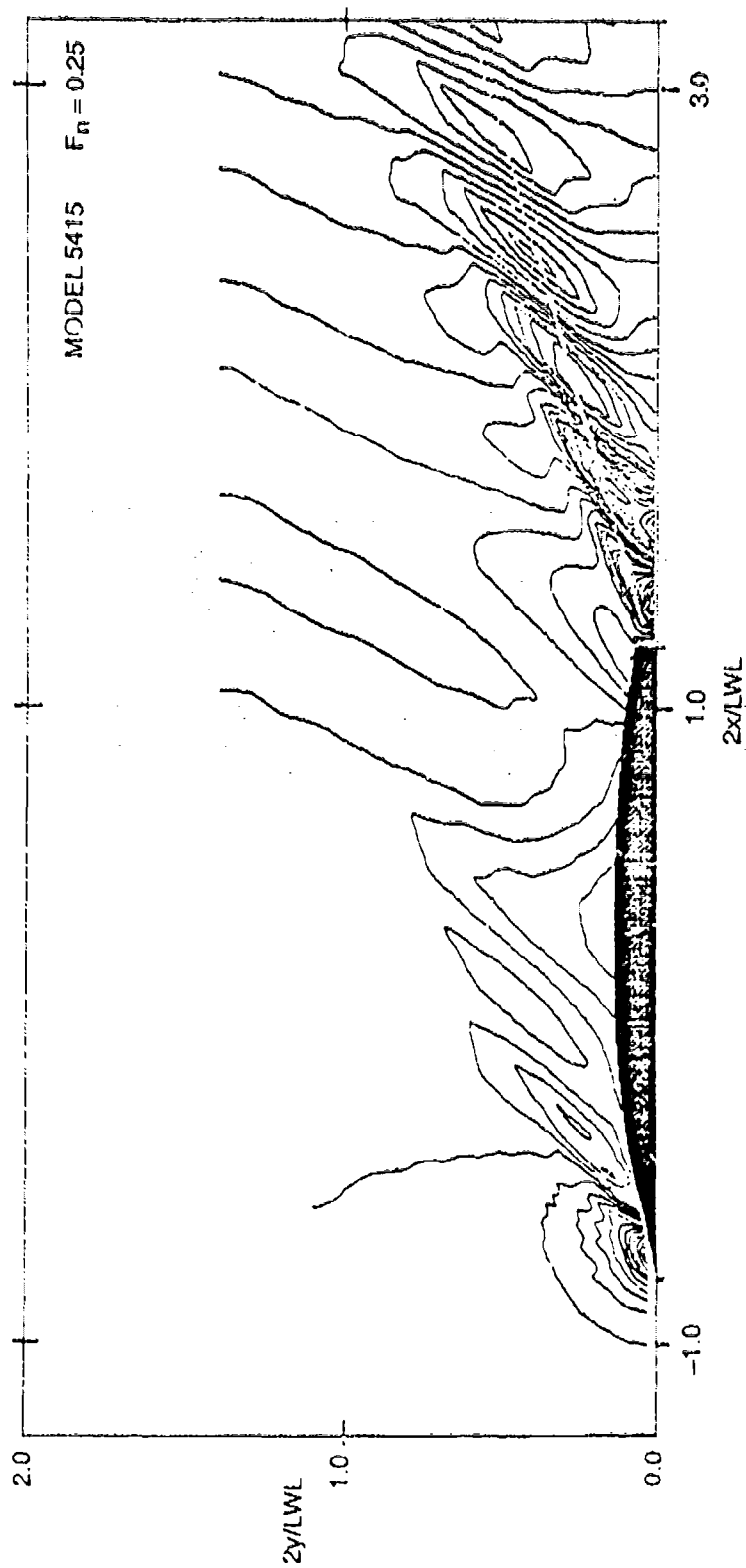


Fig. F.1. SWIFT prediction of wave contours ($0.5 < 2x/LWL < 8$) for Model 5415 at $F_n = 0.25$.

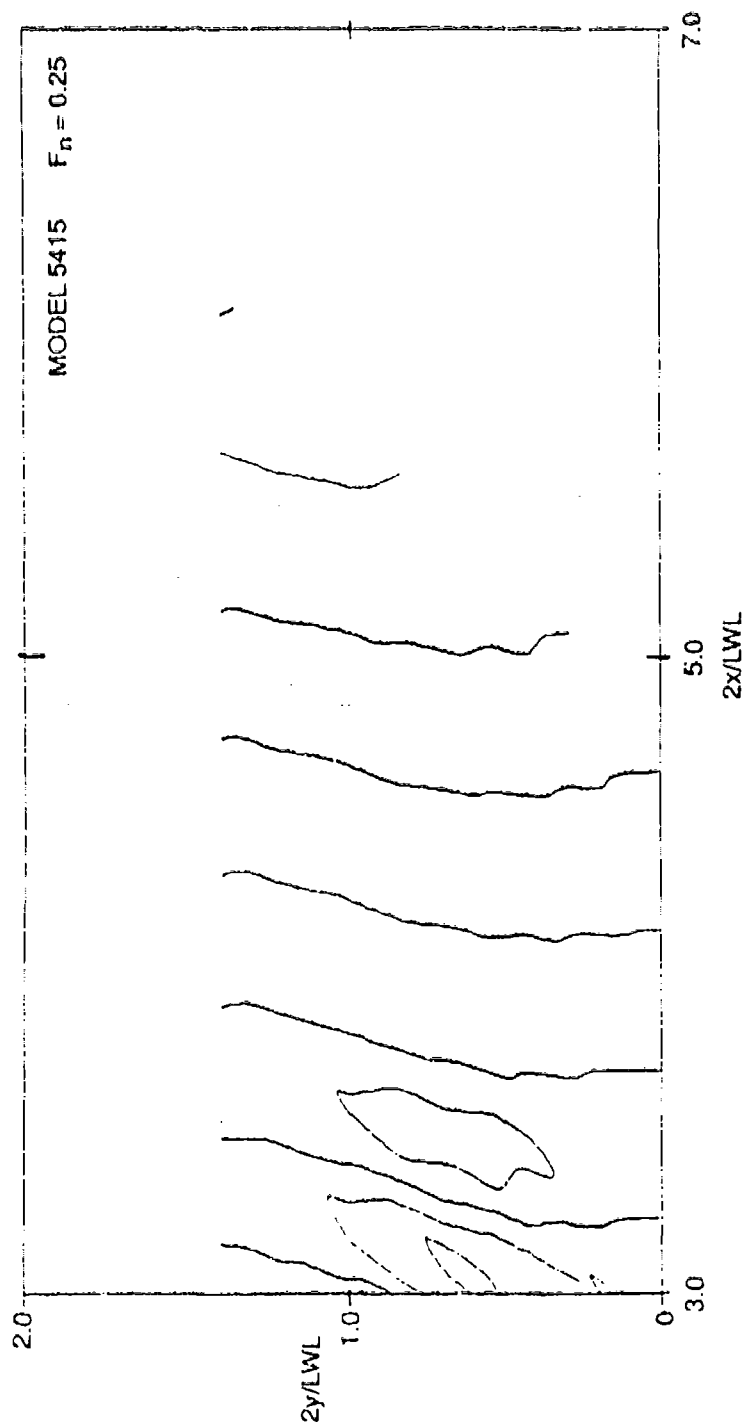


Fig. F.2. SWIFT prediction of wave contours ($4 < 2x/LWL < 8$) for Model 5415 at $F_n = 0.25$.

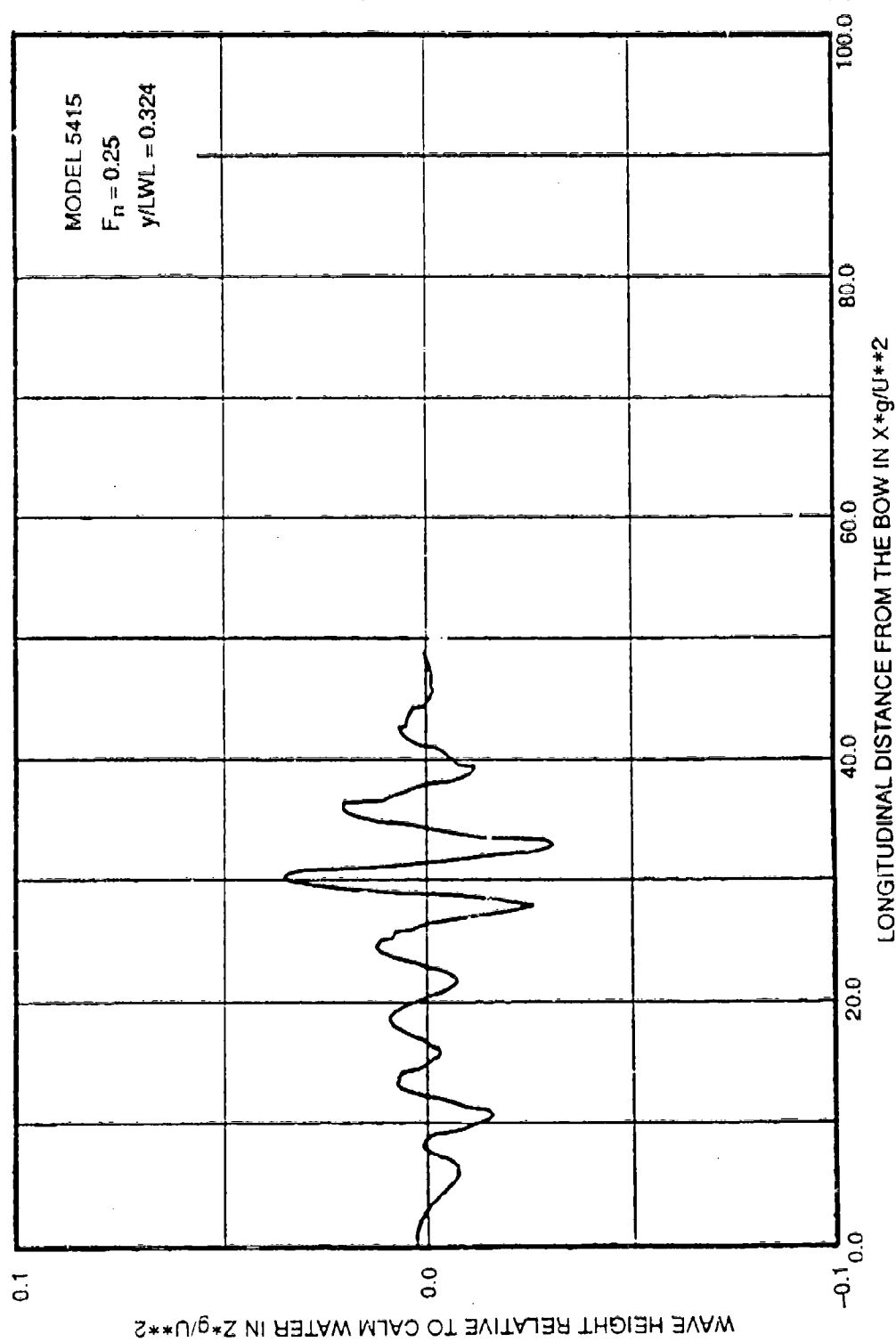


Fig. F.3. SWIFT prediction of wave cut for Model 5415 at $F_n = 0.250$.

MODEL 5415 $F_n = 0.2755$

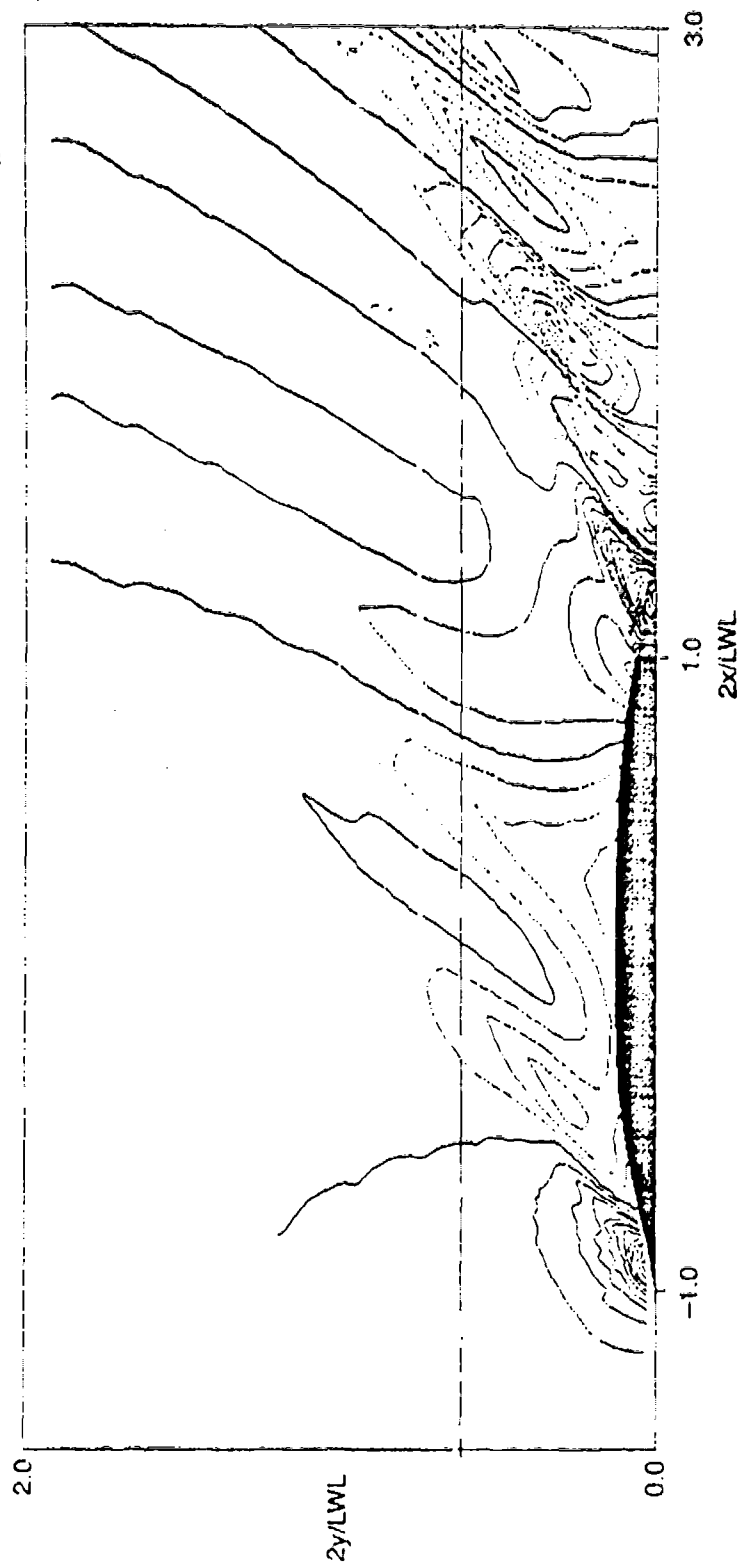


Fig. F.4. SWIFT prediction of wave contours ($-0.5 < 2x/LWL < 4$) for Model 5415 at $F_n = 0.2755$.

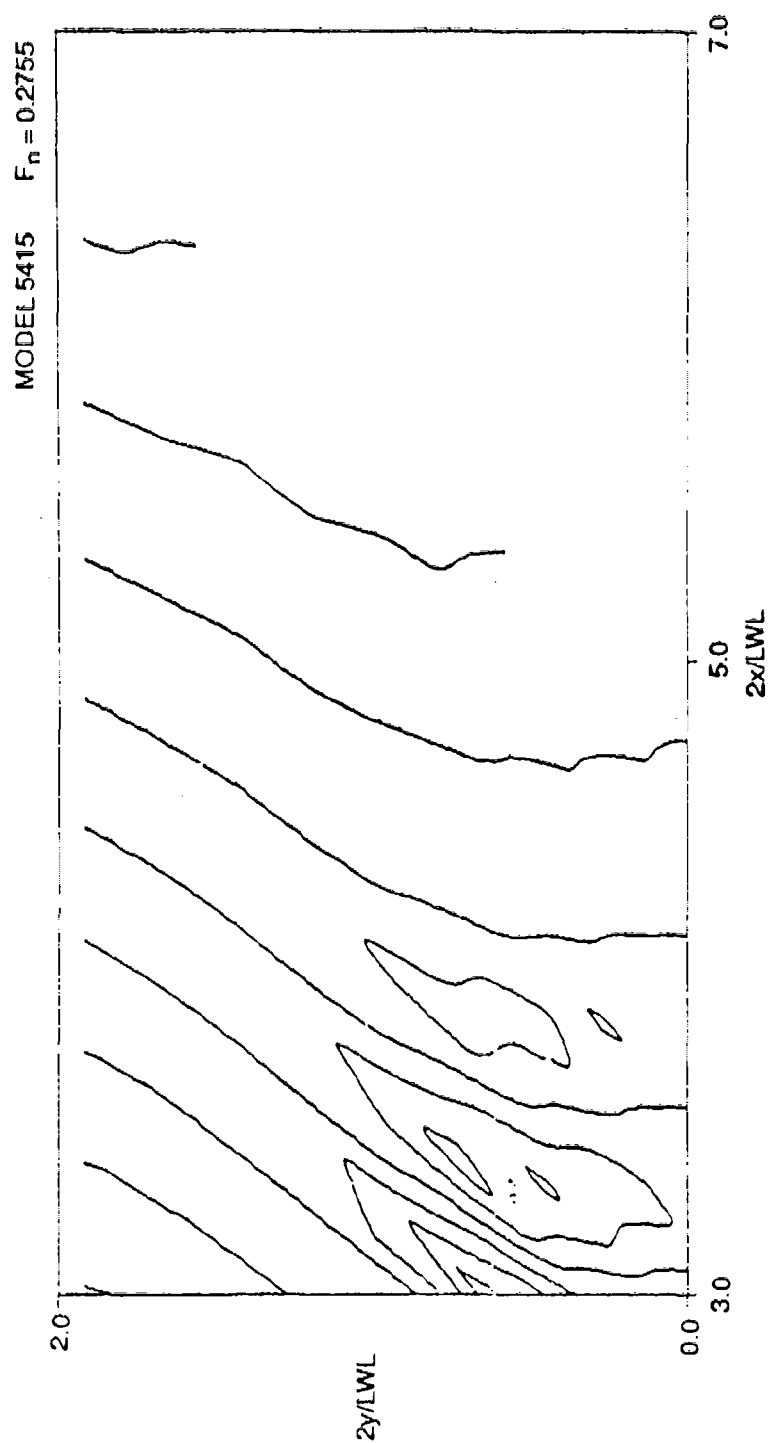


Fig. F.5. SWIFT prediction of wave contours ($4 < 2x/LWL < 8$) for Model 5415 at $F_n = 0.2755$.

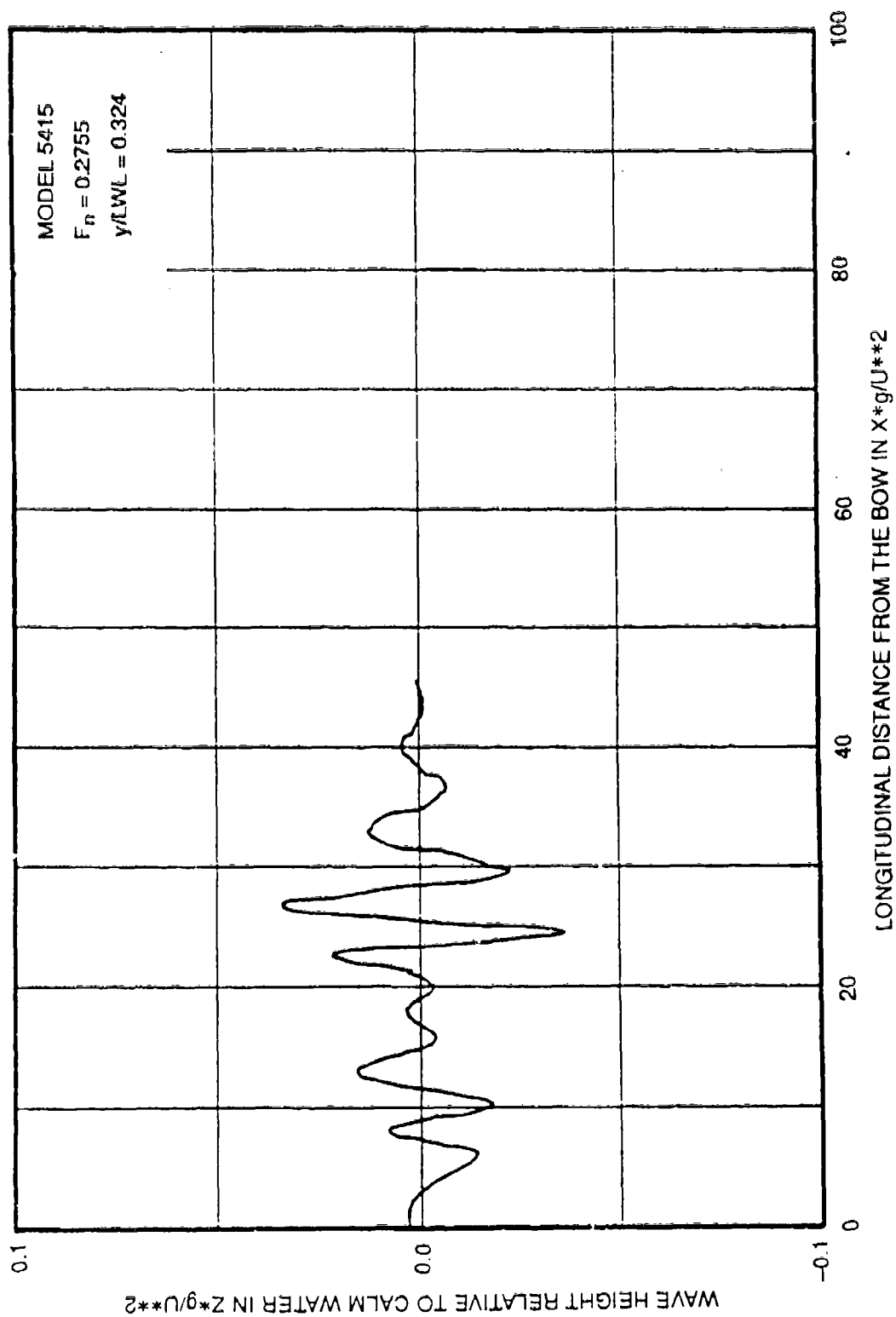


Fig. F.6. SWIFT prediction of wave cut for Model 5415 at $F_n = 0.2755$.

MODEL 5415 $F_n = 0.4136$

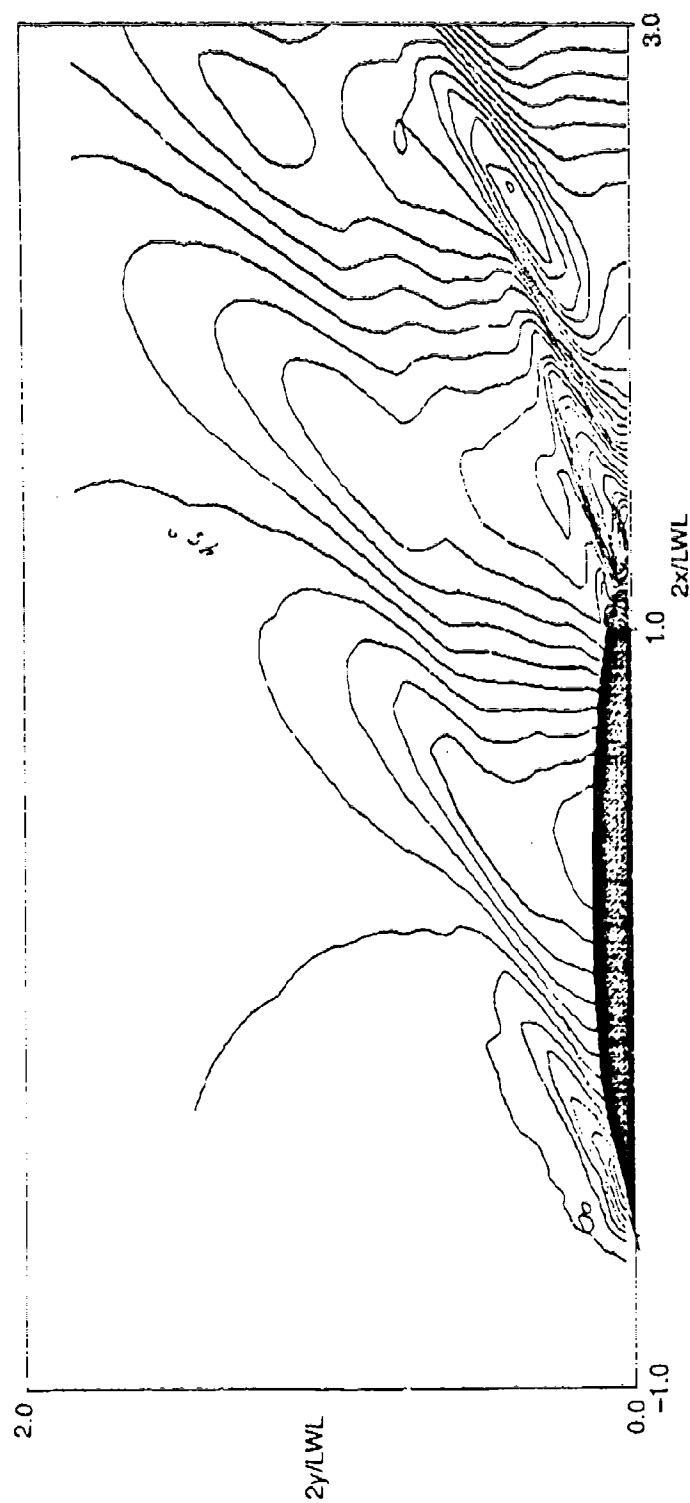


Fig. F.7. SWIFT prediction of wave contours ($-0.5 < 2x/LWL < 4$) for Model 5415 at $F_n = 0.4136$.

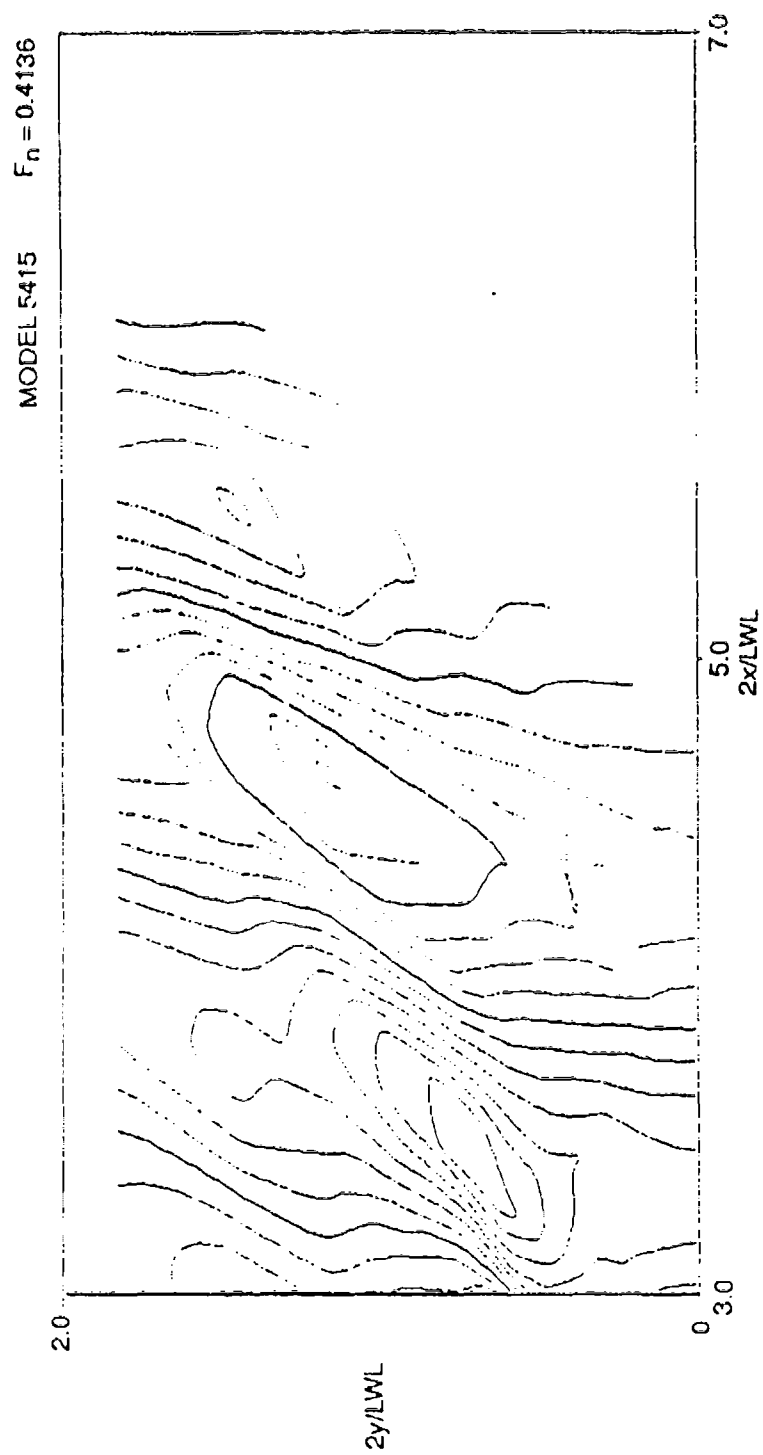


Fig. F.8. SWIFT prediction of wave contours ($4 < 2x/LWL < 8$) for Model 5415 at $F_n = 0.4136$.

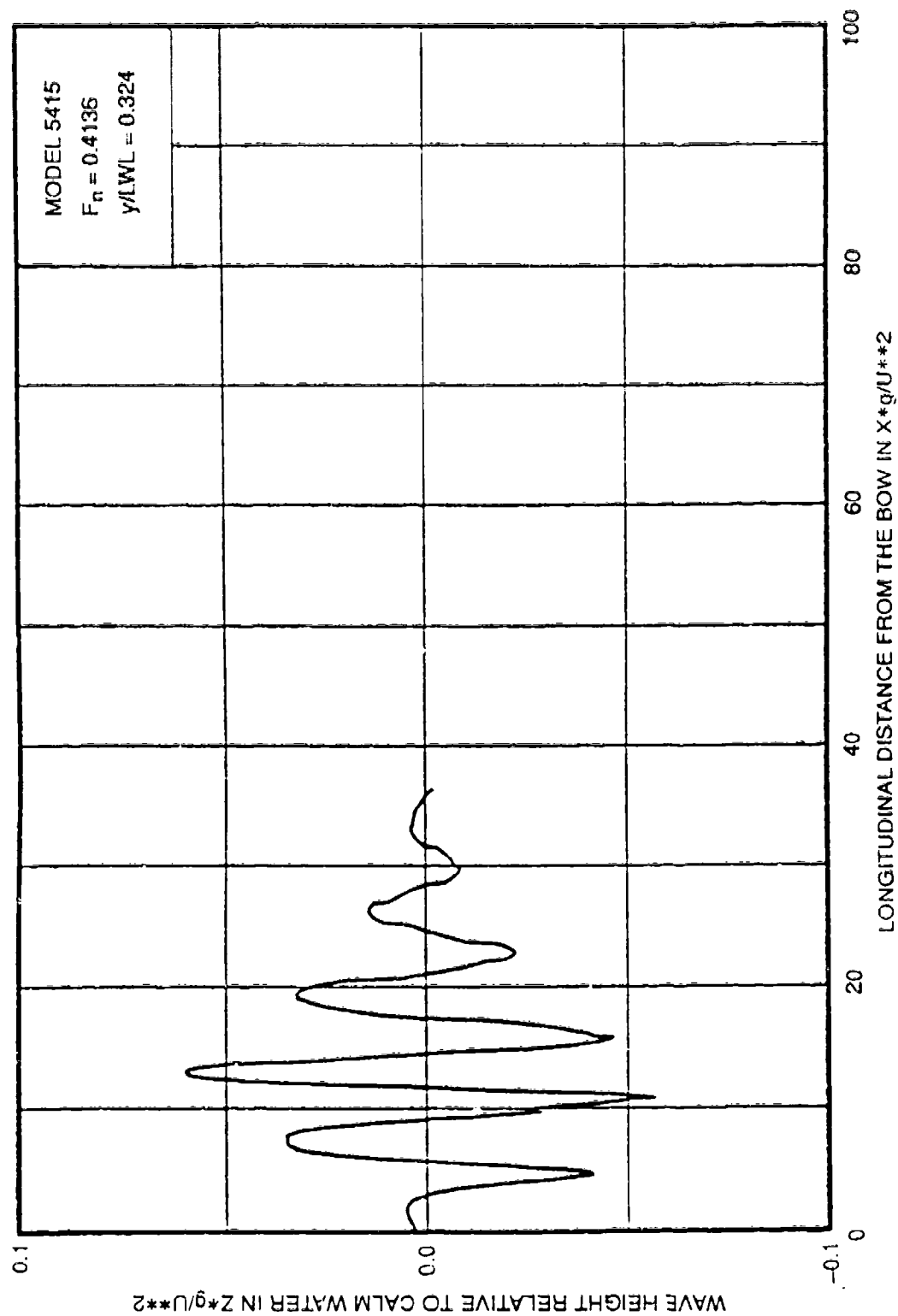


Fig. F.9. SWIFT prediction of wave cut for Model 5415 at $F_n = 0.4136$.

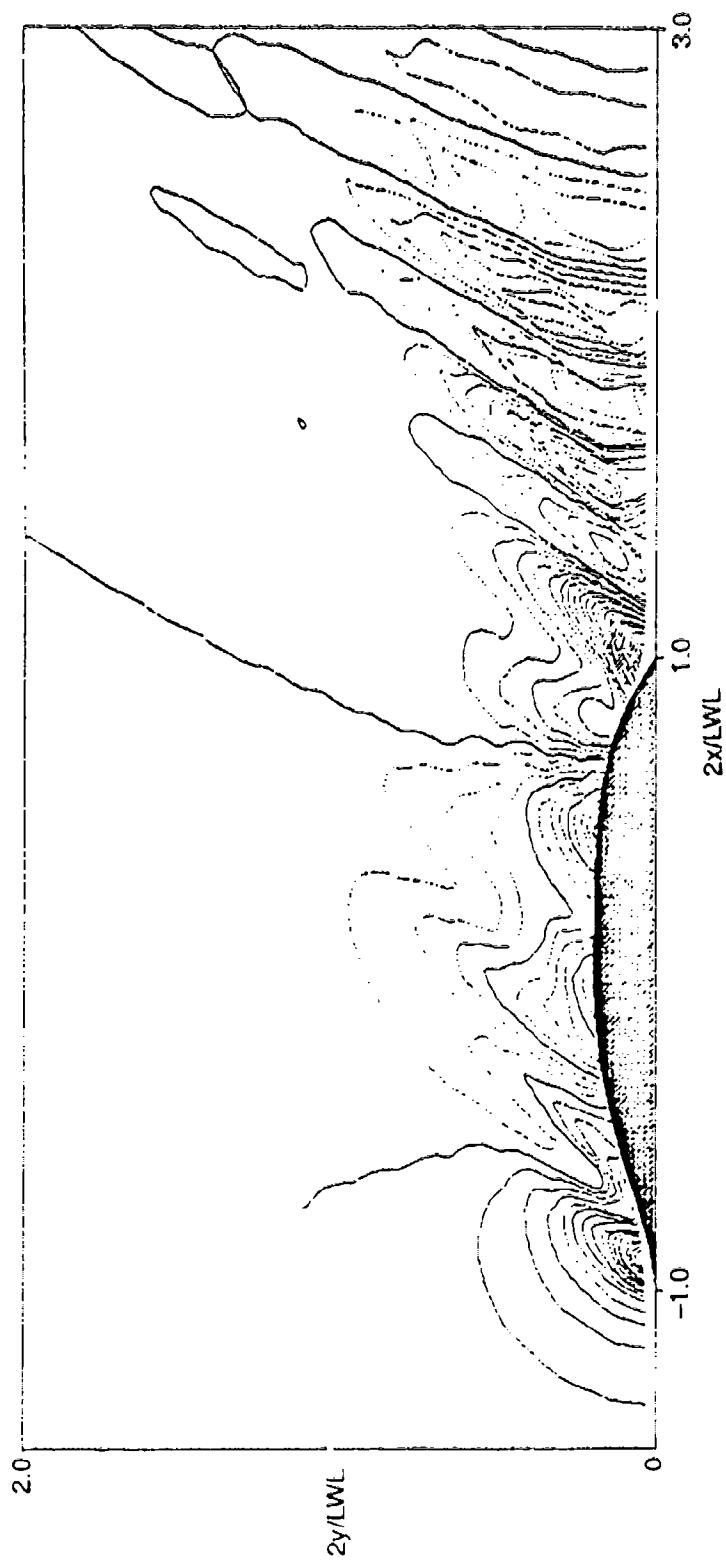


Fig. F.10. SWIFT prediction of wave contours ($-0.5 < 2x/LWL < 4$) for QUIAPAW at $F_n = 0.2131$.

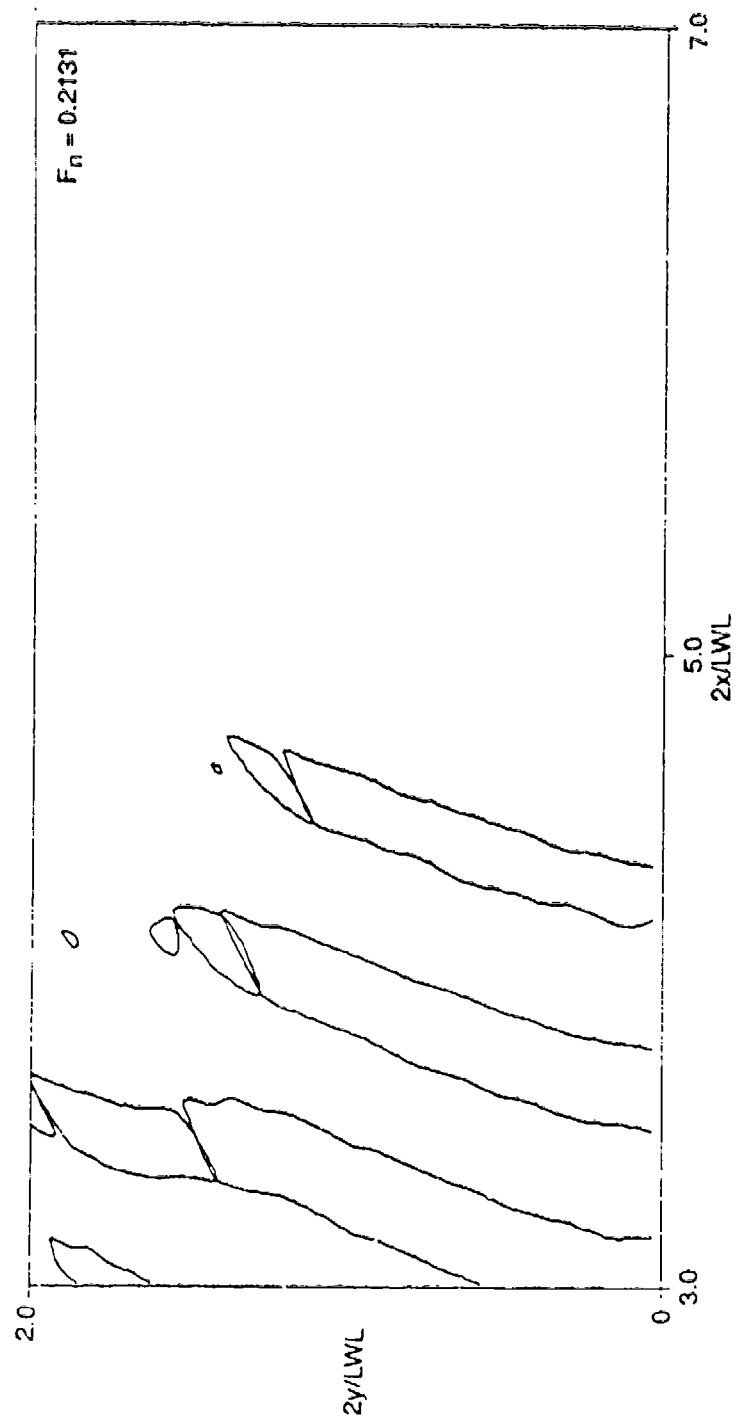


Fig. F.11. SWIFT prediction of wave contours ($4 < 2x/LWL < 8$) for QUAPAW at $F_n = 0.2131$.

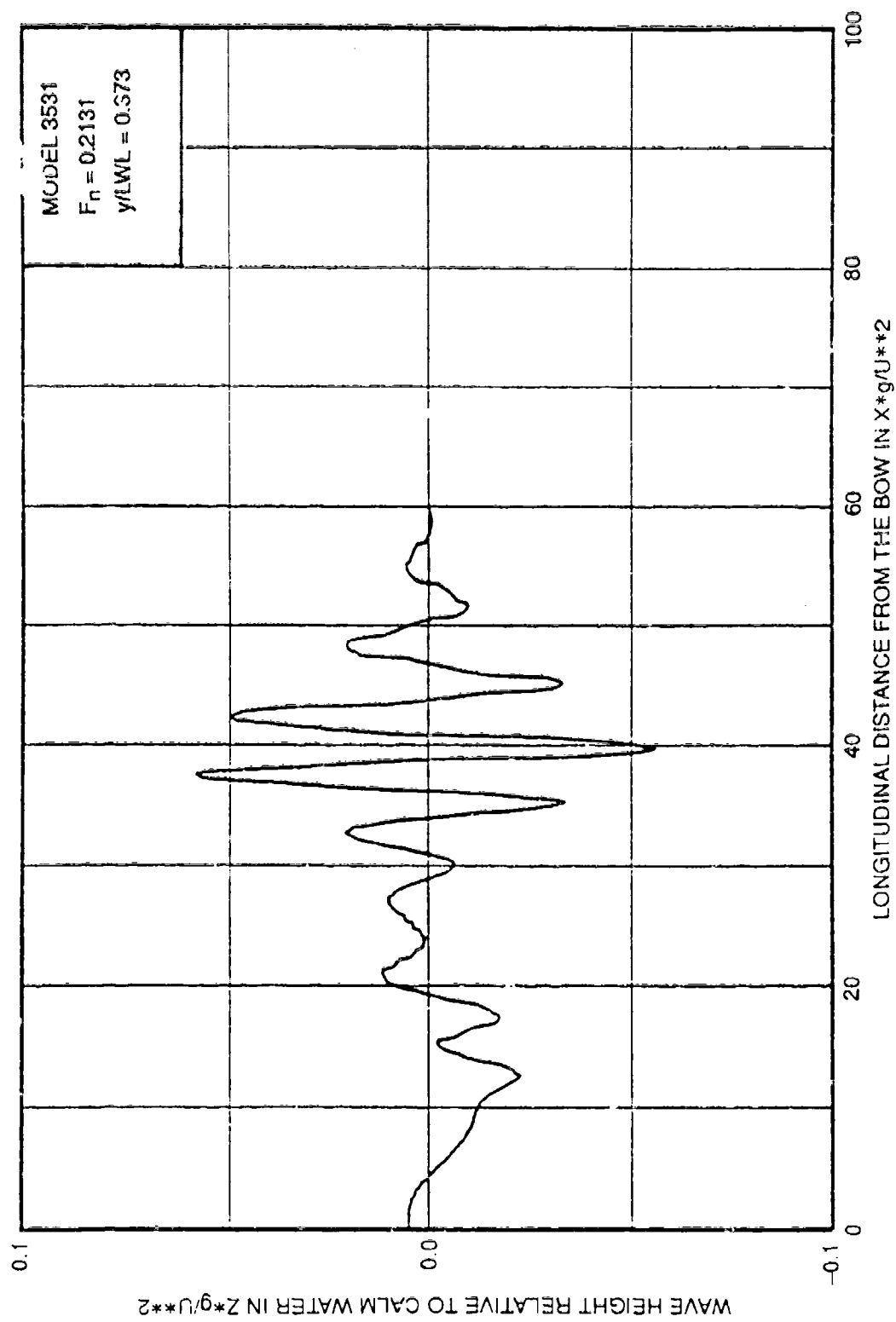


Fig. F.12. SWIFT prediction of wave cut for QUJAPAW at $F_n = 0.2131$.

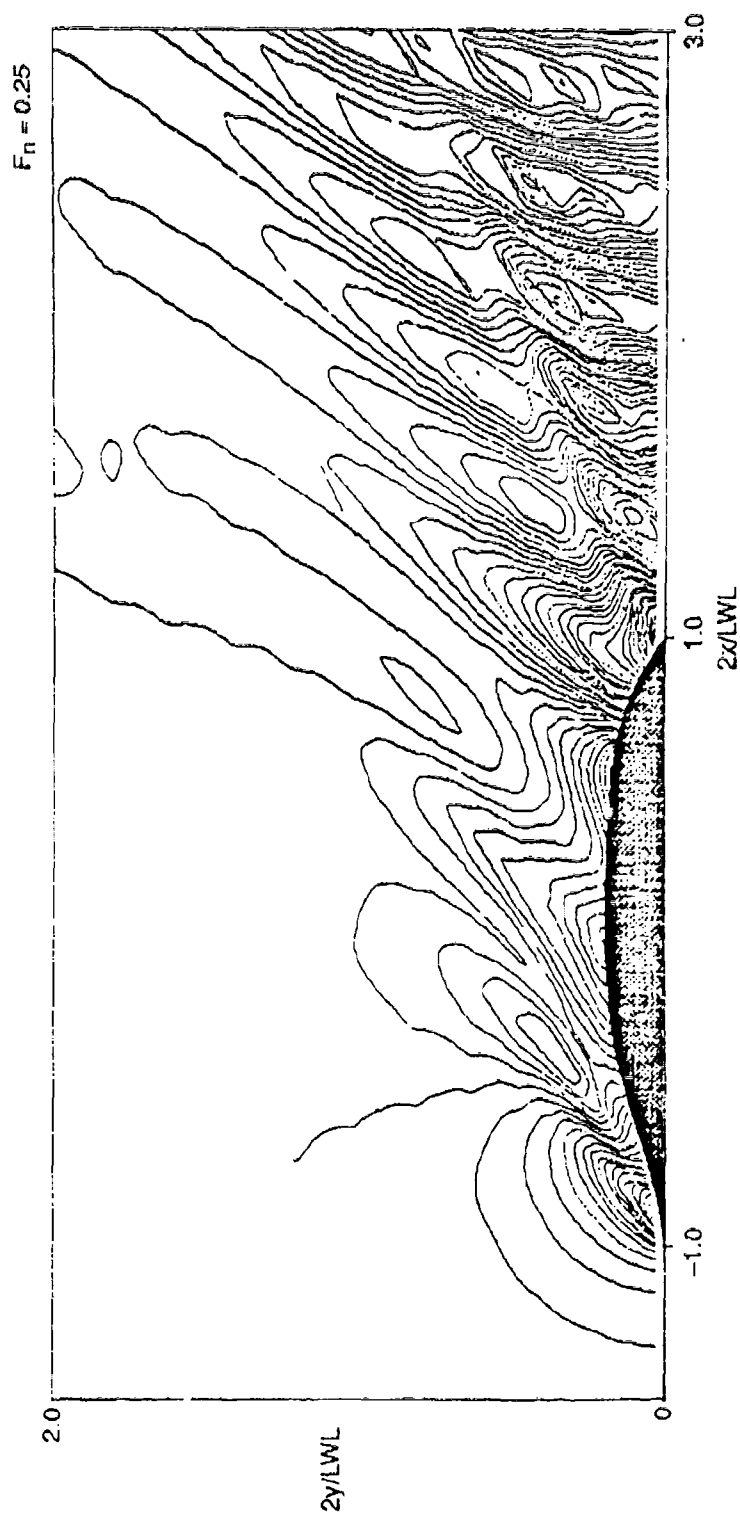


Fig. F.13. SWIFT prediction of wave contours ($-0.5 < 2x/LWL < 4$) for QUAPAW at $F_n = 0.25$.

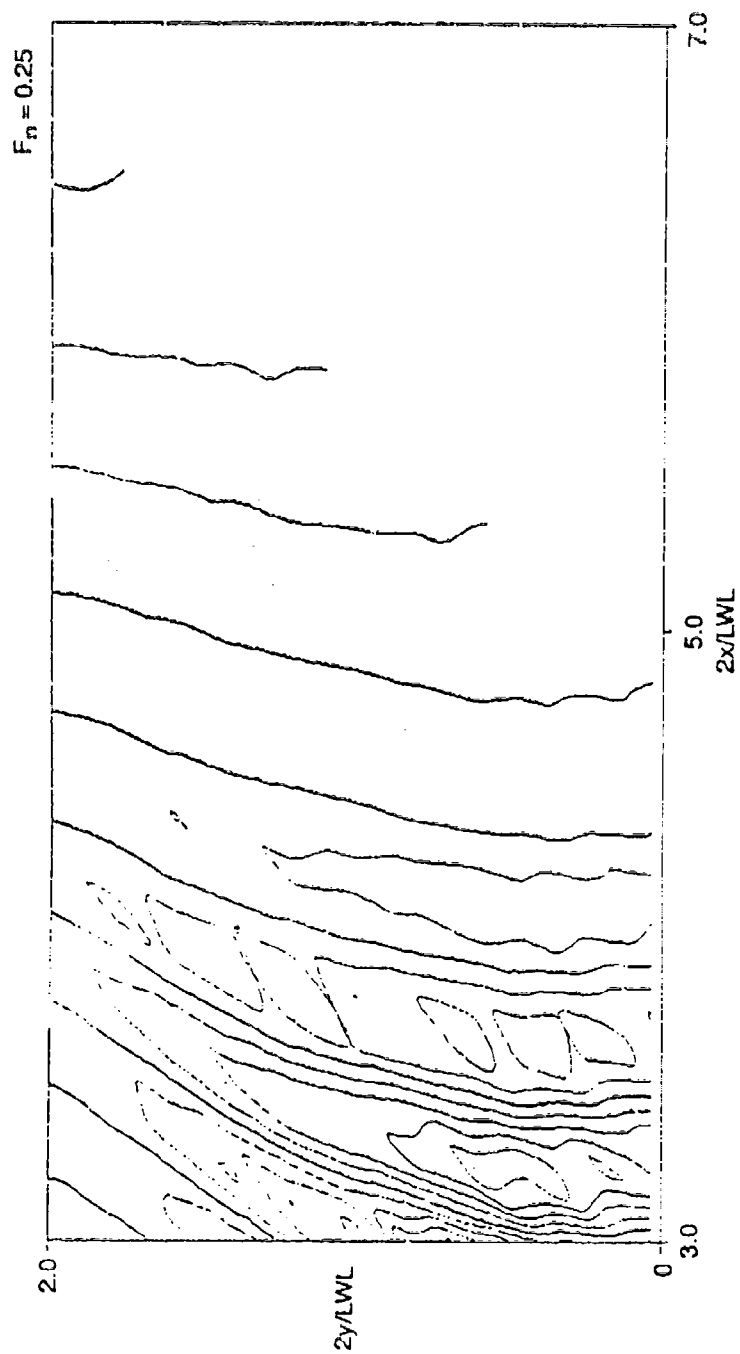


Fig. F.14. SWIFT prediction of wave contours ($4 < 2x/LWL < 8$) for QUAPAW at $F_n = 0.25$.

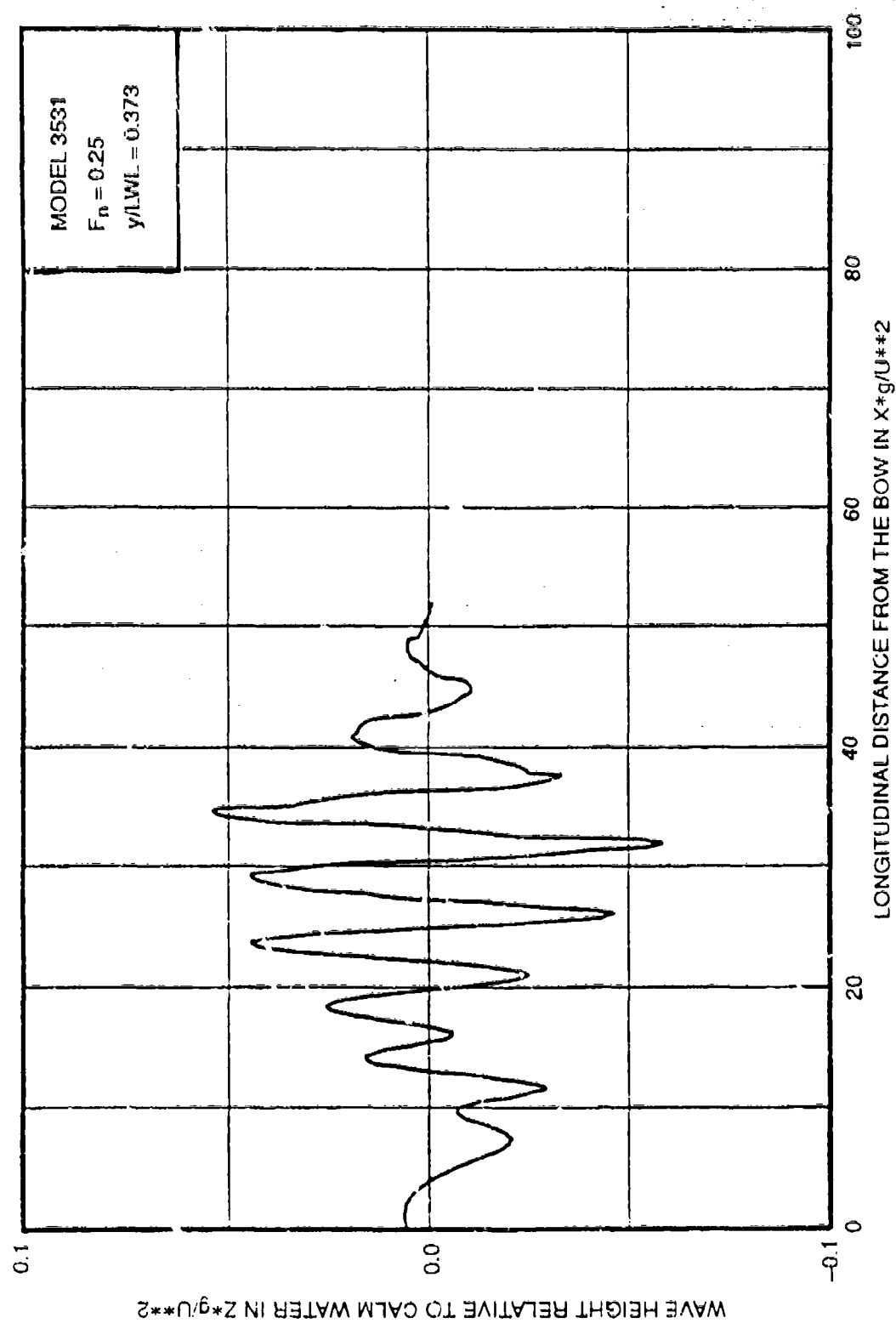


Fig. F.15. SWIFT prediction of wave cut for QUAPAW at $F_n = 0.25$.

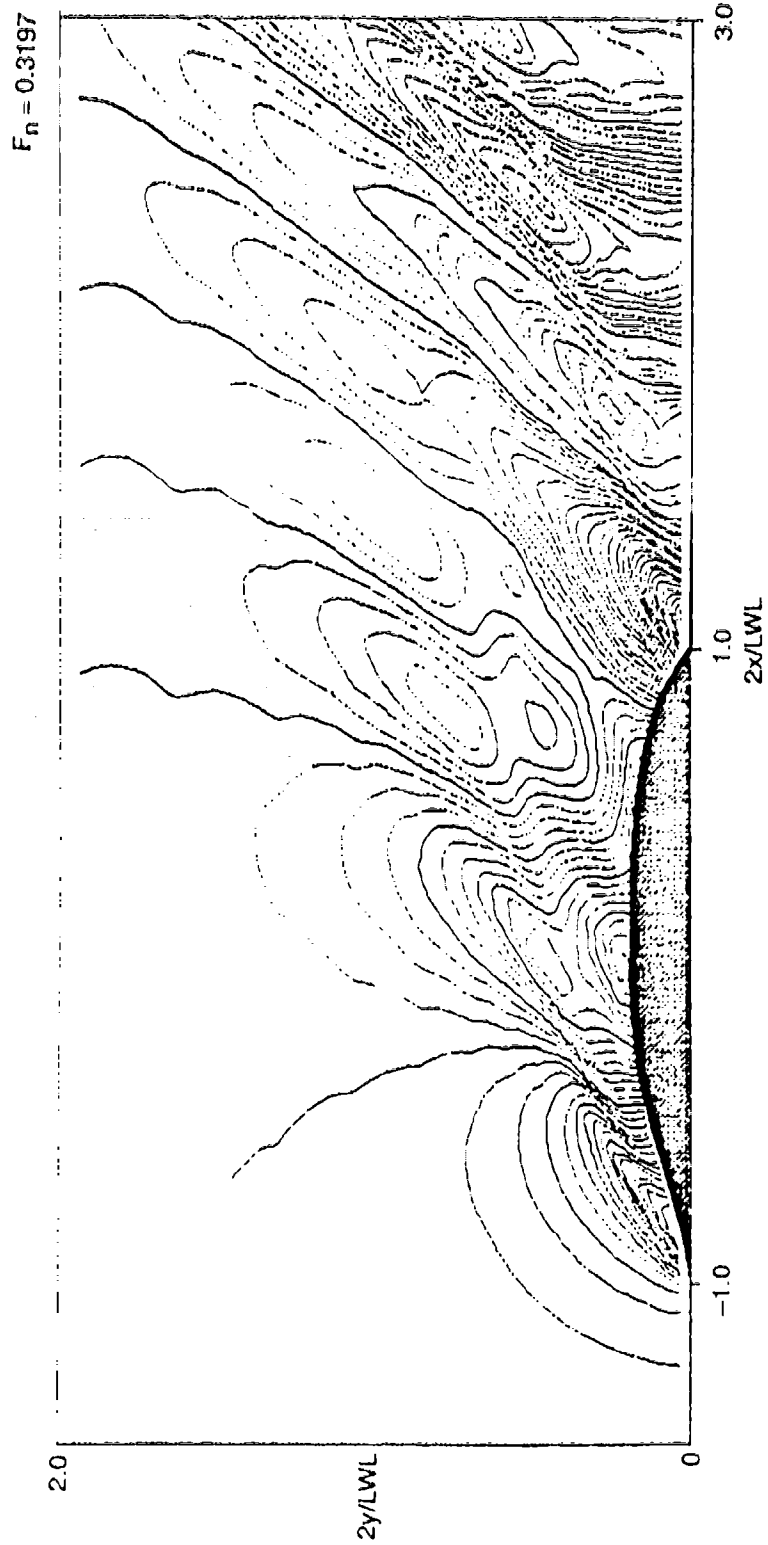


Fig. F.16. SWIFT prediction of wave contours ($-0.5 < 2x/LWL < 4$) for QUAPAW at $F_n = 0.3197$.

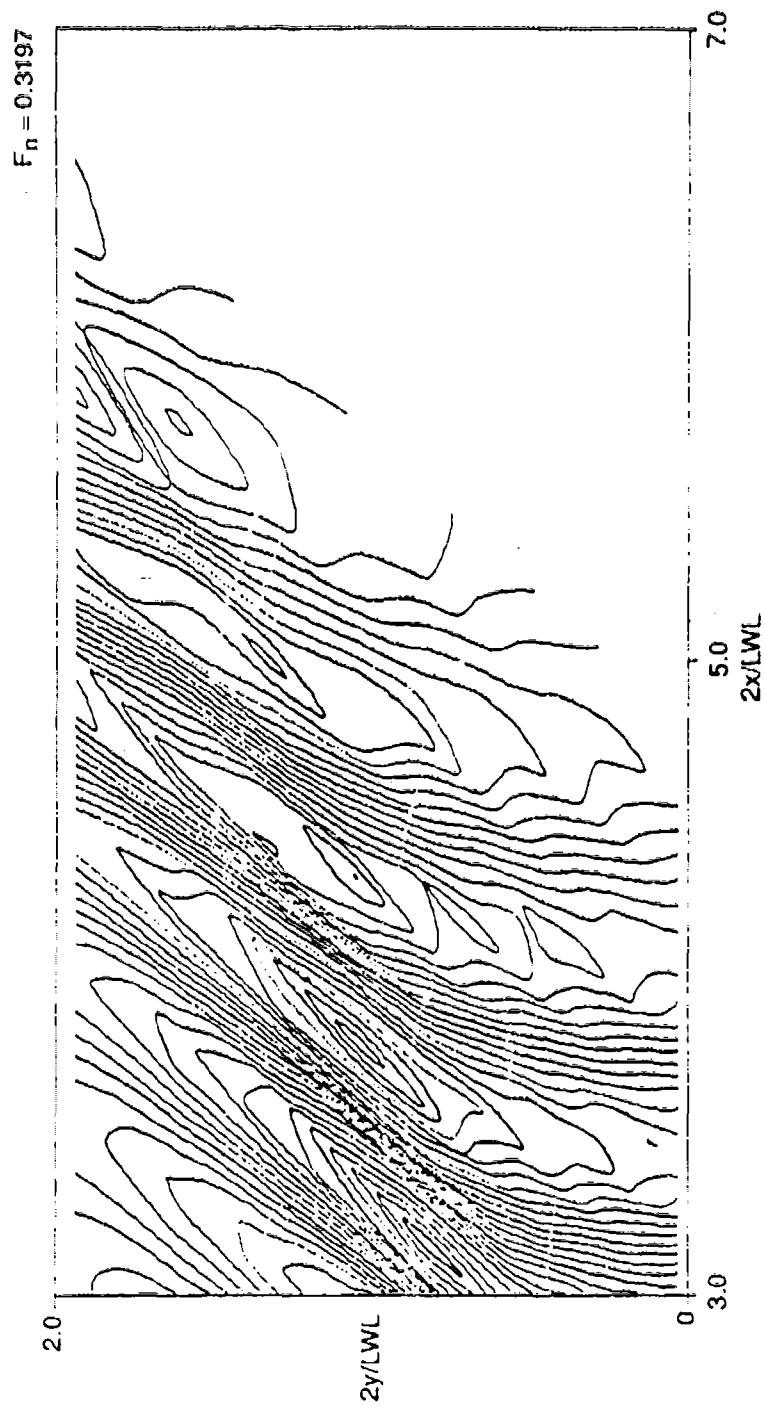


Fig. F.17. SWIFT prediction of wave contours ($4 < 2x/LWL < 8$) for QUAPAW at $F_n = 0.3197$.

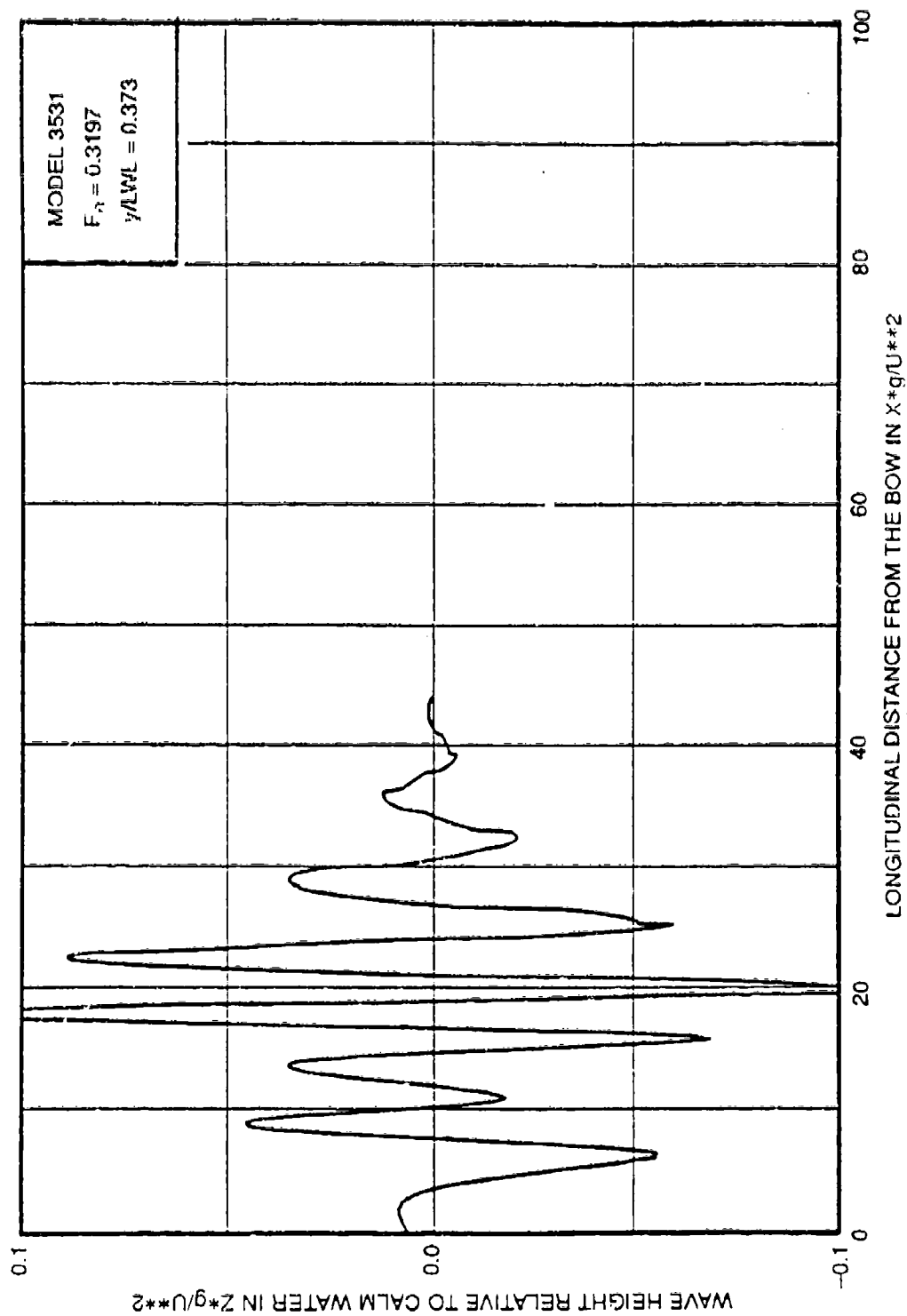


Fig. F.18. SWIFT prediction of wave cut for QUAPAW at $F_n = 0.3197$.

THIS PAGE INTENTIONALLY LEFT BLANK

APPENDIX G
NKSHIP PREDICTIONS

WAKE-OFF QUESTIONNAIRE

Response from MIT

COMPUTATIONAL CODE

- (1) *Name of Code?*
NKSHIP
- (2) *Who many lines of Coding?*
1550 plus standard routines (RPAN, GEOM, etc.).
- (3) *How many subroutines?*
12 plus standard routines.
- (4) *What are the limitations on the number of panels which can be used?*
Specified by available machine memory. If direct solver is used on VAX-750 1500/3000
- (5) *Describe the status of the program documentation.*
Under development, not commercialized.
- (6) *Does a user's manual exist?*
No.
- (7) *What hardware could/has the code run on? With what modifications?*
On any machine that supports FORTRAN 77, without any modifications.
- (8) *Can the Wave Resistance Coefficient, C_w , be predicted?*
Yes, but the prediction is not reliable.
- (9) *Can/Does the Code include lift? Describe the difficulties of modifying the code to include lift and/or non-linearities.*
No, at least at this stage.
- (10) *Can/Does the Code include provision for a propulsor/Actuator disc?*
No, at least at this stage.
- (11) *Are on-body and/or off-body streamlines calculated?*
Yes, on the body and on the free surface.
- (12) *What kind of boundary conditions or numerical techniques are used to deal with the radiation condition?*
The freesurface elevation and slope vanish at the upstream boundary of the free surface computational domain, while no conditions are imposed at the downstream boundary.
(*Note:* the shape function used for the approximation of the potential is a quadratic spline that needs, in general, two end-conditions in each direction.)
- (13) *Is the Code suitable for transon-stern type hull forms?*
It has not been tried yet.
- (14) *What experience level is necessary to prepare the input data, run the program and display the results?*
The code is not commercialized yet.
- (15) *Describe the "user-friendliness" aspects of the code.*
The code is not commercialized yet.

KELVIN WAVE COMPUTATIONS

- (1) *On what machine were the computations run?*
VAX-750 and CRAY-XMP.
- (2) *How long (CPU time) did it take to run each case?*
3 hrs on a VAX-750.
- (3) *How involved, streamlined, and time consuming is the input data preparation process?*
The code is not commercialized yet.
- (4) *Was a check done for convergence during or after the computations?*
Yes - we think that this is essential.
- (5) *How many panels were used (for each case/hull)?*
905, of which 585 are on the free surface and 320 on the body.
- (5) *What is the nature of the panel shape and distribution and singularity distributions?*
Plane quadrilaterals, quadratic spline.
- (6) *If C_w was calculated, please provide the predictions for each case.*
Yes, but without being reliable.

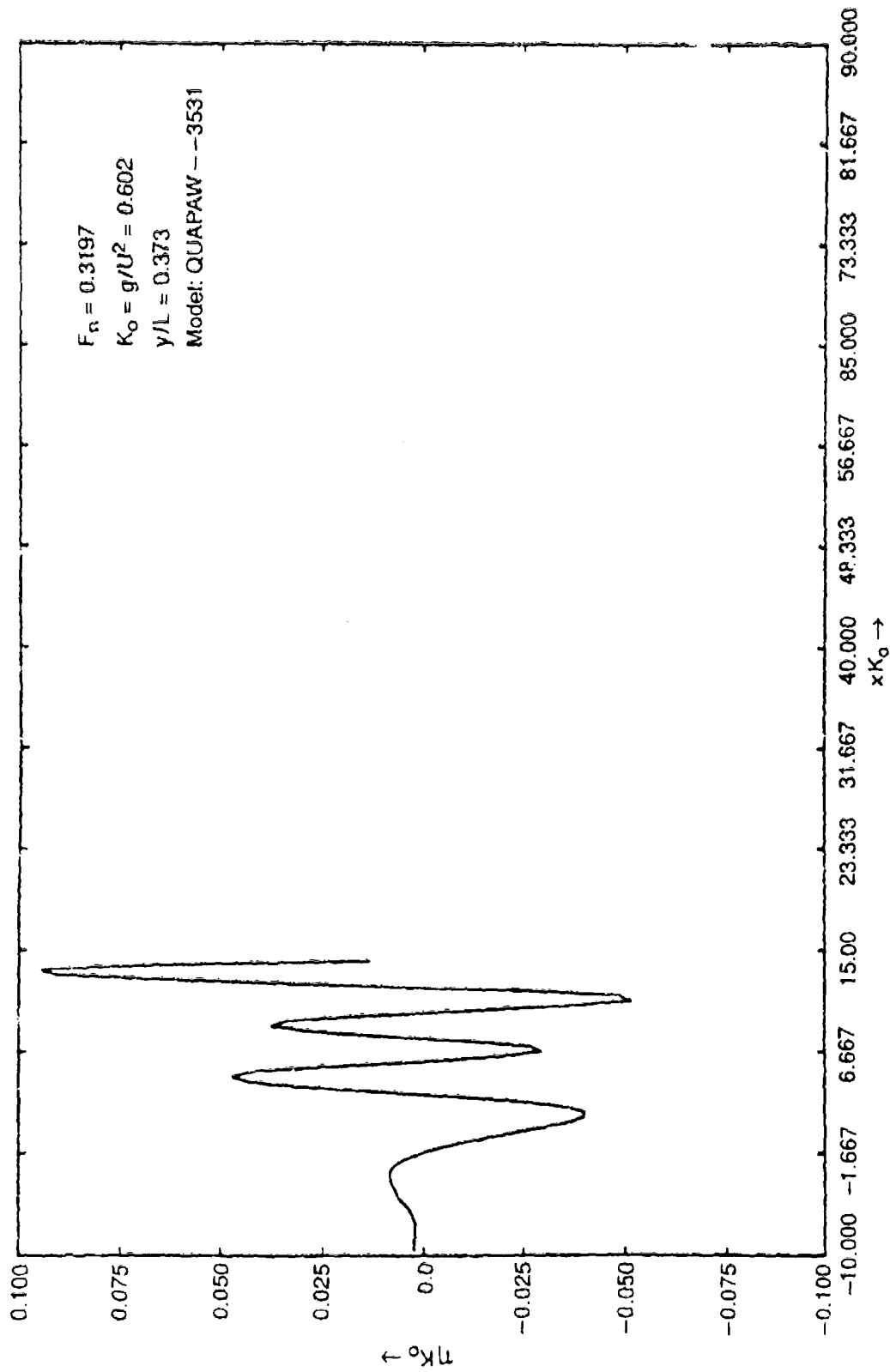


Fig. G.1. NKSHIP prediction of wave contours for QUAPAW at $F_n = 0.3197$.

FROUDE No. 0.32000

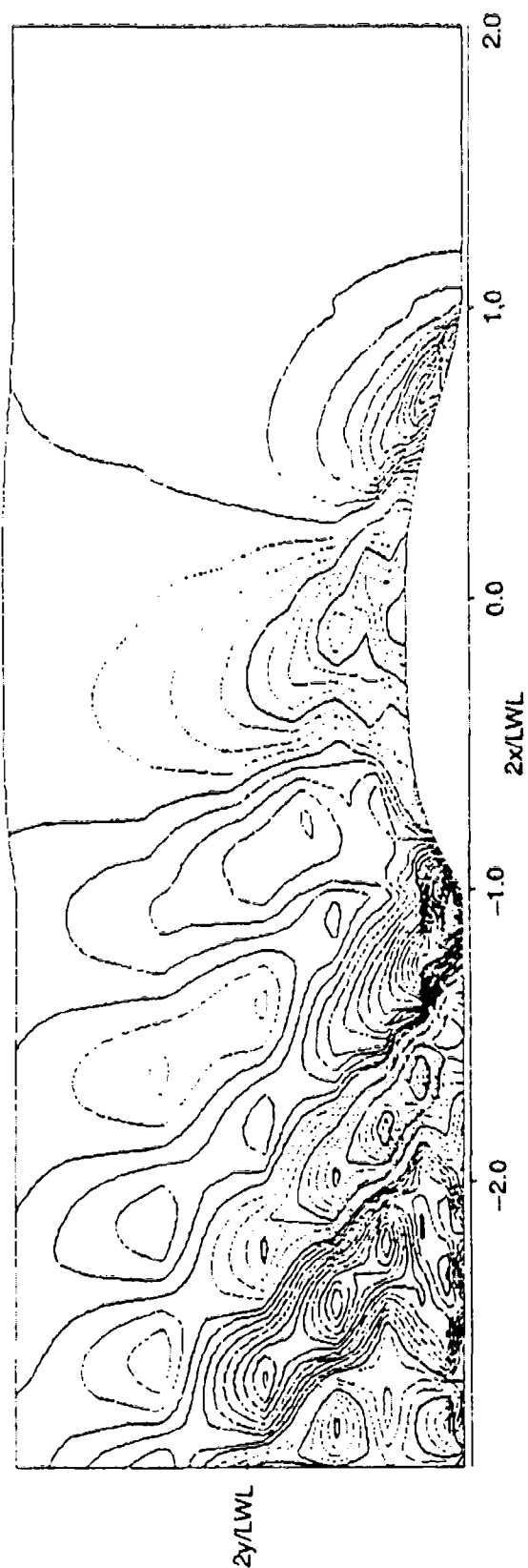


Fig. G.2. NKSHIP prediction of wave cut for QUAPAW at $F_n = 0.3197$.

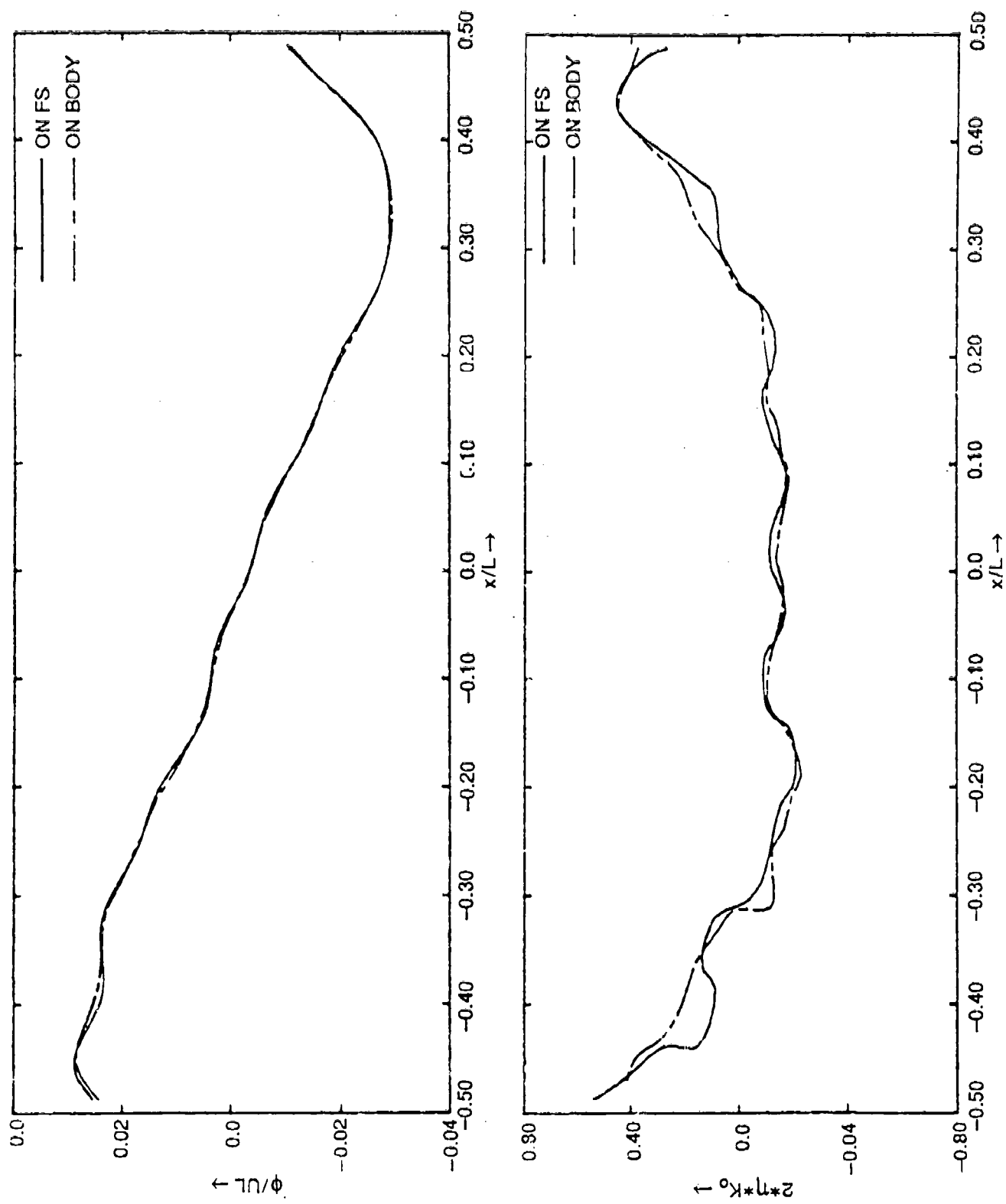


Fig. G.3. NKSHIP prediction of wave profiles along QUAPAW hull at $F_n = 0.2131$.

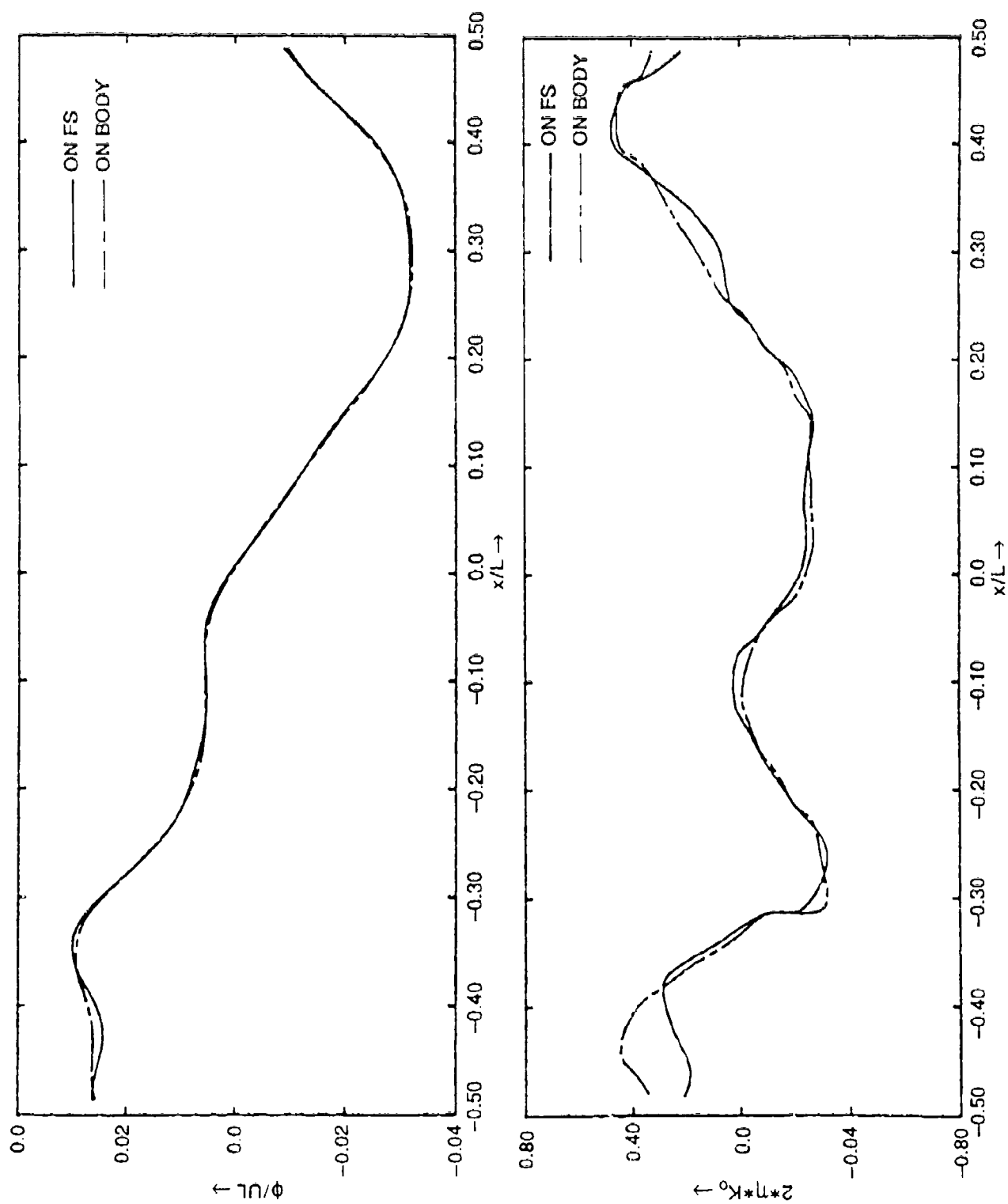


Fig. G.4. NKSHIP prediction of wave profiles along QUAPAW hull at $F_n = 0.25$.

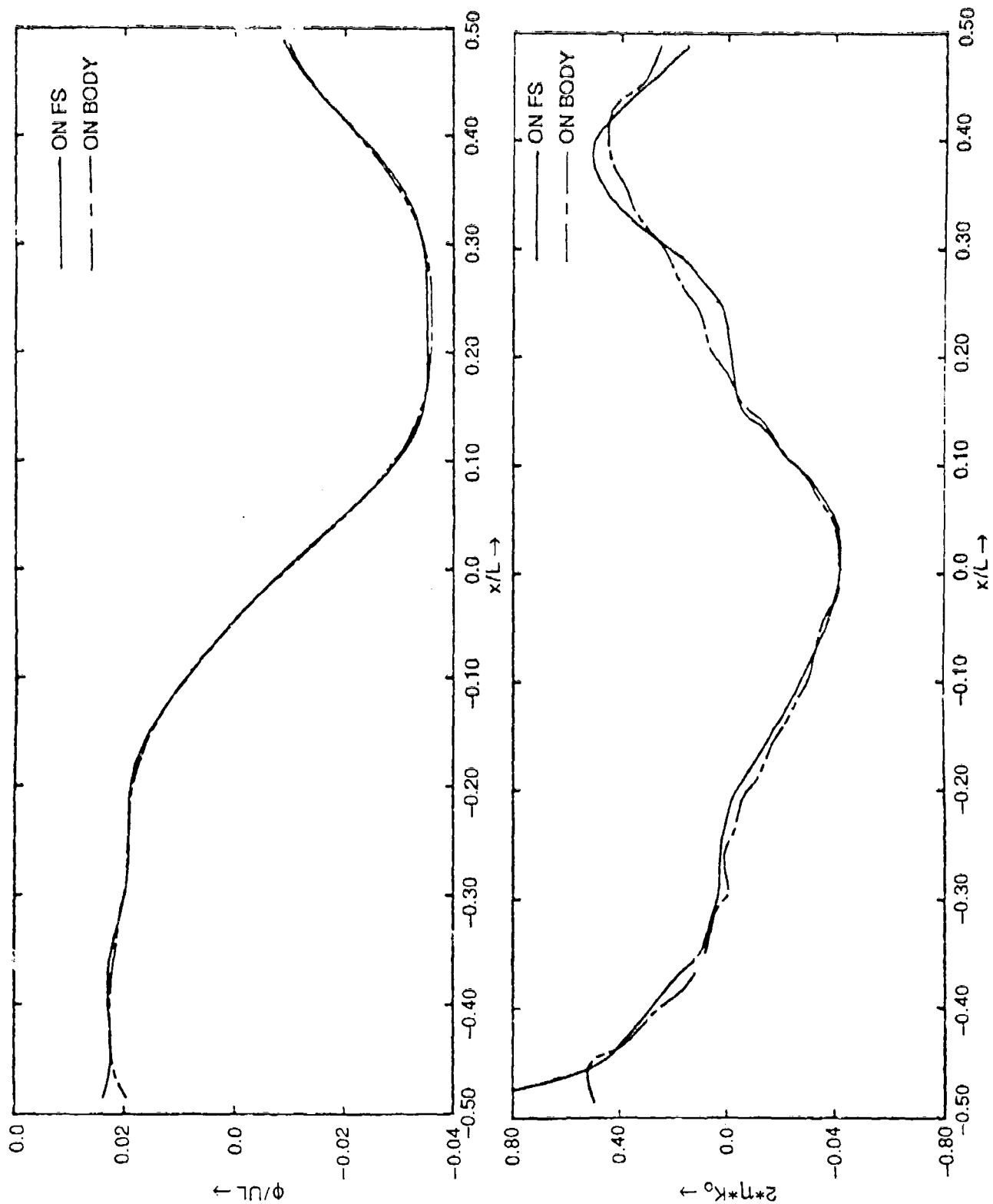
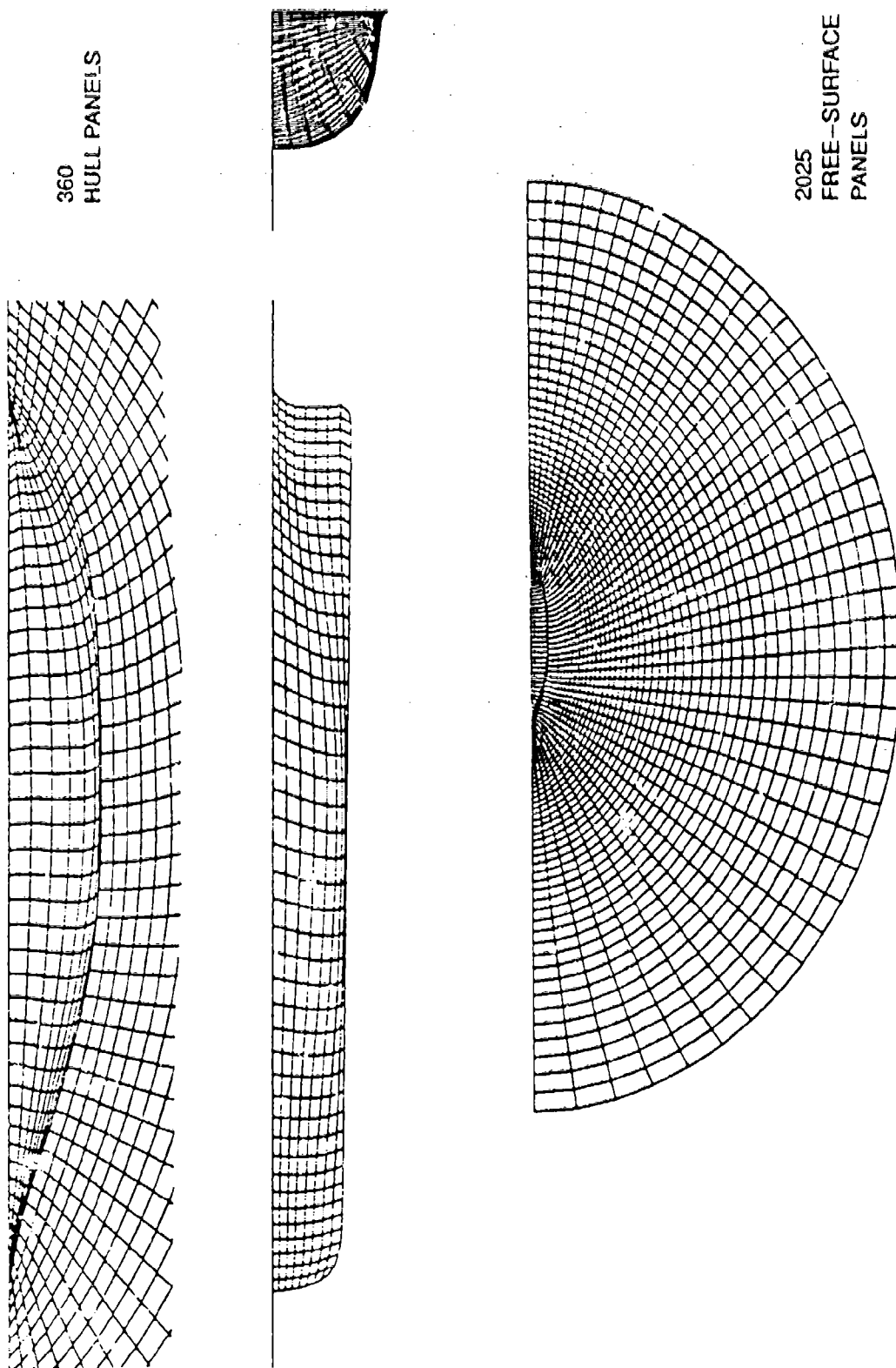


Fig. G.5. NKSHIP prediction of wave profiles along QUAPAW hull at $F_n = 0.3197$.

APPENDIX H
FLOPAN PREDICTIONS



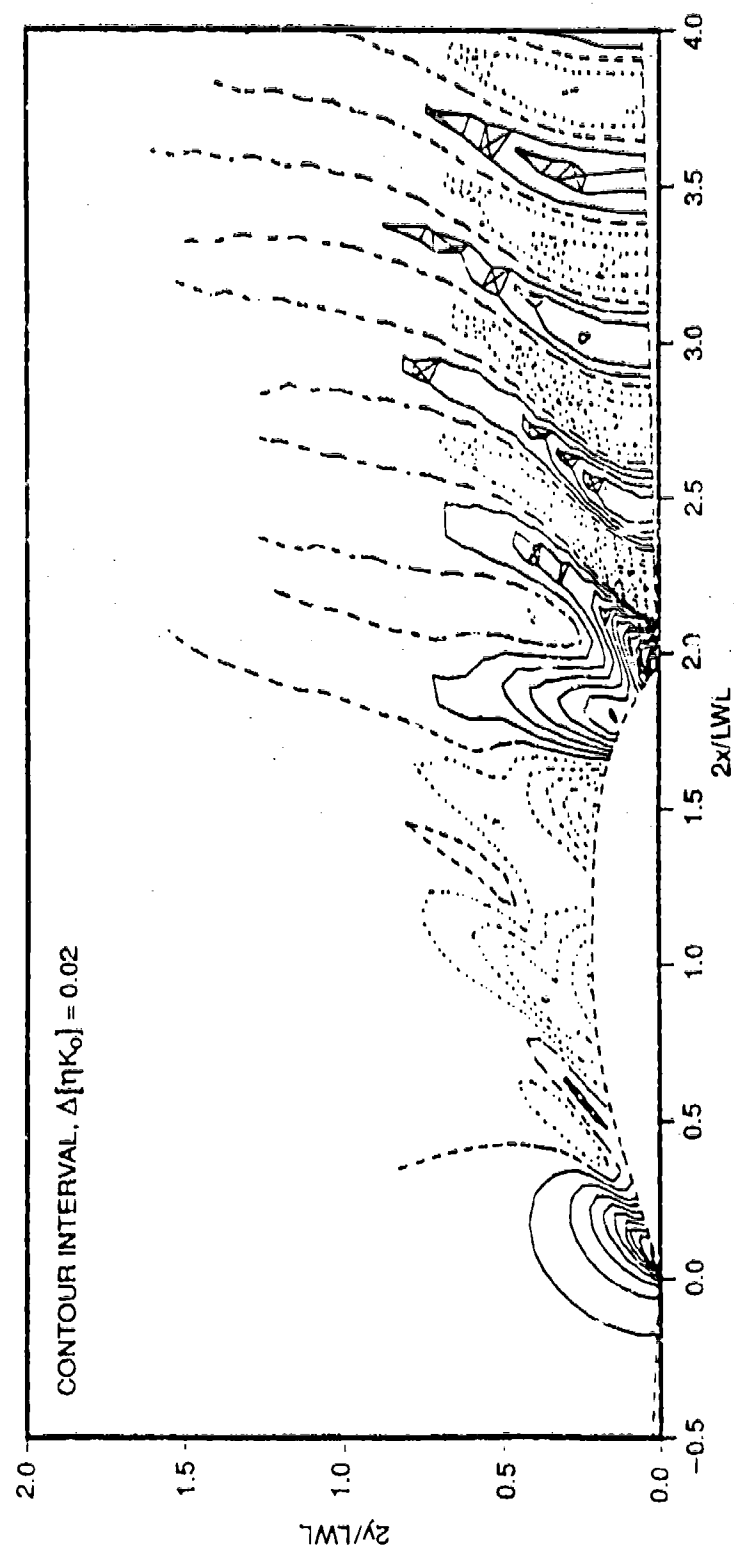


Fig. H.2. FLOPAN prediction of wave contours for QUAPAW at $F_n = 0.2131$.

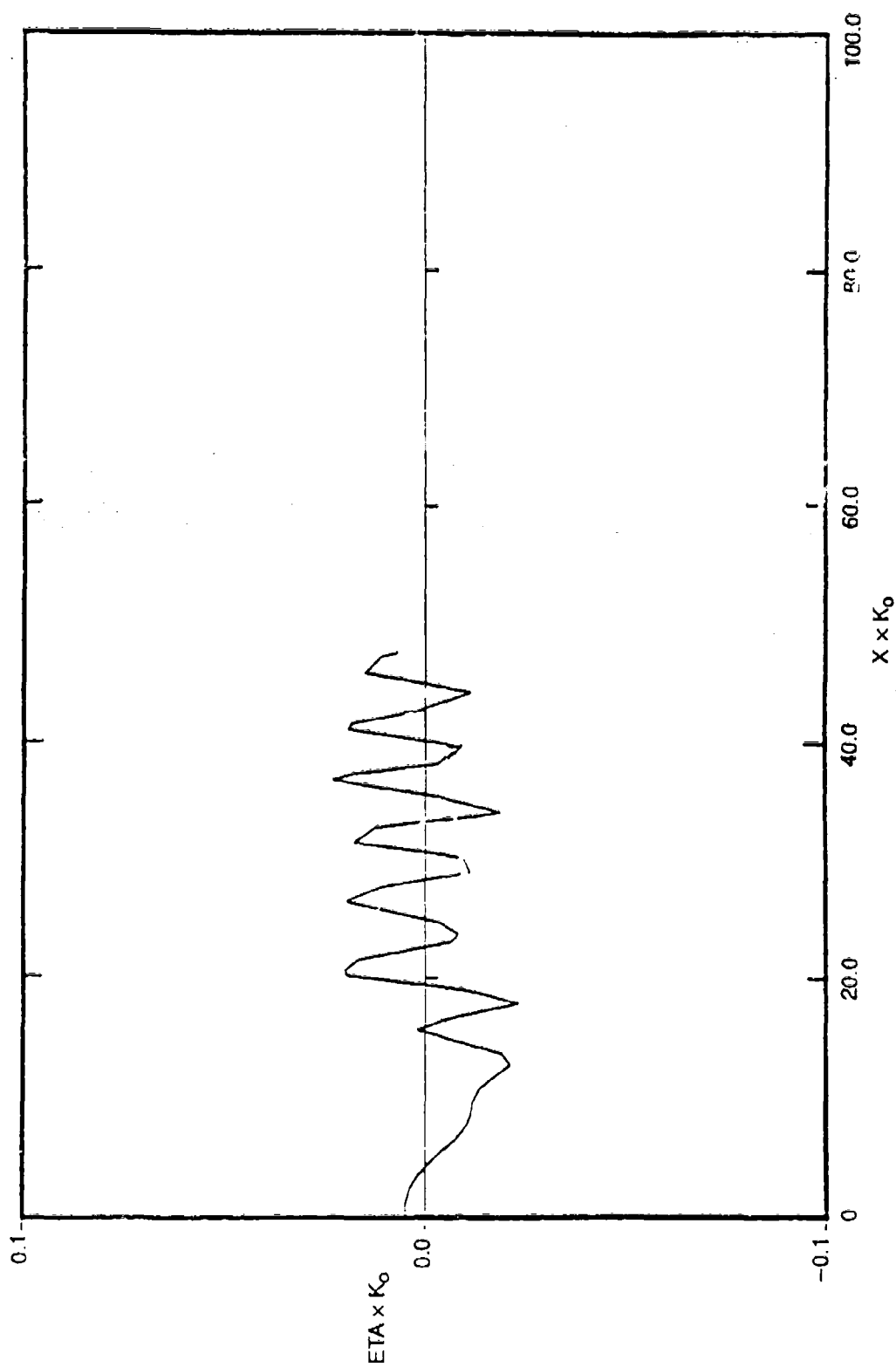


Fig. H.3. FLOPAN prediction of wave cut for QUAPAW at $F_n = 0.2131$.

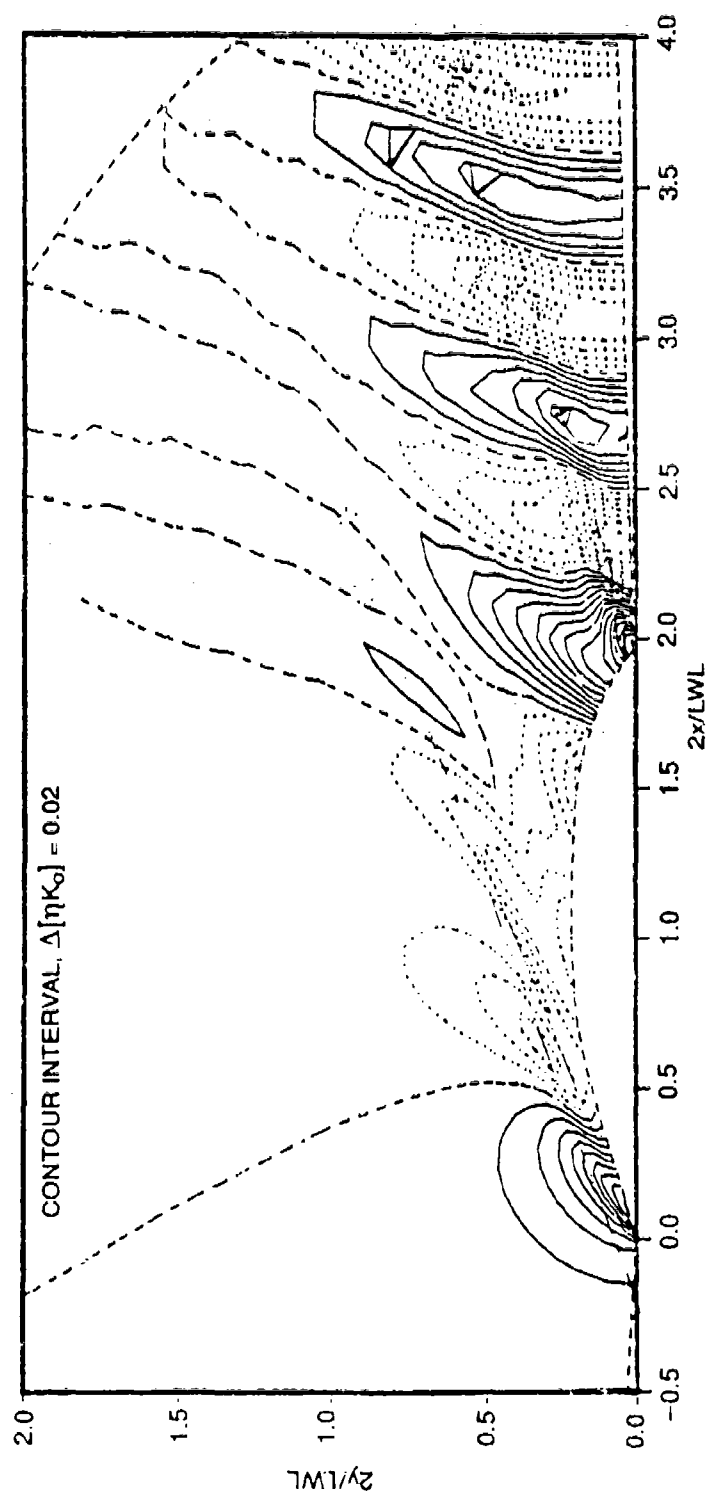


Fig. H.4. FLOPAN prediction of wave contours for QUAPAW at $F_n = 0.25$.

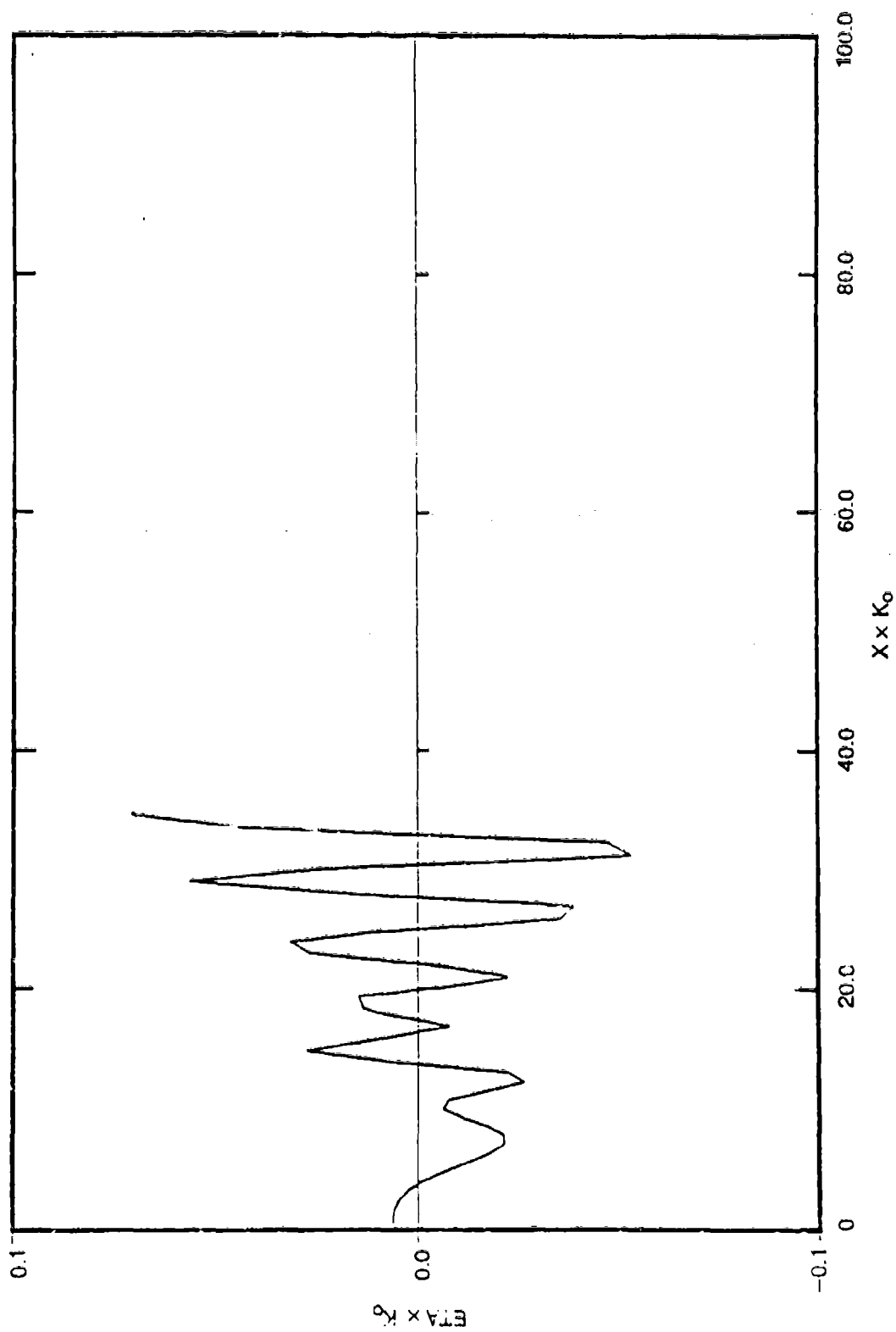


Fig. H.5. FLOPAN prediction of wave cut for QUAPAW at $F_n = 0.25$.

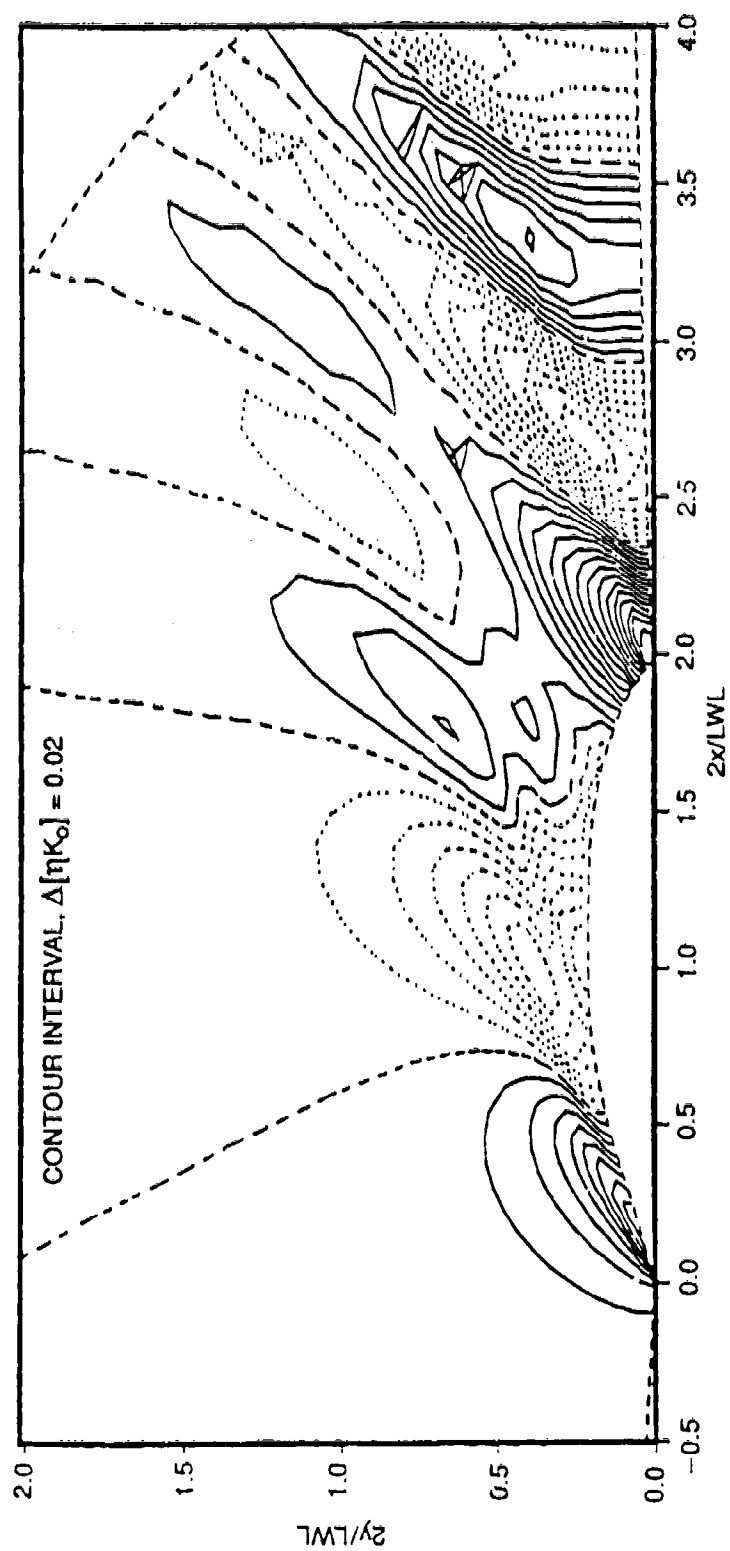


Fig. H.6. FLOPAN prediction of wave contours for QUAPAW at $F_n = 0.3197$.

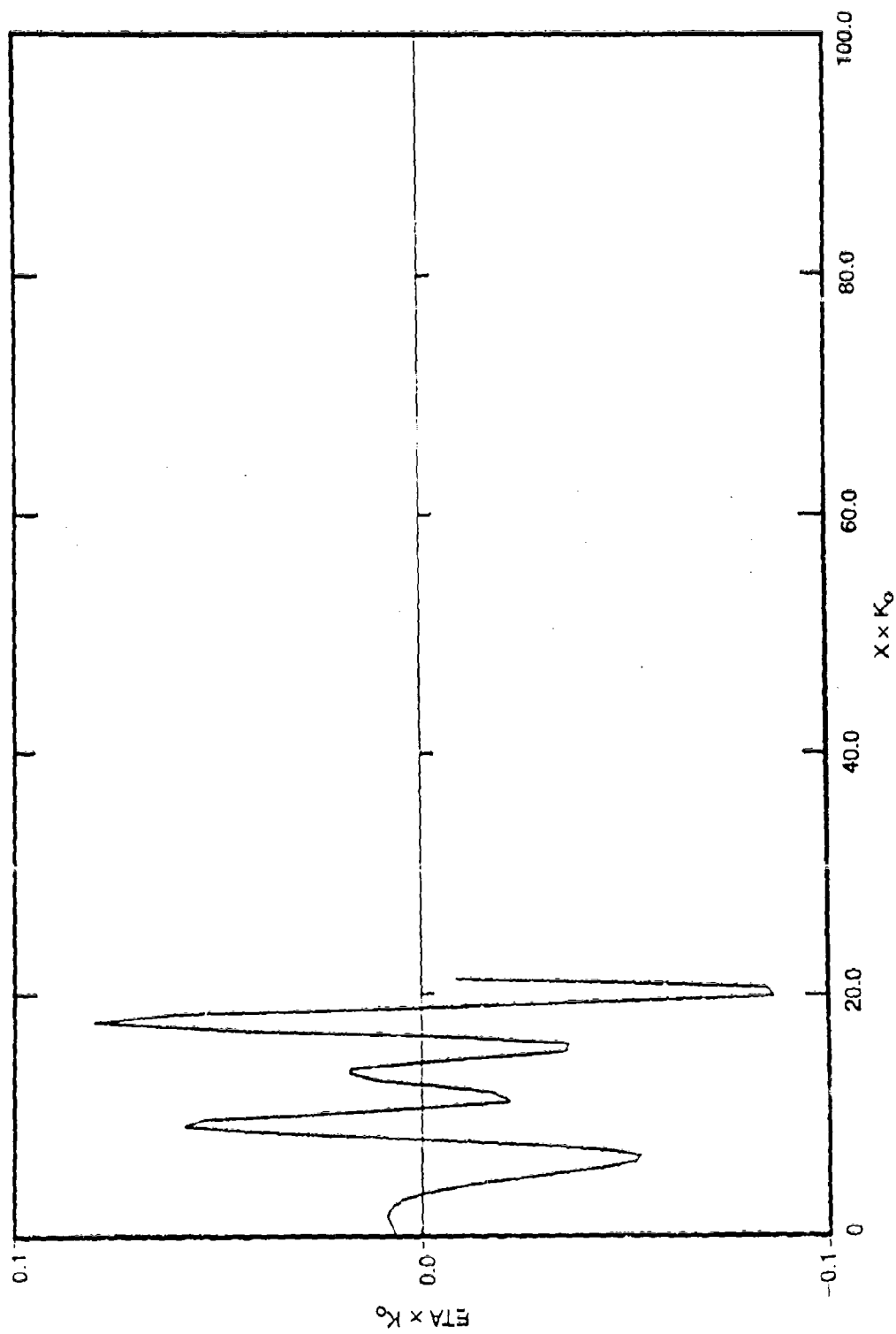


Fig. H.7. FLOPAN prediction of wave cut for QUAPAW at $F_0 = 0.3197$.

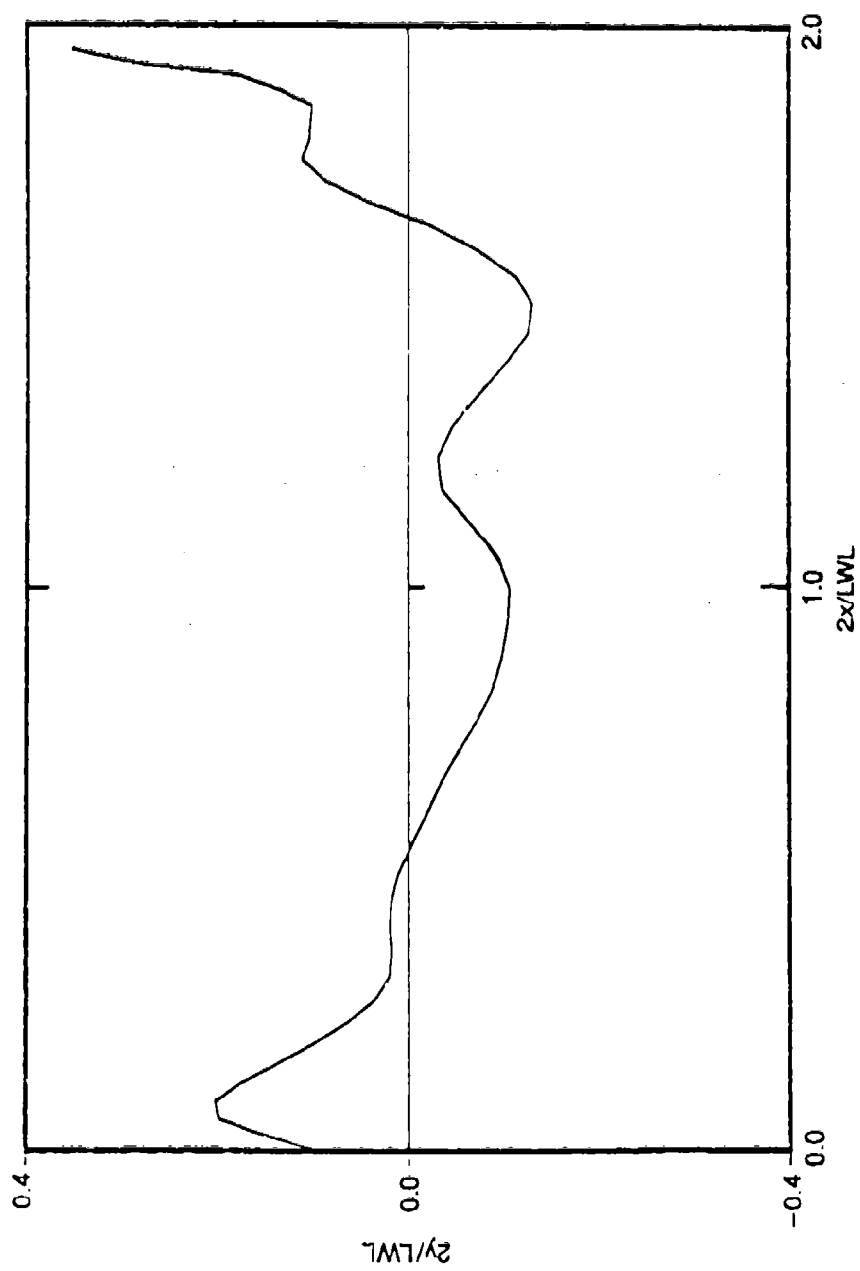


Fig. H.8. FLOPAN prediction of wave profile along QUAPAW hull at $F_n = 0.2131$.

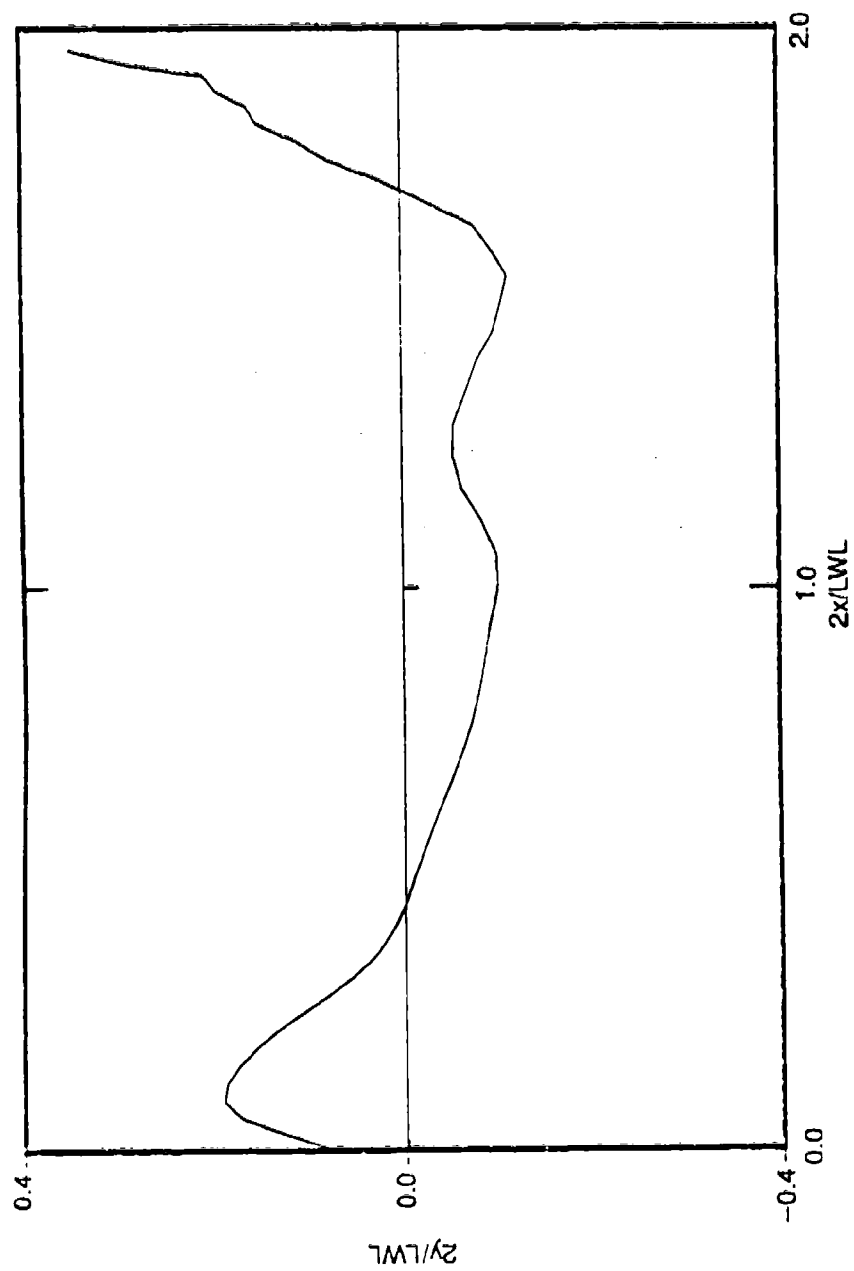


Fig. H.9. FLOFAN prediction of wave profile along QUAPAW hull at $F_n = 0.25$.

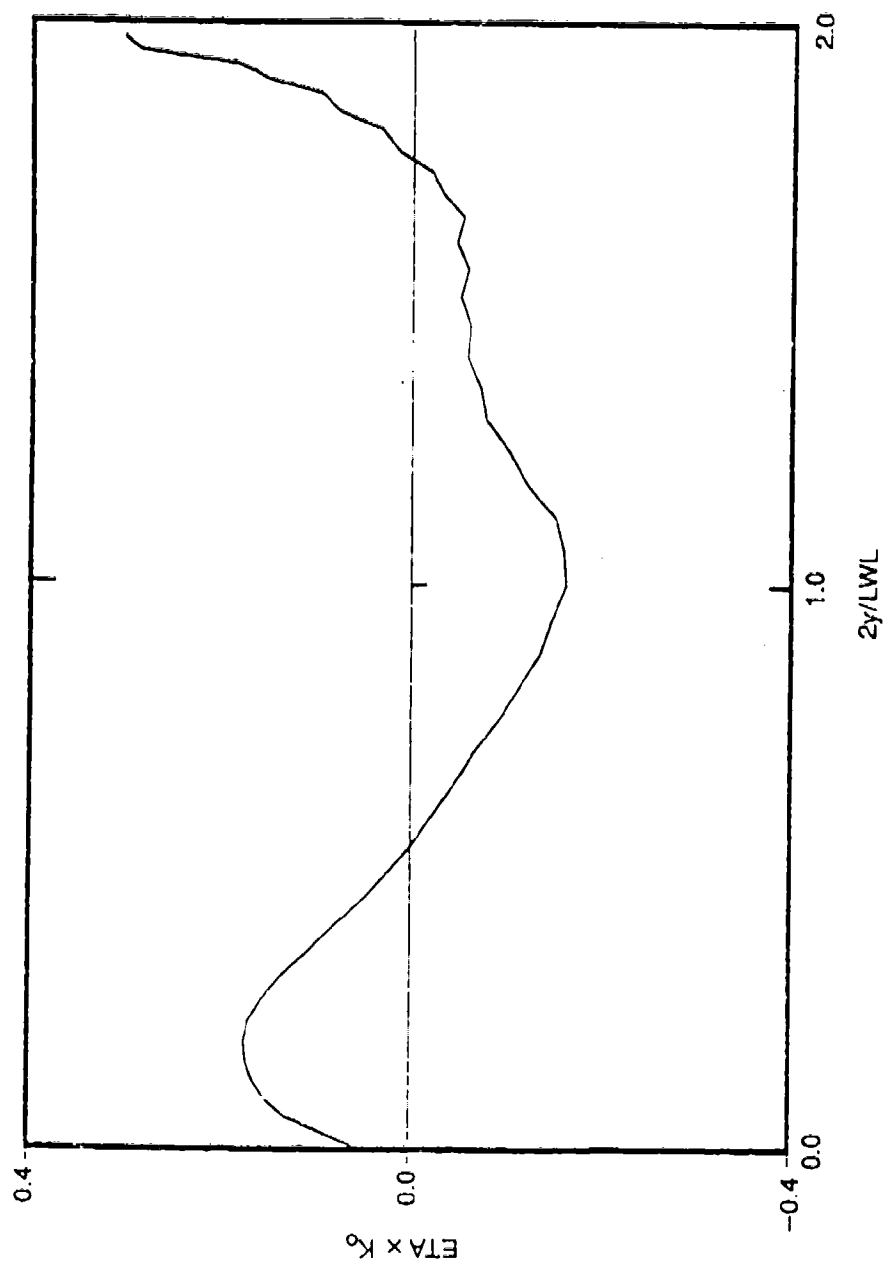


Fig. H.10. FLOPAN prediction of wave profile along QUAPAW hull at $F_n = 0.3197$.

THIS PAGE INTENTIONALLY LEFT BLANK

APPENDIX I
XYZFS PREDICTIONS

XYZFS PROGRAM

- GENERAL DESCRIPTION

- Originally developed by Charles Dawson
- Further developed by Bill Cheng and Janet Dean
- Rankine source panel method
- Computes 3D flow fields around a ship in forward motion
- 2000 lines
- Seven segments plus numerous preprocessors and postprocessors
- XYZFS runs on CRAY 1S and CRAY XMP-24. Number of panels limited only by computer memory (currently 1500).
- Preprocessors and postprocessors run on Apollo workstations.

- COMPUTATIONAL METHODS

- Double model
- Free surface solution
- Direct solution method (Gaussian Elimination)
- Radiation condition satisfied by a four-point upstream finite difference operator.
- Velocity induced by a panel is computed using exact integration and multiple expansion methods developed by Hess and Smith (1962).

- USER REQUIREMENT / BACKGROUND

- Input preparation — ship geometry and lines drawing
- Program execution — previous computer usage
- Results display — computer graphics (2D, 3D and contour plots)
- Results analysis — physics of ship waves

- USER-FRIENDLINESS

- User's manual available
- Provisions for error checkings of panel data such as aspect ratio, outward normal, deviations from a flat panel.

- RESEARCH AREAS OF PANEL METHODS

- Nonlinearities — Nonlinear free surface work has been reported by Ogiwara and Maruo (1985), Xia (1986), Bugarelli (1987), and Ni (1987).
- Lifting Surface — Work on linear free surface with lift has been reported by Slooff (1984) and Larsson and Xia (1986).

KELVIN WAKE COMPUTATIONS USING XYZFS

- Computations for QUAPAW and DDG51
- Machine used: CRAY XMP-24
- CPU time: approximately 1 minute per Froude number
- Number of panels used:

	HULL	FREE SURFACE
QUAPAW	192	1220
MODEL 5415	320	1128

- Quadrilateral panels of constant source strength were used. The panels are organized by station lines; points on a station line are selected by specified percentages in girth using B-splines.
- Convergence check was made as the width and length of the FS computational domain were changed.

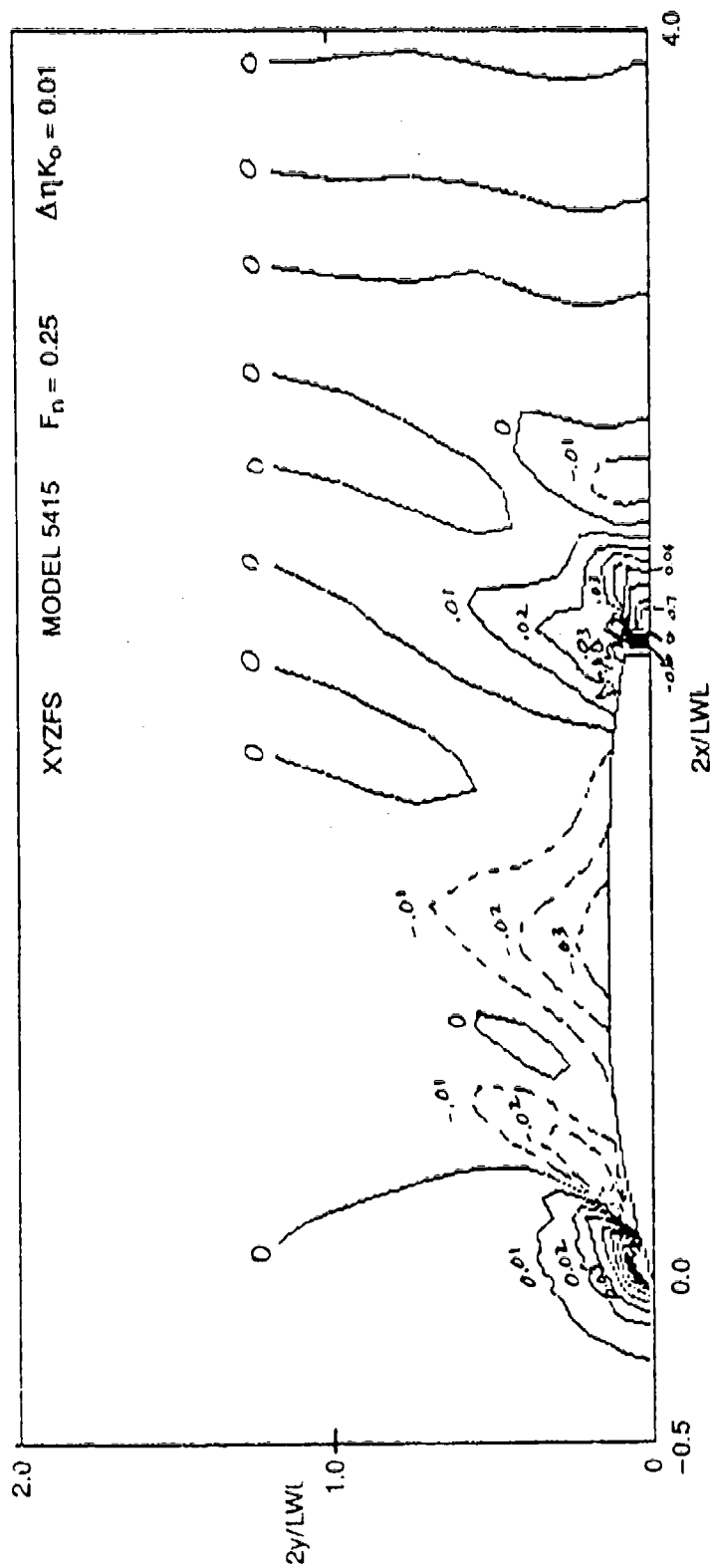


Fig. 1.1. XYZFS prediction of wave contour for Model 5415 at $F_n = 0.25$.

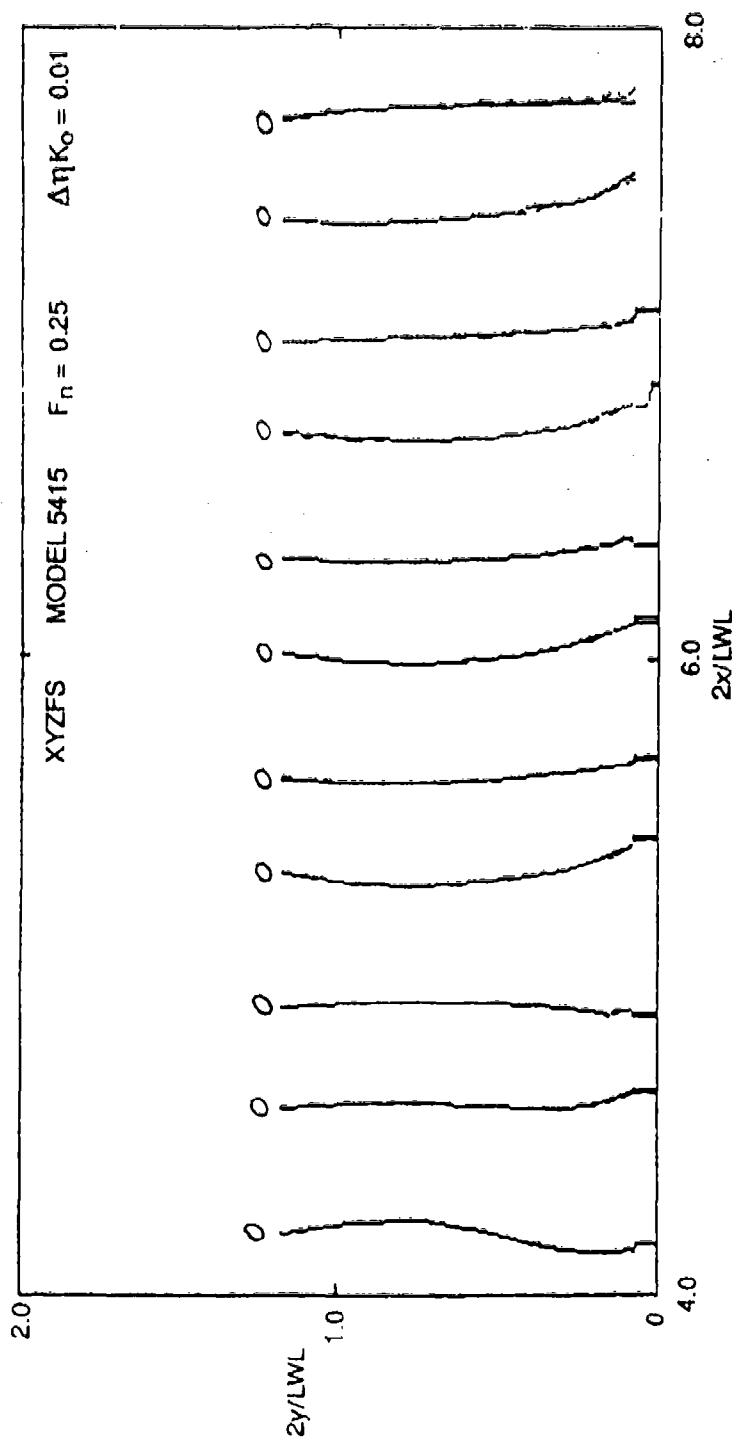


Fig. I.1. (Continued).

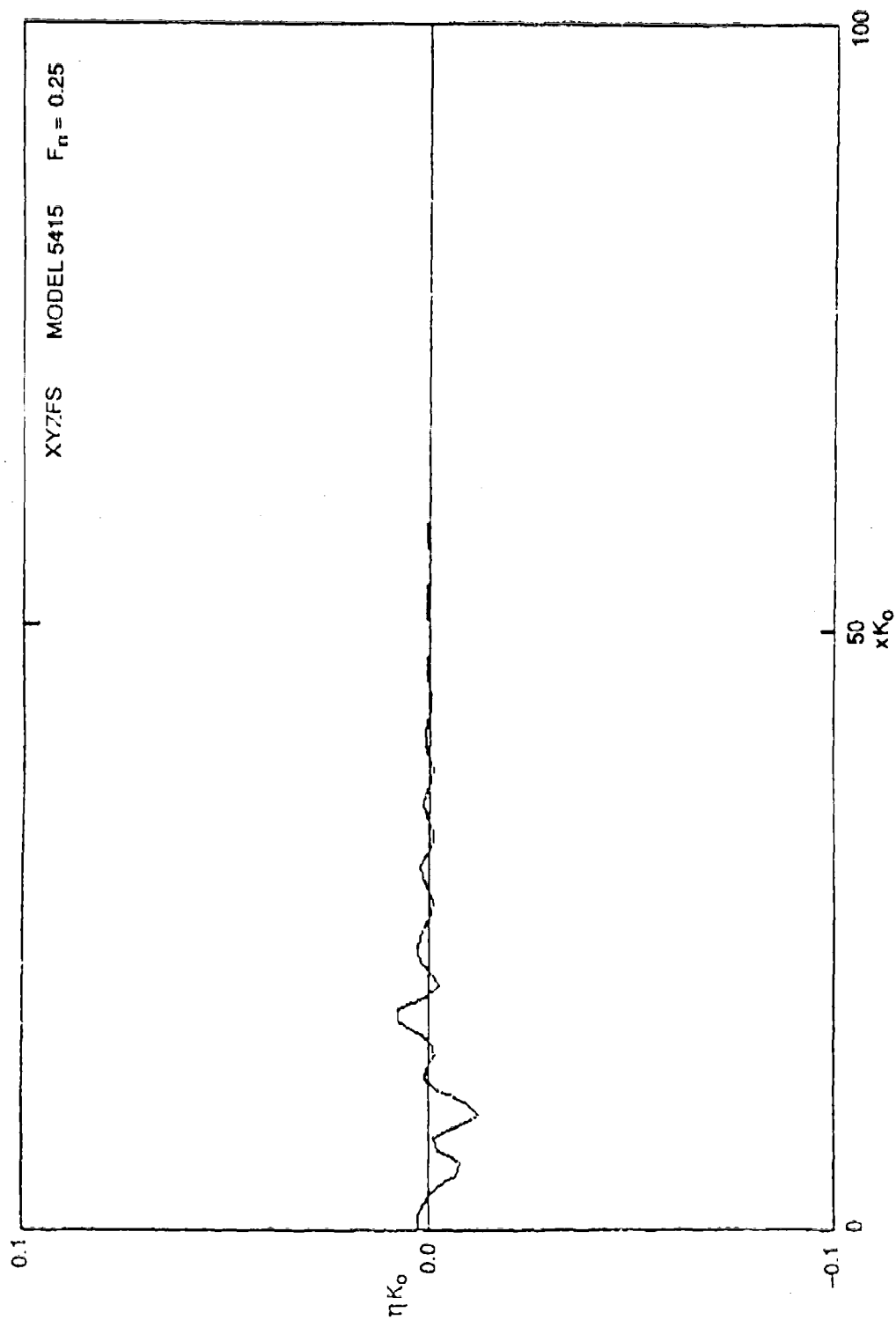


Fig. 1.2. XYZFS prediction of wave cut for Model 5415 at $F_n = 0.25$.

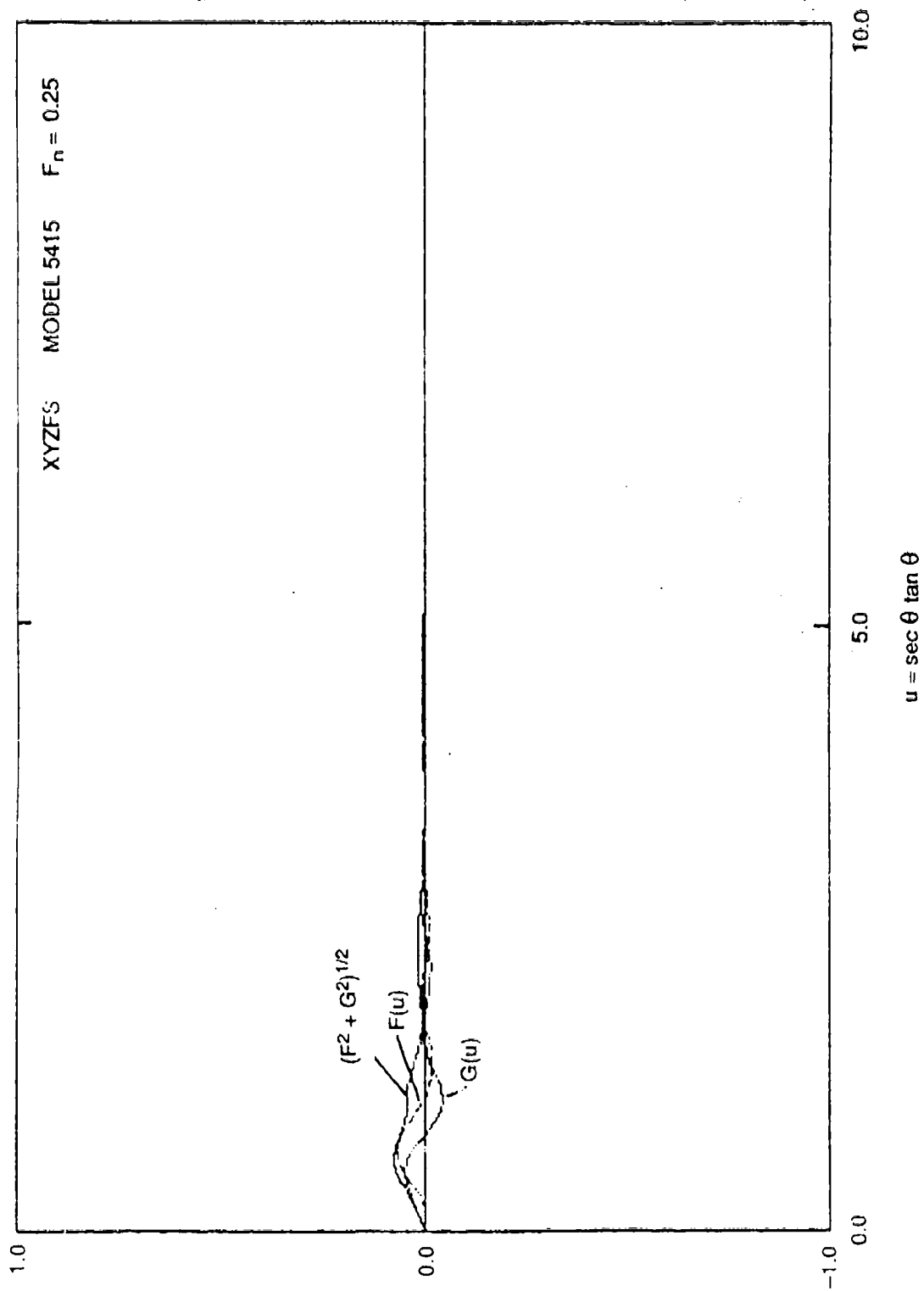


Fig. I.3. XYZFS prediction of wave spectrum for Model 5415 at $F_n = 0.25$.

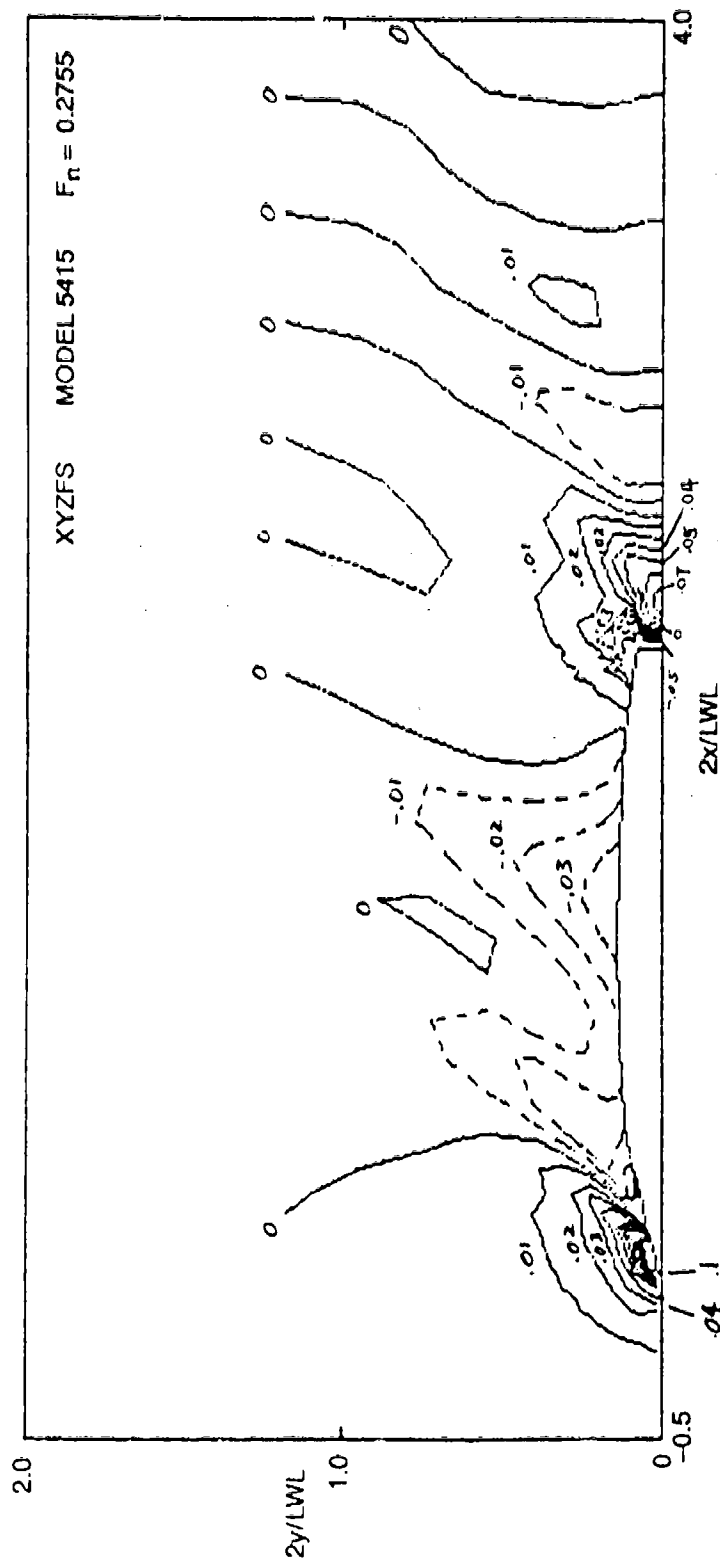


Fig. 1.4. XYZFS prediction of wave contour for Model 5415 at $F_n = 0.2755$.

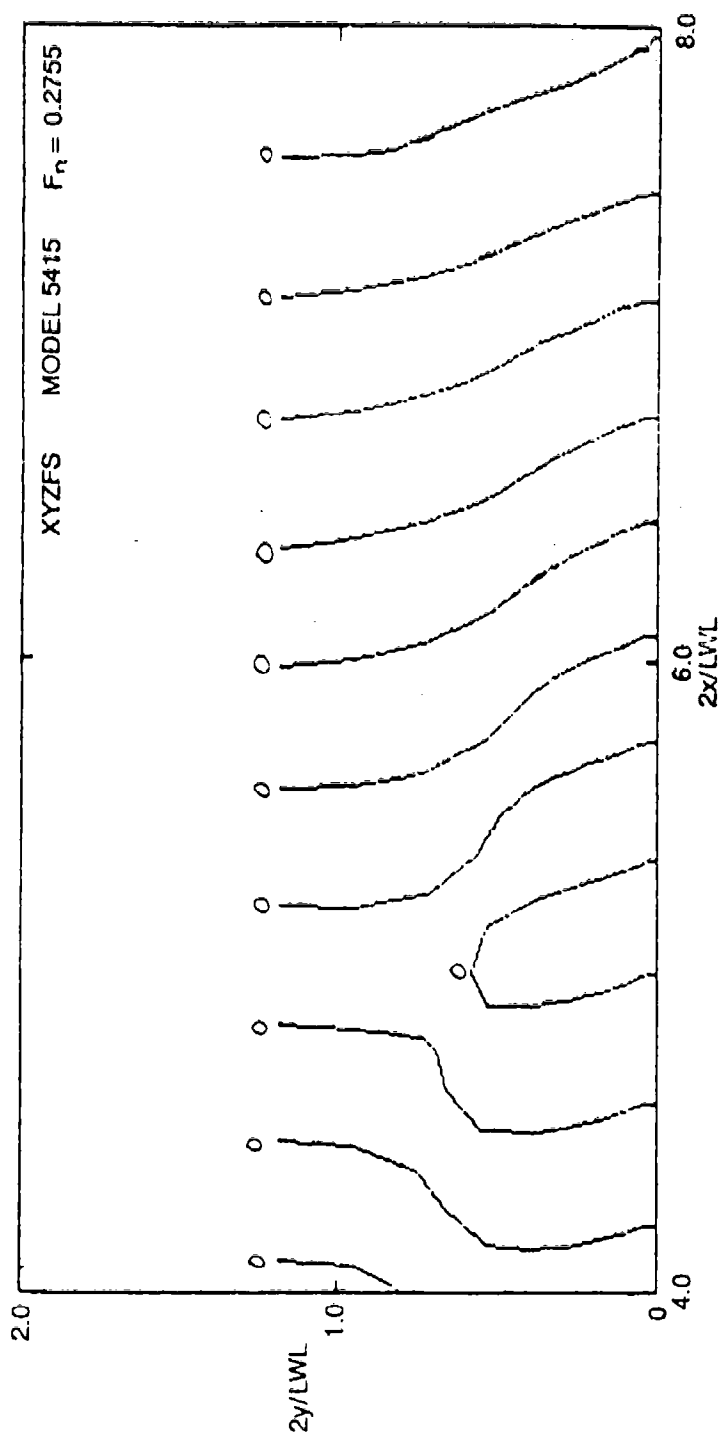


Fig. 1.4. (Continued).

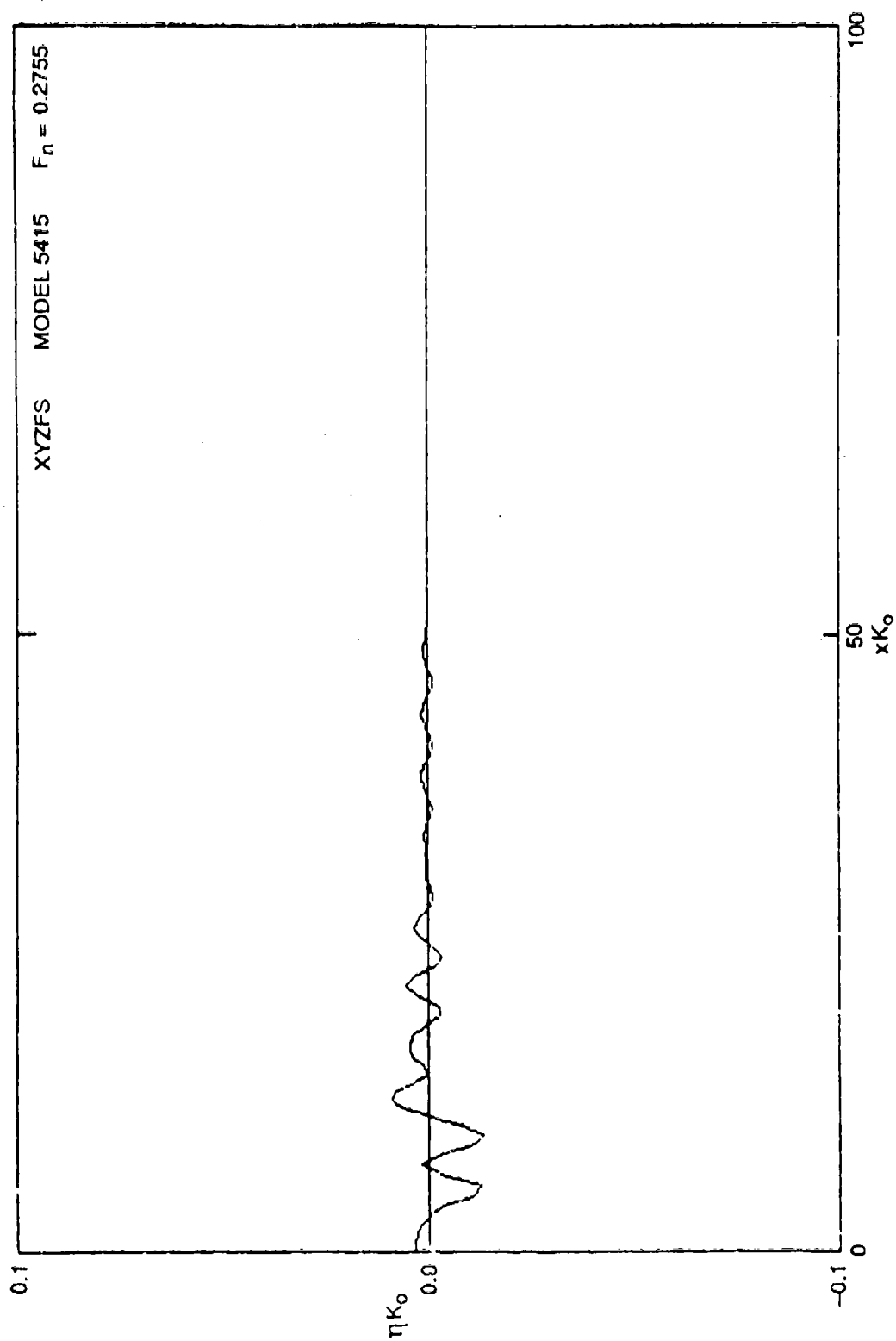


Fig. I.5. XYZFS prediction of wave cut for Model 5415 at $F_n = 0.2755$.

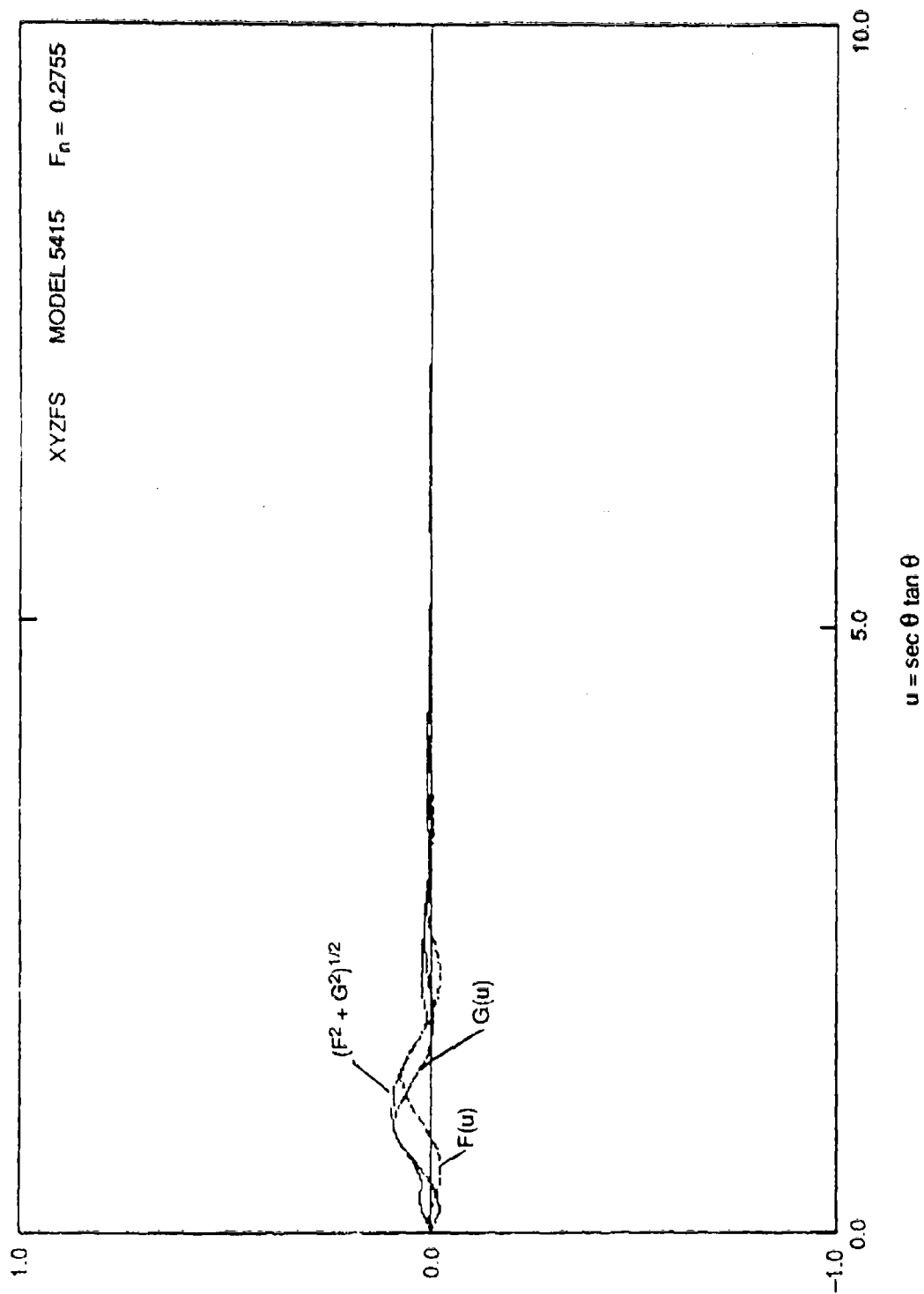


Fig. 1.6. XYZFS prediction of wave spectrum for Model 5415 at $F_n = 0.2755$.

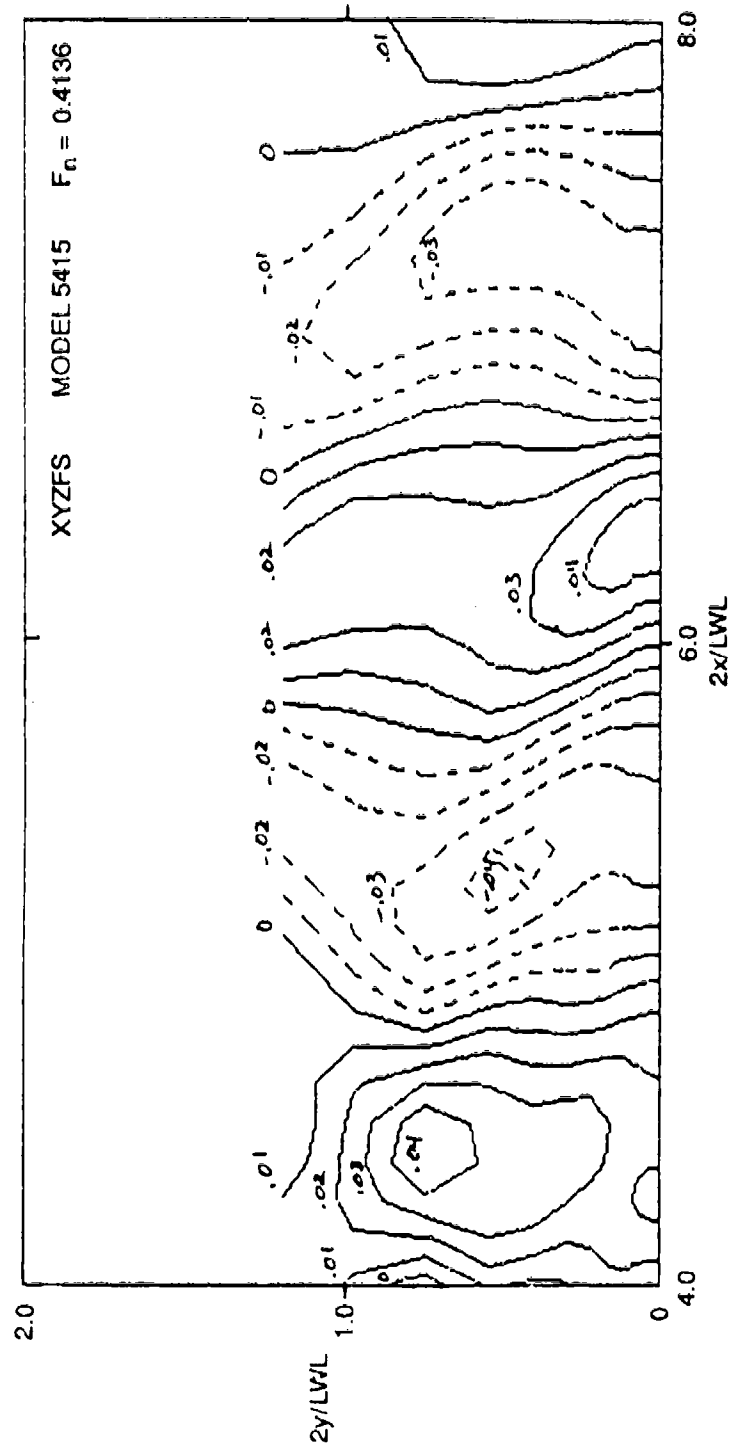


Fig. I.7. XYZFS prediction of wave contour for Model 5415 at $F_n = 0.4136$.

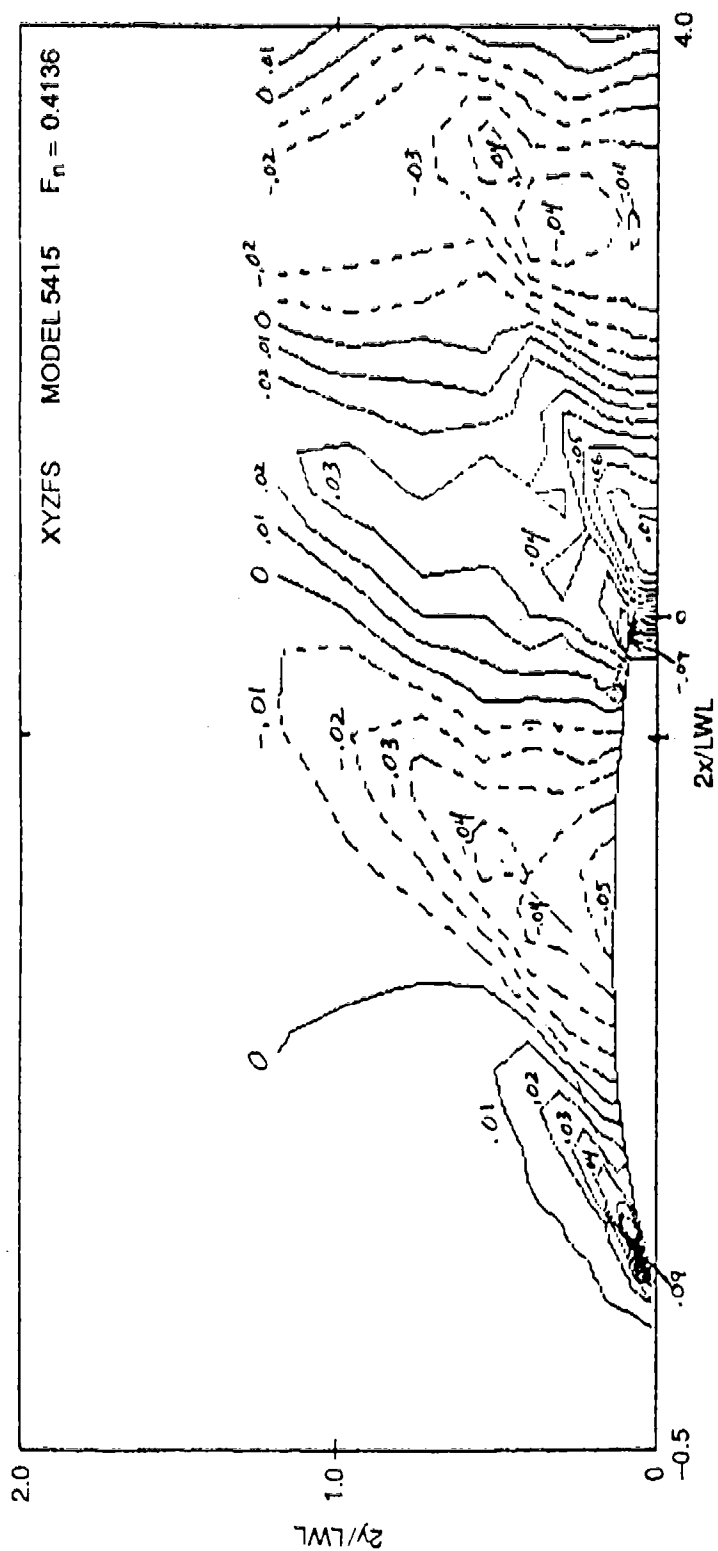


Fig. I.7. (Continued).

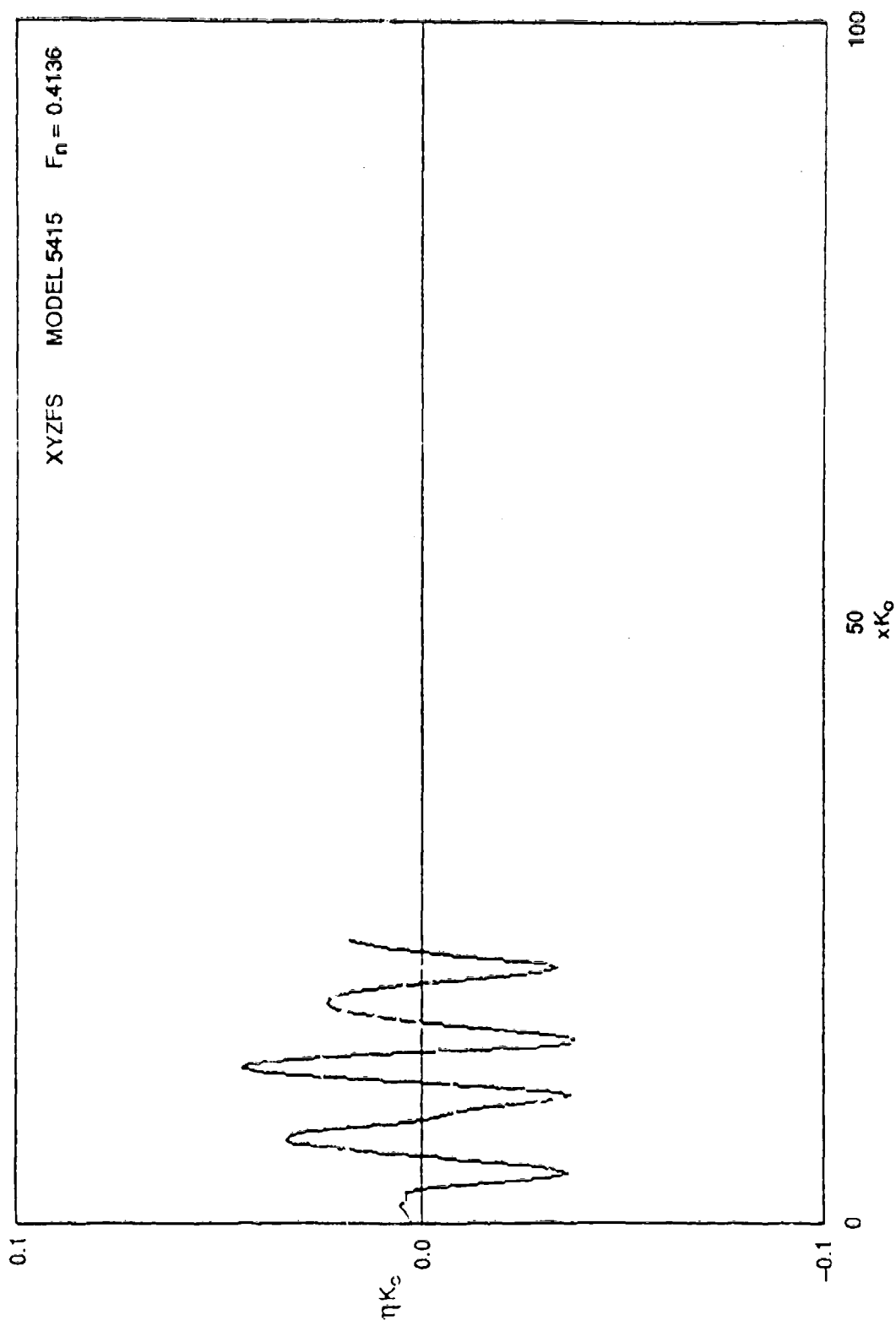


Fig. I.8. XYZFS prediction of wave cut for Model 5415 at $F_n = 0.4136$.

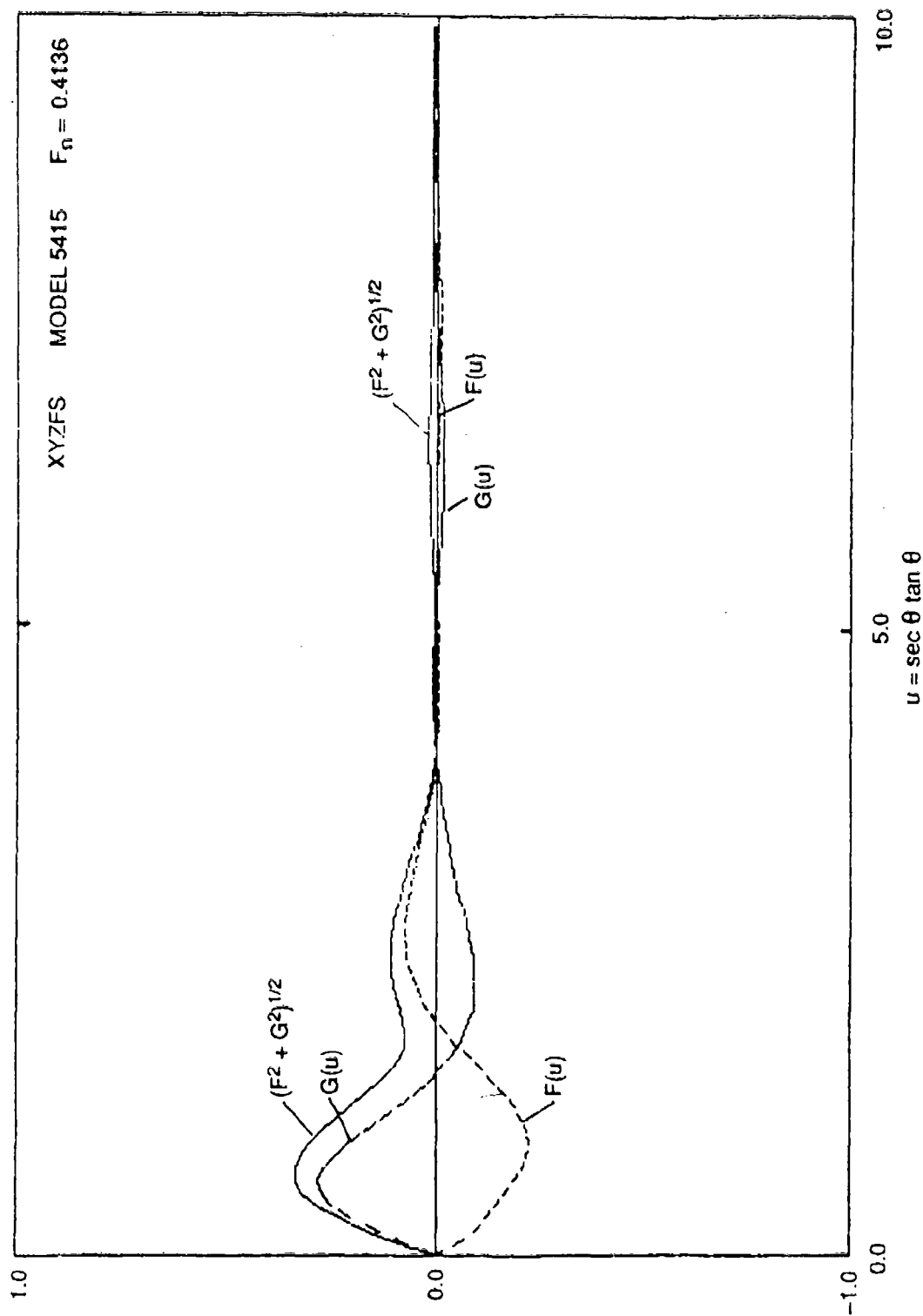


Fig. I.9. XYZFS prediction of wave spectrum for Model 5415 at $F_n = 0.4136$.

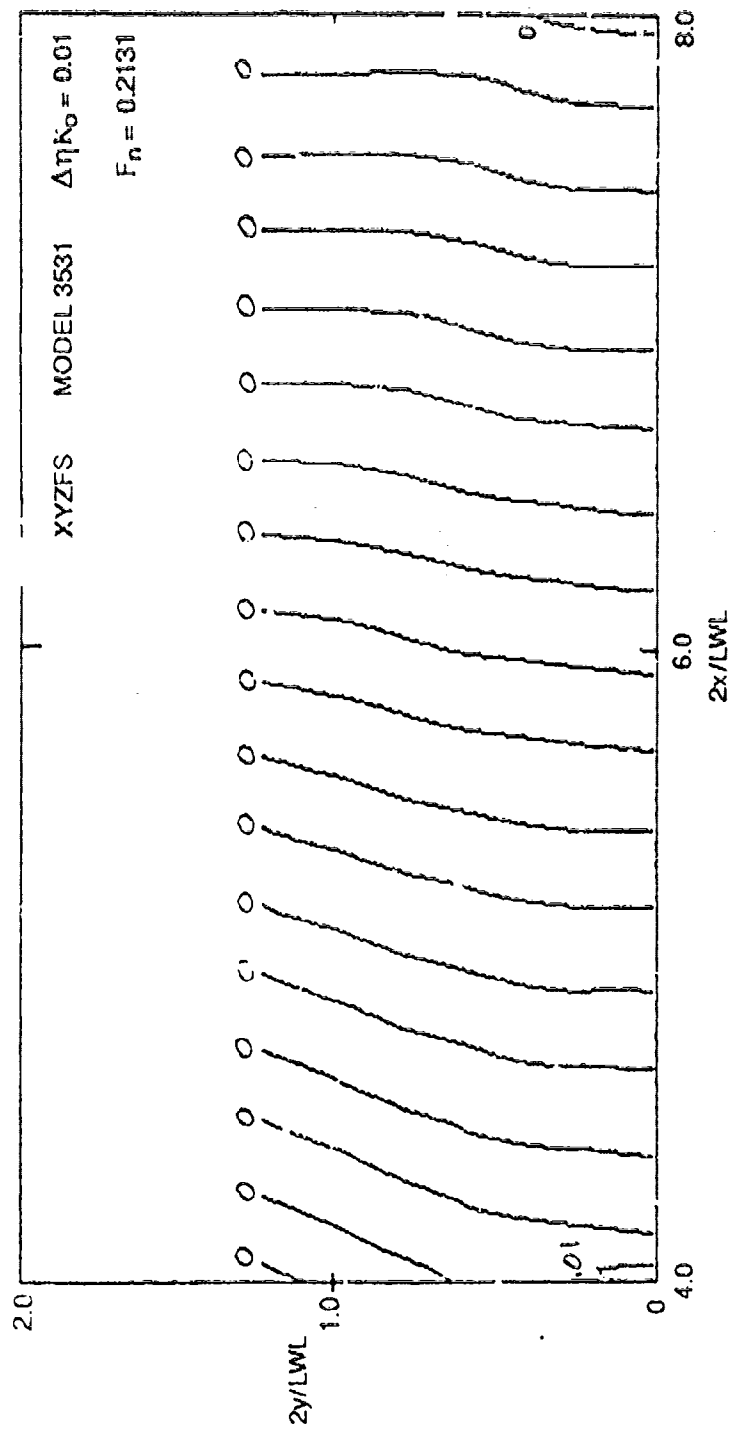


Fig. I.10. (Continued).

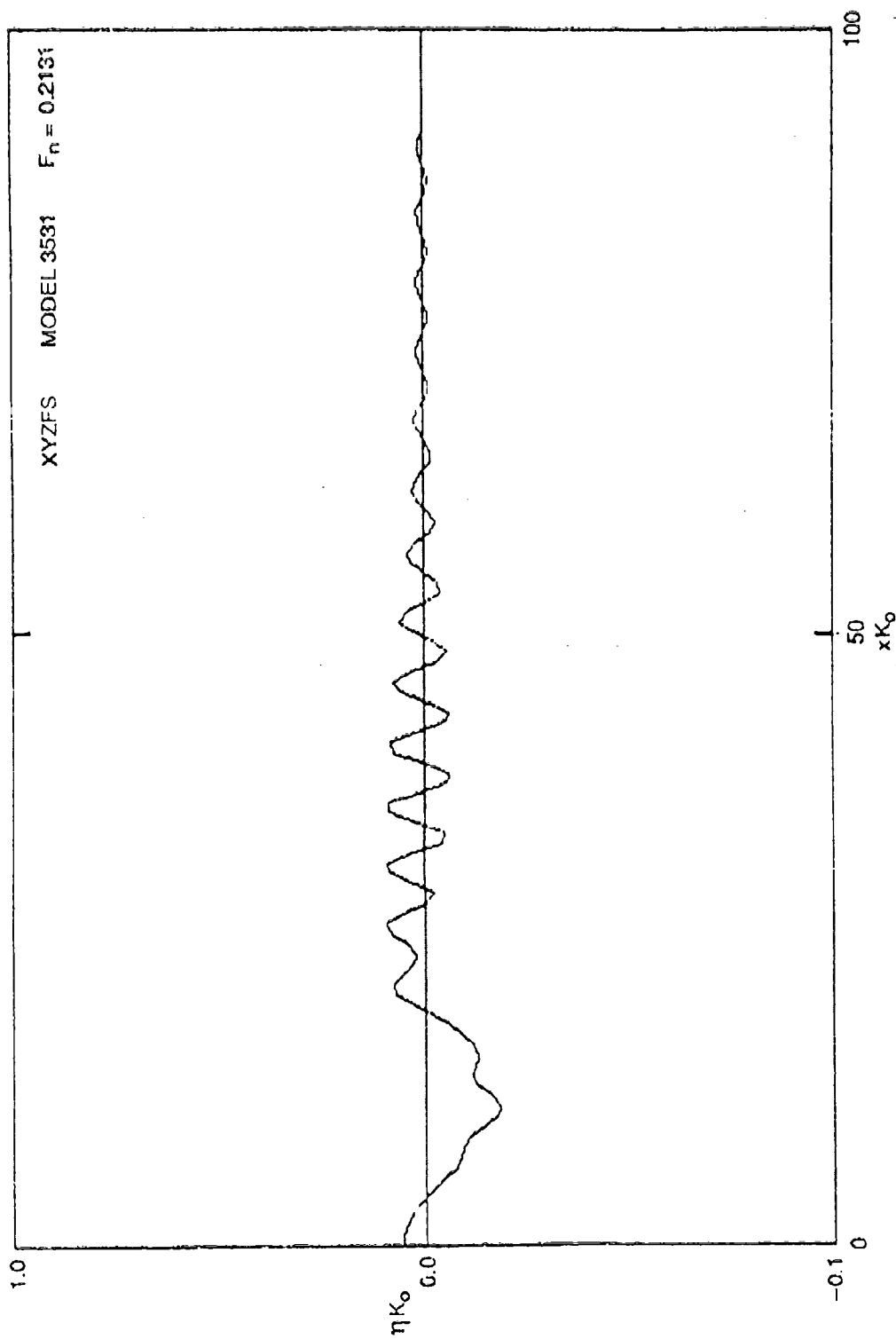


Fig. I.11. XYZFS prediction of wave cut for QUAPAW at $F_n = 0.2131$.

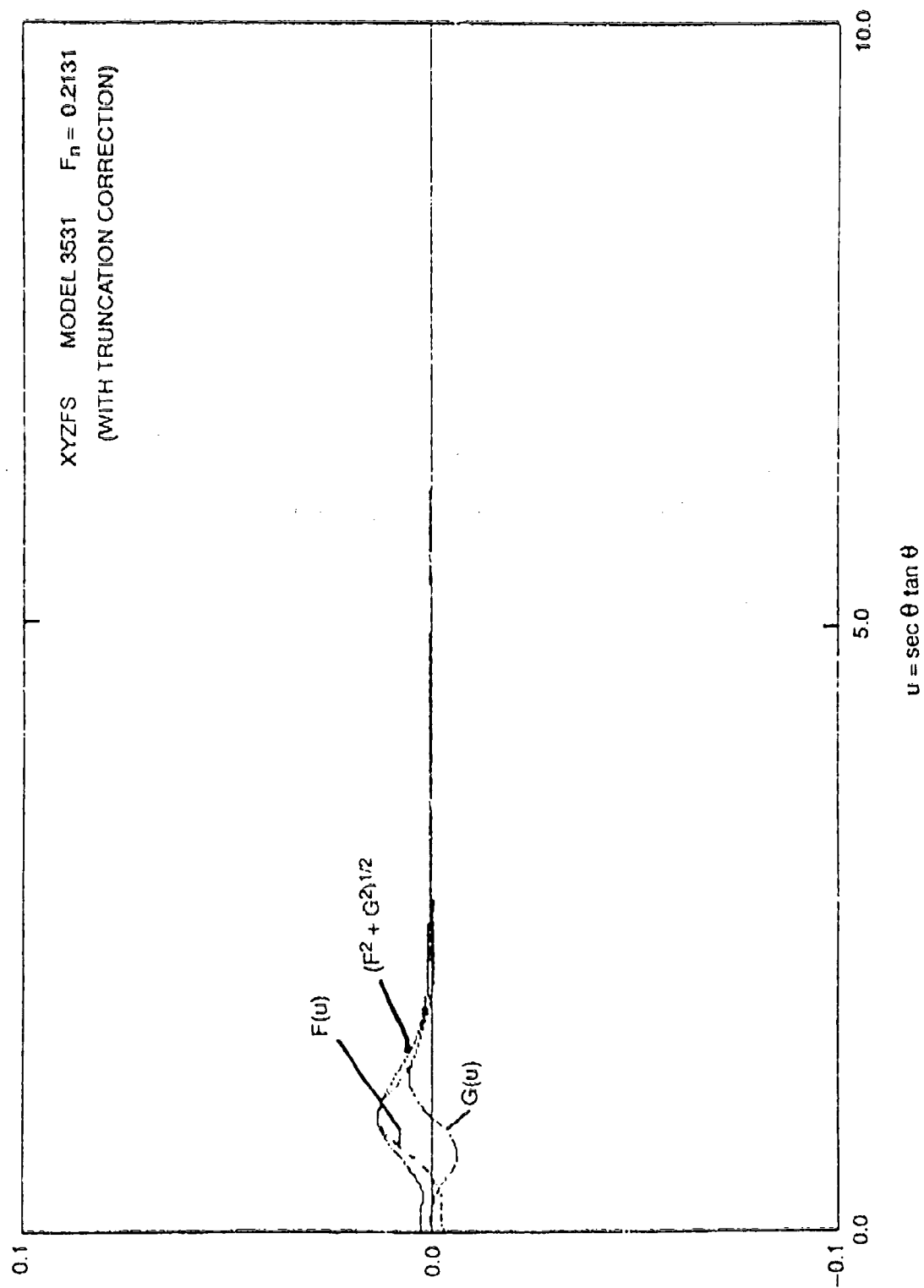


Fig. I.12. XYZFS prediction of wave spectrum for QUAPAW at $F_n = 0.2131$.

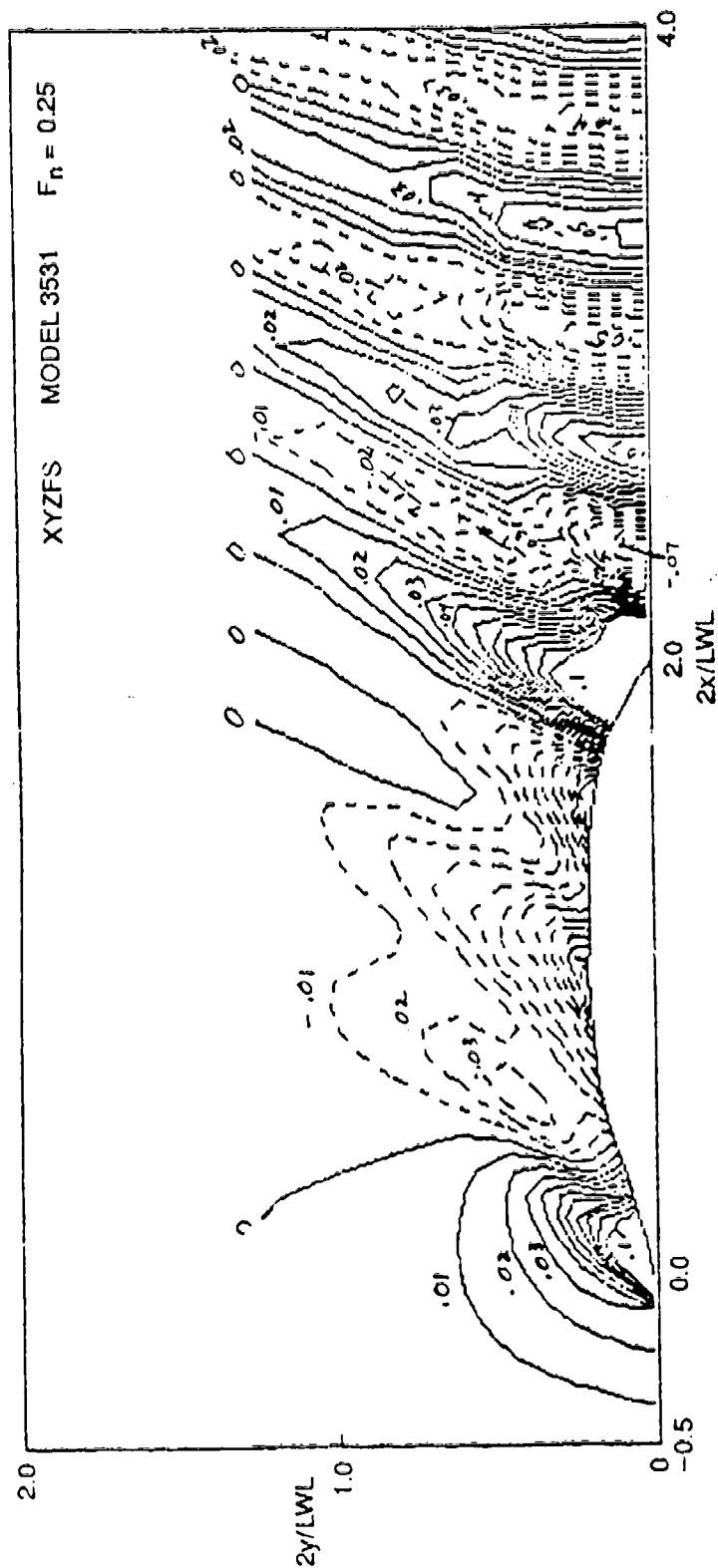


Fig. I.13. XYZFS prediction of wave contour for QUAPAW at $F_n = 0.25$.

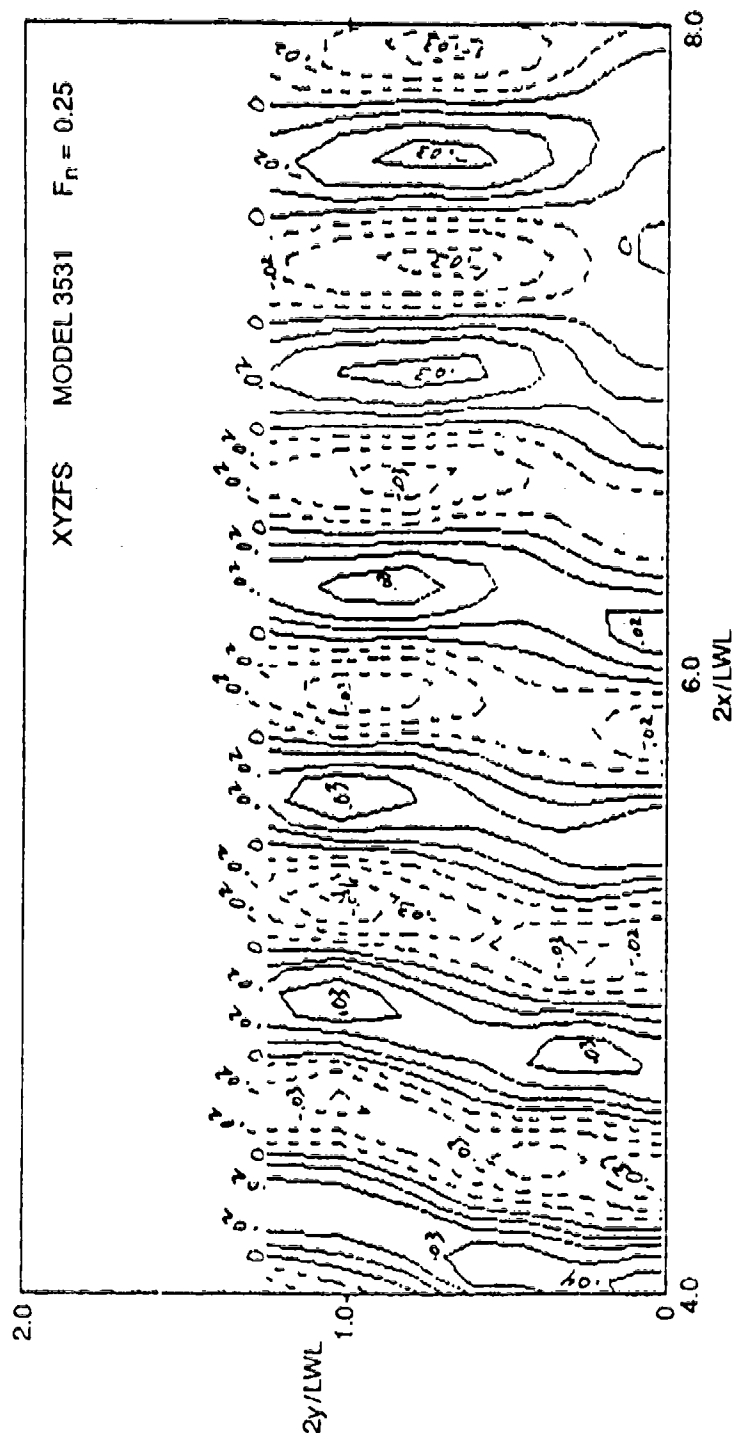


Fig. I.13. (Continued).

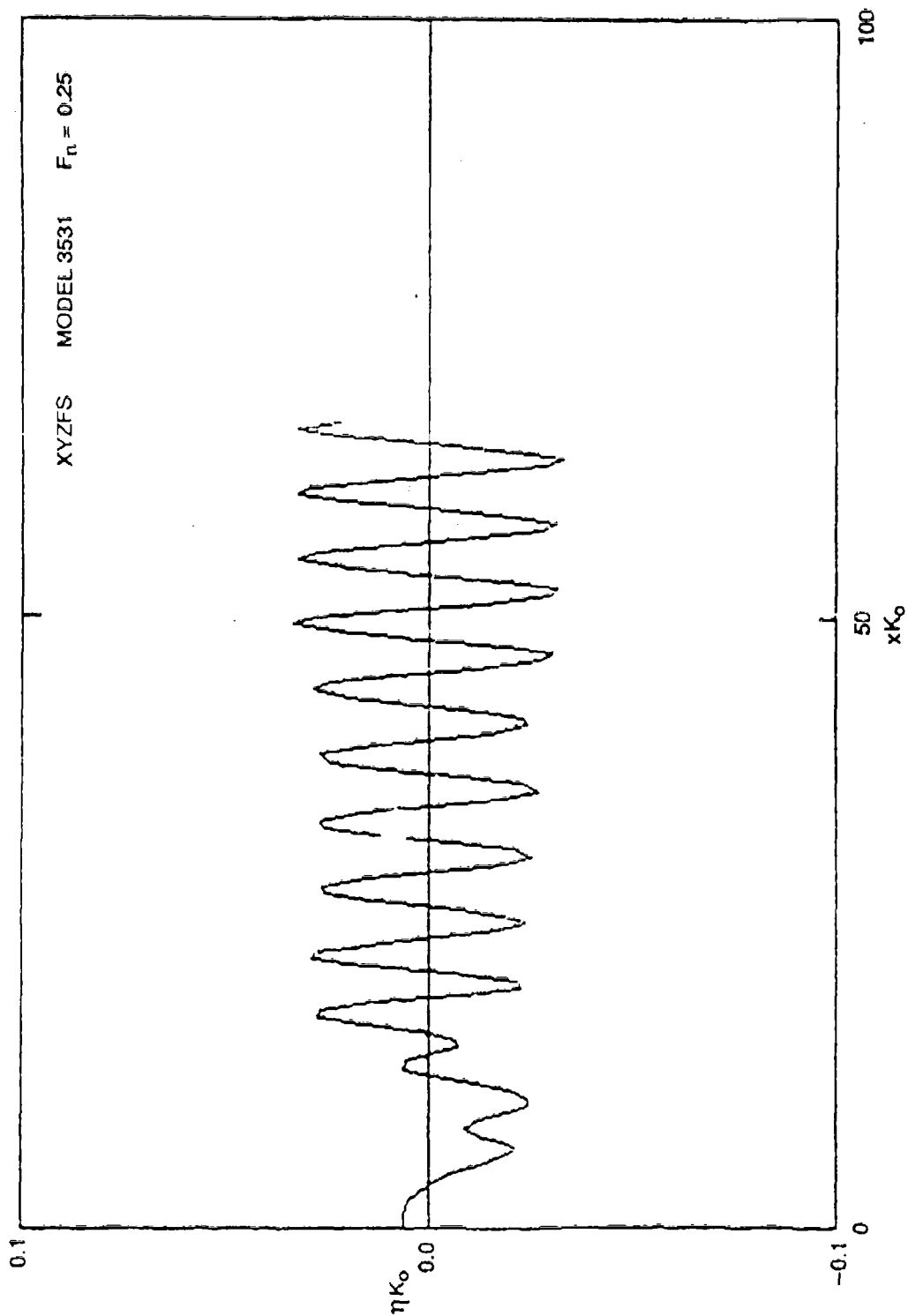


Fig. 1.14. XYZFS prediction of wave cut for QUAPAW at $F_n = 0.25$

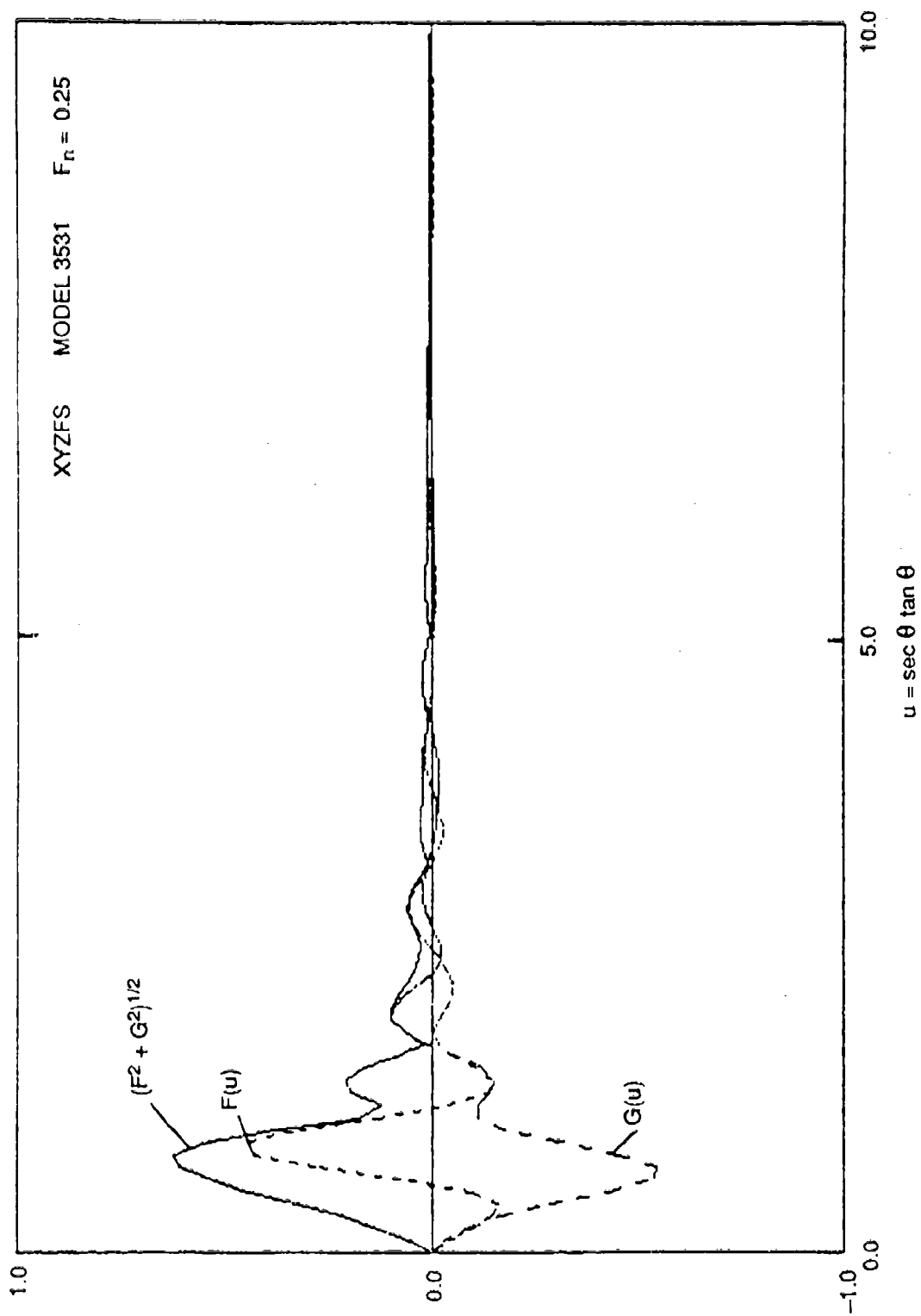


Fig. I.15. XYZFS prediction of wave spectrum for QUAPAW at $F_n = 0.25$.

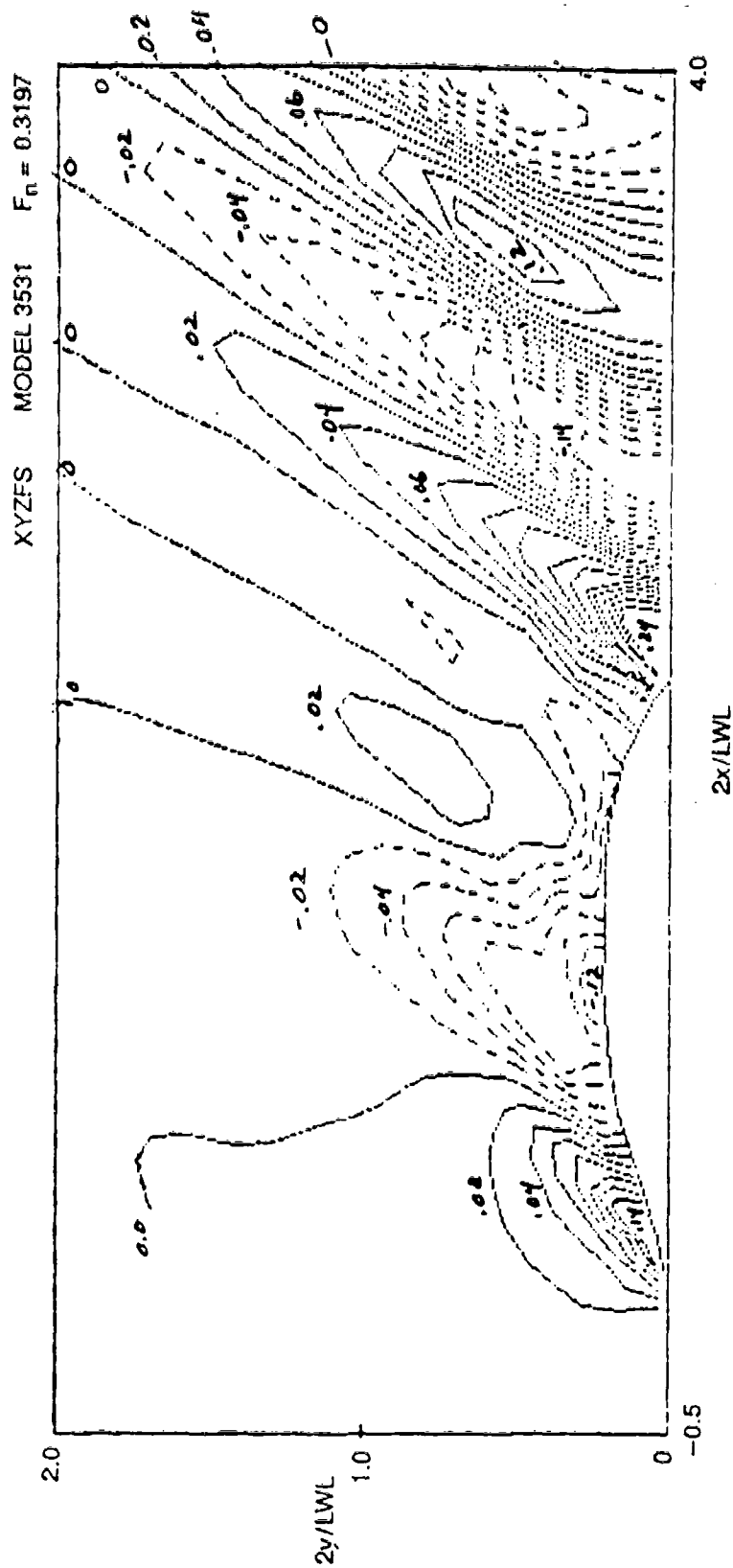


Fig. I.16. XYZFS prediction of wave contour for QUAPAW at $F_n = 0.3197$.

XYZFS MODEL 3531 $F_n = 0.3197$

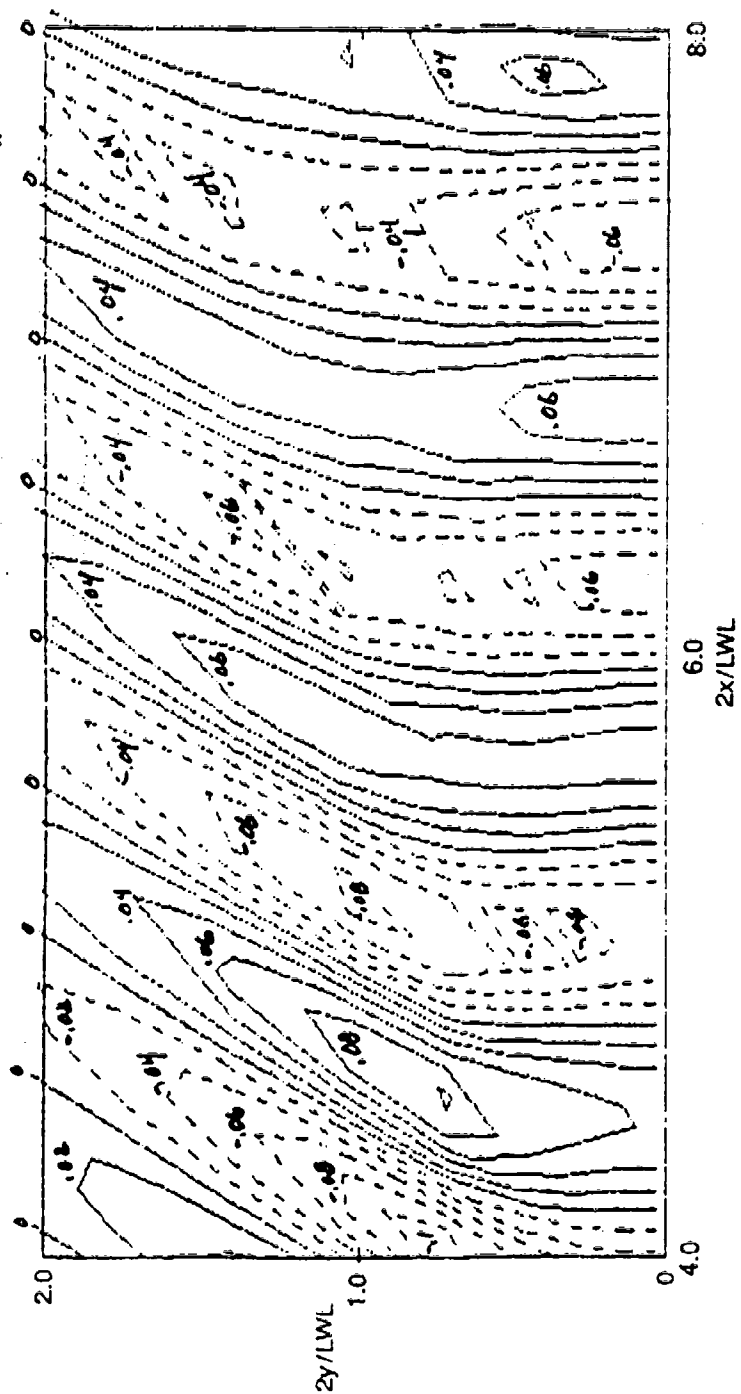


Fig. I.16. (Continued).

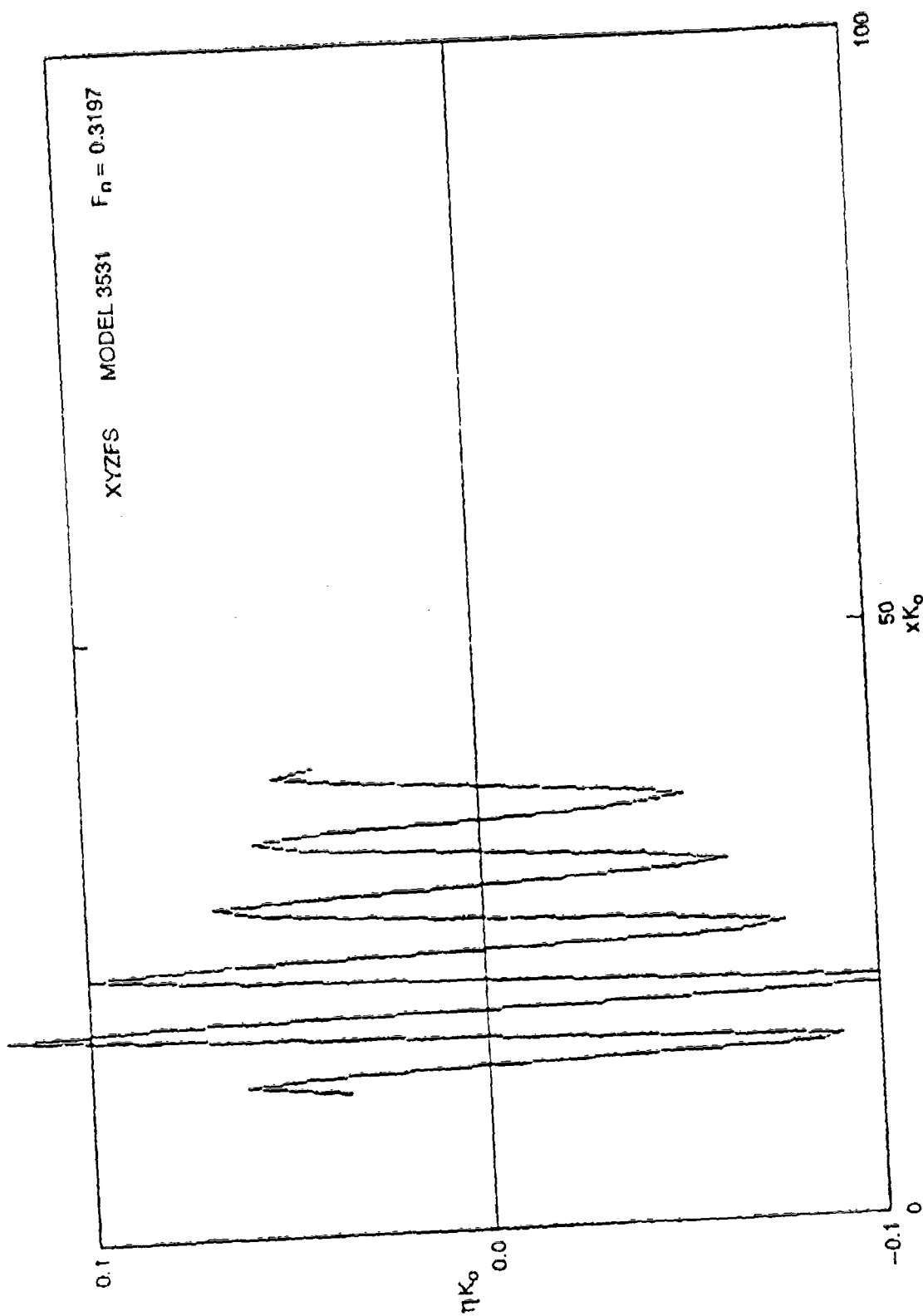


Fig. I.17. XYZFS prediction of wave cut for QUAPAW at $F_n = 0.3197$.

XYZFS MODEL 3531 $F_n = 0.3197$
 (WITH TRUNCATION CORRECTION)

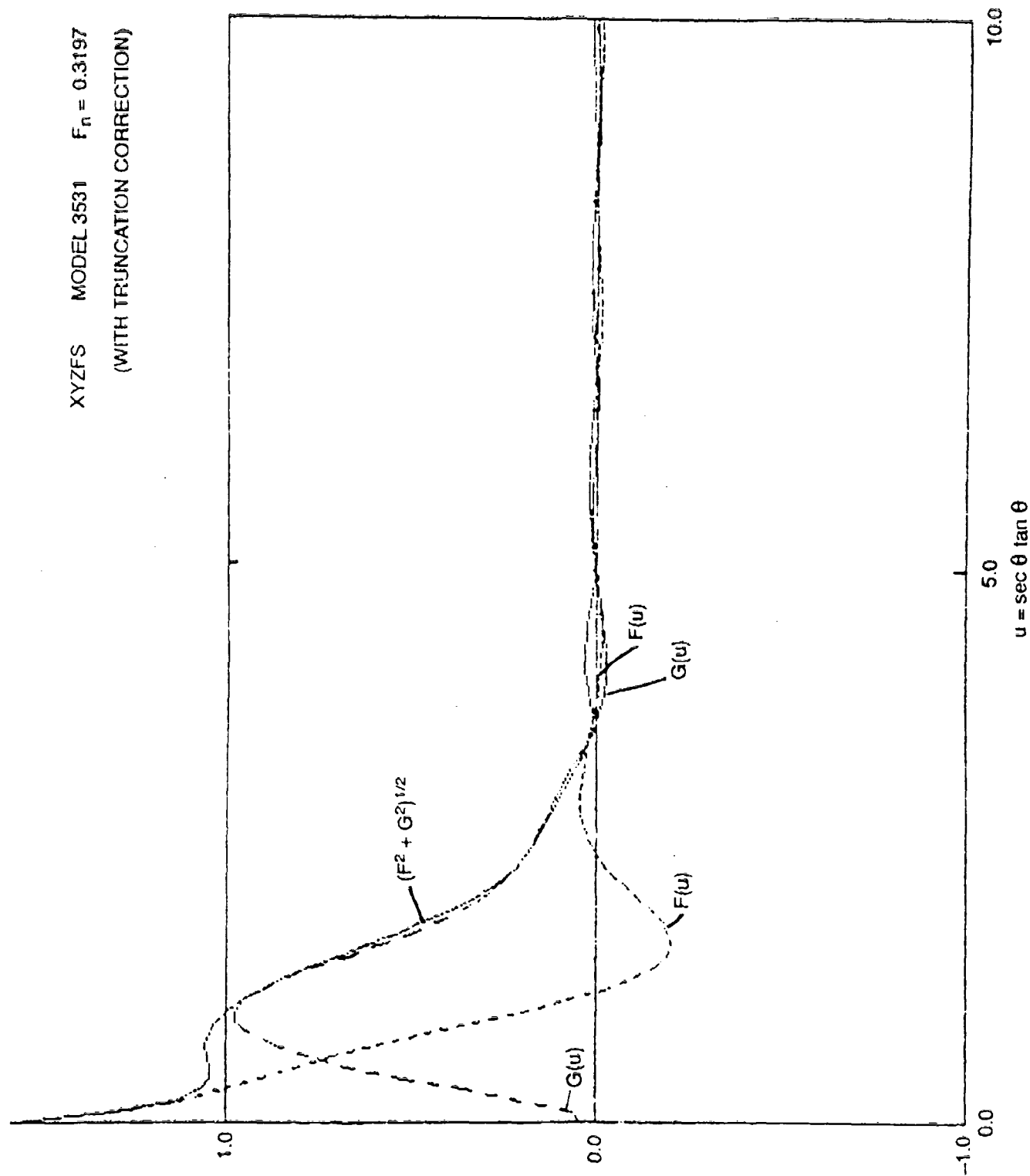


Fig. I.18. XYZFS prediction of wave spectrum for QUAPAW at $F_n = 0.3197$.

THIS PAGE INTENTIONALLY LEFT BLANK

APPENDIX J
PROPRIETARY CODE PREDICTIONS

PROPRIETARY COMPUTER CODE

- SOLUTION PROCEDURE
 - DOUBLE MODEL SOLUTION
 - CREATE FREE SURFACE GRID
 - FREE SURFACE SOLUTION
- ITERATIVE MATRIX SOLVER
- FLAT QUADRILATERAL PANELS
- HULL - CONSTANT RANKINE SOURCES
- FREE SURFACE
 - CONSTANT RANKINE SOURCES
 - CONSTANT DOUBLET
- RADIATION CONDITION
 - UPSTREAM FINITE DIFFERENCE OPERATOR
- CAPABILITIES
 - COMPUTES WAVE RESISTANCE
 - INCLUDES LIFT
 - SOME ERROR CHECKING
 - NO SINKAGE / TRIM
 - NO STREAMLINE OPTION
 - NO PROPULSOR / ACTUATOR DISC
 - MAY BE SUITABLE FOR TRANSOM STERNS
 - NOT A DOCUMENTED OPTION
- CODING INFORMATION
 - FORTRAN
 - 15,000 LINES
 - 80 SUBROUTINES
 - VAX OR CDC COMPUTER
- DOCUMENTATION
 - SEVERAL REPORTS ON THE METHOD
 - USER'S MANUAL
 - CODE SPARSELY COMMENTED

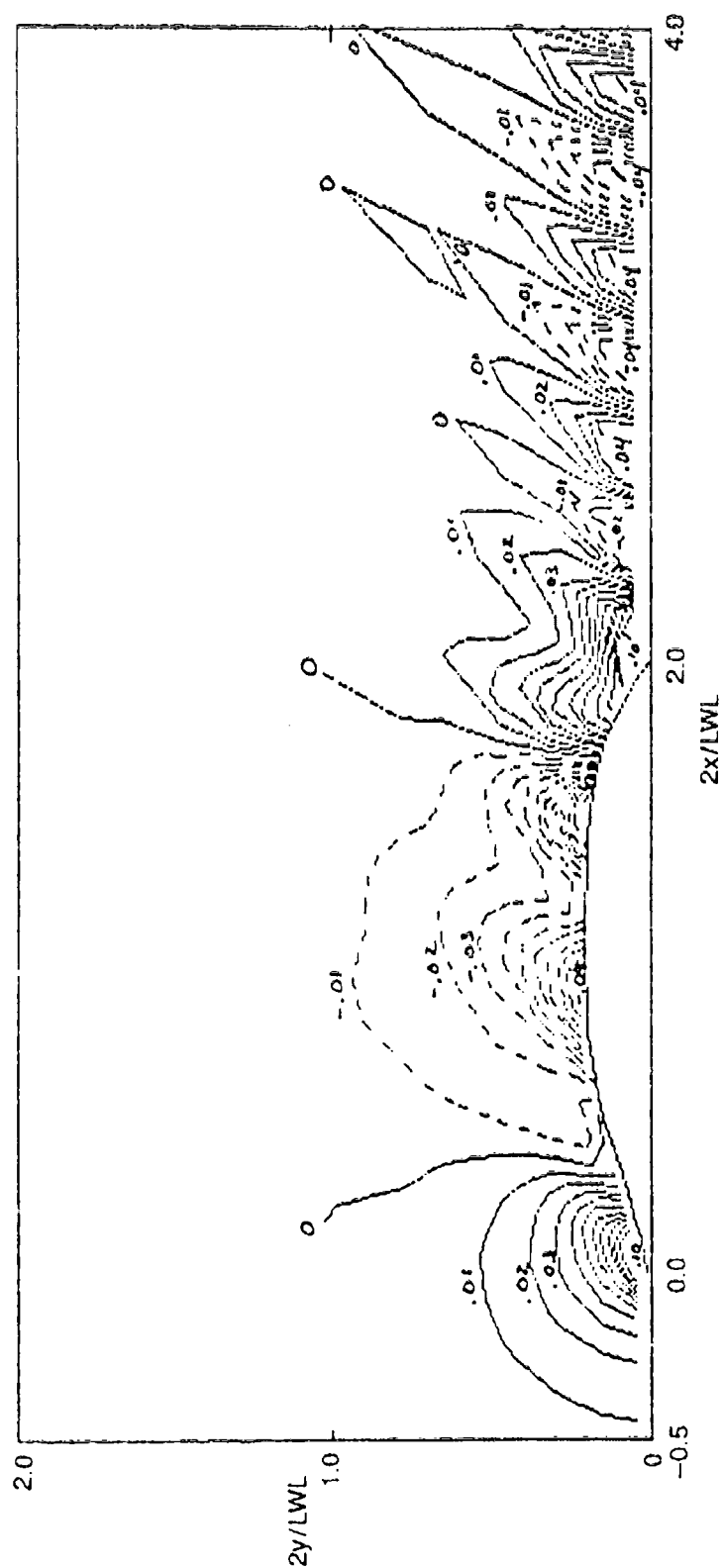


Fig. J.1. Proprietary Code prediction of wave contour for QUAPAW at $F_n = 0.2131$.

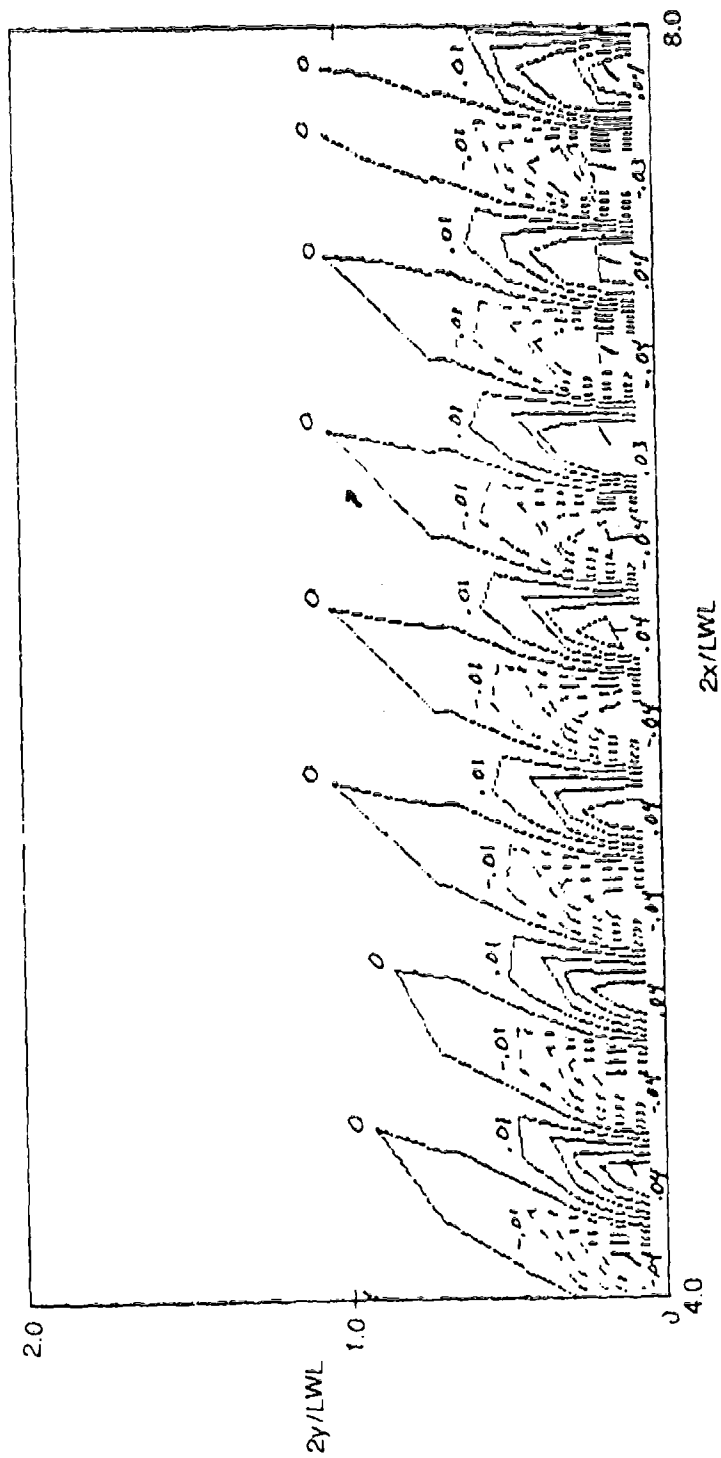


Fig. J.1. (Continued).

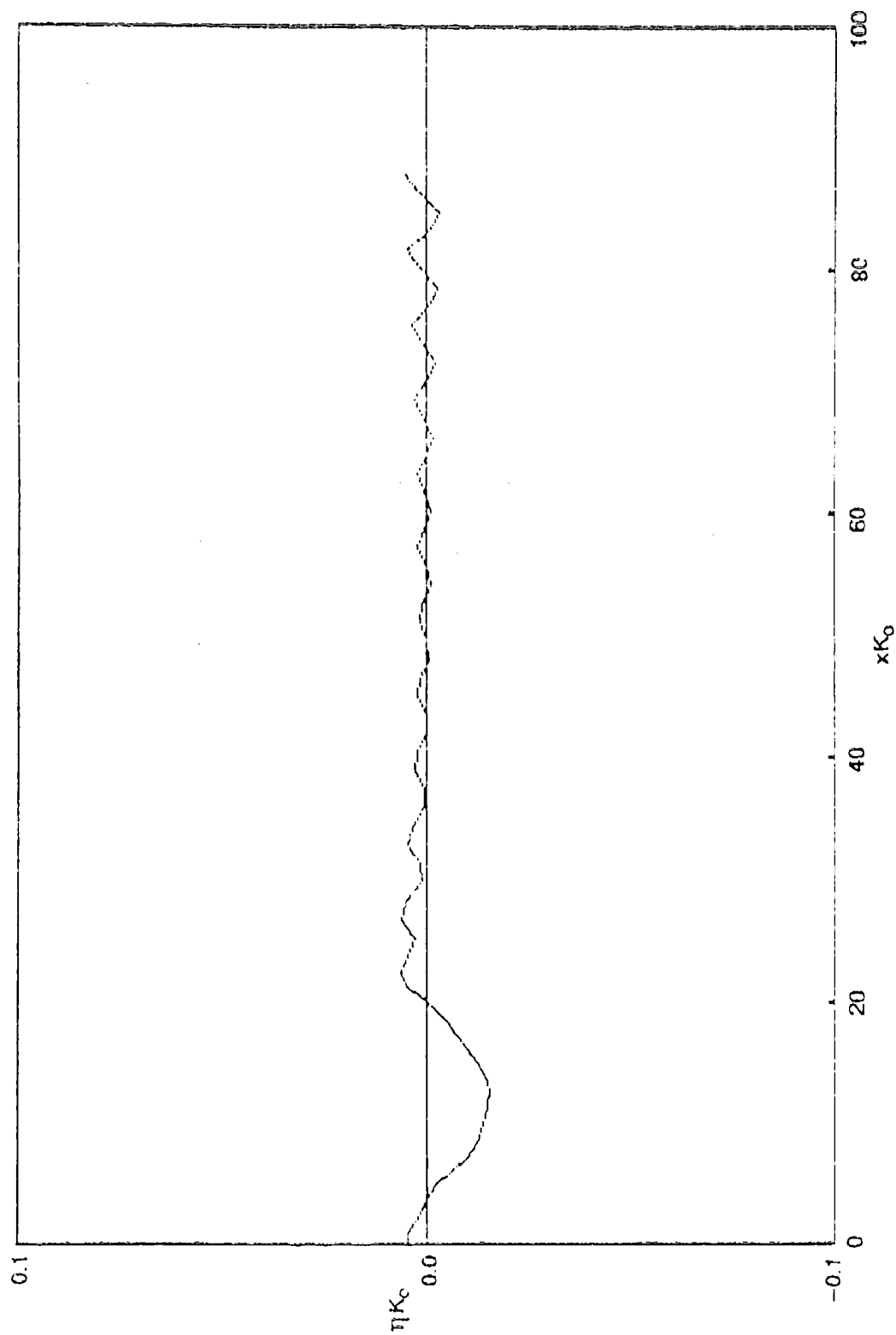


Fig. J.2. Proprietary Code prediction of wave cut for QUAPAW at $F_n = 0.2131$.

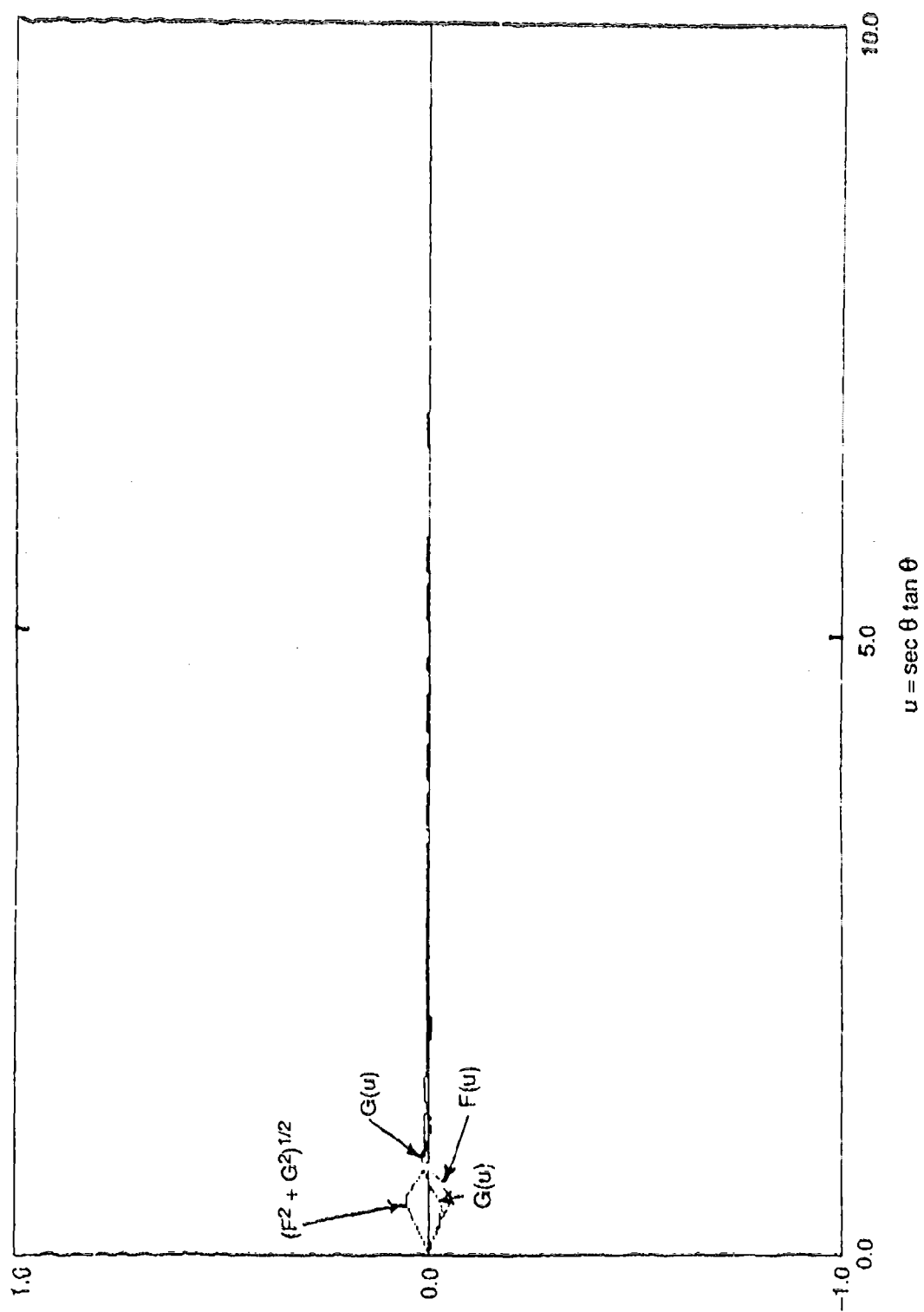


Fig. J.3. Proprietary Code prediction of wave spectrum for QUAPAW at $F_n = 0.2131$.

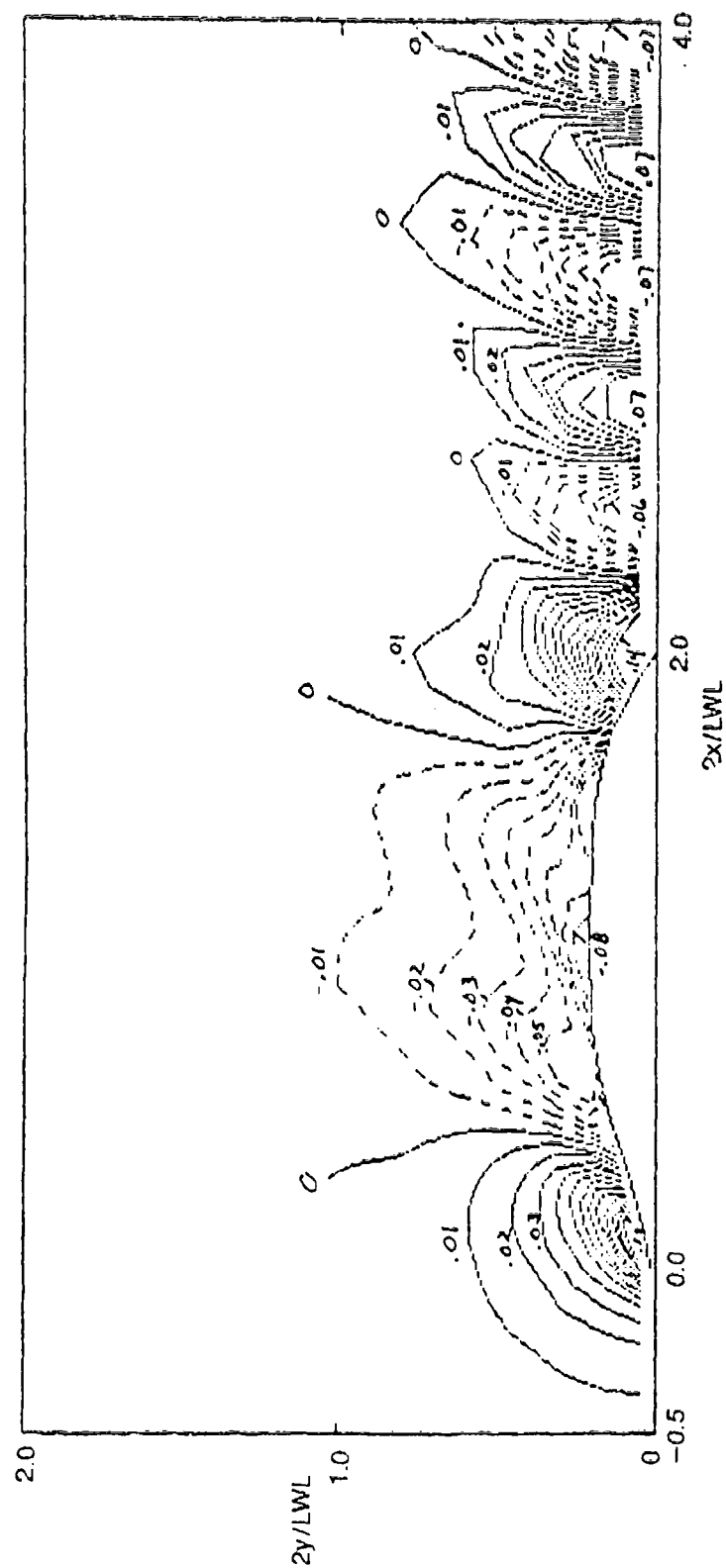


Fig. J.4. Proprietary Code prediction of wave contour for QUAPAW at $F_n = 0.25$.

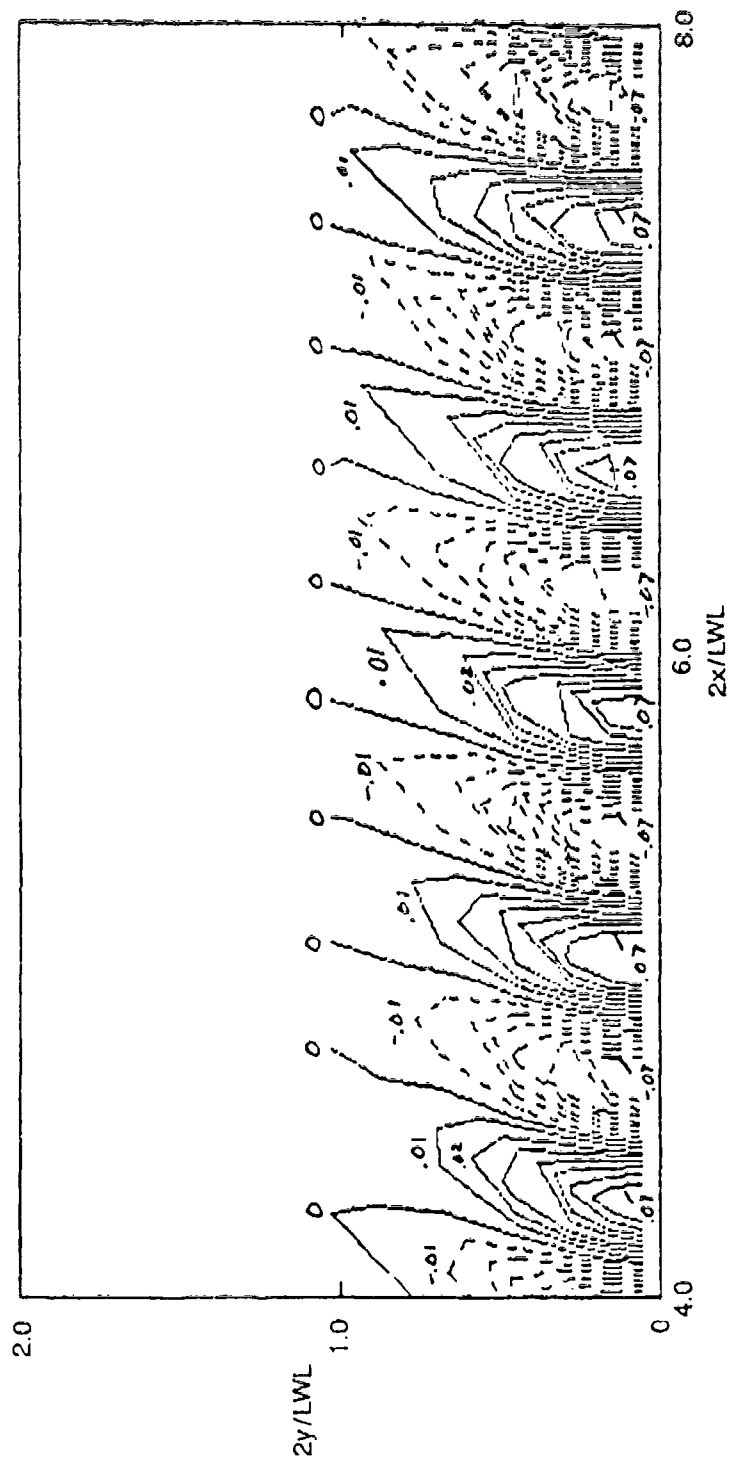


Fig. J.4. (Continued).

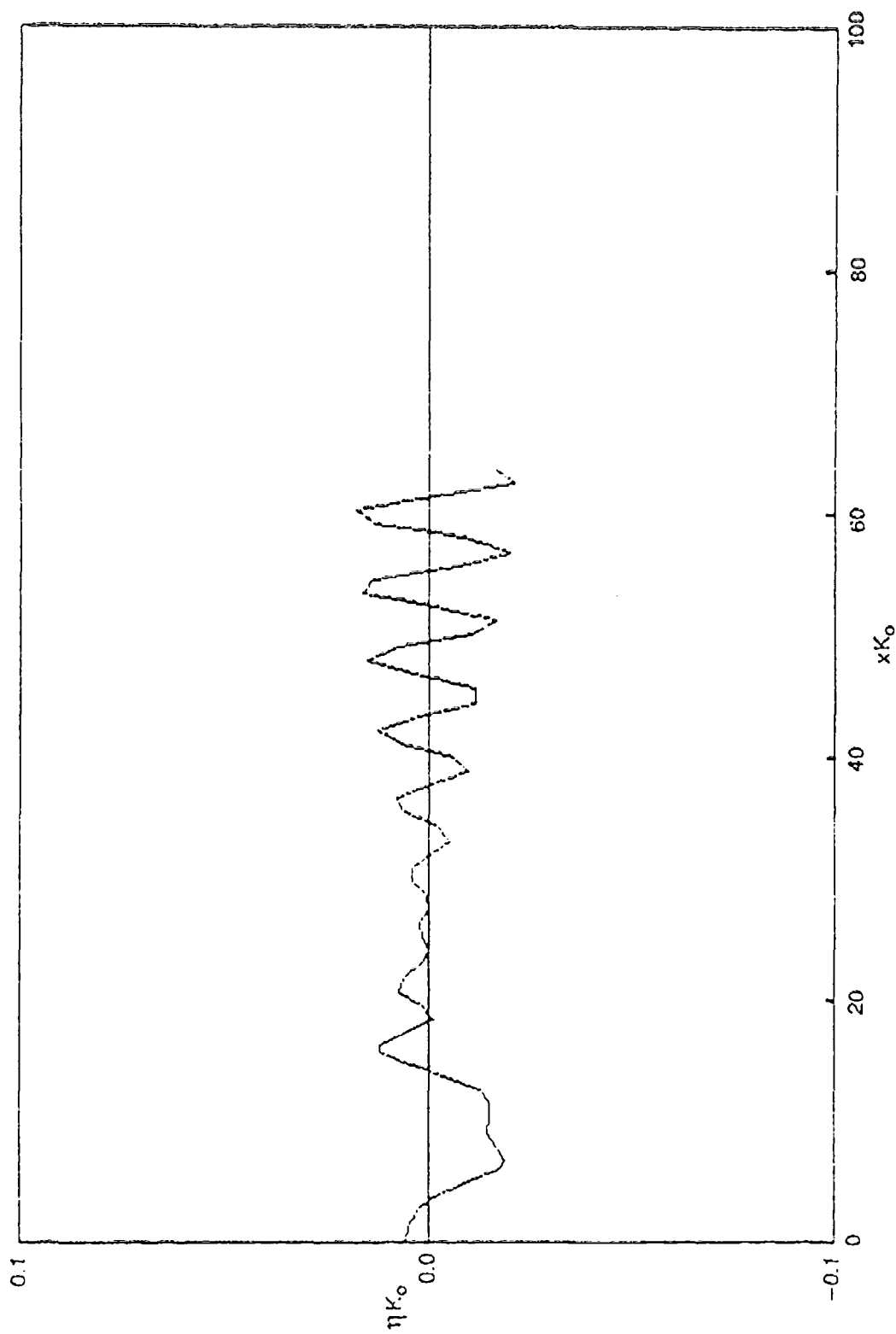


Fig. J.5. Proprietary Code prediction of wave cut for QUAPAW at $F_n = 0.25$.

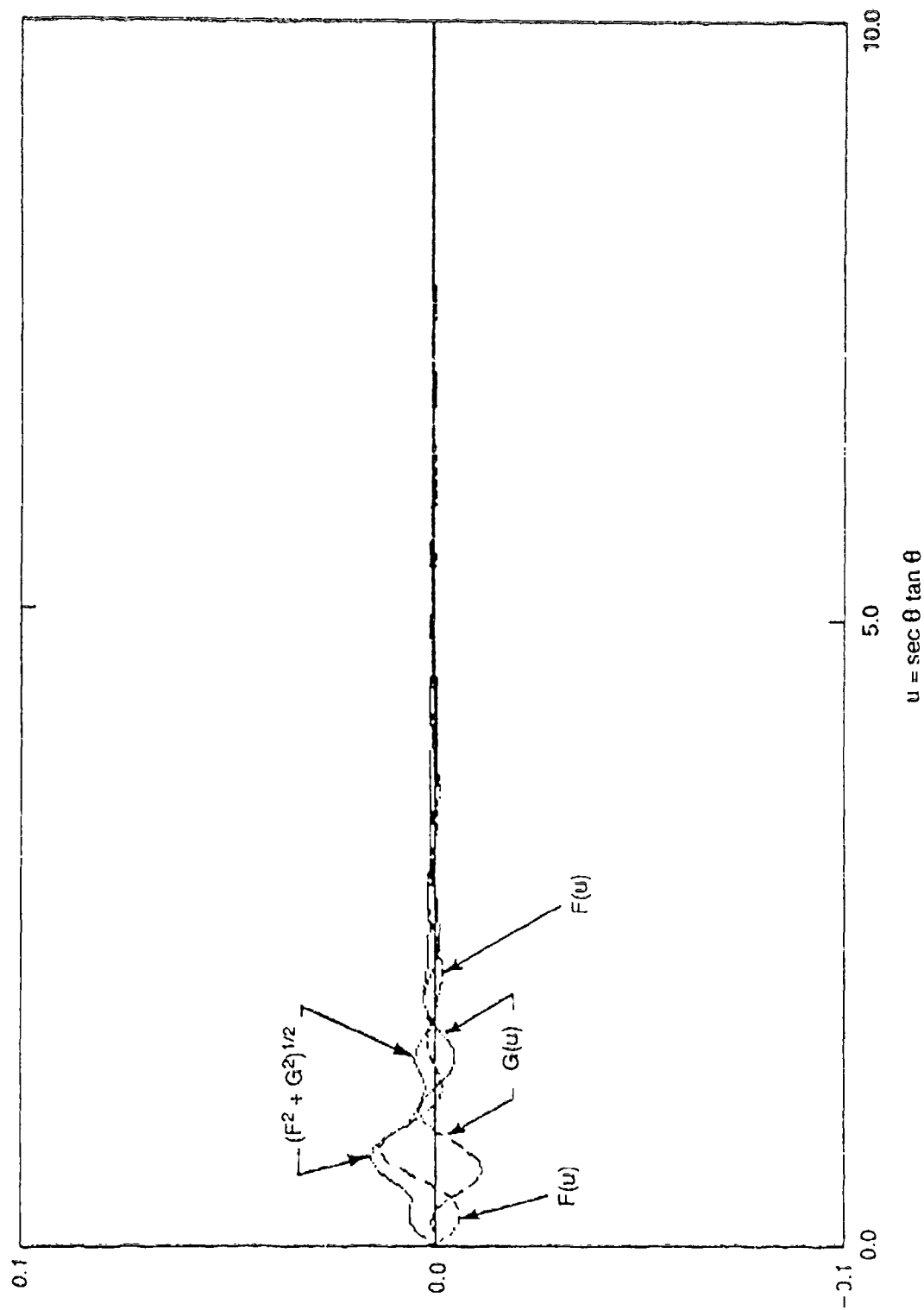


Fig. J.6. Proprietary Code prediction of wave spectrum for QUAPAW at $F_n = 0.25$

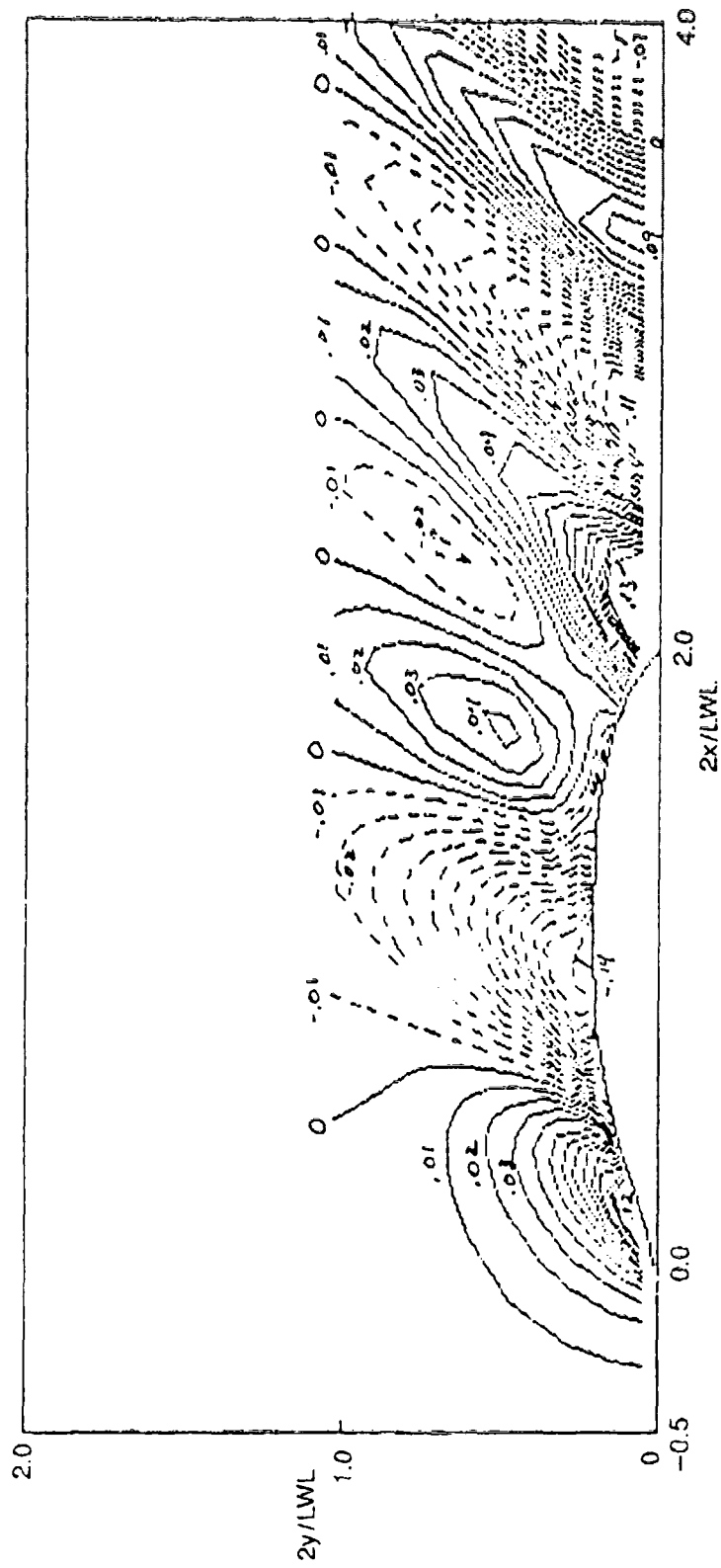


Fig. J.7. Proprietary Code prediction of wave contour for QUAPAW at $F_n = 0.3197$.

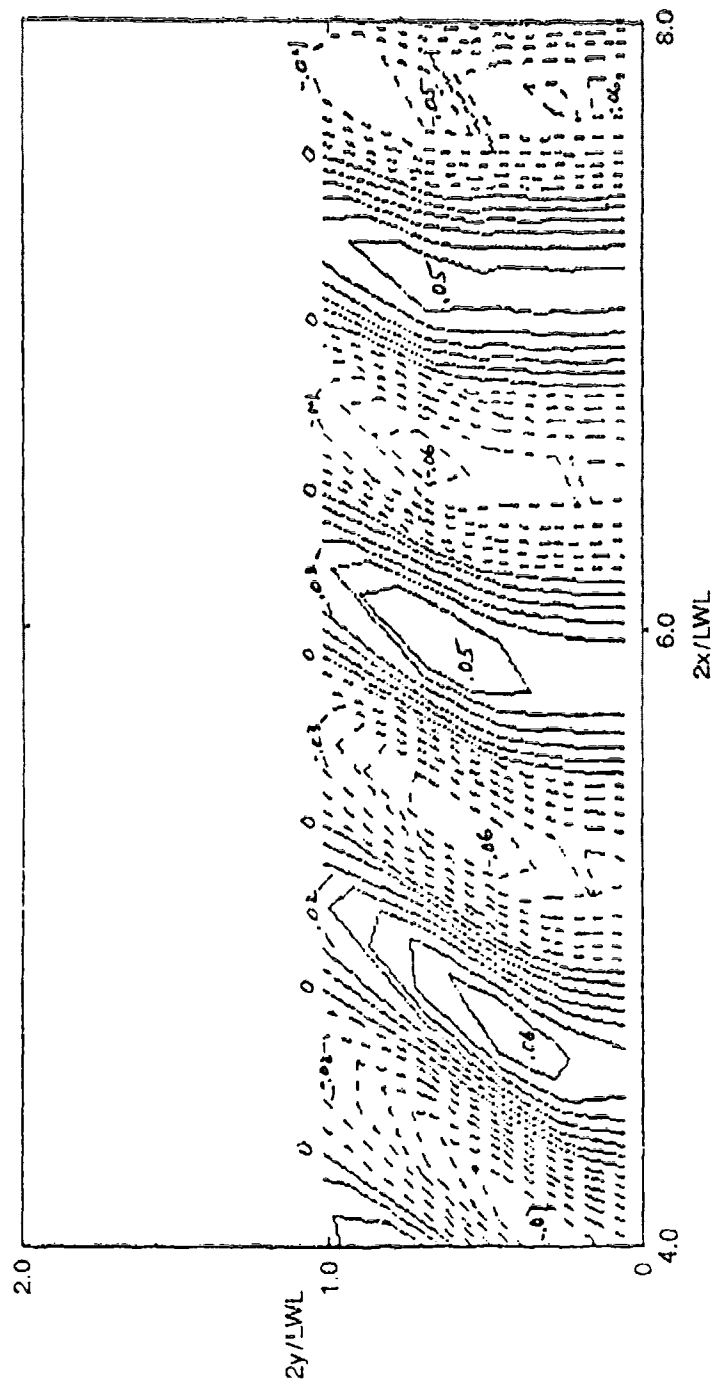


Fig. J.7. (Continued).

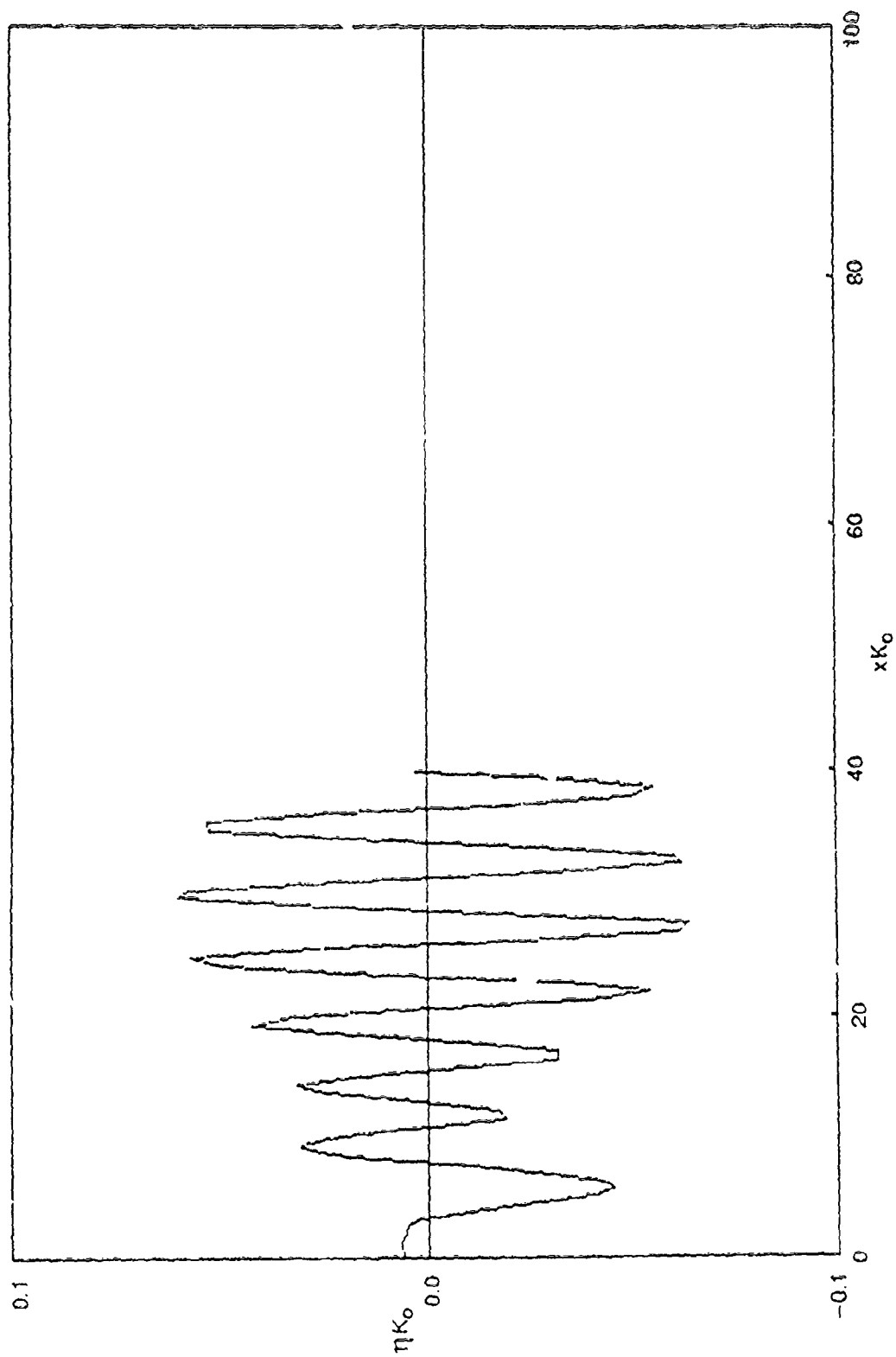


Fig. J.8. Proprietary Code prediction of wave cut for QUA PAW at $F_n = 0.3197$.

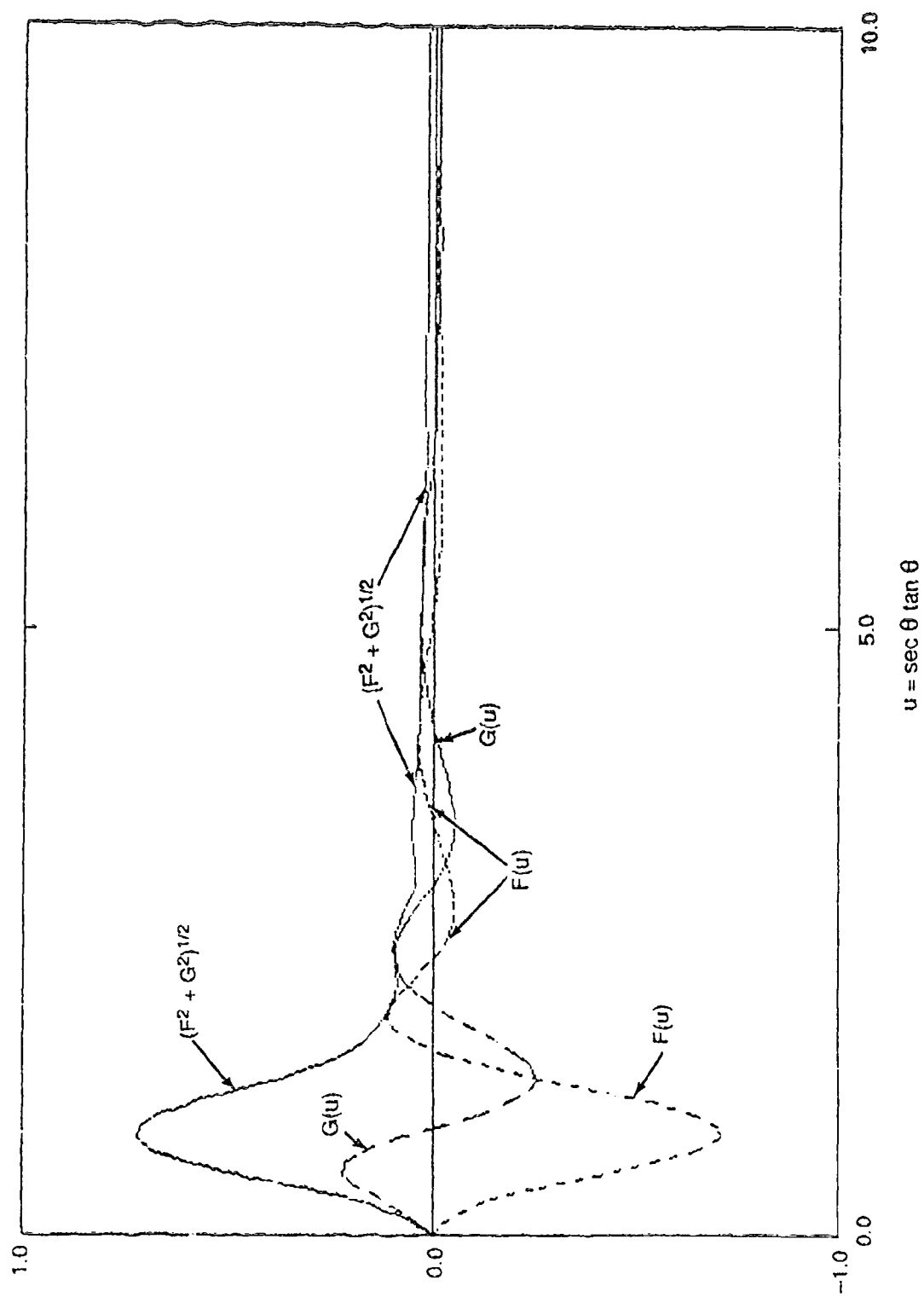


Fig. J.9. Proprietary Code prediction of wave spectrum for QUAPAW at $F_n = 0.3197$.

APPENDIX K
SWIMFS PREDICTION

SWIM/SWIMFS COMPUTER CODE — SWIM

- Developed by Ming Chang of DTRC — 1970's
- Modifications for a CRAY by T. Lucas of UNC
- Computes a Havelock source distribution on the hull
- Computes wave resistance and lift — has been used for this purpose by the Ship Performance Department at DTRC
- 1361 lines of FORTRAN (excluding comments)
- 14 subroutines

SWIM/SWIMFS — DOCUMENTATION

- A report describing the approximations in SWIM/SWIMFS has been prepared.
- No user's manual exists.
- Most of the code inadequately commented.
- Ming Chang: 2nd Int'l Conf on Num Ship Hydro — 1977
- SWIM/SWIMFS — 1985

SWIM/SWIMFS — CAPABILITIES & LIMITATIONS

SWIM/SWIMFS COMPUTER CODE — SWIMFS

- Modification of SWIM — all computations of ϕ , ϕ_r and ϕ_t were eliminated; more accurate evaluation of exponential integral
- Uses a Havelock source distribution (previously computed by SWIM) on the hull to compute wave elevations at specified points
- 553 lines of FORTRAN (excluding comments)
- 6 subroutines

- Number of panels limited only by computer memory

- SWIM has provisions for handling transom sterns

- Runs on most computers with minor modifications — has run on CDC, CRAY, VAX, Apollo computers

- No streamlines calculated

- No provision for a propulsor/actuator disc

SWIM/SWIMFS — USER-FRIENDLINESS

- No checking of geometric input — prints centroid, normal, and area of each panel.
- No informative messages if something goes wrong or is likely to go wrong in the computation.
- To prepare input —
- To run the program —
- To display results —

SWIM/SWIMFS — computations

- Sunk/trimmed Quapaw data from XYZFS
- CPU time: about 50 minutes per speed (CRAY-XMP)
- 192 (8×24) panels on half the hull
- 1200 to 1250 free-surface points for contour plotting (only inside the 19° cusp lines) — on the Quapaw:

Speed (knots)	pts./wavelength
10.0	13
11.7	8
15.0	6

- Rectangular panels. Singularity distribution of Havelock sources on panel collapsed onto line segment through centroid of panel.
- No convergence check.
- Wave spectra — from (denser) wave cut data

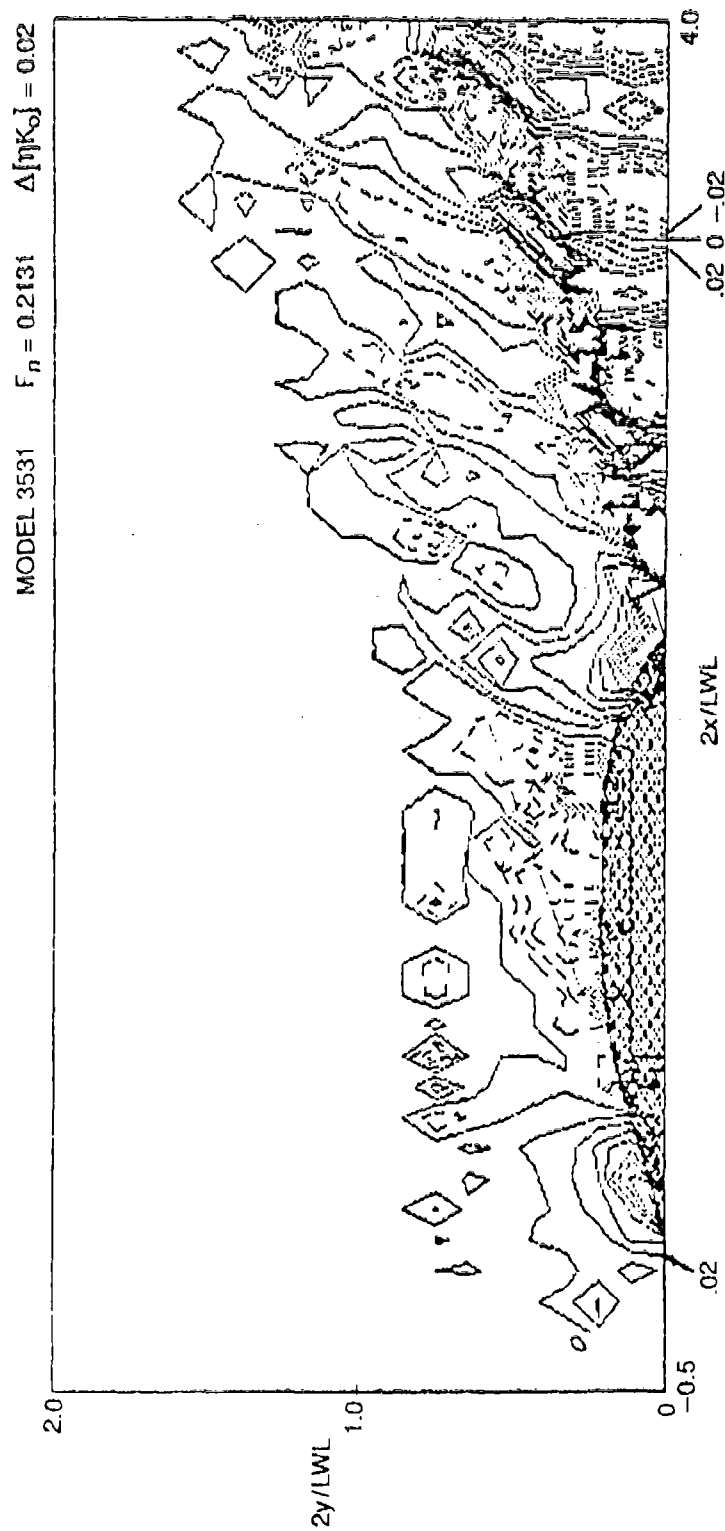


Fig. K.1. SWIMFS prediction of wave contour for QUAPAW at $F_n = 0.2131$.

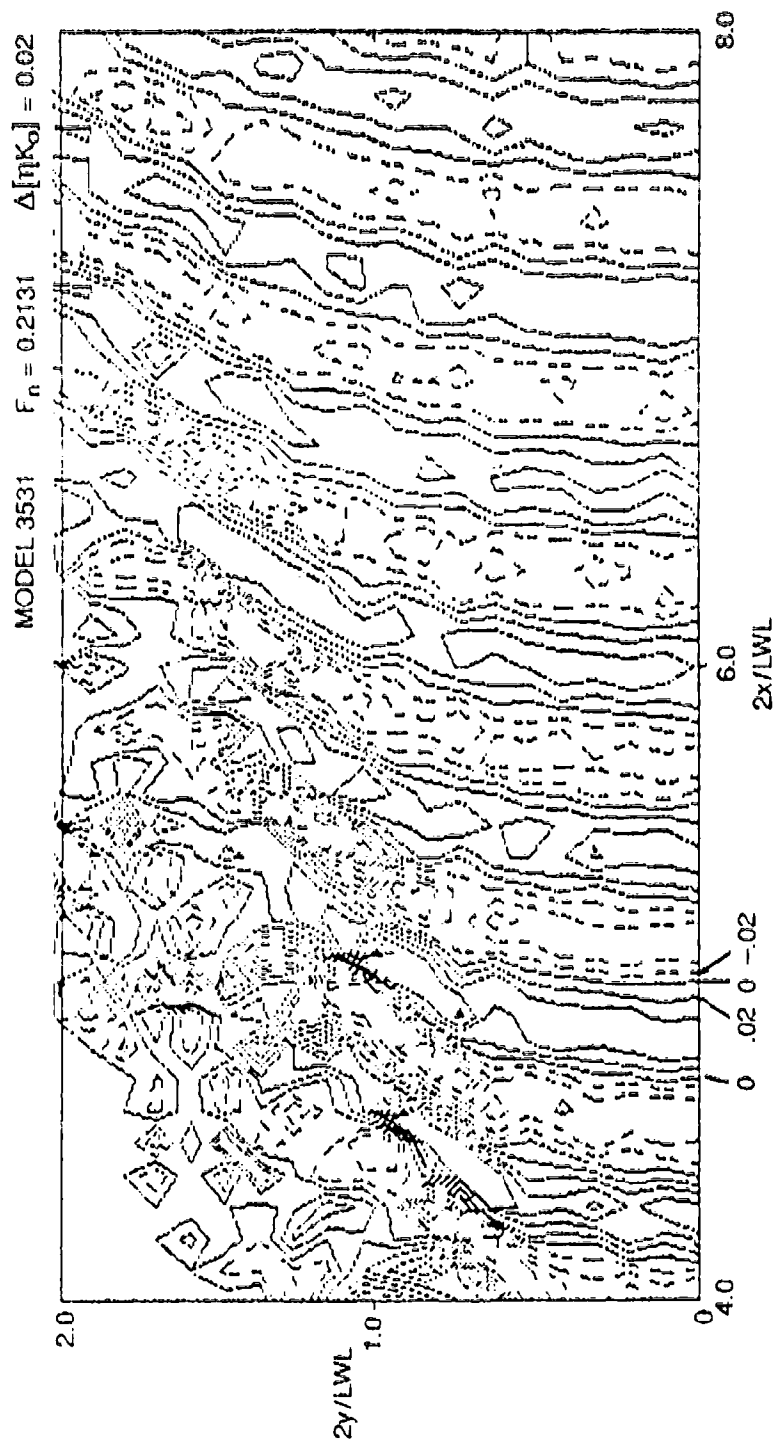


Fig. K.1. (Continued).

MODEL 3531 $F_n = 0.2131$

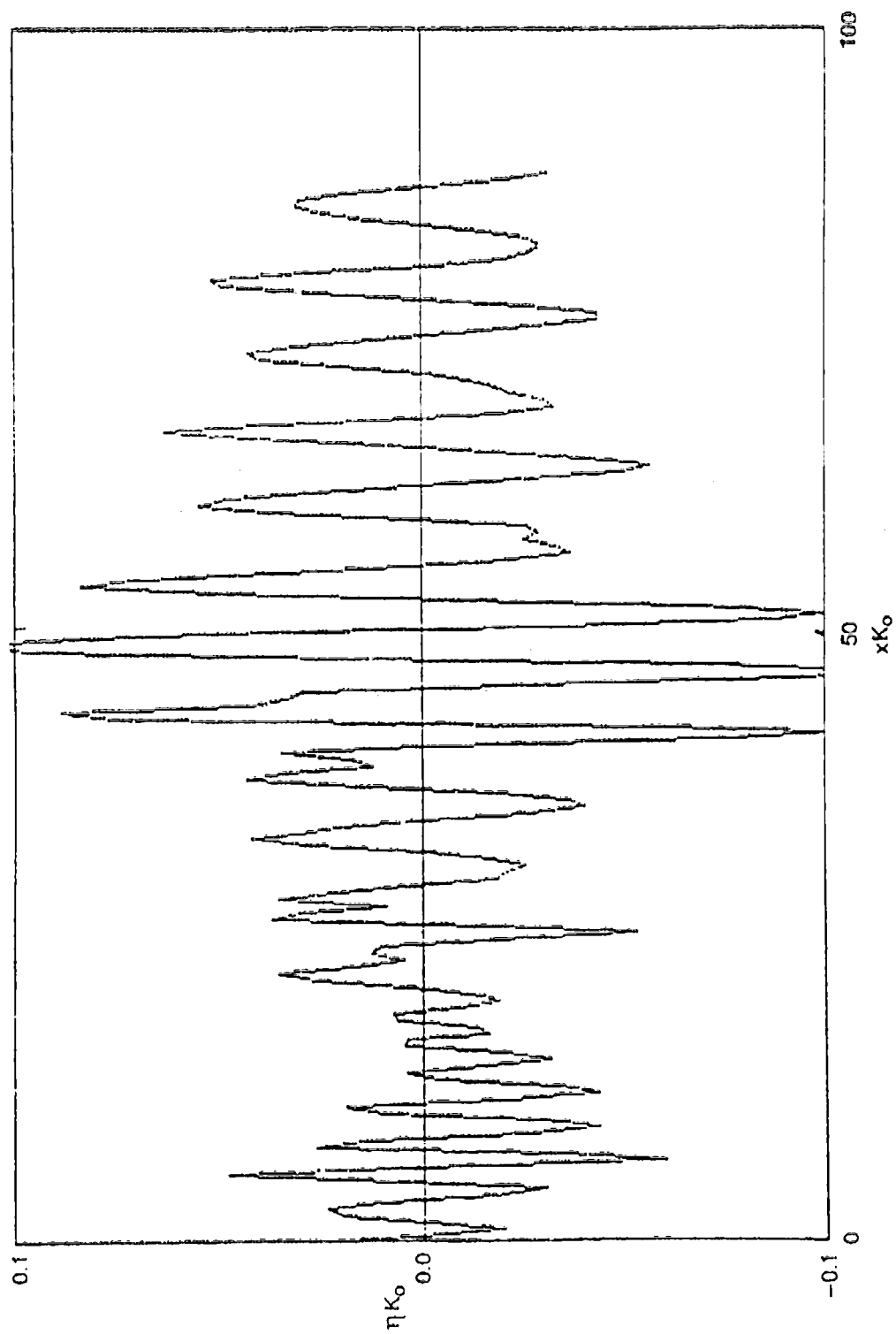


Fig. K.2. SWIMFS prediction of wave cut for QUAPAW at $F_n = 0.2131$.

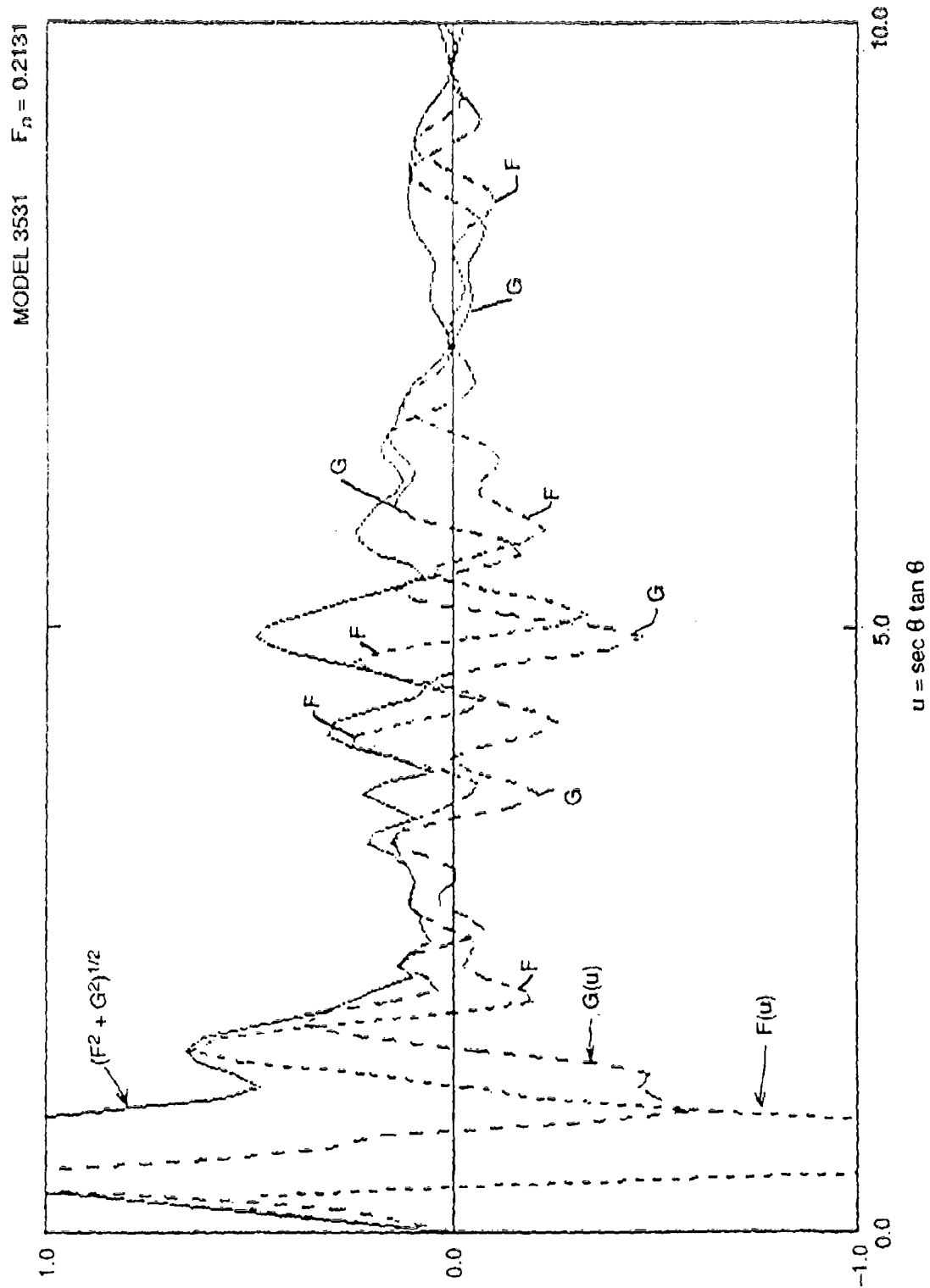


Fig. K.3. SWIMFS prediction of wave spectrum for QUAPAW at $F_n = 0.2131$.

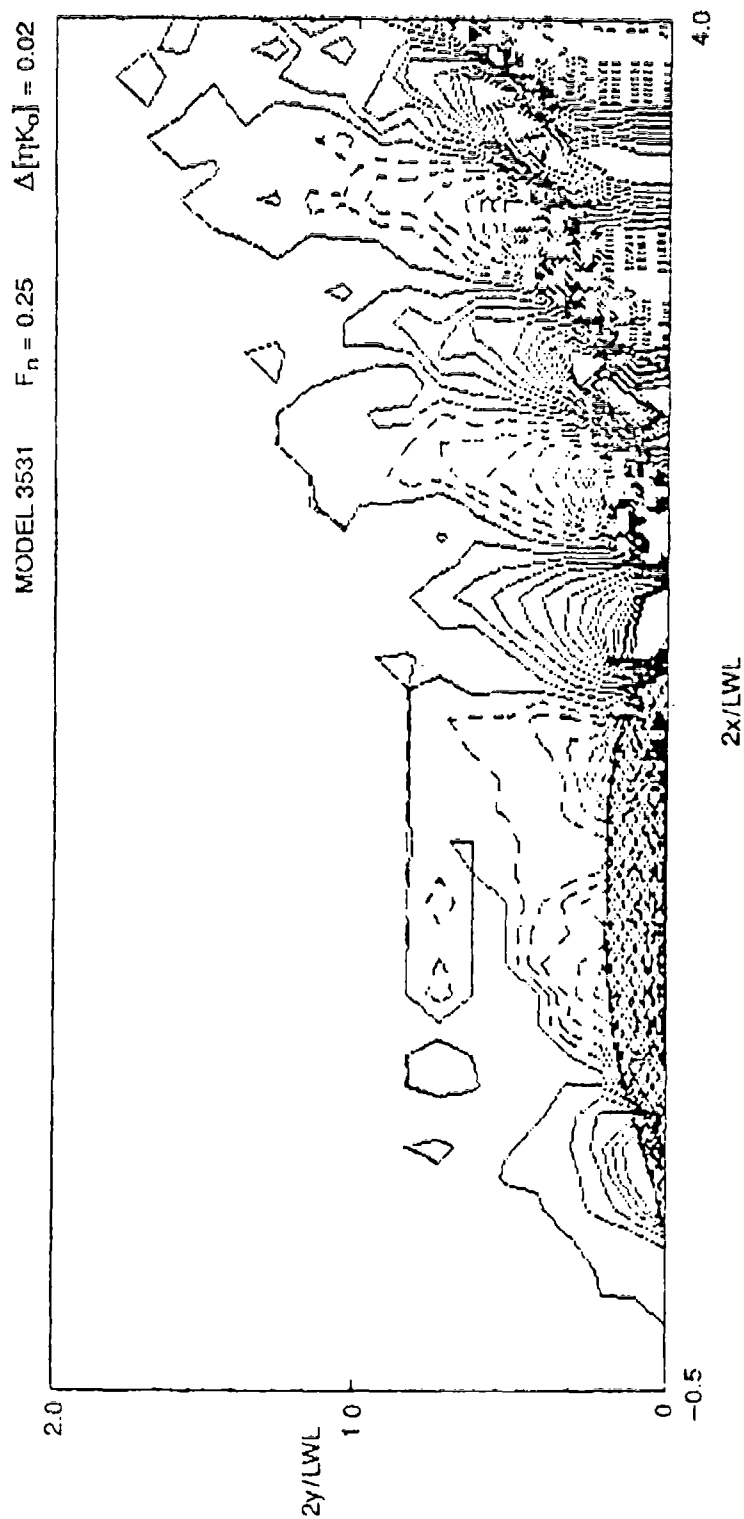


Fig. K.4. SWIMFS prediction of wave contour for QUAPAW at $F_n = 0.25$

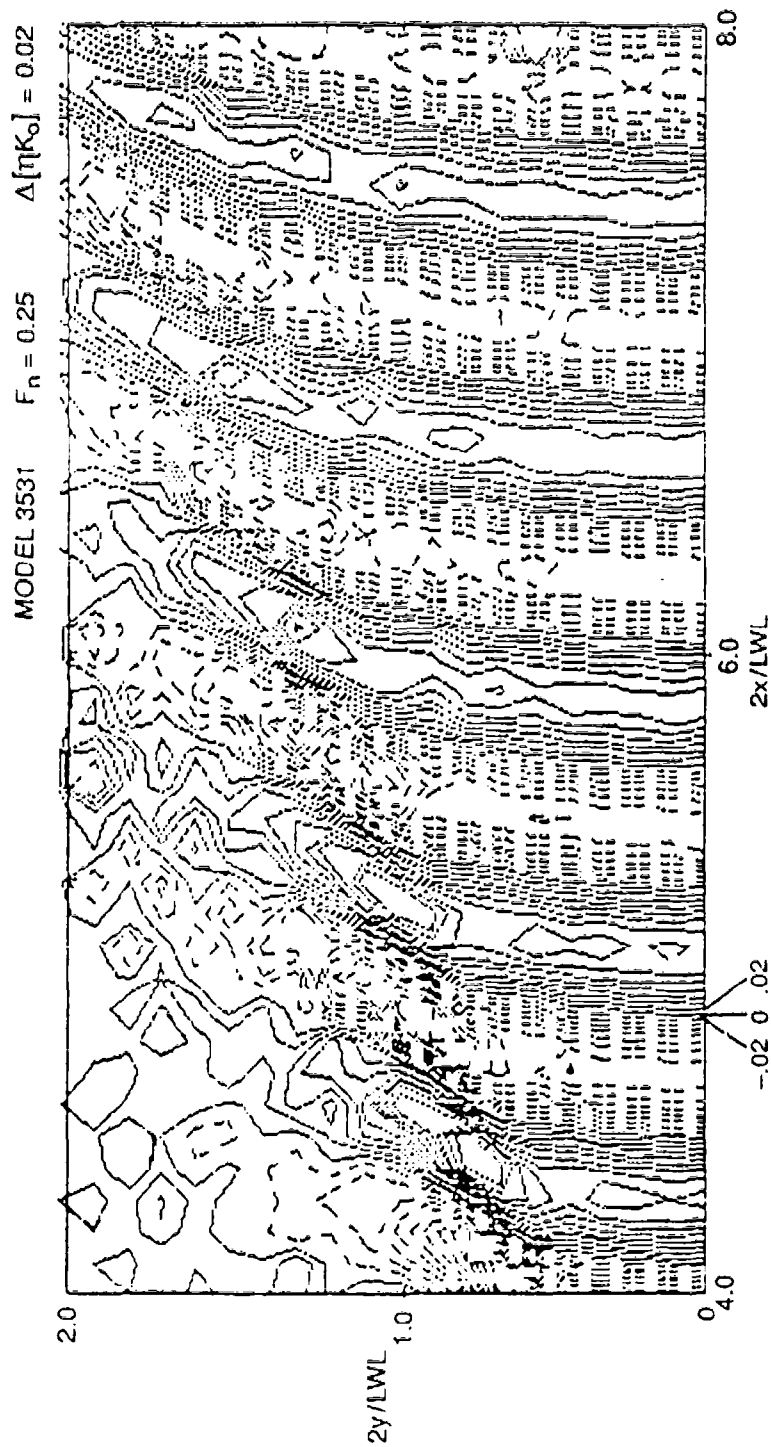


Fig. K.4. (Continued).

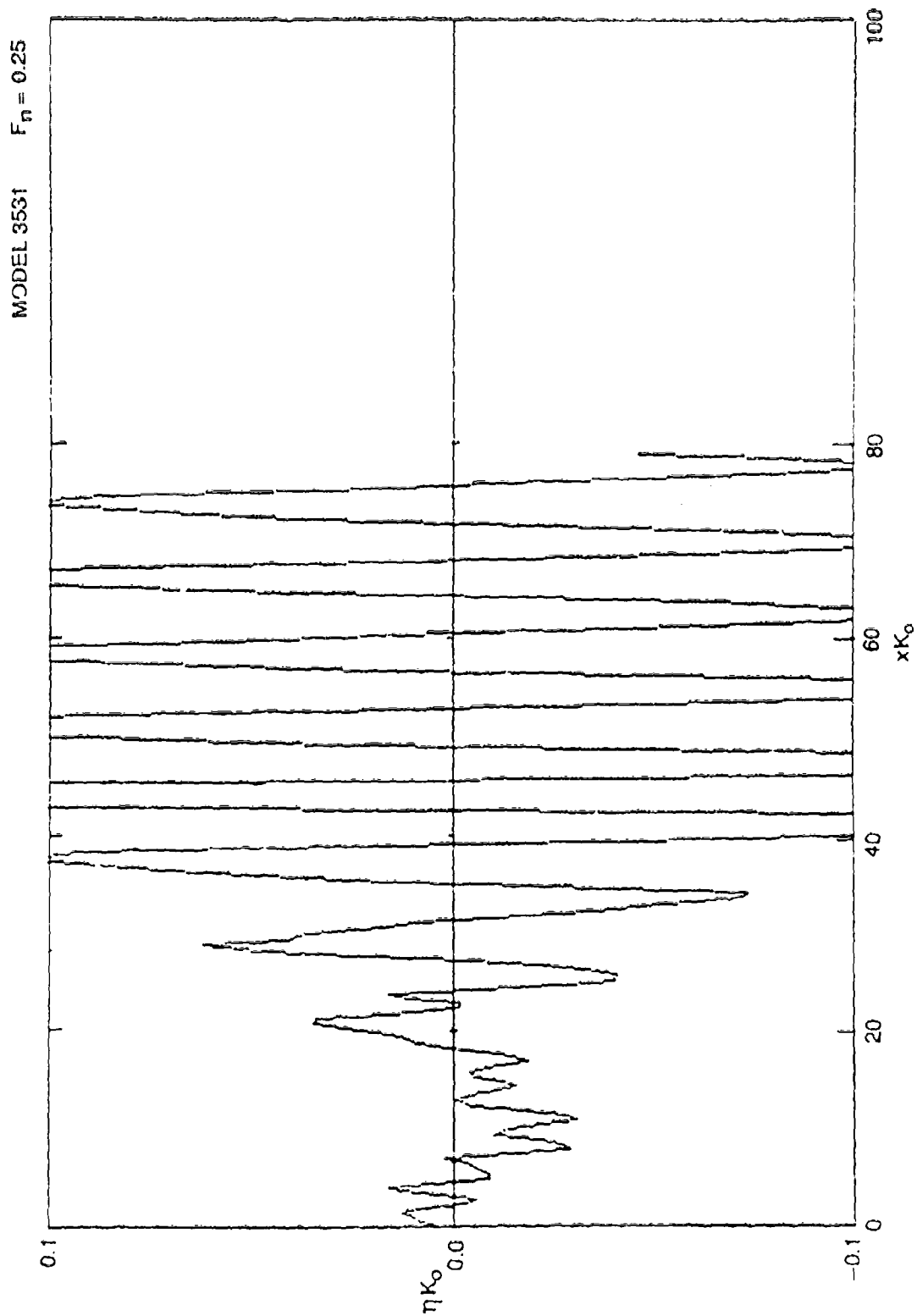


Fig. K.5. SWIMFS prediction of wave cut for QUAPAW at $F_n = 0.25$.

MODEL 3531 $F_n = 0.25$

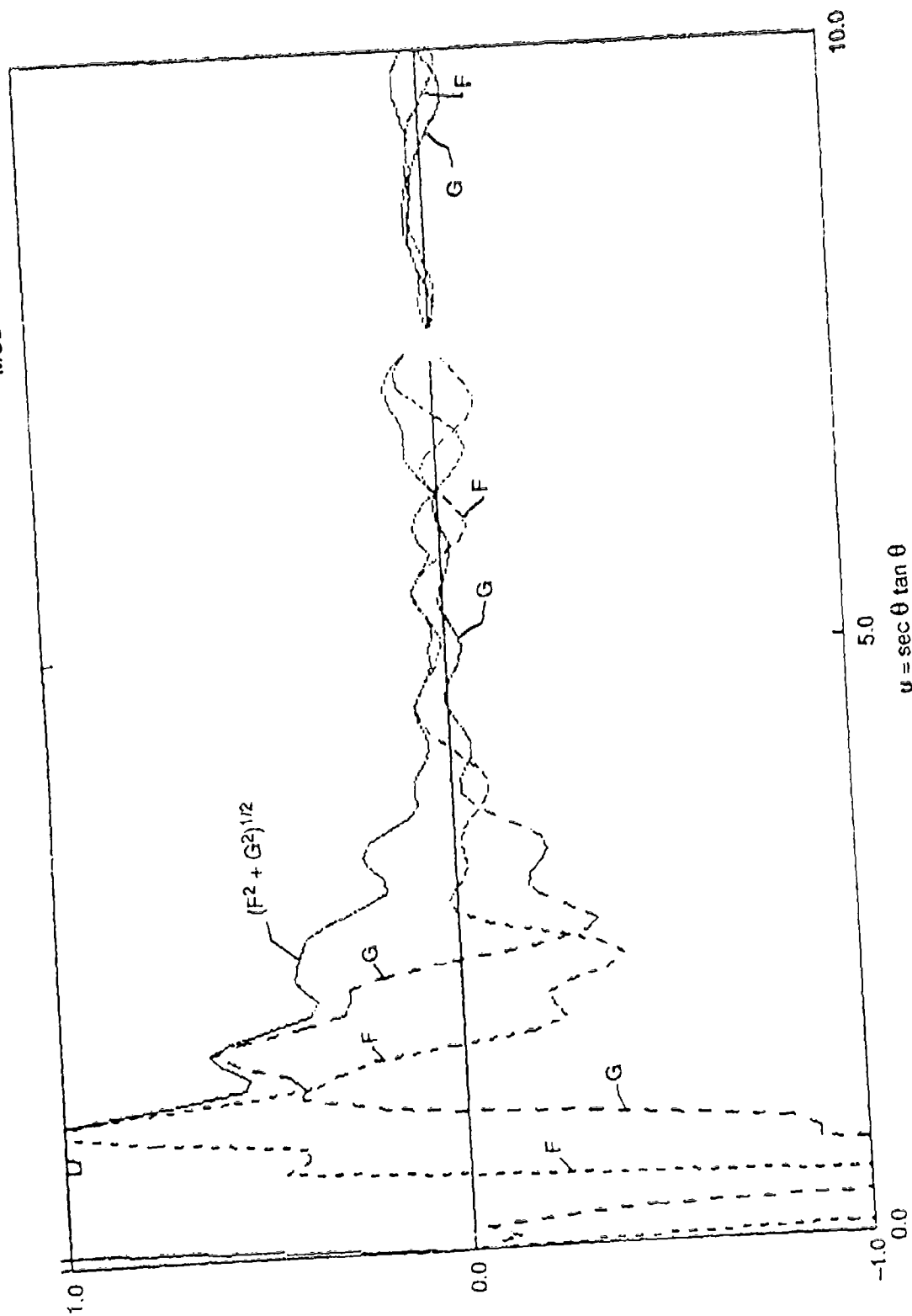


Fig. K.6. SWIMFS prediction of wave spectrum for QUAPAW at $F_n = 0.25$.

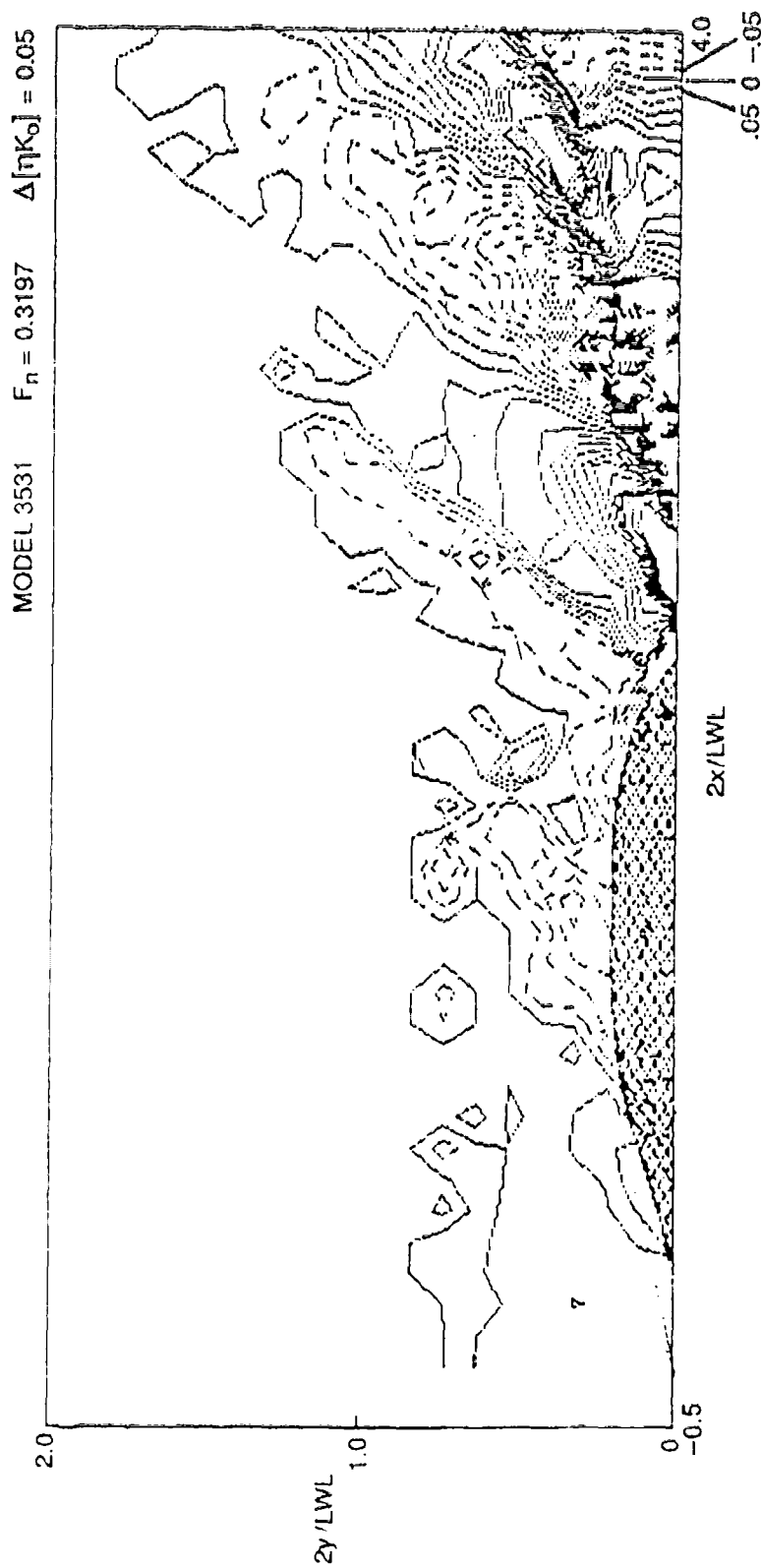


Fig. K.7. SWIMFS prediction of wave contour for QUAPAW at $F_n = 0.3197$.

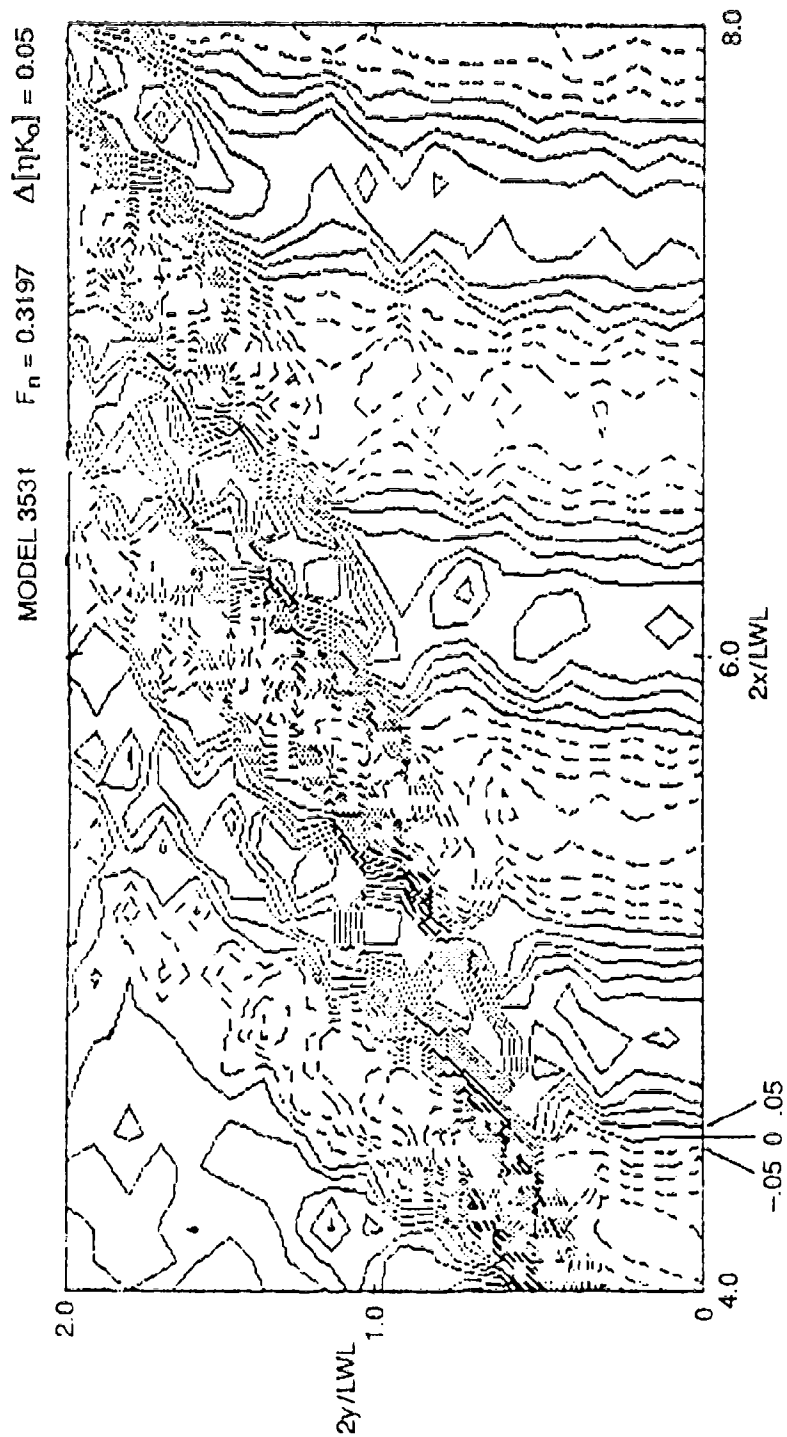


Fig. K.7. (Continued).

MODEL 3531 $F_n = 0.3197$

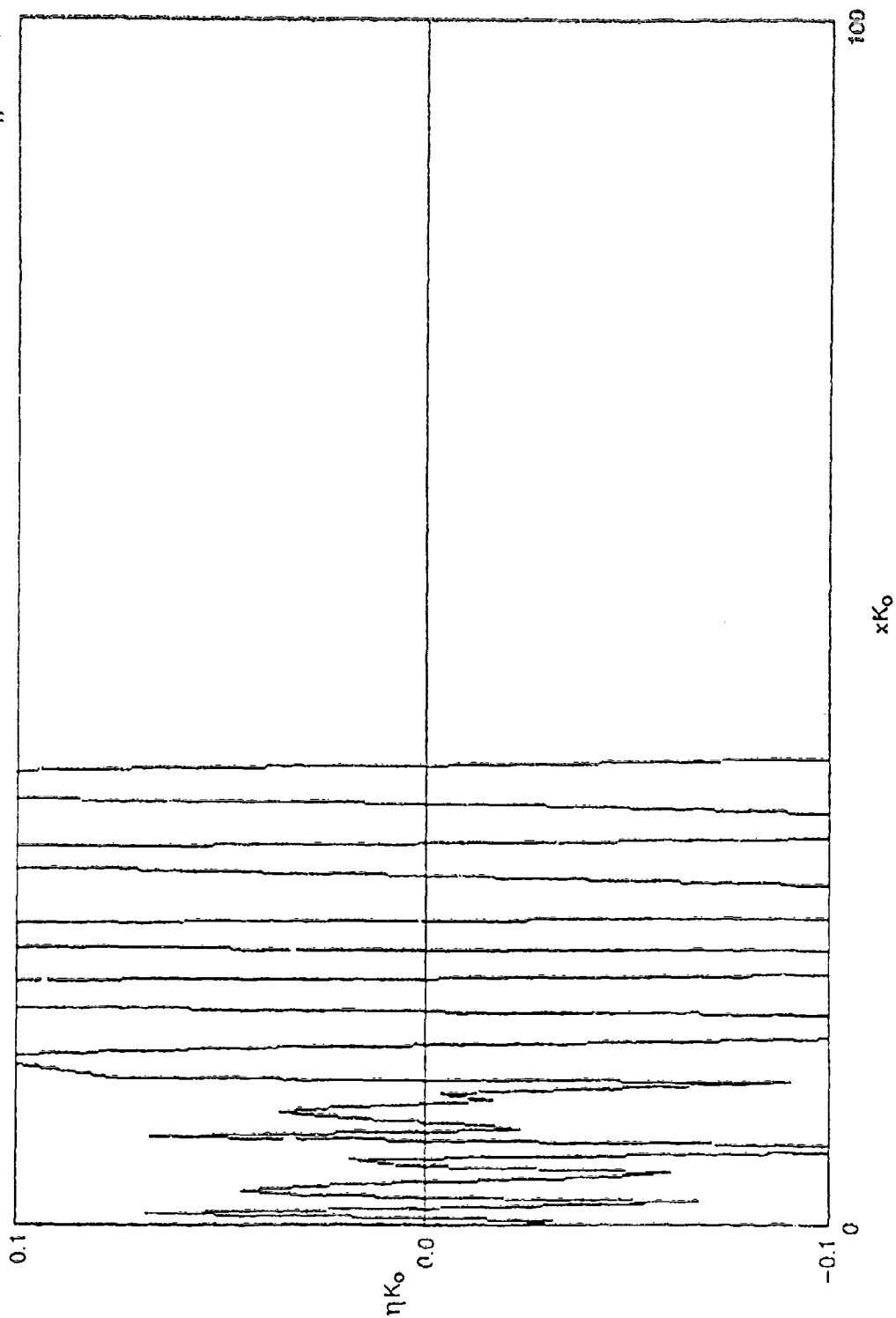


Fig. K.8. SWIMFS prediction of wave cut for QUAPAW at $F_n = 0.3197$.

MODEL 3531 $F_n = 0.3197$

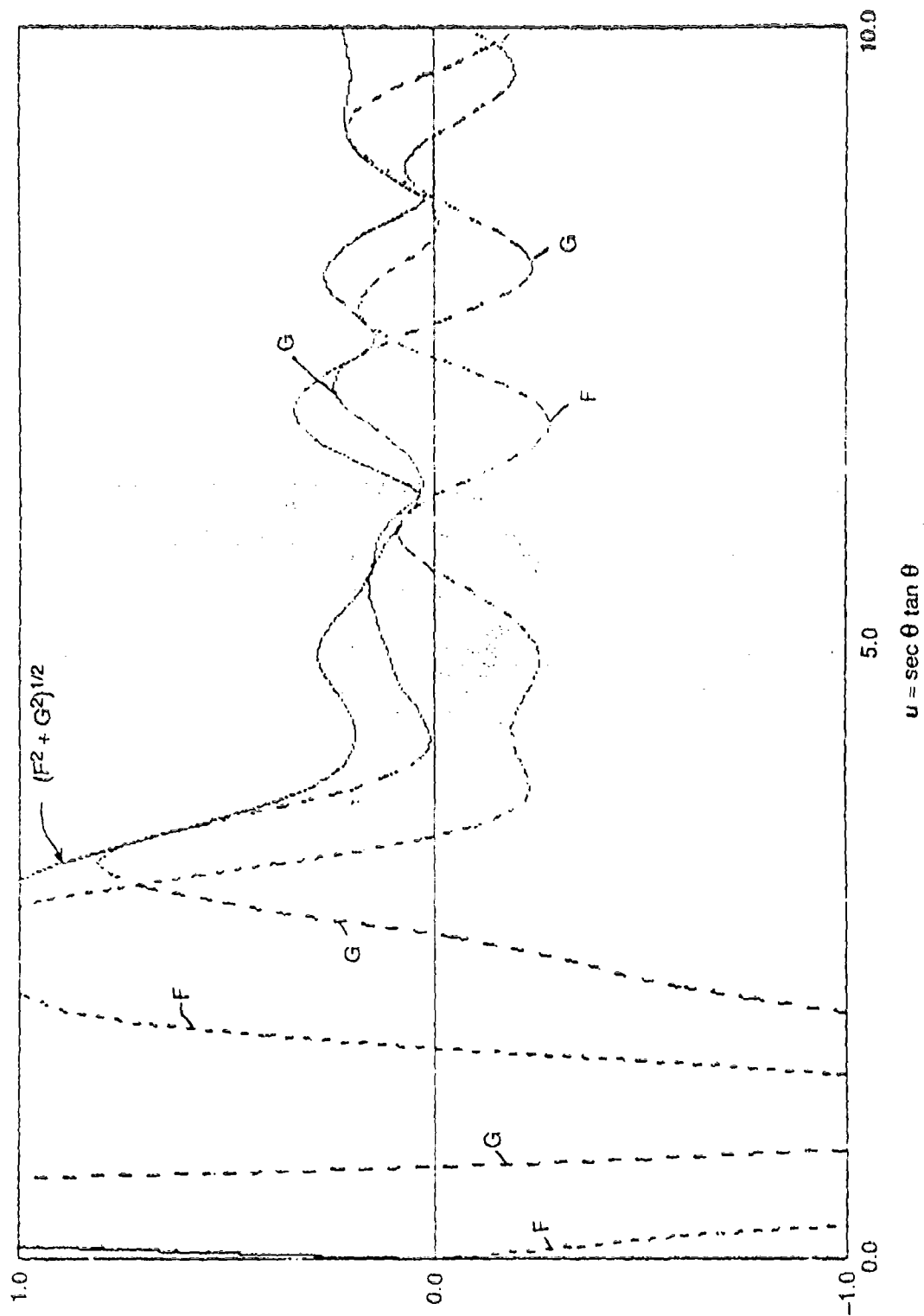


Fig. K.9. SWIMFS prediction of wave spectrum for QUAPAW at $F_n = 0.3197$.

THIS PAGE INTENTIONALLY LEFT BLANK

APPENDIX L

SAIC SLENDER-SHIP SUBMITTED AFTER WAKE-OFF

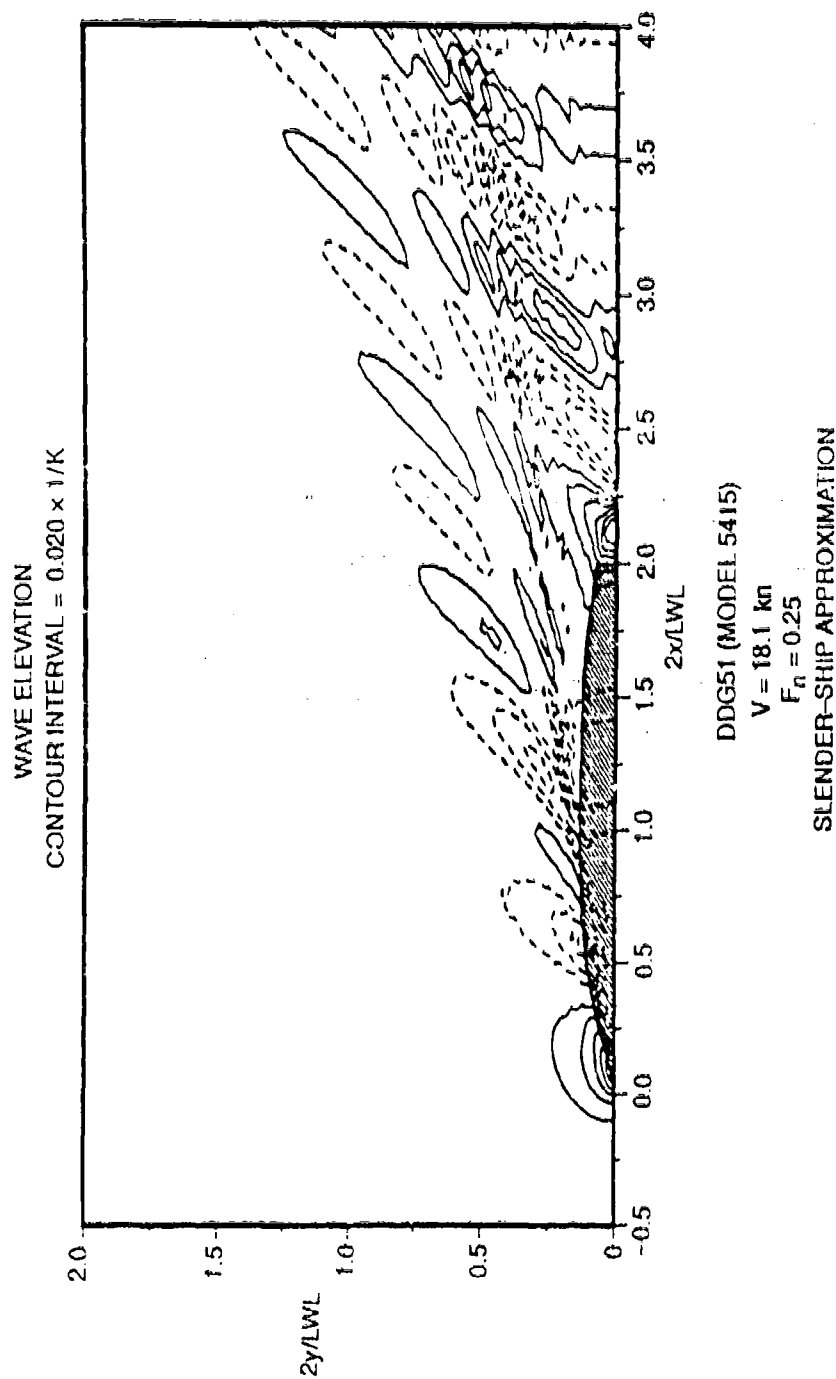


Fig. L.1. Post wake-off SAIC slender-ship prediction of wave contours ($-0.5 < 2x/LWL < 4$)
for Model 5415 at $F_n = 0.25$.

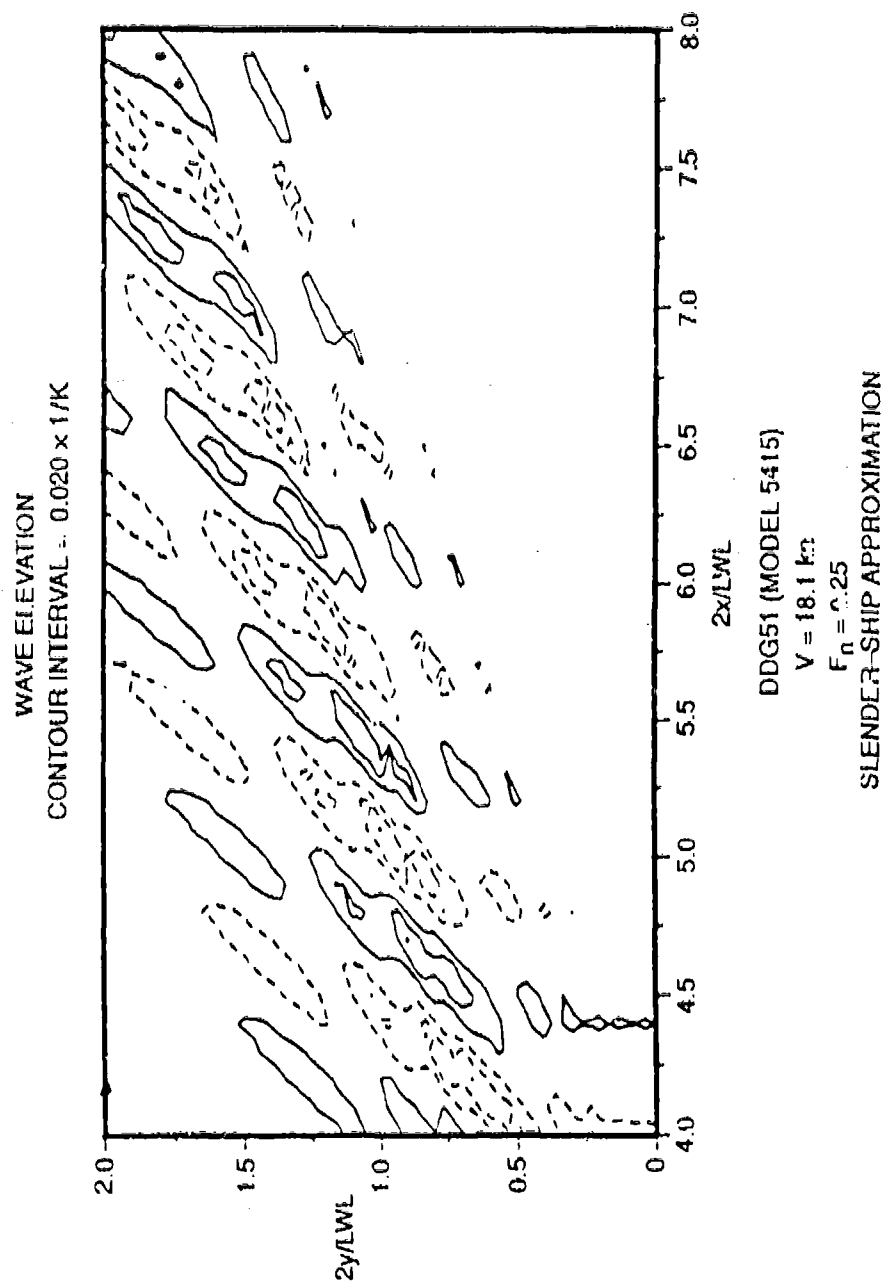


Fig. L.2. Post wake-off SAIC slender-ship prediction of wave contours ($4 < 2x/LWL < 8$)
for Model 5415 at $F_n = 0.25$.

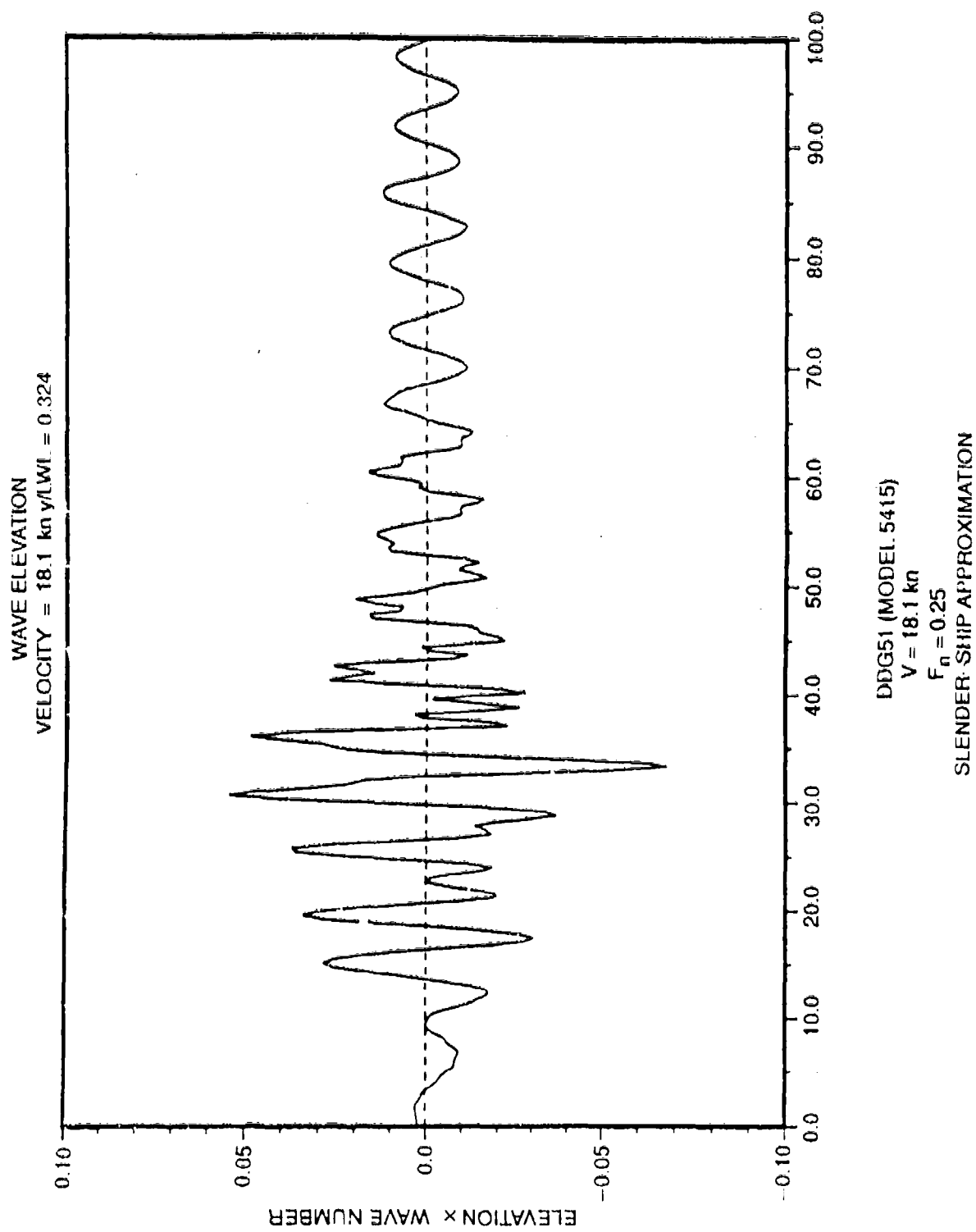


Fig. L.3. Post wake-off SAIC slender-ship prediction of wave cut for Model 5415 at $F_n = 0.25$.

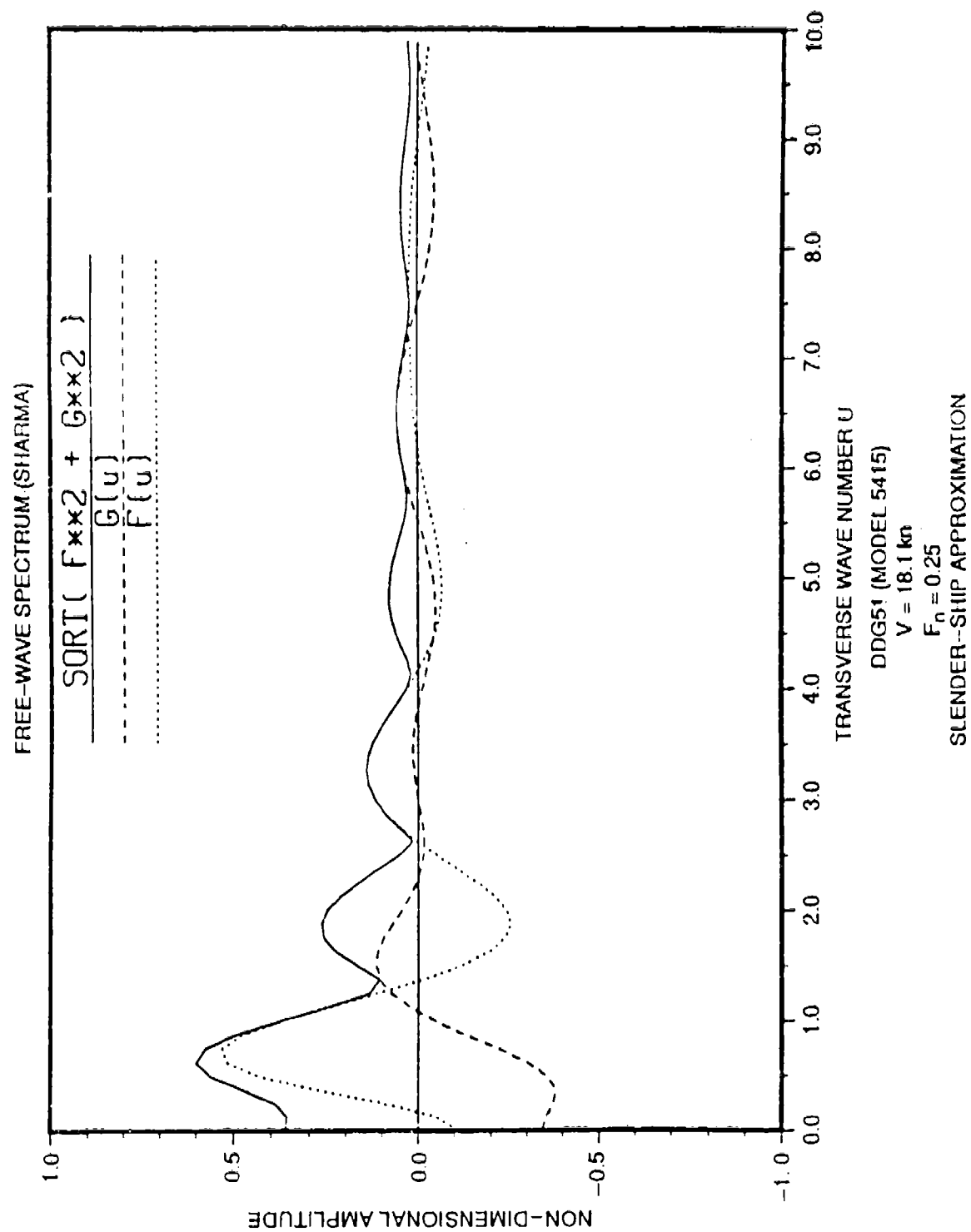


Fig. L.4. Post wake-off SAIC slender-ship prediction of wave spectrum for Model 5415 at $F_n = 0.25$

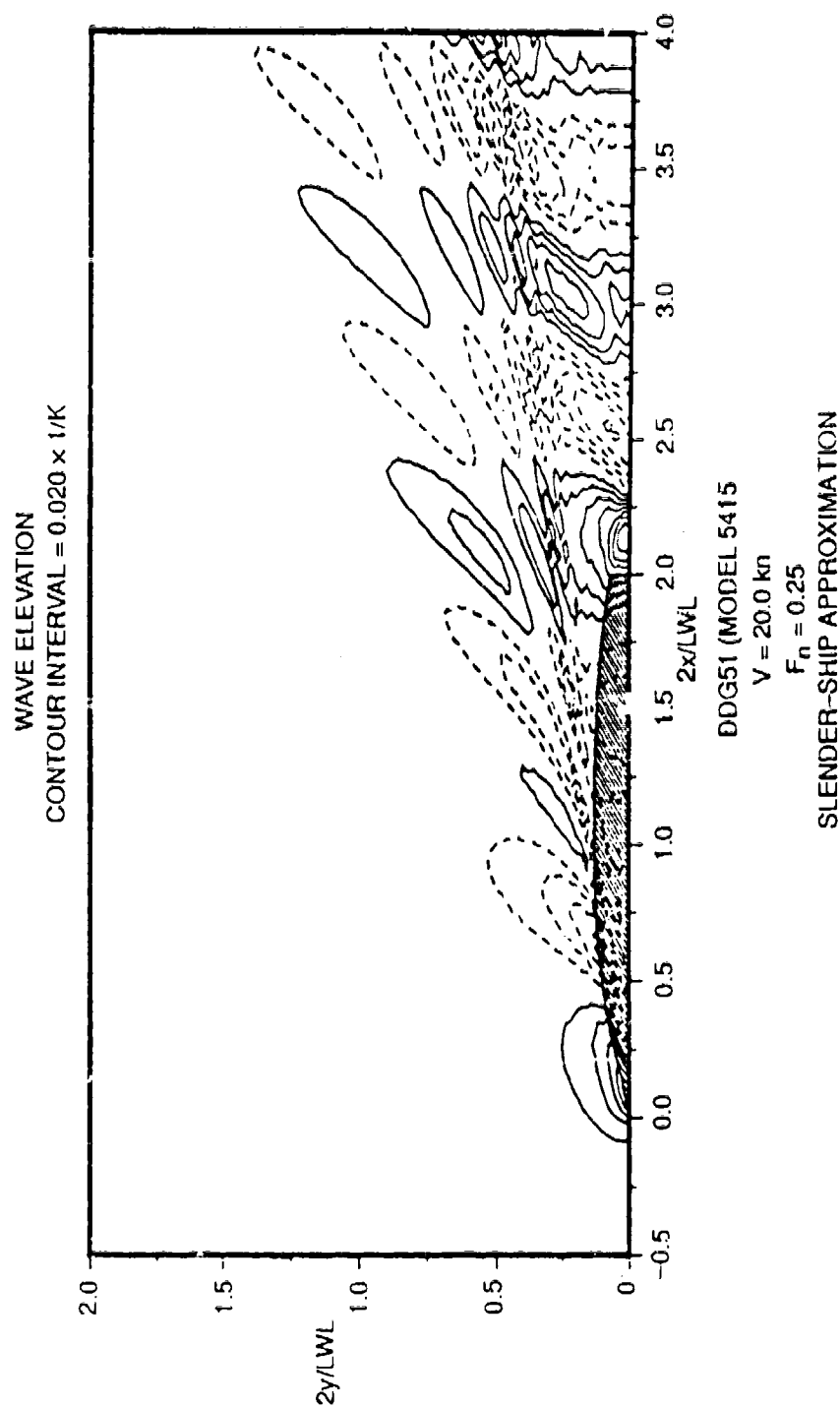


Fig. L.5. Post wake-off SAIC slender-ship prediction of wave contours ($-0.5 < 2x/LWL < 4$) for Model 5415 at $F_n = 0.2755$.

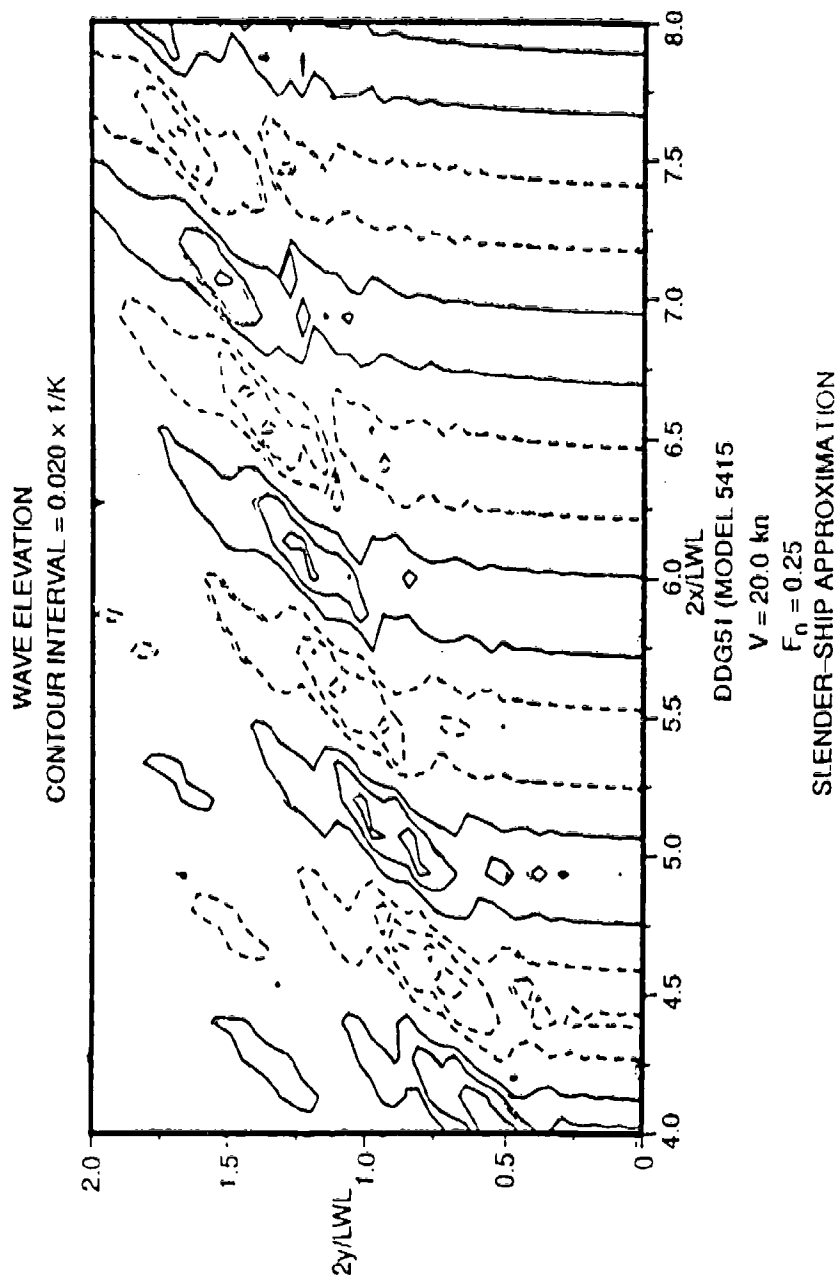


Fig. L.6. Post wake-off SAIC slender-ship prediction of wave contours ($4 < 2x/LWL < 8$) for Model 5415 at $F_n = 0.2755$.

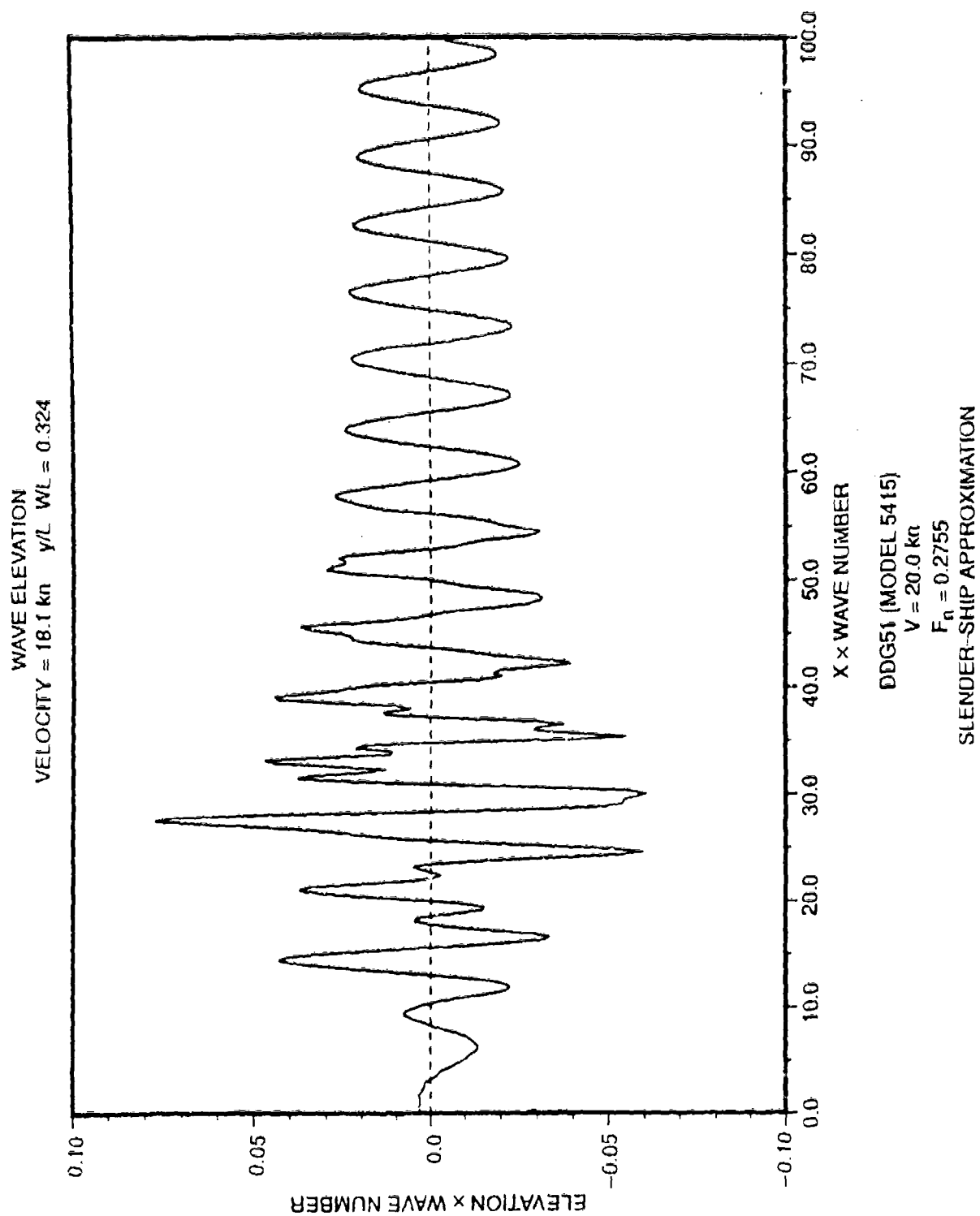


Fig. L.7. Post wake-off SAIC slender-ship prediction of wave cut for Model 5415 at $F_n = 0.2755$.

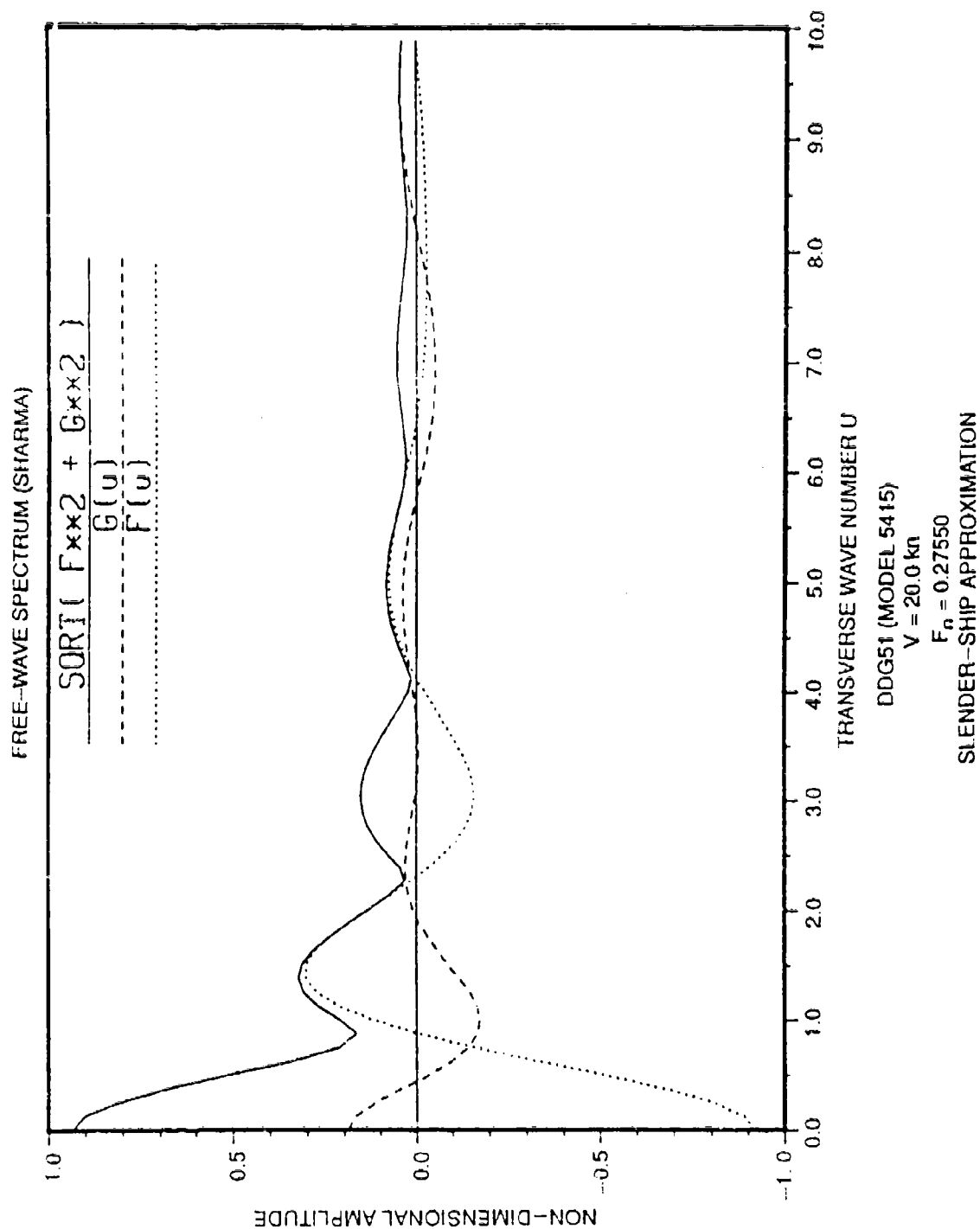


Fig. L.8. Post wake-off SAIC slender-ship prediction of wave spectrum for Model 5415 at $F_n = 0.2755$.

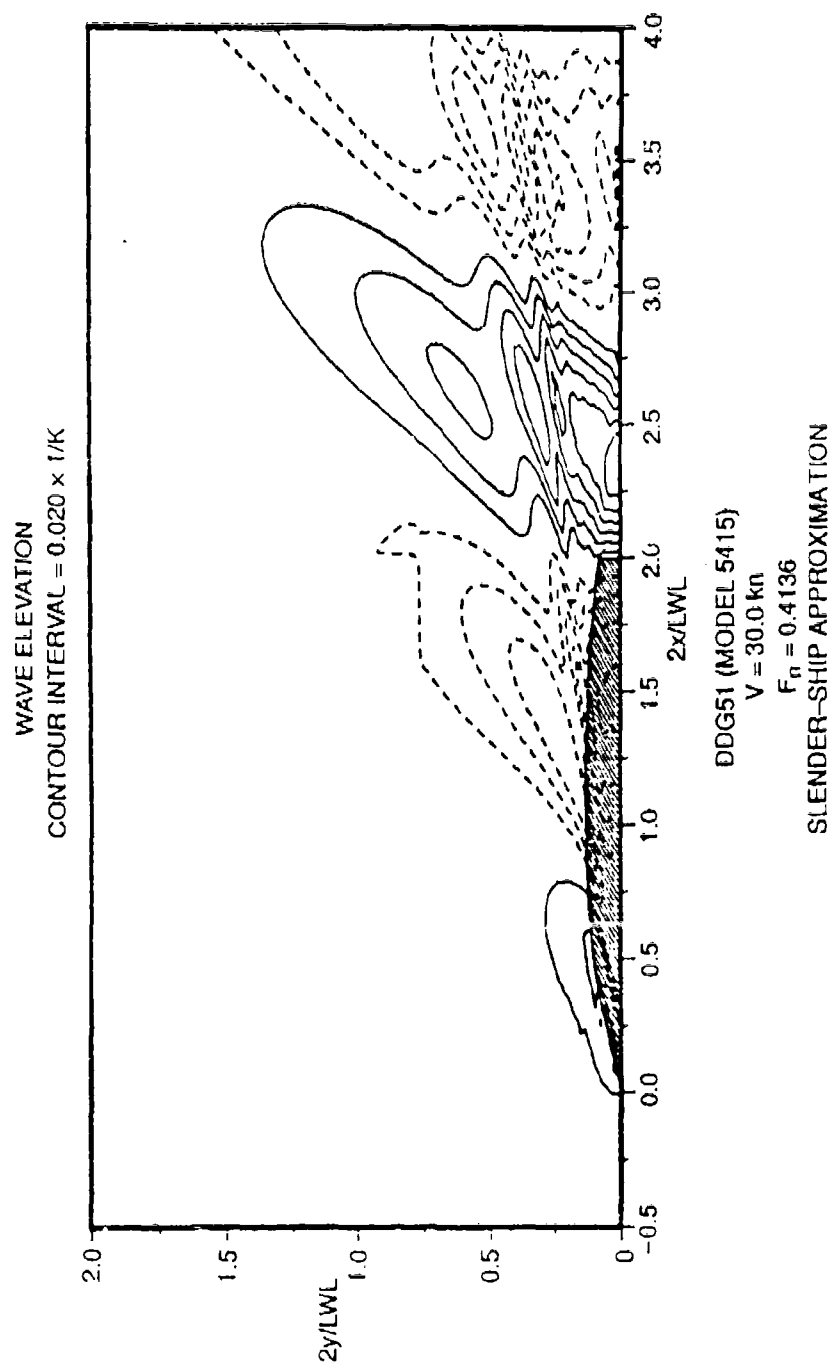
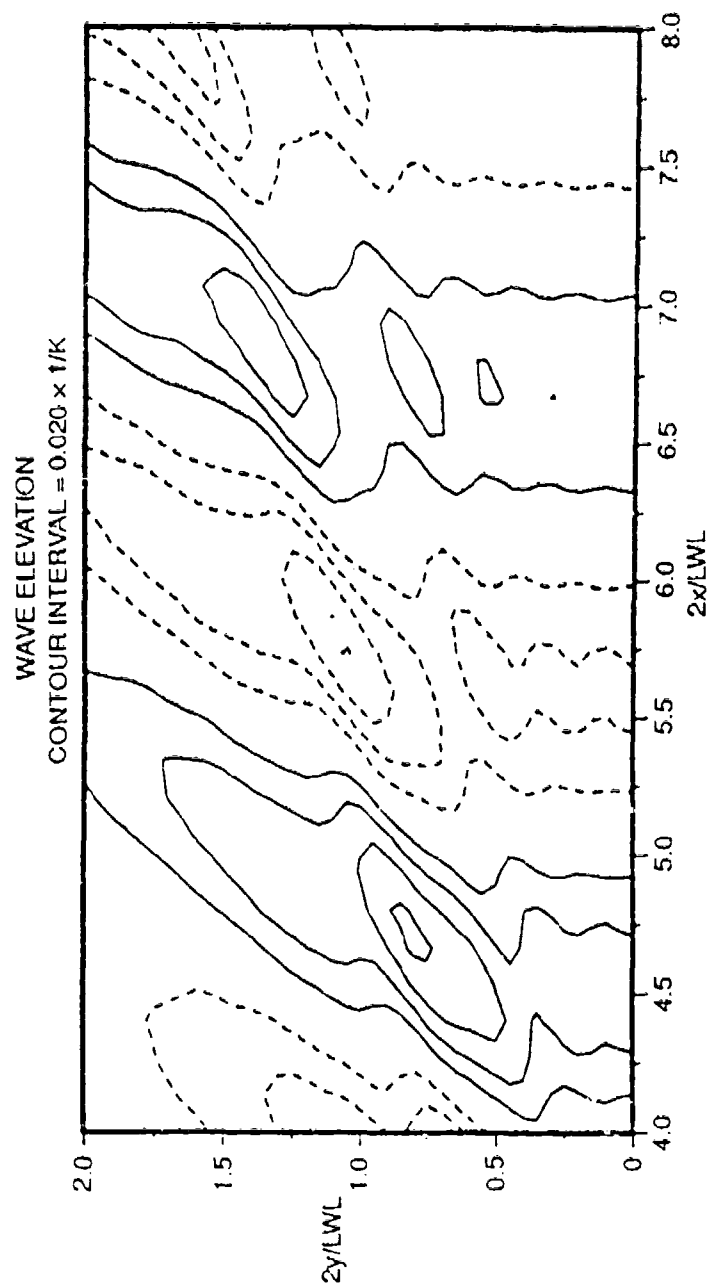


Fig. L.9. Post wake-off SAIC slender-ship prediction of wave contours ($-0.5 < 2x/LWL < 4$) for Model 5415 at $F_n = 0.4136$.



DDG51 (MODEL 5415)

$V = 30.0$ kn

$F_n = 0.4136$

SLENDER-SHIP APPROXIMATION

Fig. L.10. Post wake-off SAIC slender-ship prediction of wave contours ($4 < 2x/LWL < 8$) for Model 5415 at $F_n = 0.4136$.

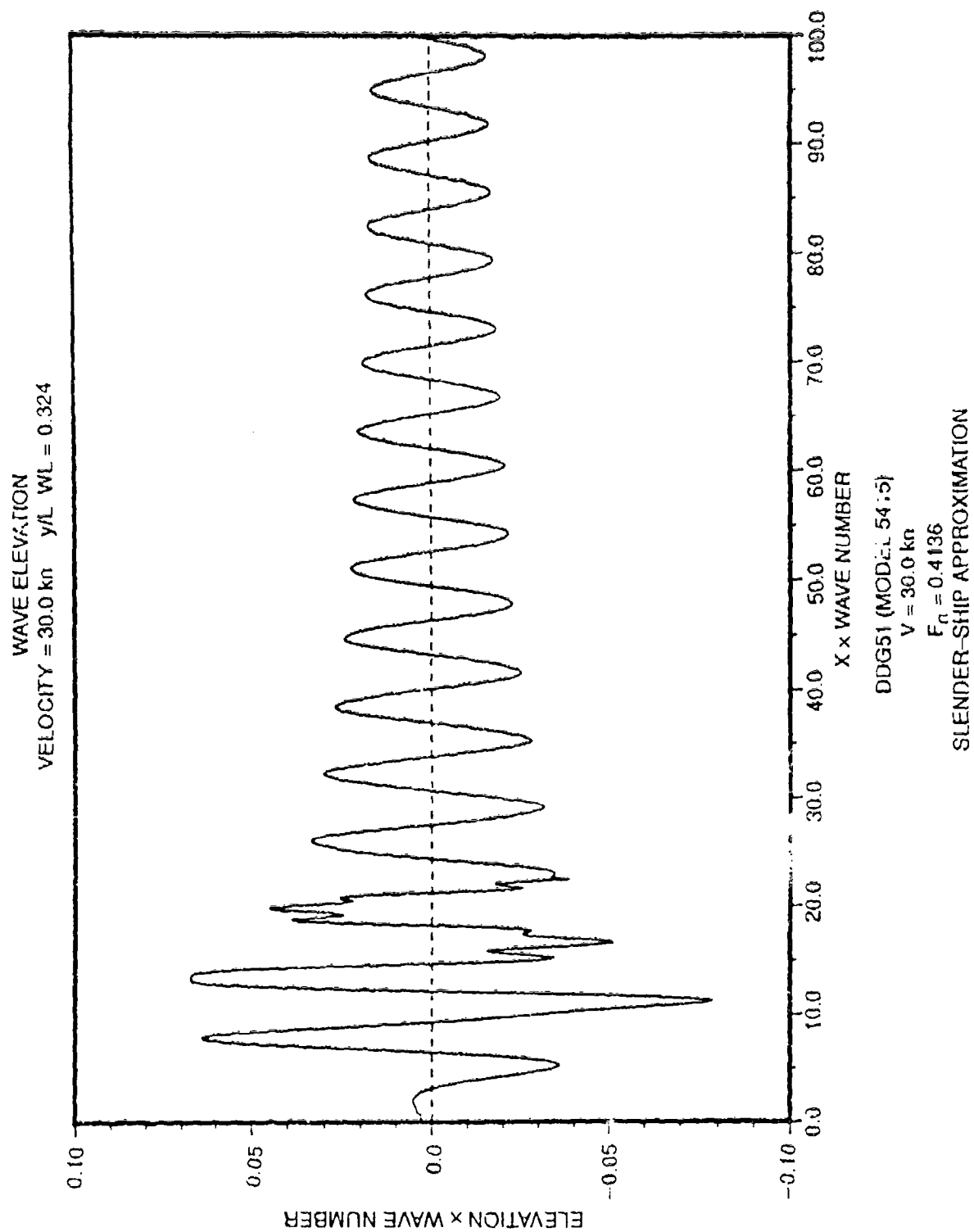


Fig. L.11. Post wake-off SAIC slender-ship prediction of wave cut for Model 5415 at $F_n = 0.4136$.

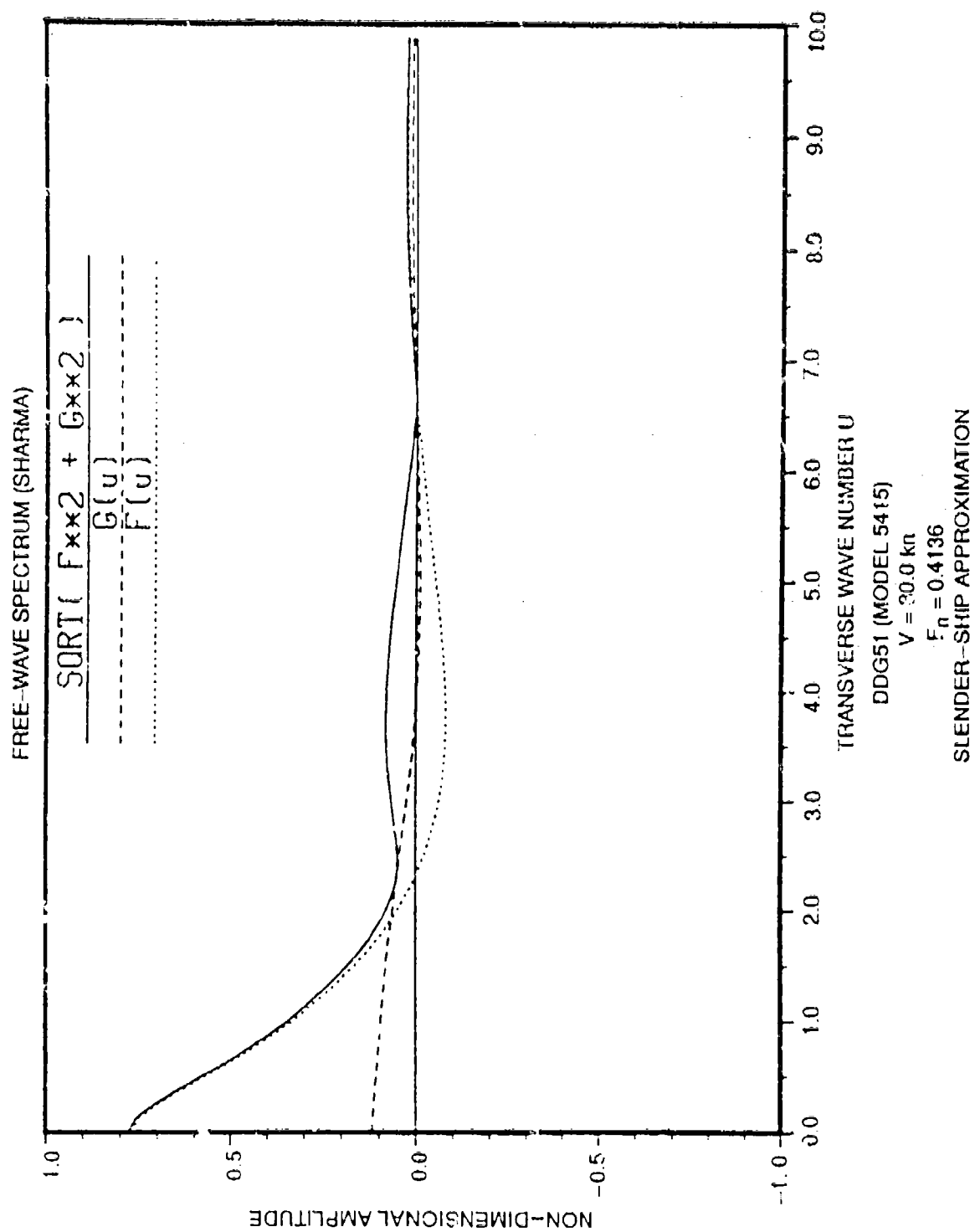
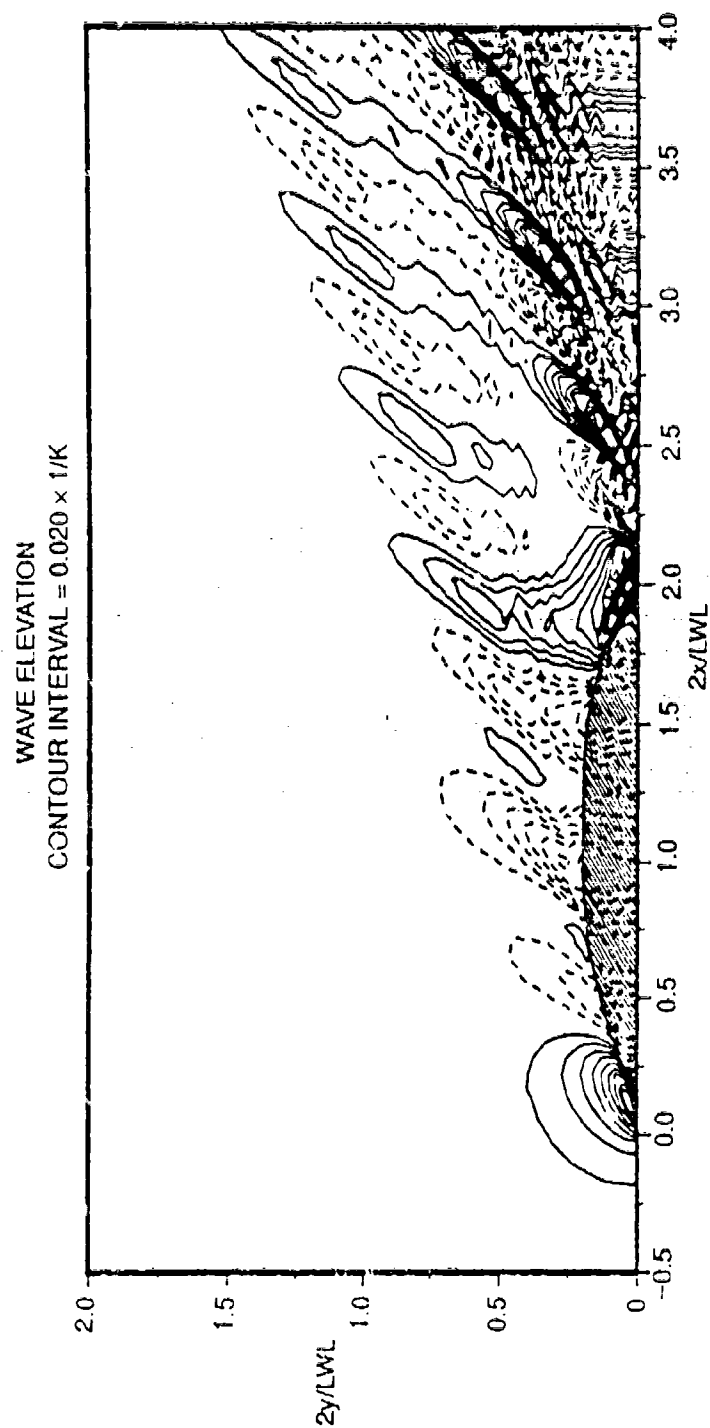


Fig. L.12. Post wake-off SAIC slender-ship prediction of wave spectrum for Model 5415 at $F_n = 0.4136$.



QUAPAW (MODEL 3531)

$V = 10.0$ kn

$F_n = 0.2131$

SLENDER-SHIP APPROXIMATION

Fig. L.13. Post wake-off SAIC slender-ship prediction of wave contours ($-0.5 < 2x/LWL < 4$) for QUAPAW at $F_n = 0.2131$.

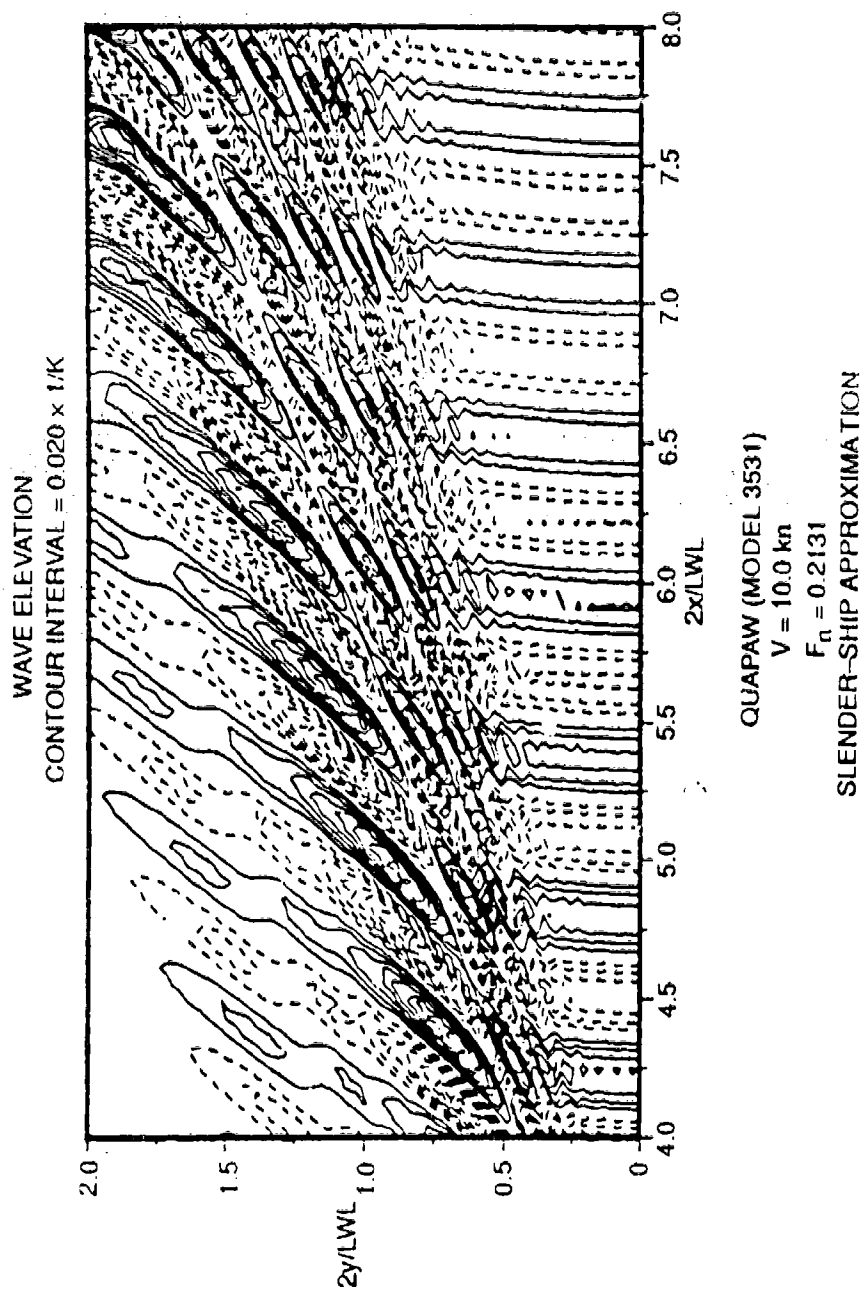


Fig. L.14. Post wake-off SAIC slender-ship prediction of wave contours ($4 < 2x/LWL < 8$) for QUAPAW at $F_n = 0.2131$.

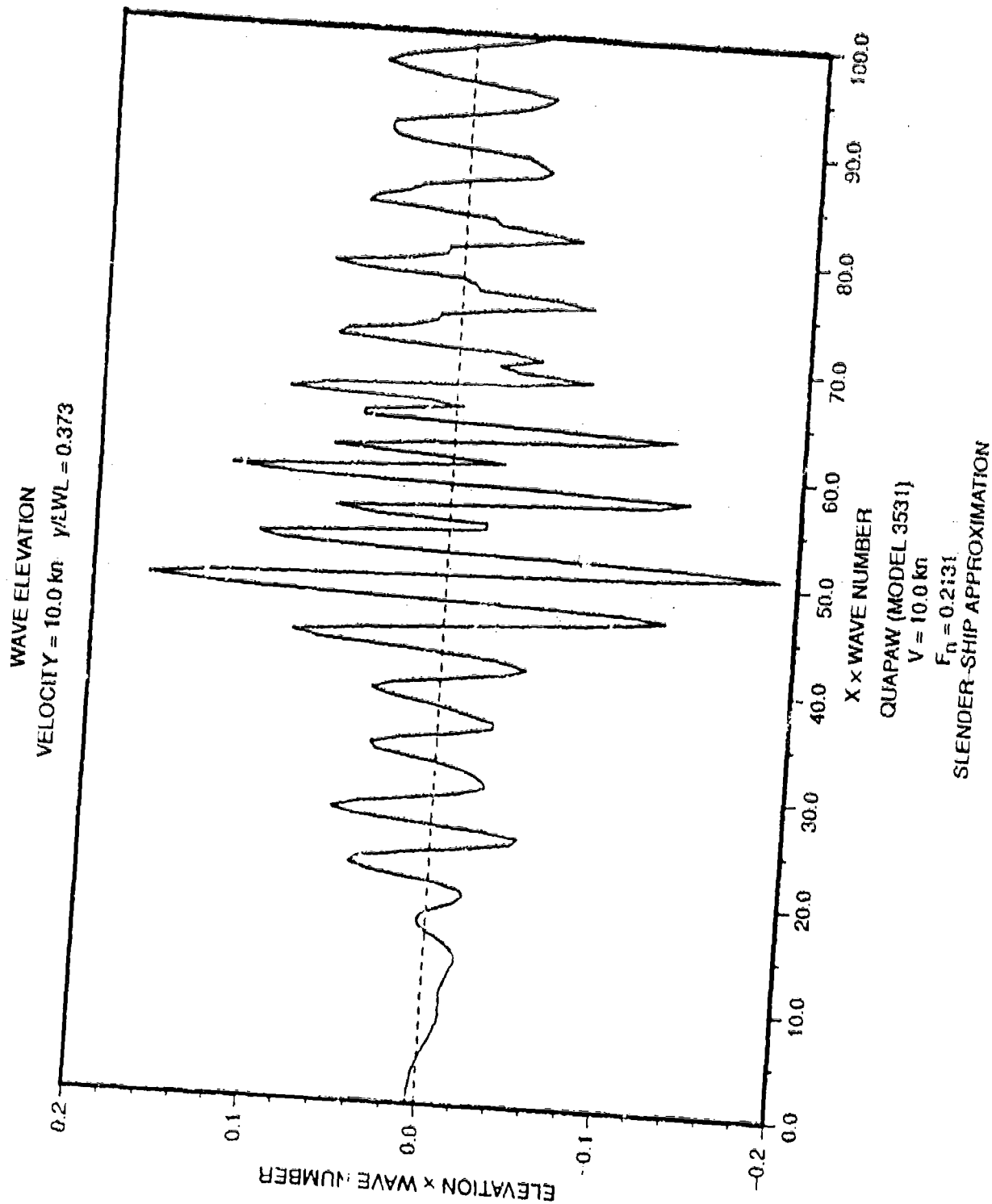


Fig. L.15. Post wake-off SAIC slender-ship prediction of wave cut for QUAPAW at $F_n = 0.2131$.

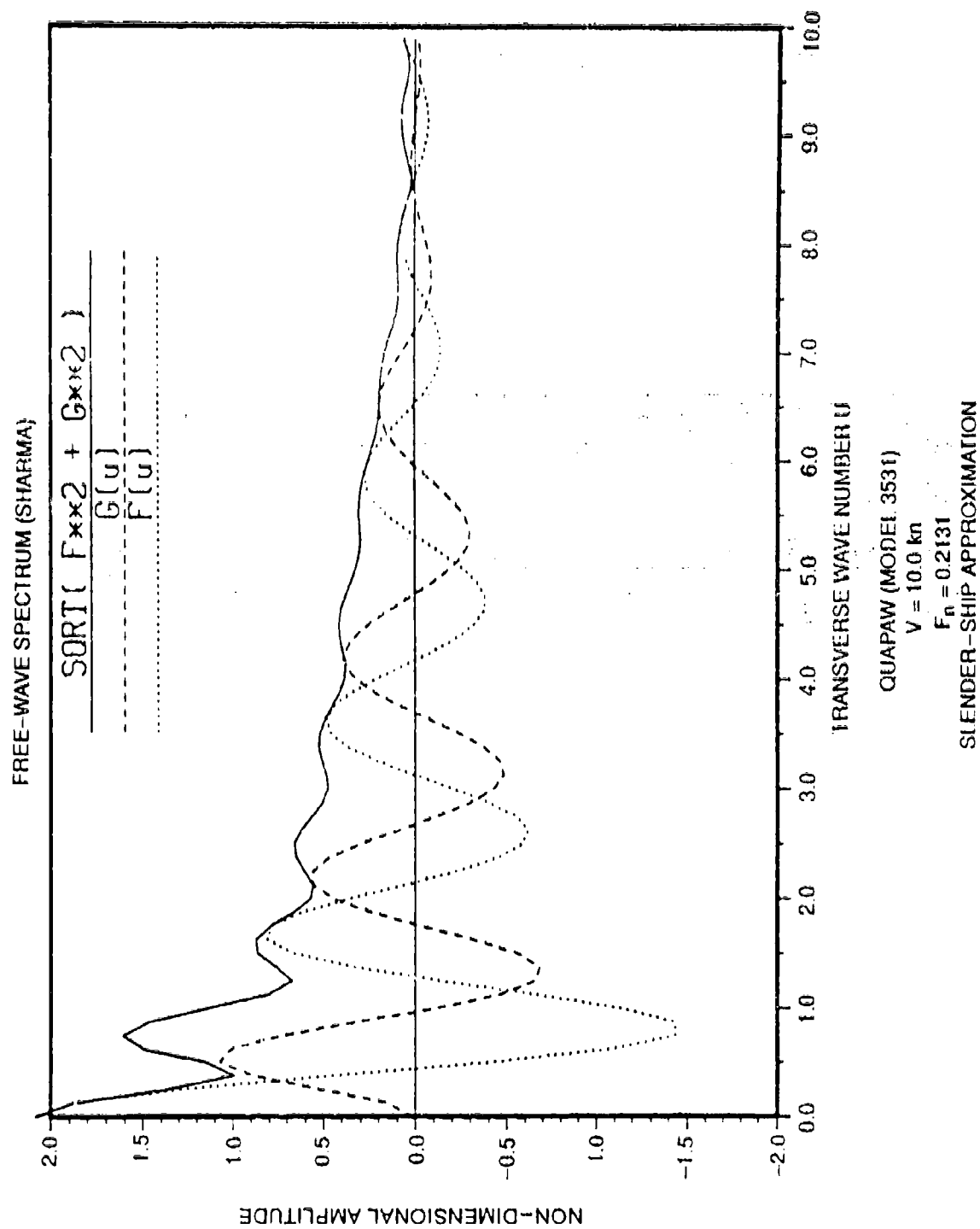


Fig. L.16. Post wake-off SAIC slender-ship prediction of wave spectrum for QUAPAW at $F_n = 0.2131$.

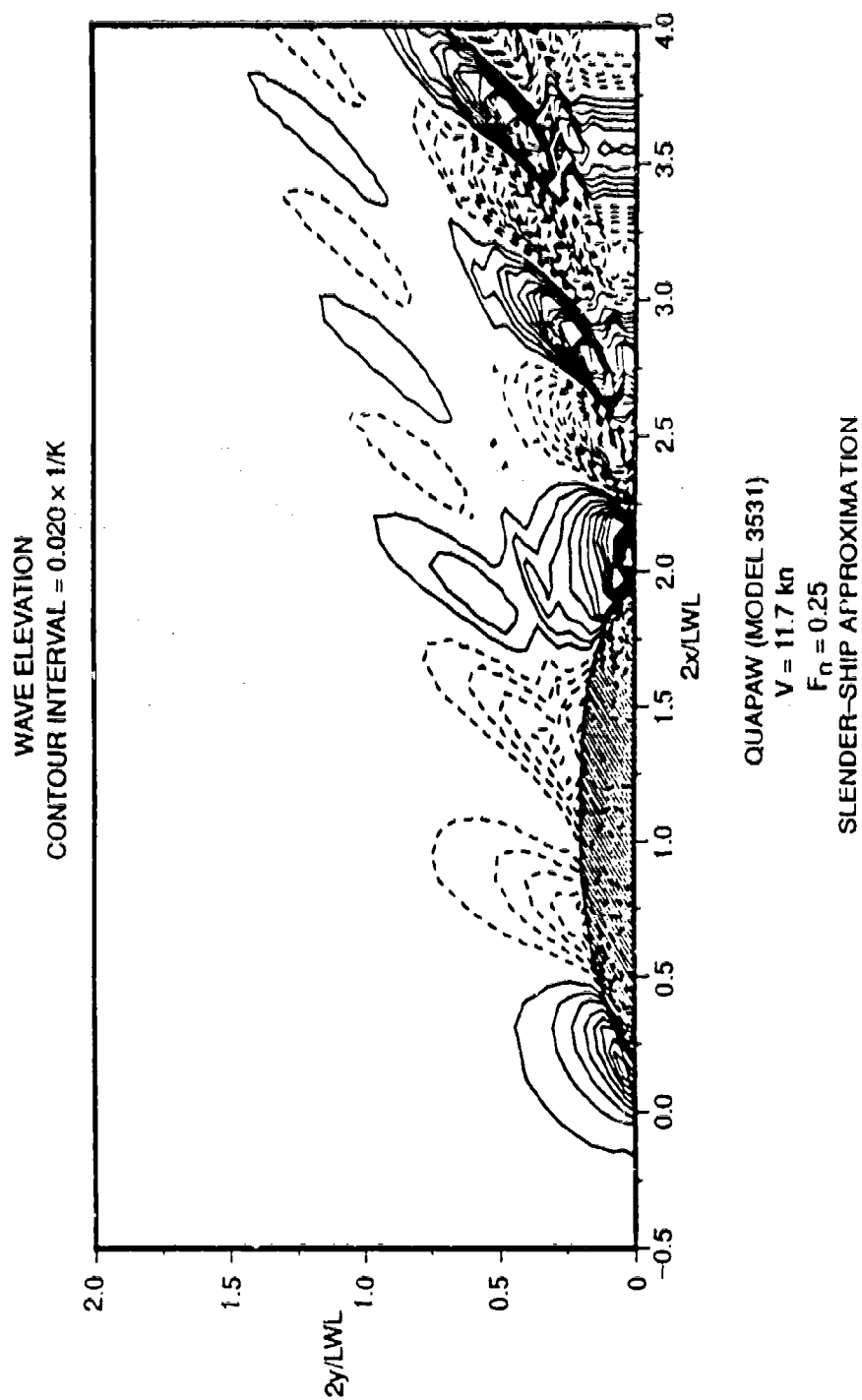


Fig. L.17. Post wake-off SAIC slender-ship prediction of wave contours ($-0.5 < 2x/LWL < 4$) for QUAPAW at $F_n = 0.25$.

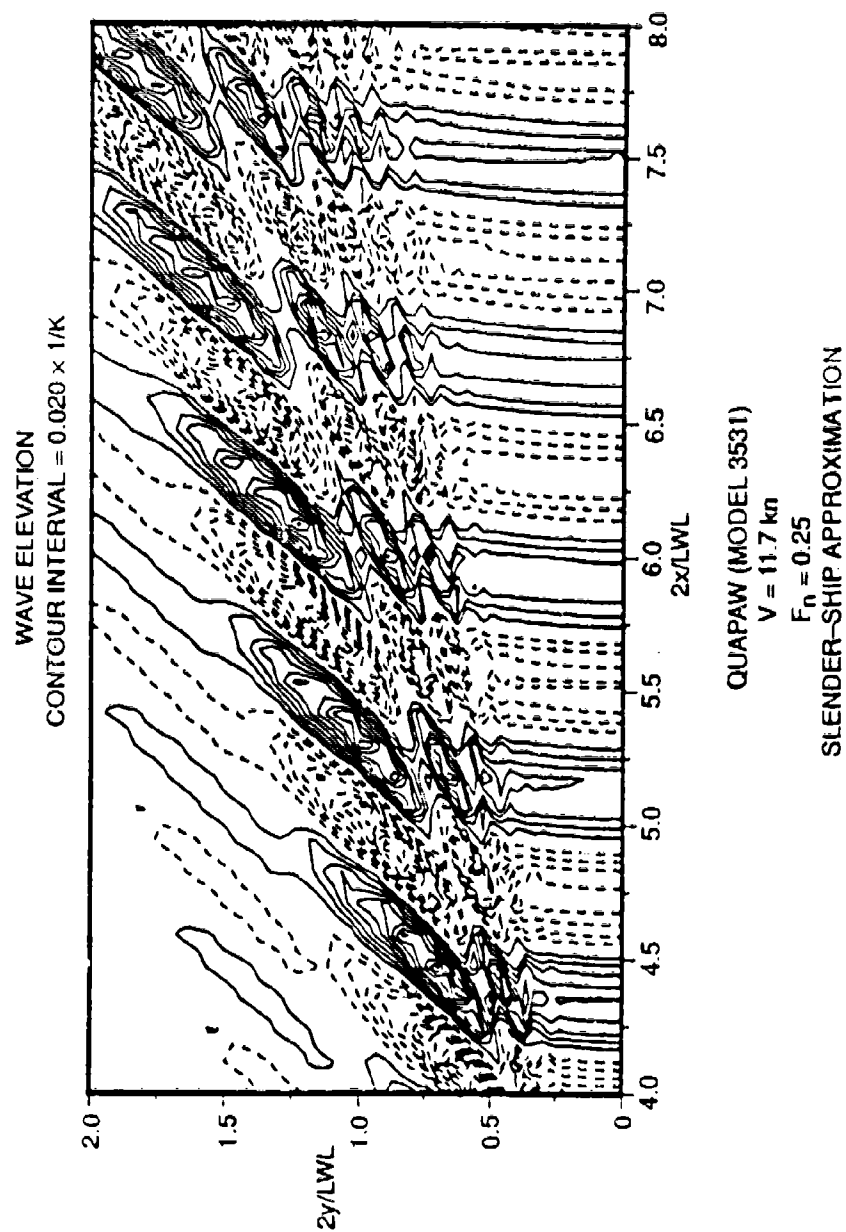


Fig. L.18. Post wake-off SAIC slender-ship prediction of wave contours ($4 < 2x/LWL < 8$) for QUAPAW at $F_n = 0.25$.

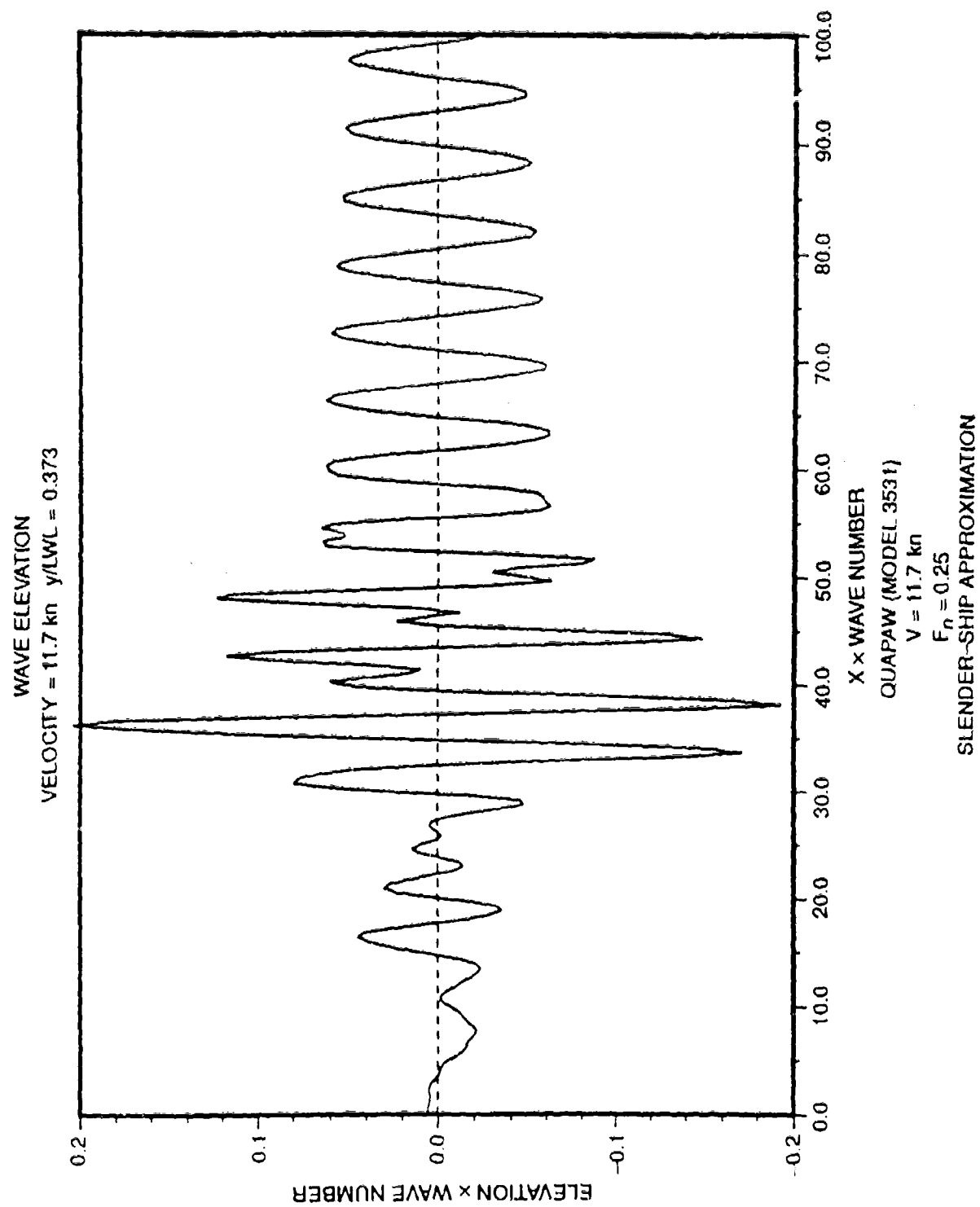


Fig. L.19. Post wake-off SAIC slender-ship prediction of wave cut for QUAPAW at $F_n = 0.25$.

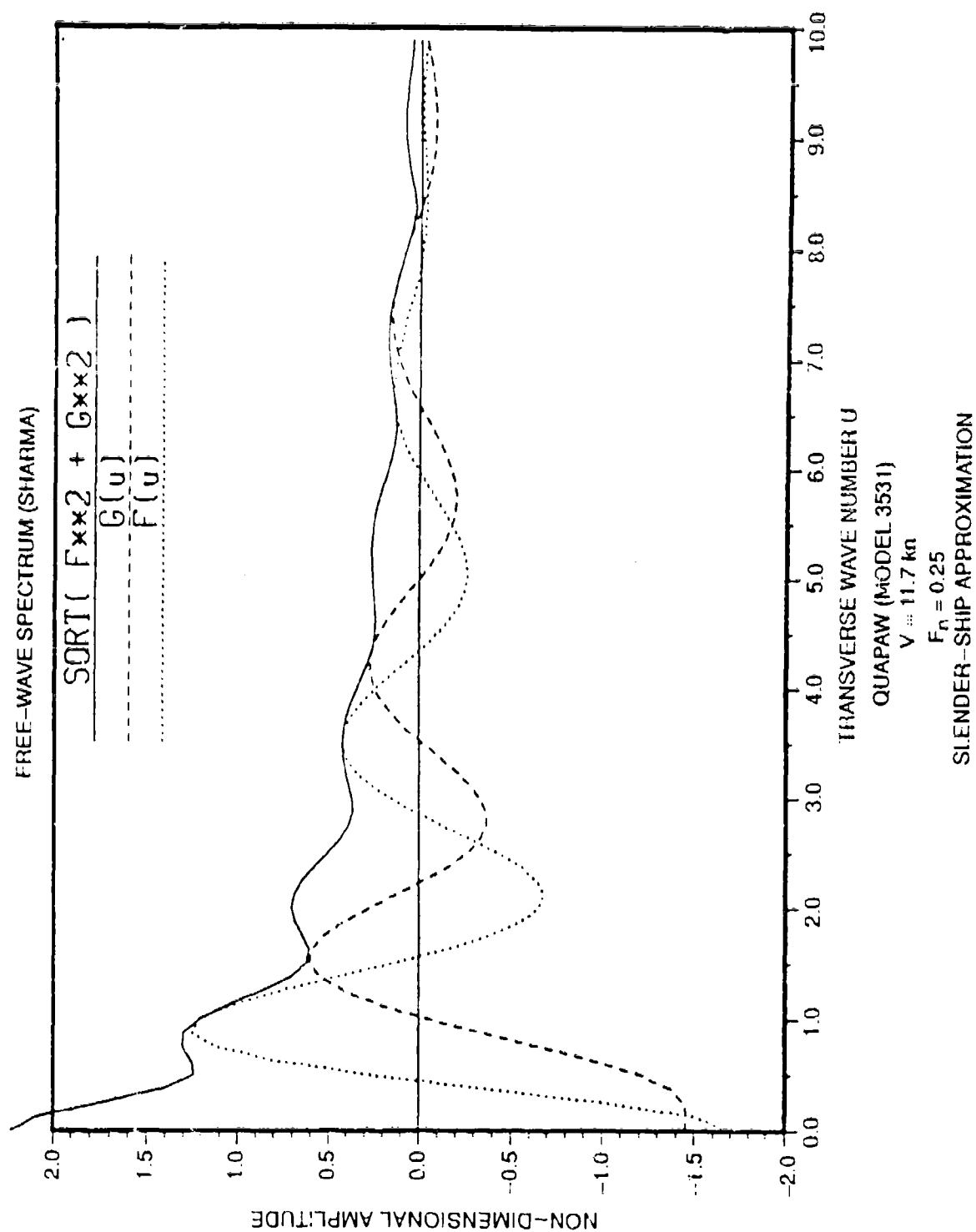


Fig. L.20. Post wake-off SAiC slender-ship prediction of wave spectrum for QUAPAW at $F_n = 0.25$.

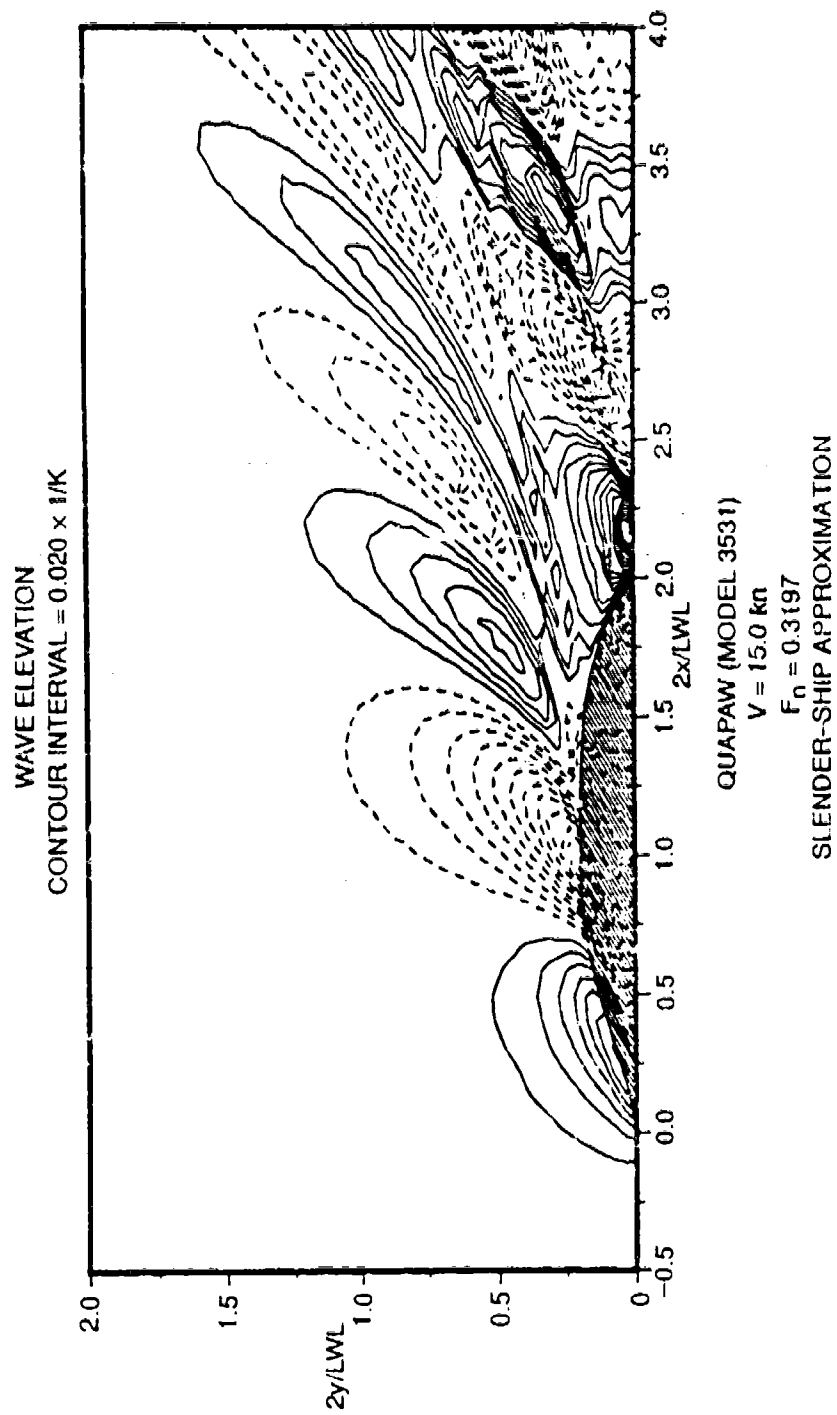


Fig. L.21. Post wake-off SAIC slender-ship prediction of wave contours ($-0.5 < 2x/LWL < 4$) for QUAPAW at $F_n = 0.3197$.

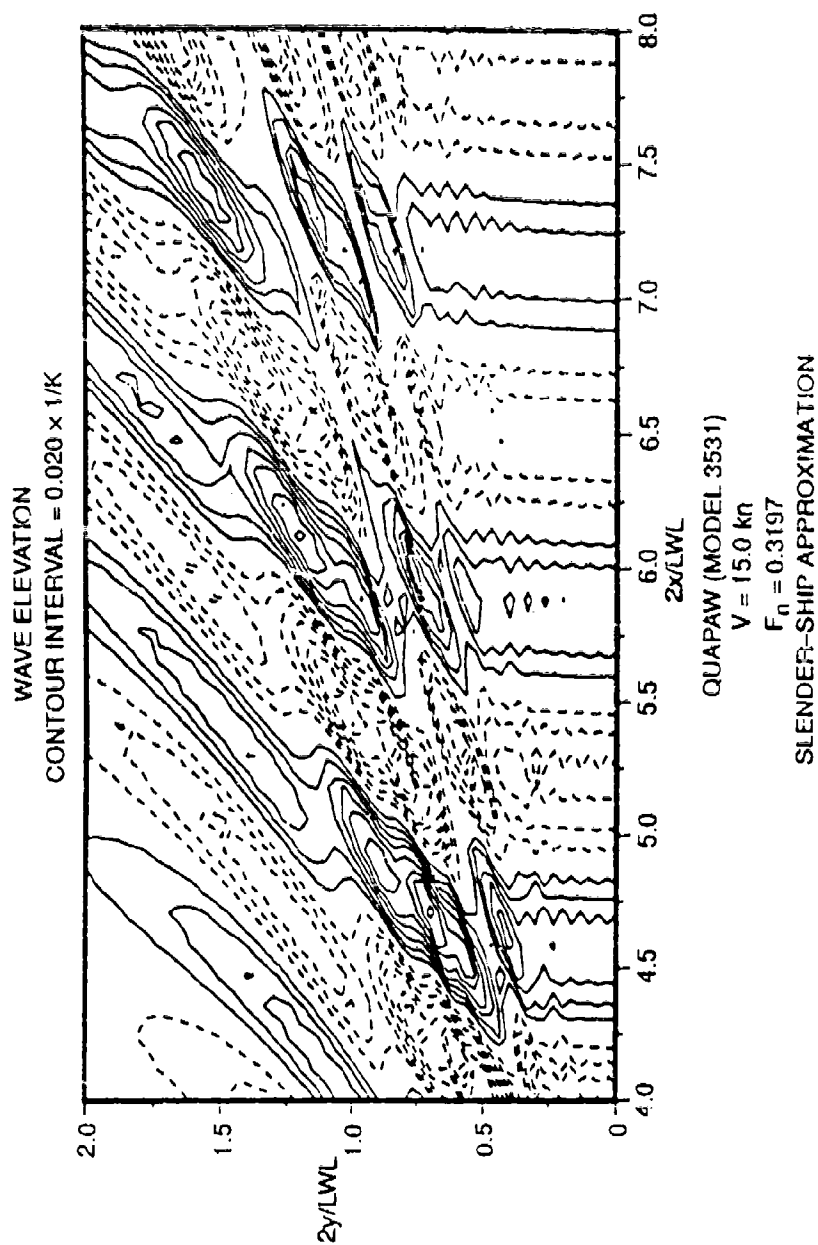


Fig L.22. Post wake-off SAIC slender-ship prediction of wave contours ($4 < 2x/LWL < 8$) for QUAPAW at $F_n = 0.3197$.

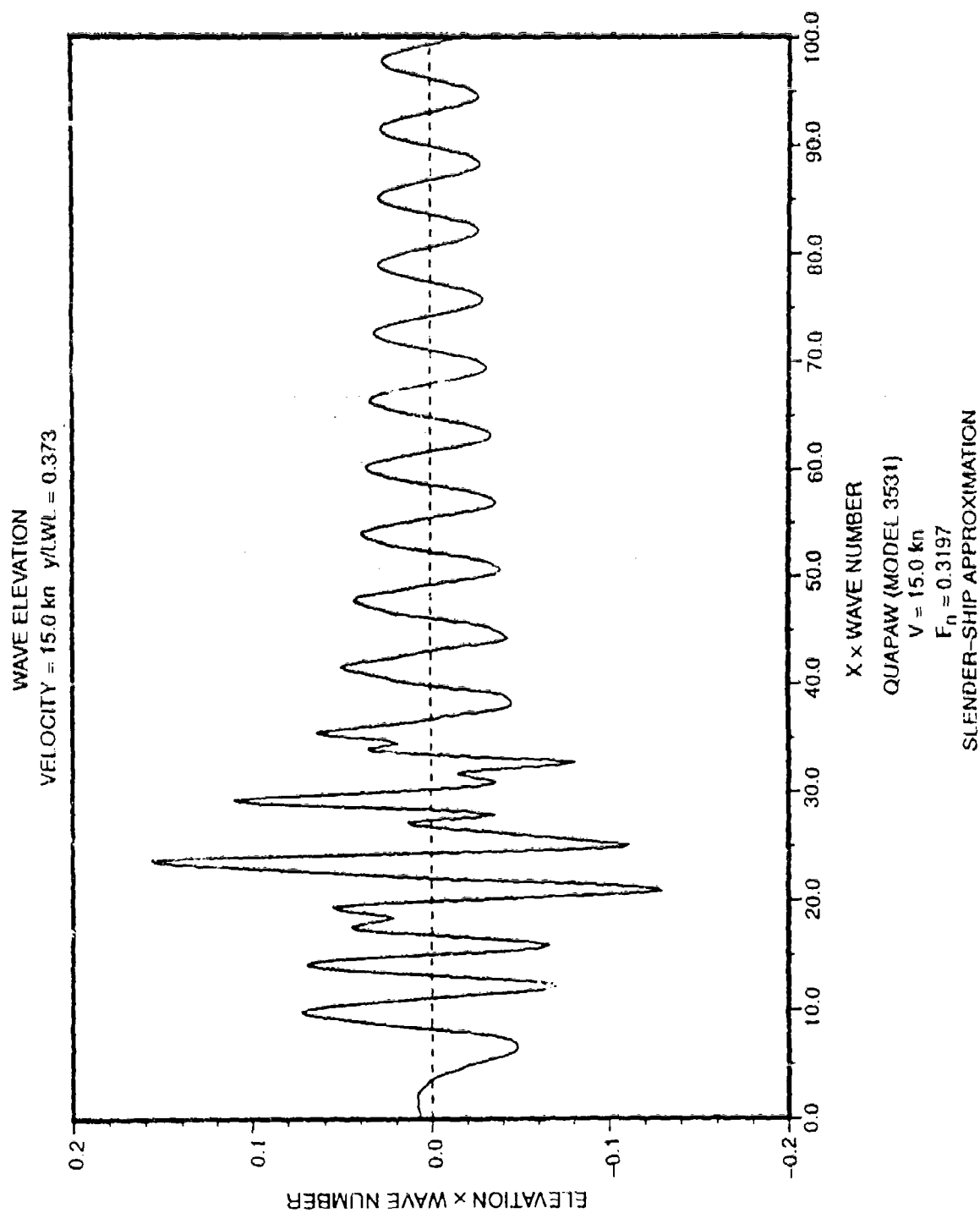


Fig. L.23. Post wake-off SAIC slender-ship prediction of wave cut for QUAPAW at $F_n = 0.3197$.

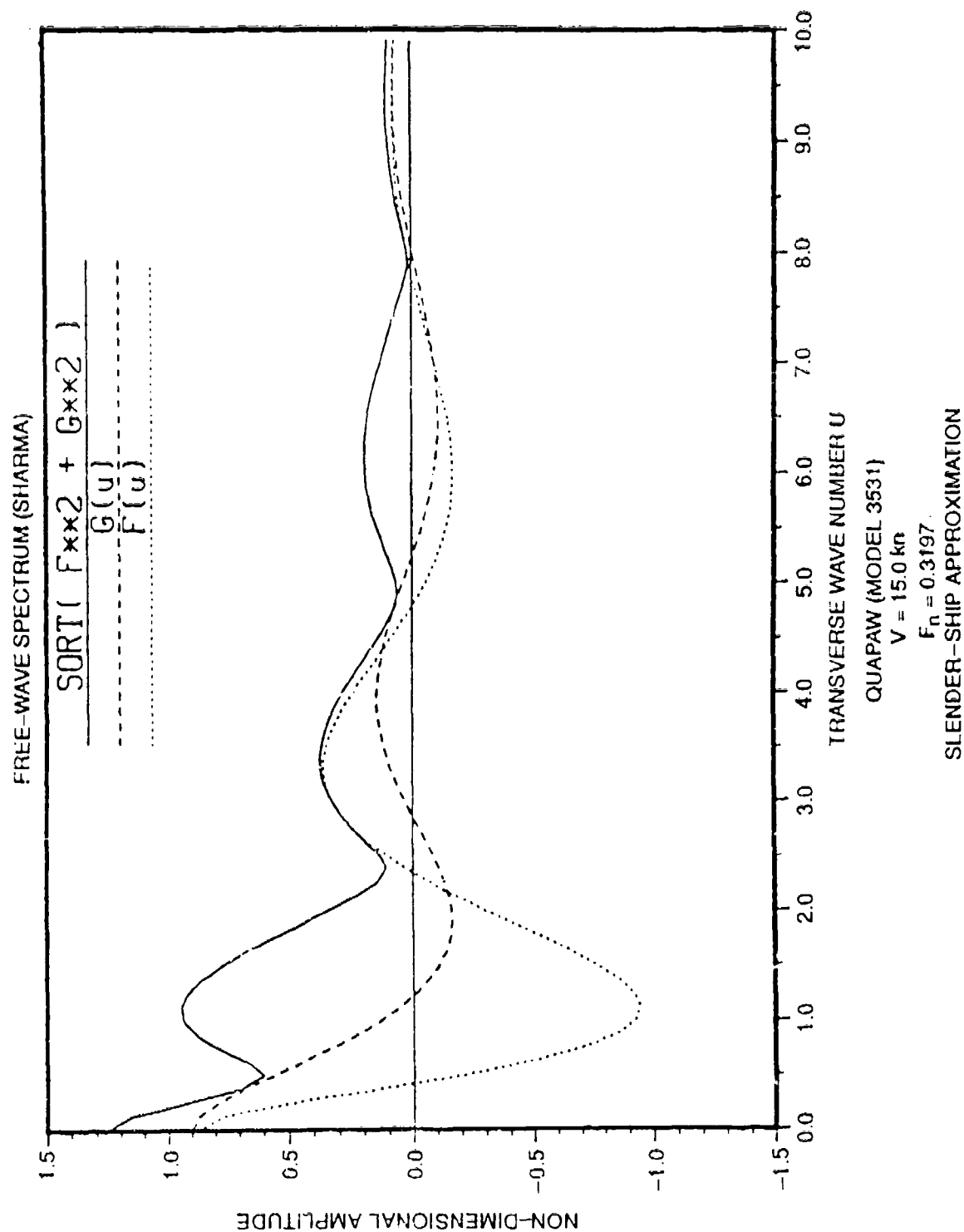


Fig. L.24. Post wake-off SAIC slender-ship prediction of wave spectrum for QUAPAW at $F_n = 0.3197$.

Table L.1. Summary of Kelvin Wake computations performed by SAIL in conjunction with the wake-off.

SUMMARY OF COMPUTATIONS PERFORMED FOR THE 1988 KELVIN WAKE COMPARISONS									
QUAPAW (Model 3531)									
Speed	# of Panels	# of Rows	# of Columns	Source Strengths*	Free Wave Spectrum	Wave Resistance	Near-Field Elevations	Far-Field Elevations	Wave-Cuts
10.0 kts (Fn=0.213)	432	16	24 [1]	N-K	X	X	X	X	X
	432	16	24 [1]	S-S	X	X	X	X	X
	192	8	24	N-K	X	X			
	192	8	24	S-S	X	X			
11.7 kts (Fn=0.250)	432	16	24 [1]	N-K	X	X	X	X	X
	432	16	24 [1]	S-S	X	X	X	X	X
	384	16	24	N-K	X	X			
	384	16	24	S-S	X	X			
	384	8	48	N-K	X	X			
	384	8	48	S-S	X	X			
	384 [2]	8	24	N-K	X	X			
	384 [2]	8	24	S-S	X	X			
	192	8	24	N-K	X	X			
	192	8	24	S-S	X	X			
15.0 kts (Fn=0.320)	432	16	24 [1]	N-K	X	X	X	X	X
	432	16	24 [1]	S-S	X	X	X	X	X
	192	8	24	N-K	X	X			
	192	8	24	S-S	X	X			
	432 [3]	16	24 [1]	N-K	X	X	X		
Notes: [1] Two rows nearest the waterline contain twice as many panels									
[2] Each panel has been divided into two triangles									
[3] Top row of panels has been made wall-sided									
* N-K = Neumann-Kelvin Solution, S-S = Zeroth-Order Slender-Ship Approximation of Noblesse									

Table L.1. (Continued)

SUMMARY OF COMPUTATIONS PERFORMED FOR THE 1908 KELVIN WAKE COMPARISONS																			
DDG 51 (Model 5415)																			
Speed	# of Panels	# of Rows	# of Columns	Source Strengths	Free Wave Spectrum	Wave Resistance	Near-Field Elevations	Far-Field Elevations	Wave-Cuts										
11.8 kts (Fn=0.163)	376 [4] 376 [4]	8 8	28 [1] 28 [1]	N-K S-S	X X	X X													
18.1 kts (Fn=0.250)	376 [4] 376 [4] 320 [4] 320 [4]	8 8 8 8	28 [1] 28 [1] 28 28	N-K S-S N-K S-S	X X X X	X X X X	X X	X X	X X										
20.0 kts (Fn=0.276)	376 [4] 376 [4] 320 [4] 320 [4] 376 [3,4]	8 8 8 8 8	28 [1] 28 [1] 26 28 28 [1]	N-K S-S N-K S-S N-K	X X X X X	X X X X X		X X	X X	X X									
30.0 kts (Fn=0.414)	376 [4] 376 [4] 320 [4] 320 [4]	8 8 8 8	28 [1] 28 [1] 28 28	N-K S-S N-K S-S	X X X X	X X X X	X X	X X	X X										
Notes: [1] Two rows nearest the waterline contain twice as many panels [2] Each panel has been divided into two triangles [3] Top row of panels has been made wall-sided [4] Includes 96 panels on the bulb										Ship Approximation of Noblesse									
* N-K = Neumann-Kelvin Solution, S-S = Zeroth-Order Slender-Ship Approximation of Noblesse																			

THIS PAGE INTENTIONALLY LEFT BLANK

APPENDIX M

FLOPAN PREDICTIONS SUBMITTED AFTER WAKE-OFF

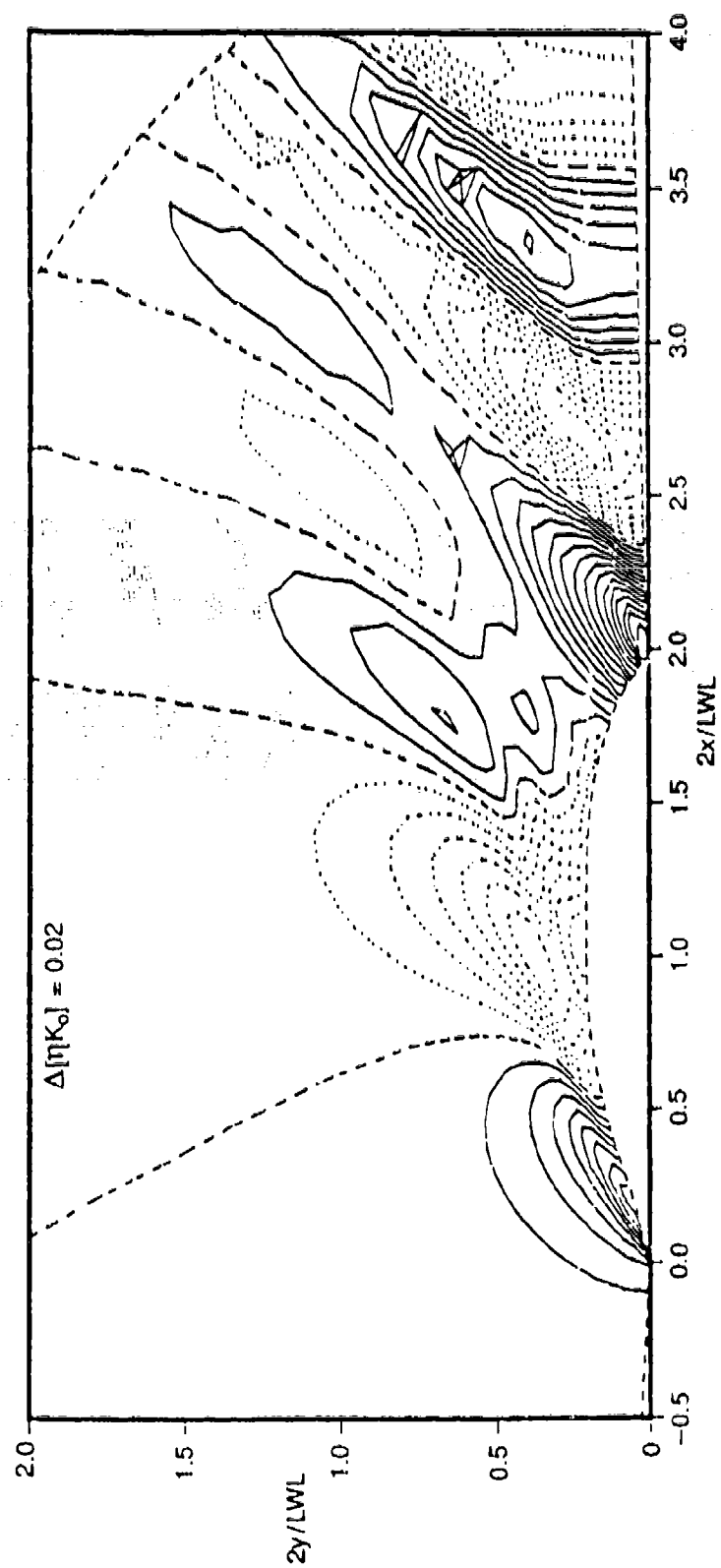


Fig. M.1. Post wake-off FLOPAN prediction of QUAPAW at $F_n = 0.3197$ using blended 3/4/5 point upwind formula.

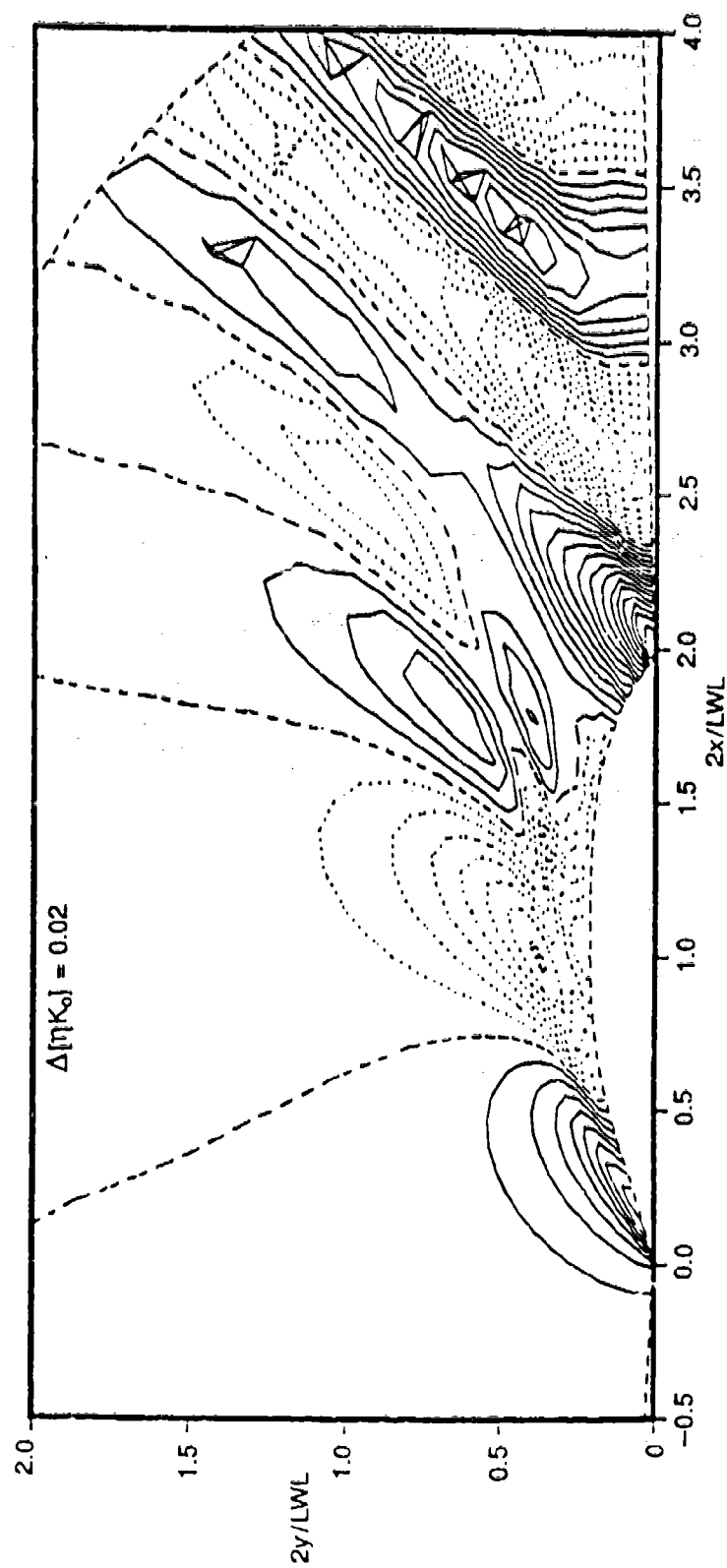


Fig. M.2. Post wake-off FLOPAN ; rediction of QUAPAW at $F_n = 0.3197$ using blended 4/5 point upwind formula.

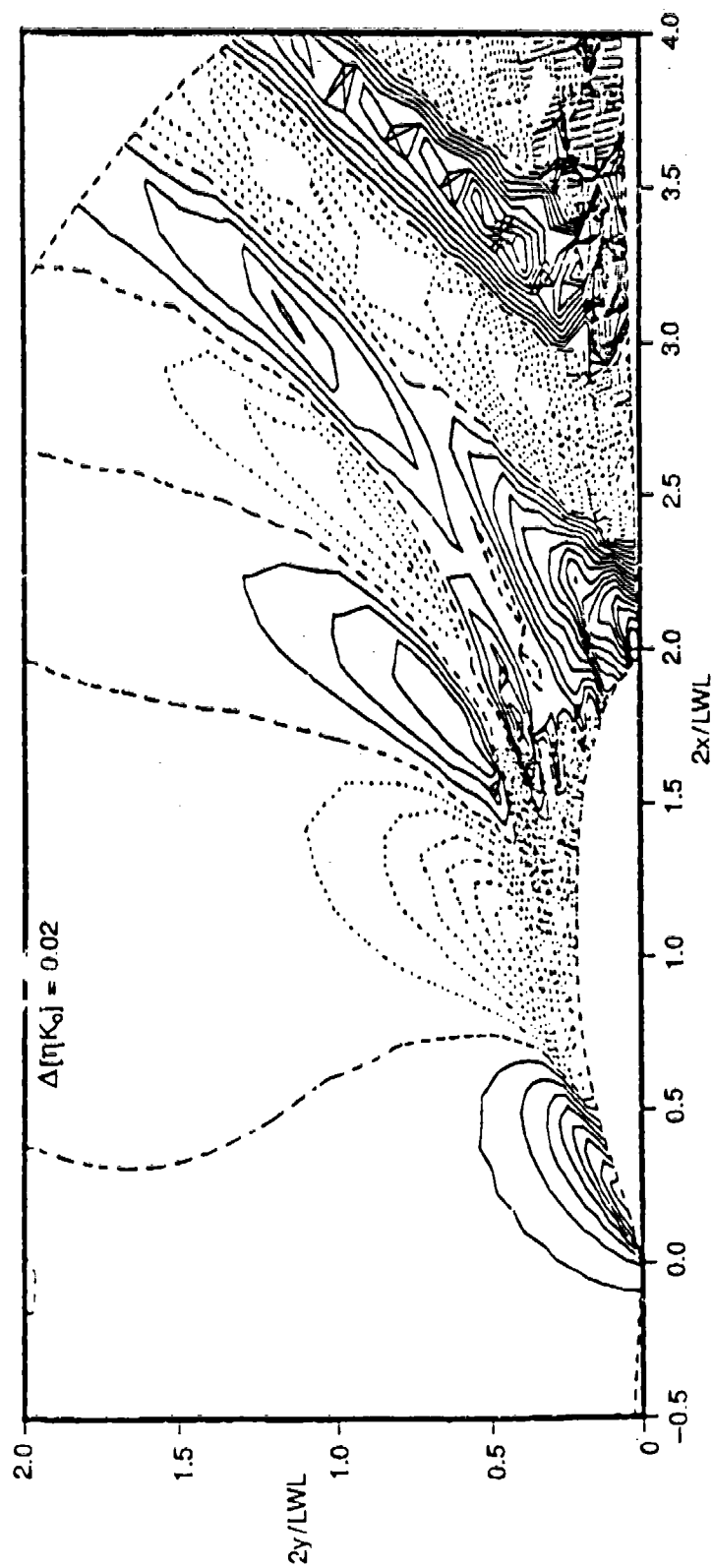


Fig. M.3. Post wake-off FLOPAN prediction of QUAPAW at $F_n = 0.3197$ using blended 5 point upwind formula.

APPENDIX N
XYZFS PREDICTIONS SUBMITTED
AFTER WAKE-OFF

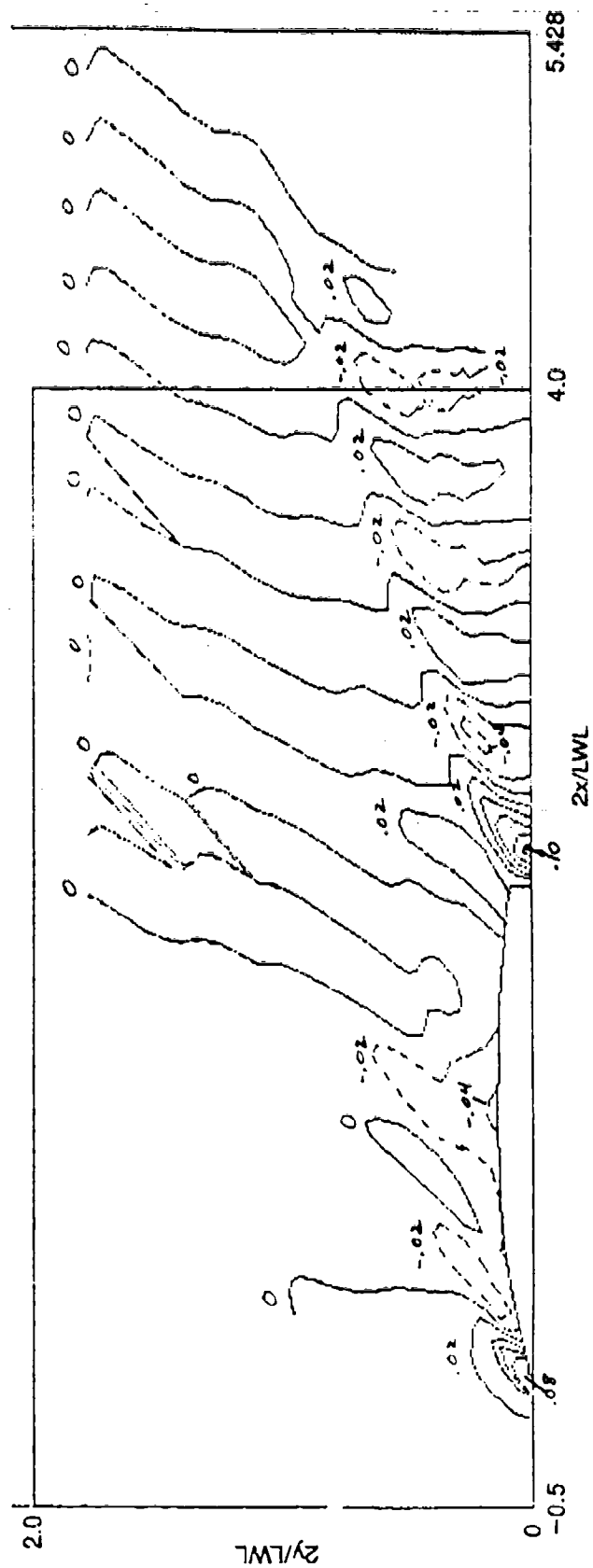


Fig. N.1. Post wake-off XYZFS prediction of wave contours for Model 5415 at $F_n = 0.25$.

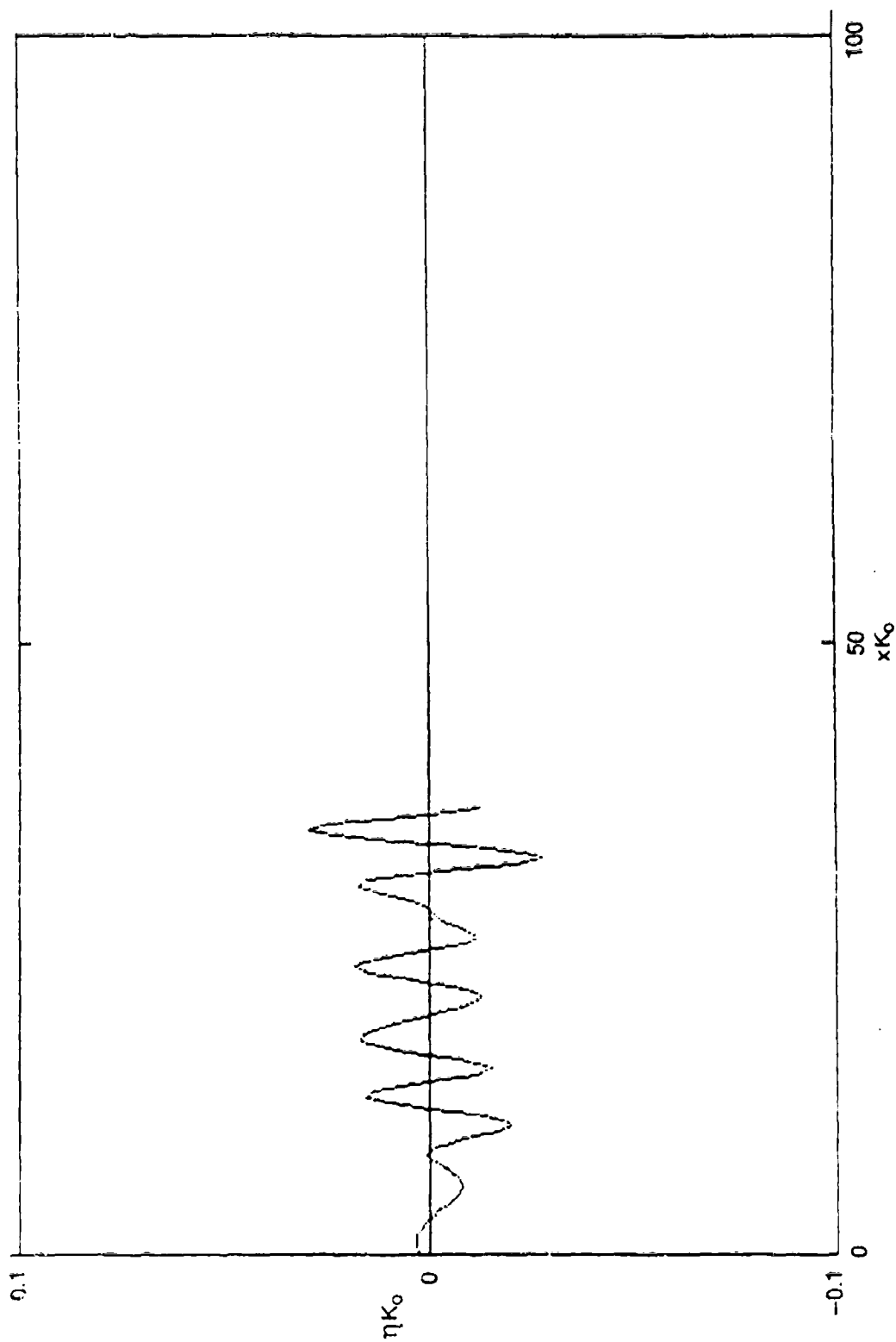


Fig. N.2. Post wake-off XYZFS prediction of wave cut for Model 5415 at $F_n = 0.25$.

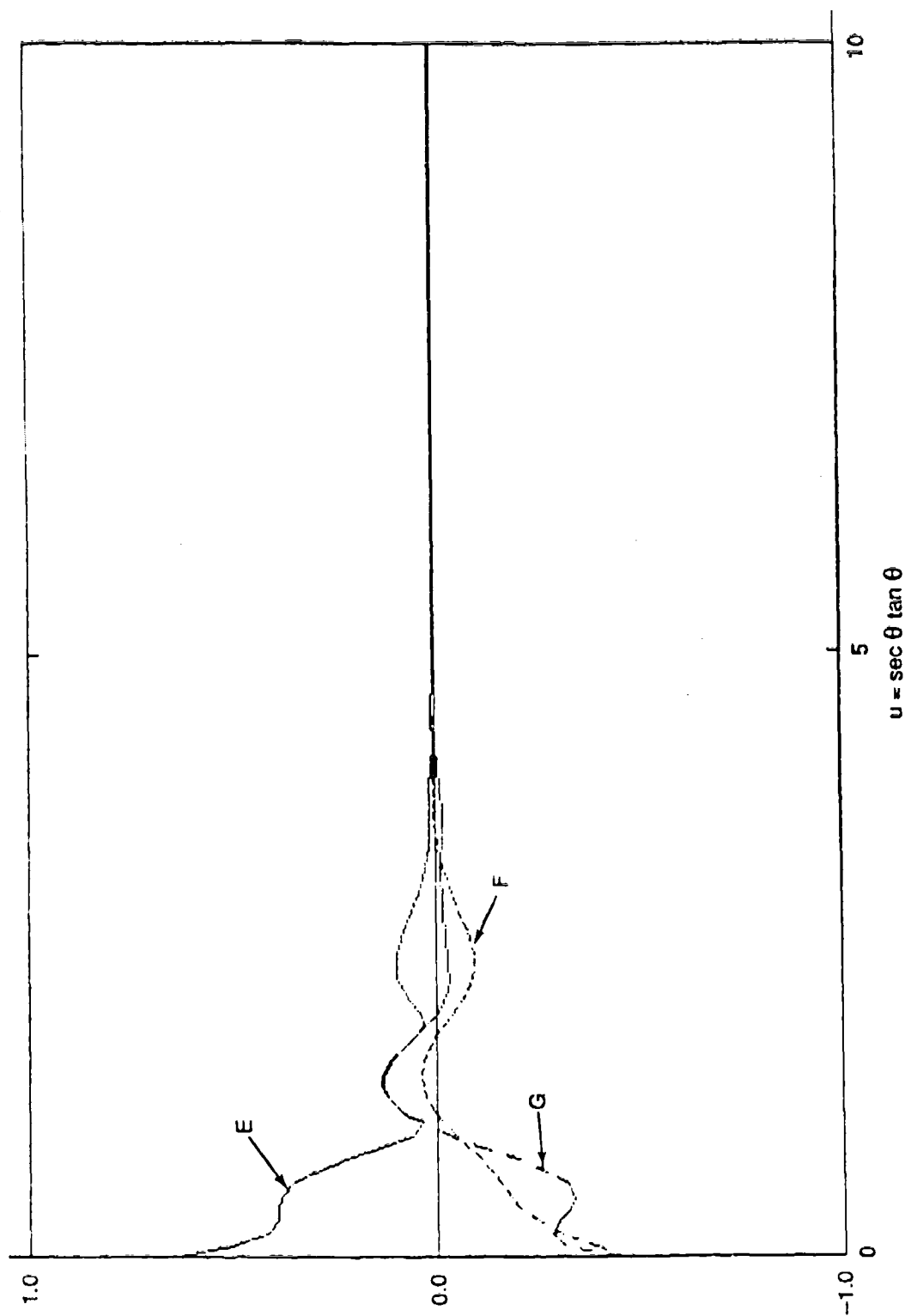


Fig. N.3. Posi wake-off XYZFS prediction of wave spectrum for Model 5415 at $F_n = 0.25$.

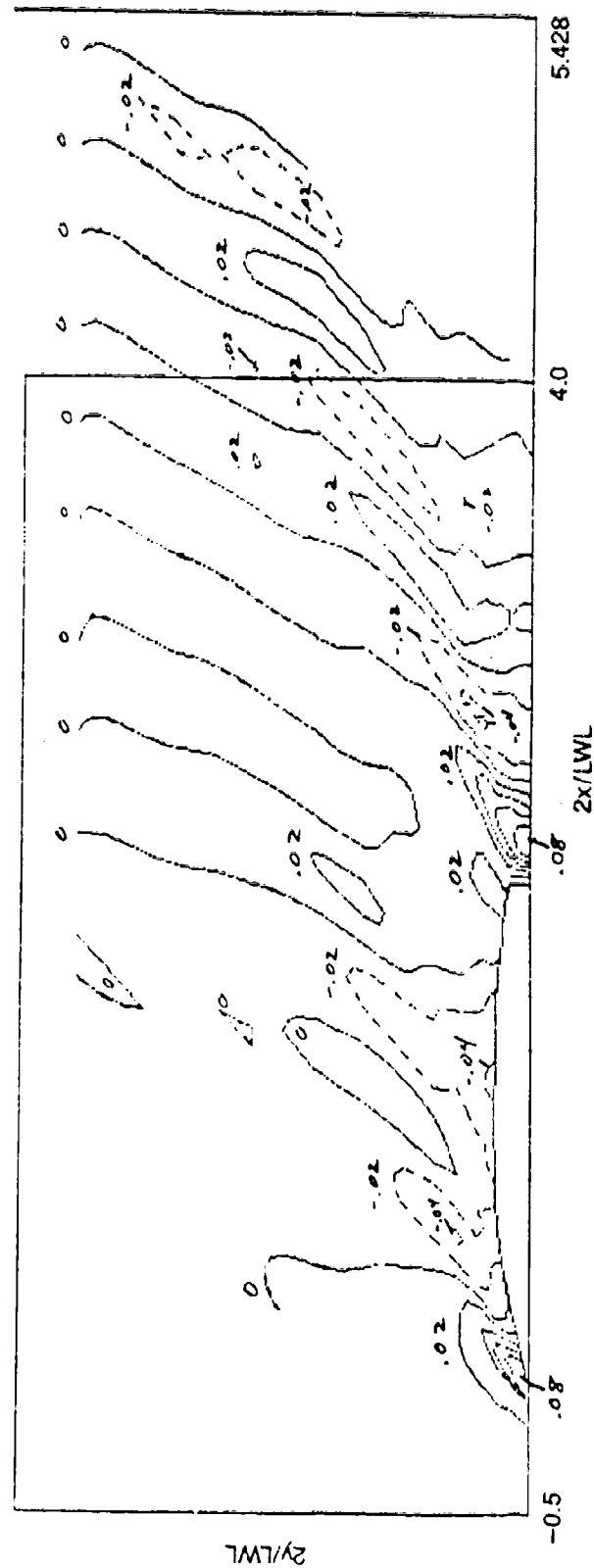


Fig. N.4. Post wake-off XYZFS prediction of wave contours for Model 5415 at $F_n = 0.2755$.

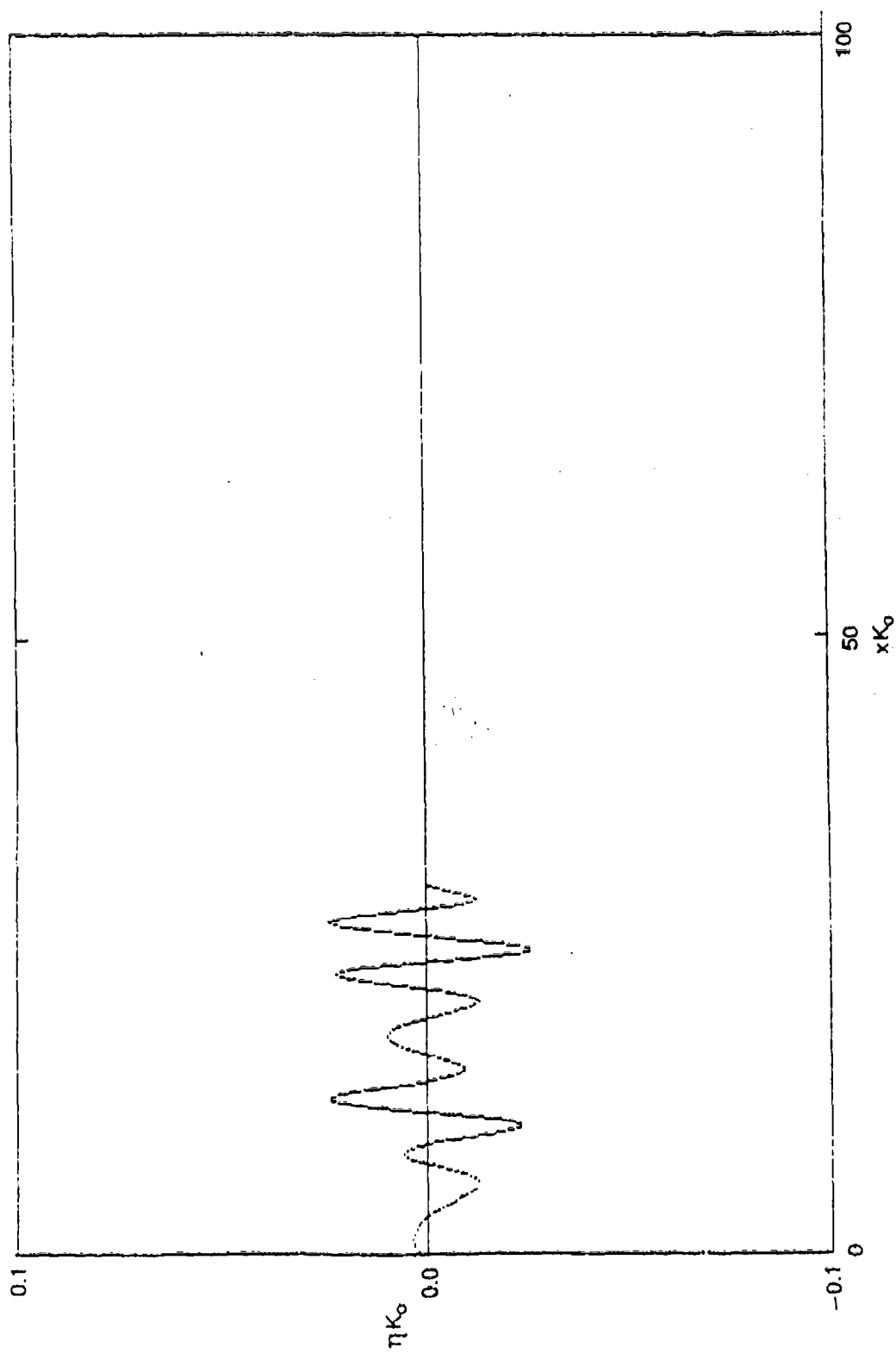


Fig. N.5. Post wake-off XYZFS prediction of wave cut for Model 5415 at $F_n = 0.2755$.

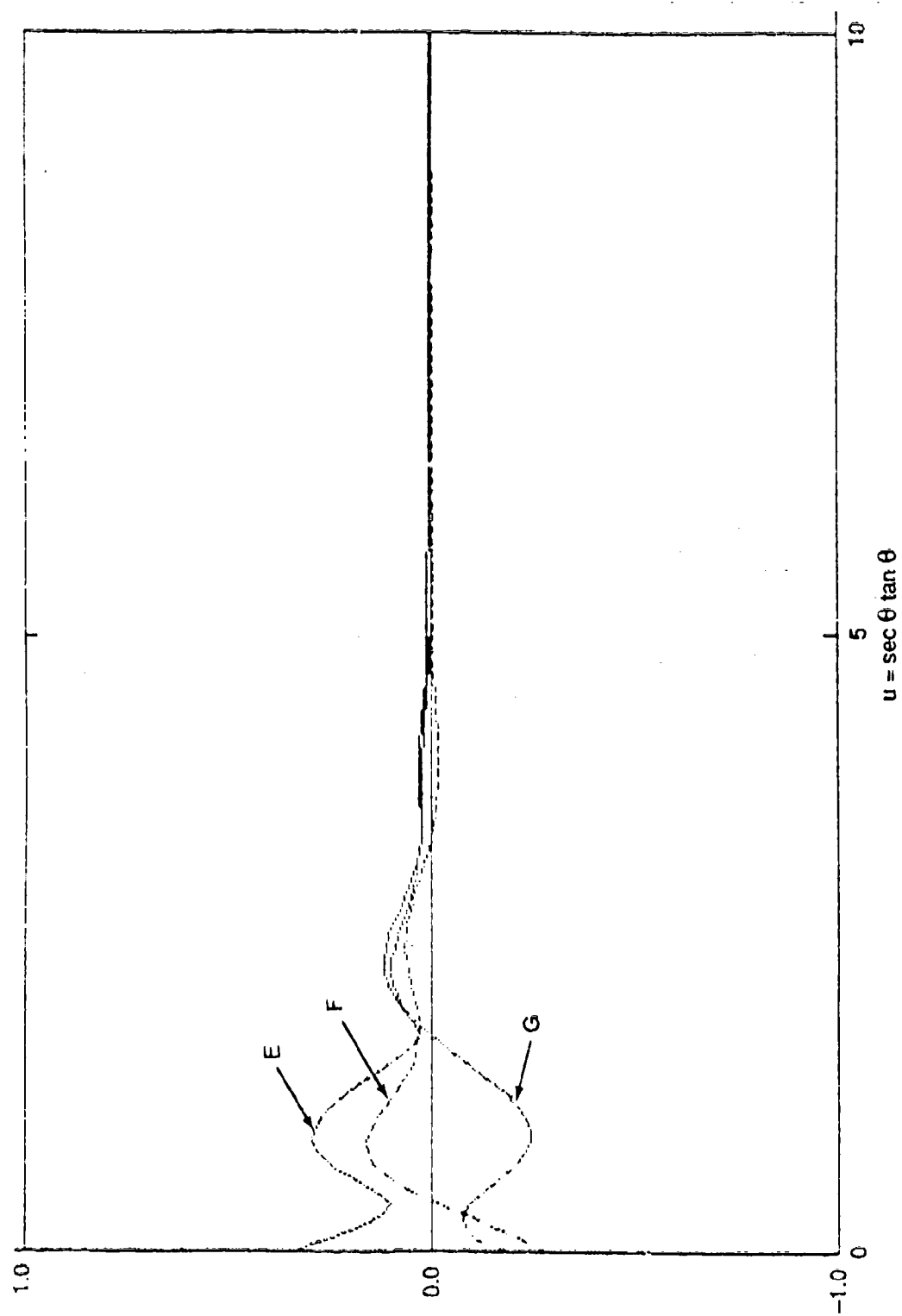


Fig. N.6. Post wake--off XYZFS prediction of wave spectrum for Model 5415 at $F_n = 0.2755$.

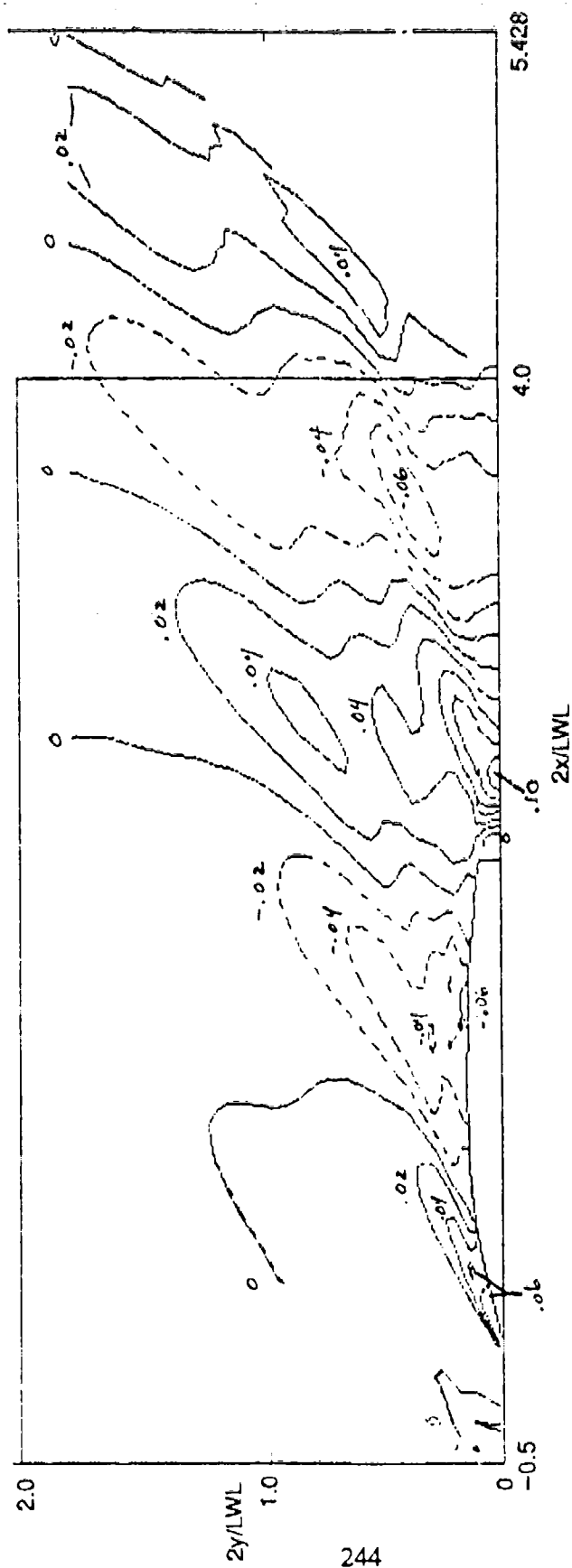


Fig. N.7. Post wake-off XYZFS prediction of wave contours for Model 5415 at $F_n = 0.4136$.

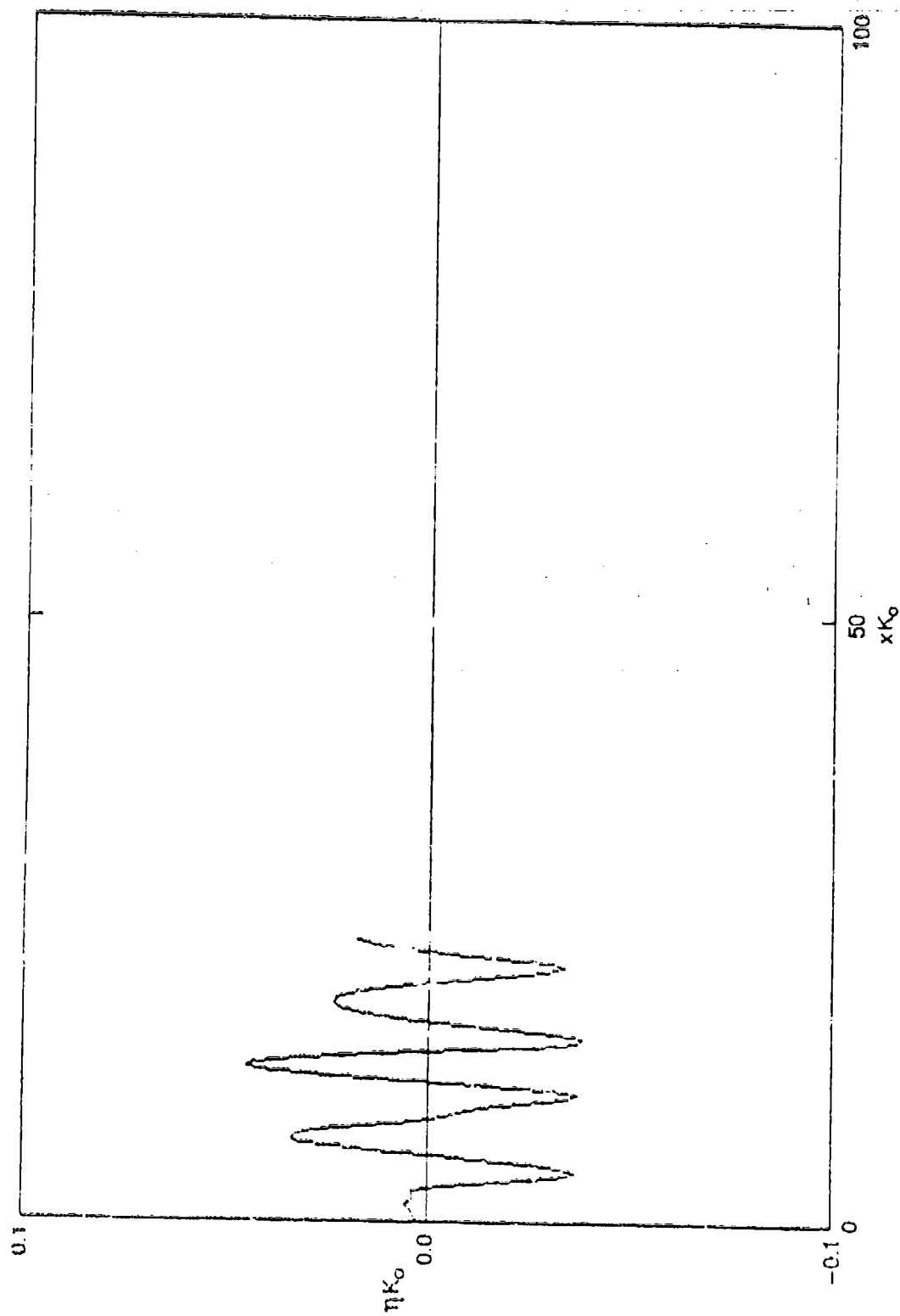


Fig. N.8. Post wake-off XYZFS prediction of wave cut for Model 5415 at $F_n = 0.4136$.

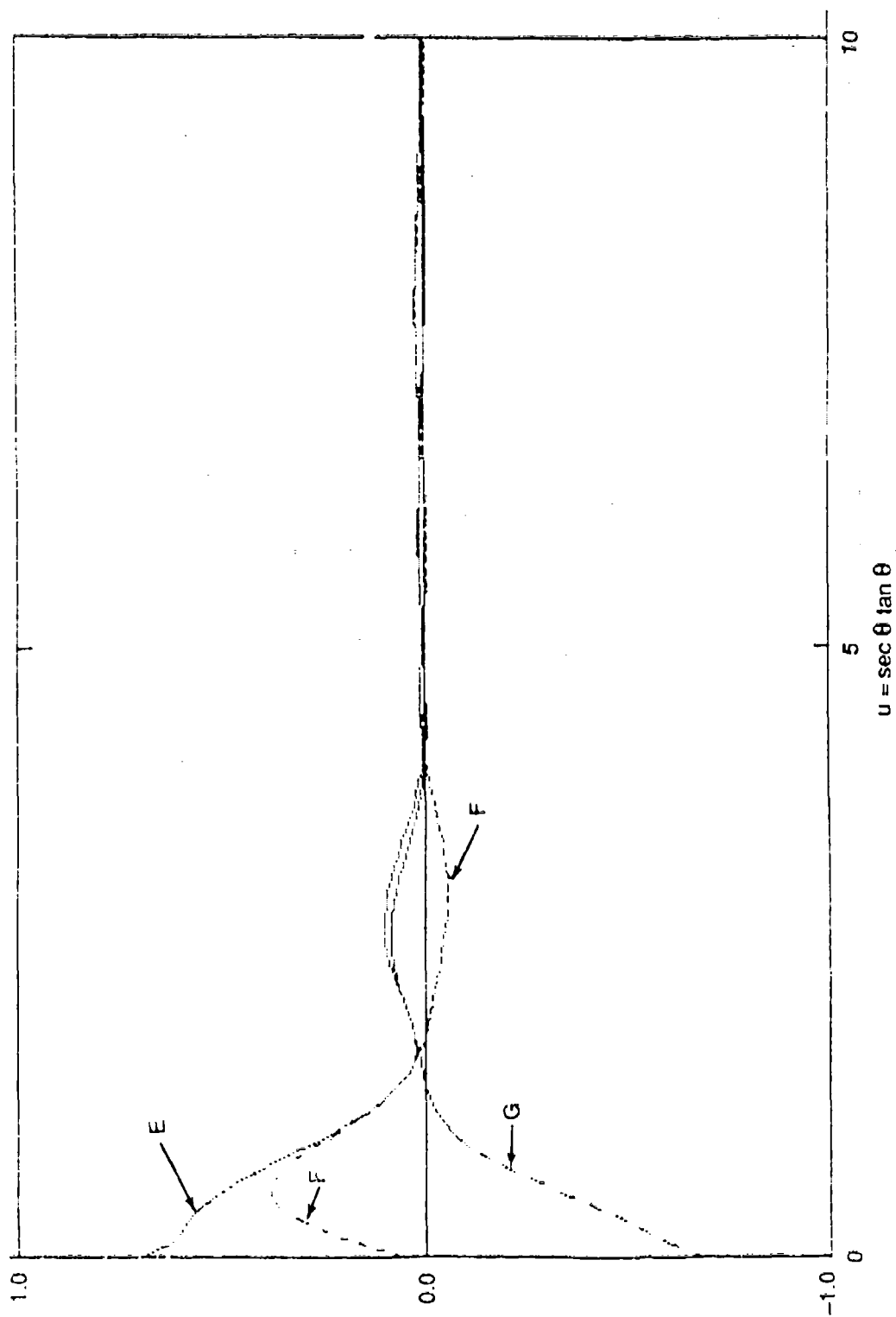


Fig. N.9. Post wake-off XYZFS prediction of wave spectrum for Model 5415 at $F_n = 0.4136$.

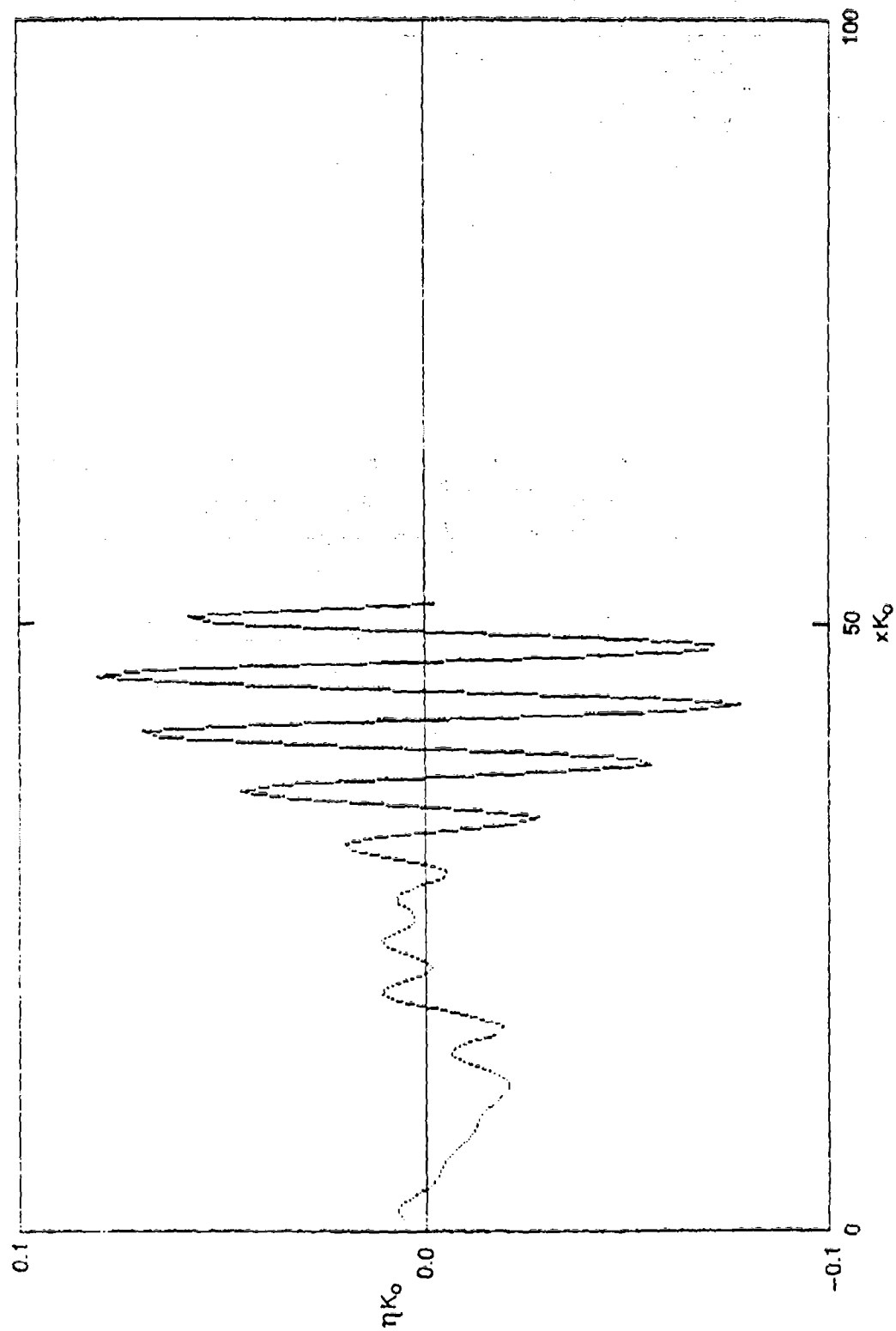


Fig. N.11. Post wake-off XYZFS prediction of wave cut for QUAPAW at $F_n = 0.2131$.

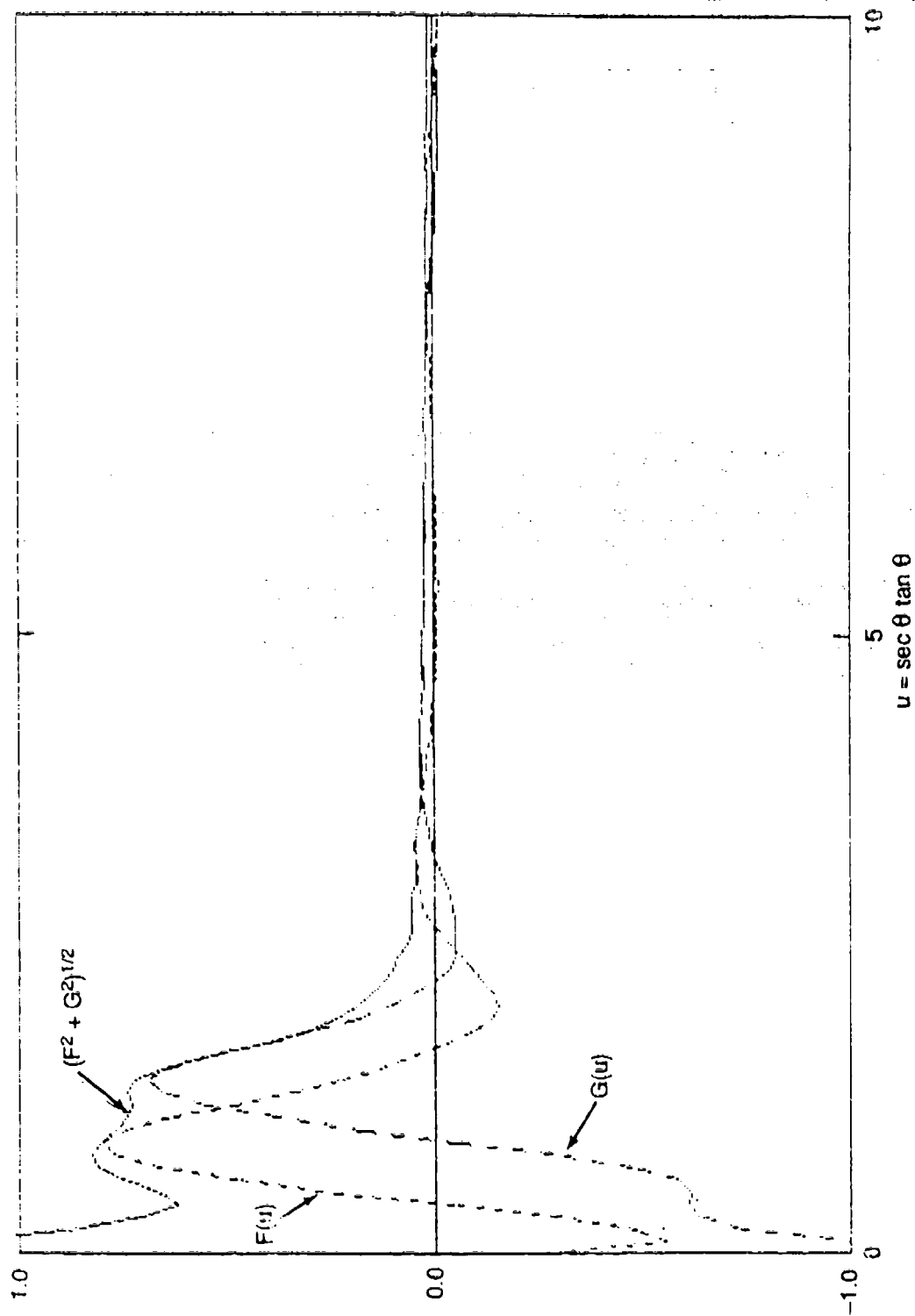


Fig. N.12. Post wake-off XYZFS prediction of wave spectrum for QUAPAW at $F_n = 0.2131$.

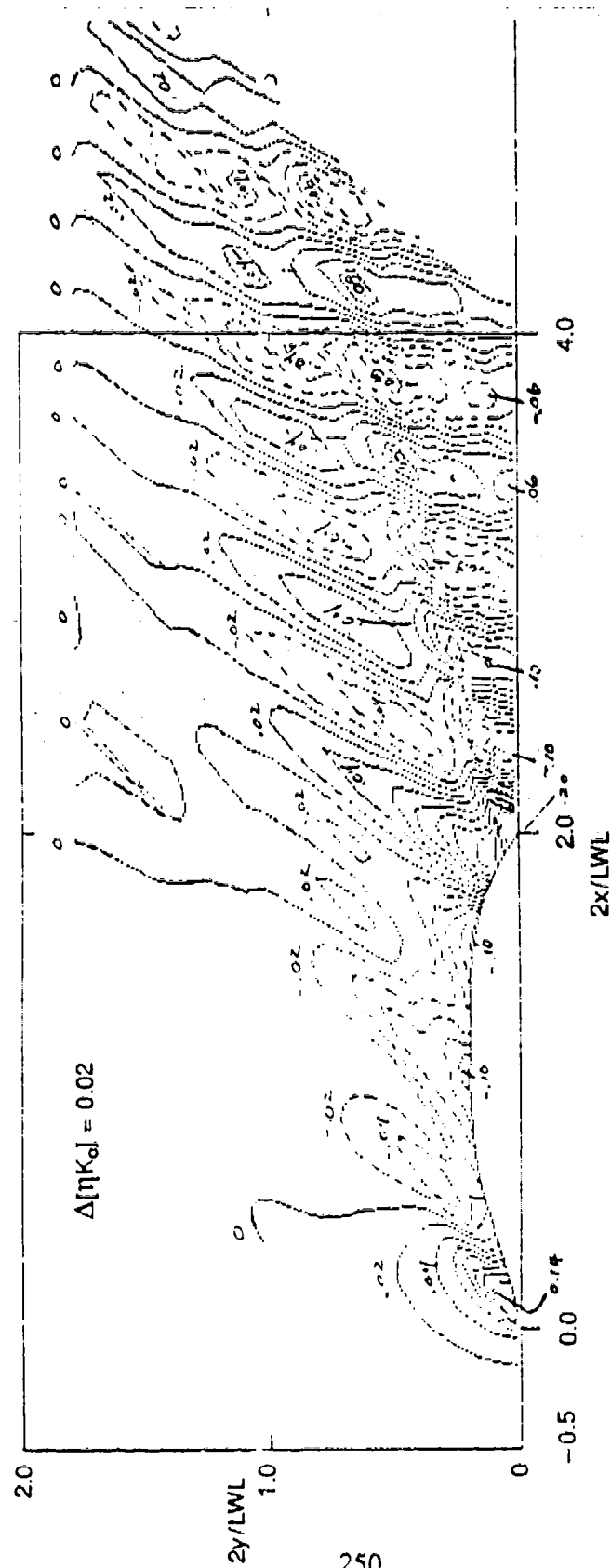


Fig. N.13. Post wake-off XYZFS prediction of wave contours for QUAPAW at $F_n = 0.25$.

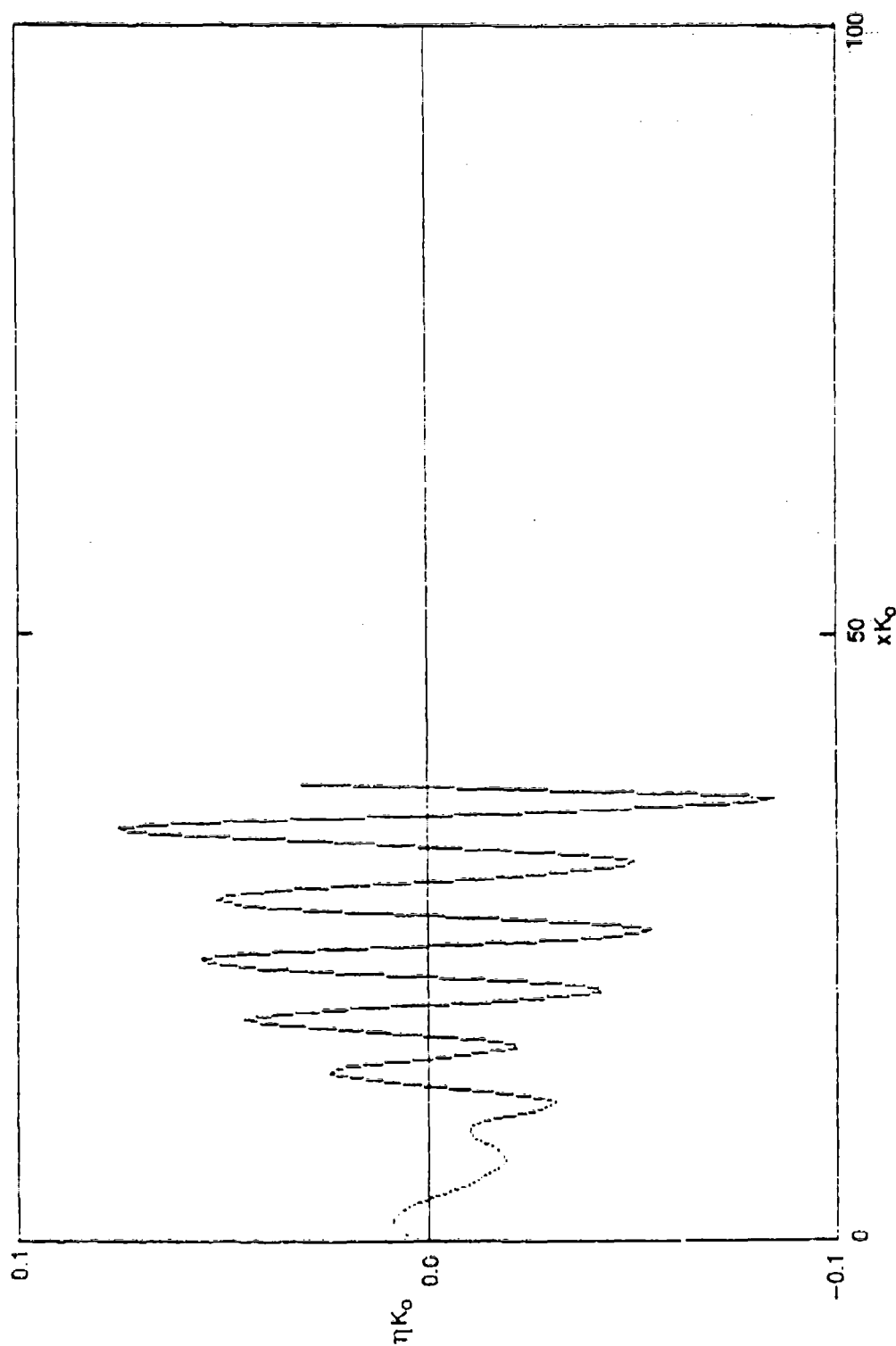


Fig. N.14. Post wake-off XYZFS prediction of wave cut for QUAPAW at $F_n = 0.25$.

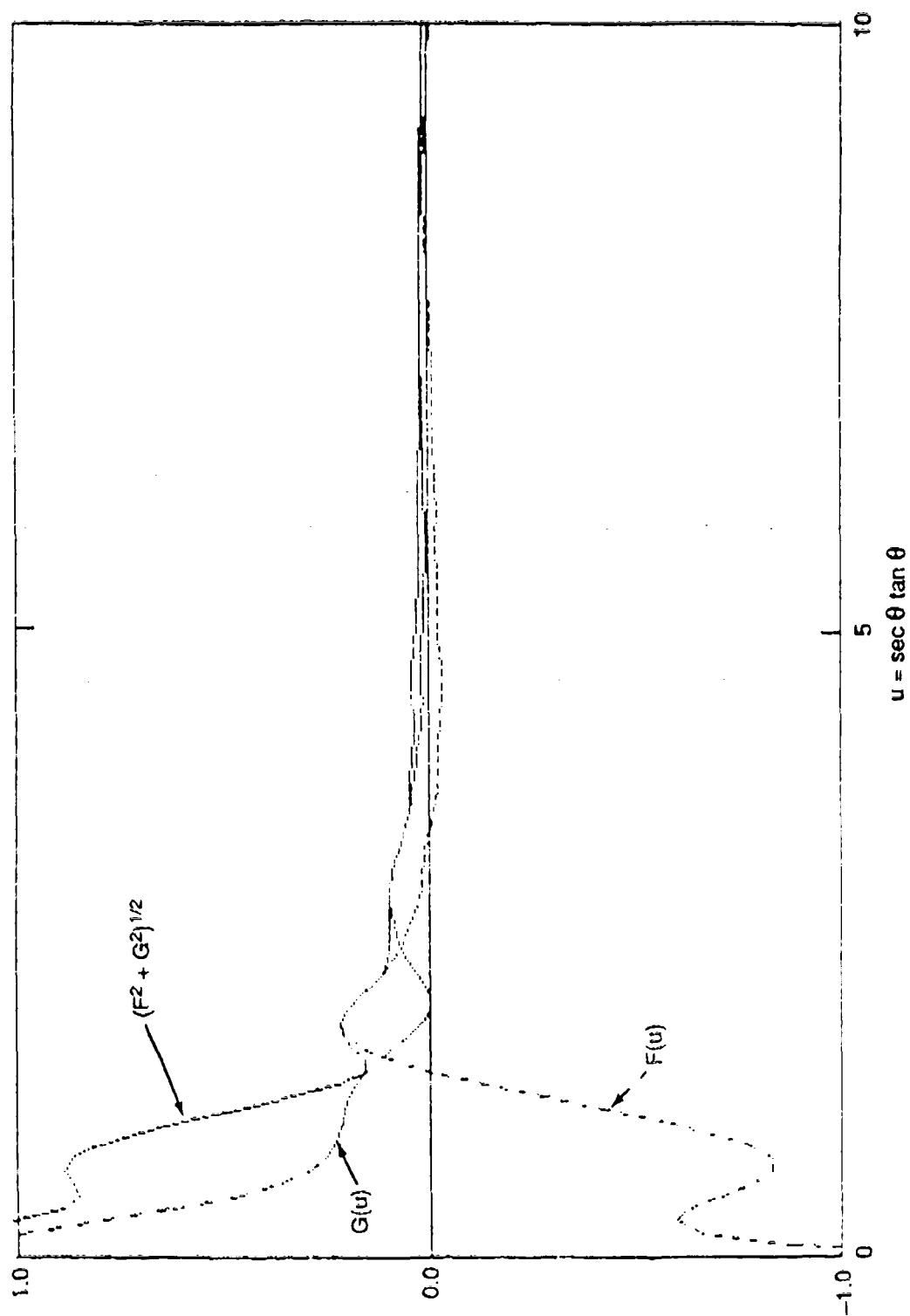


Fig. N.15. Post wake-off XYZFS prediction of wave spectrum for QUAPAW at $F_n = 0.25$.

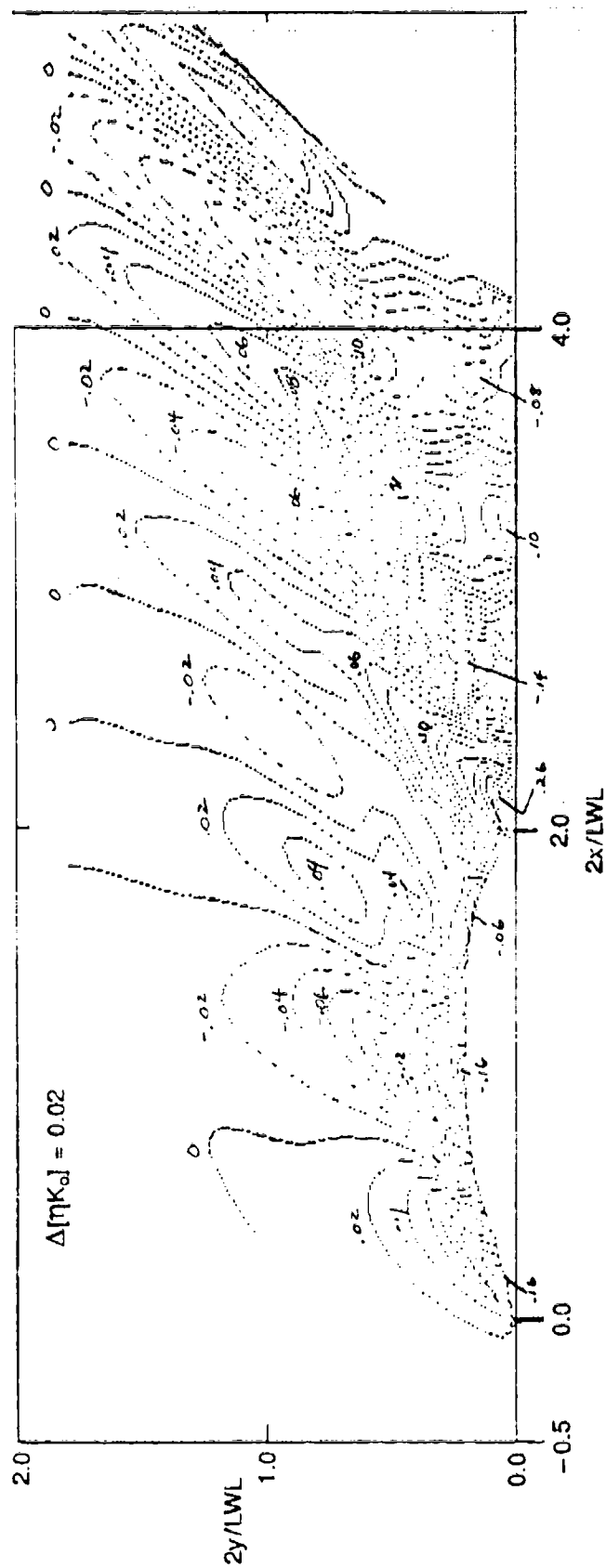


Fig. N.16. Post wake-off XYZFS prediction of wave contours for QUAPAW at $F_n = 0.3197$.

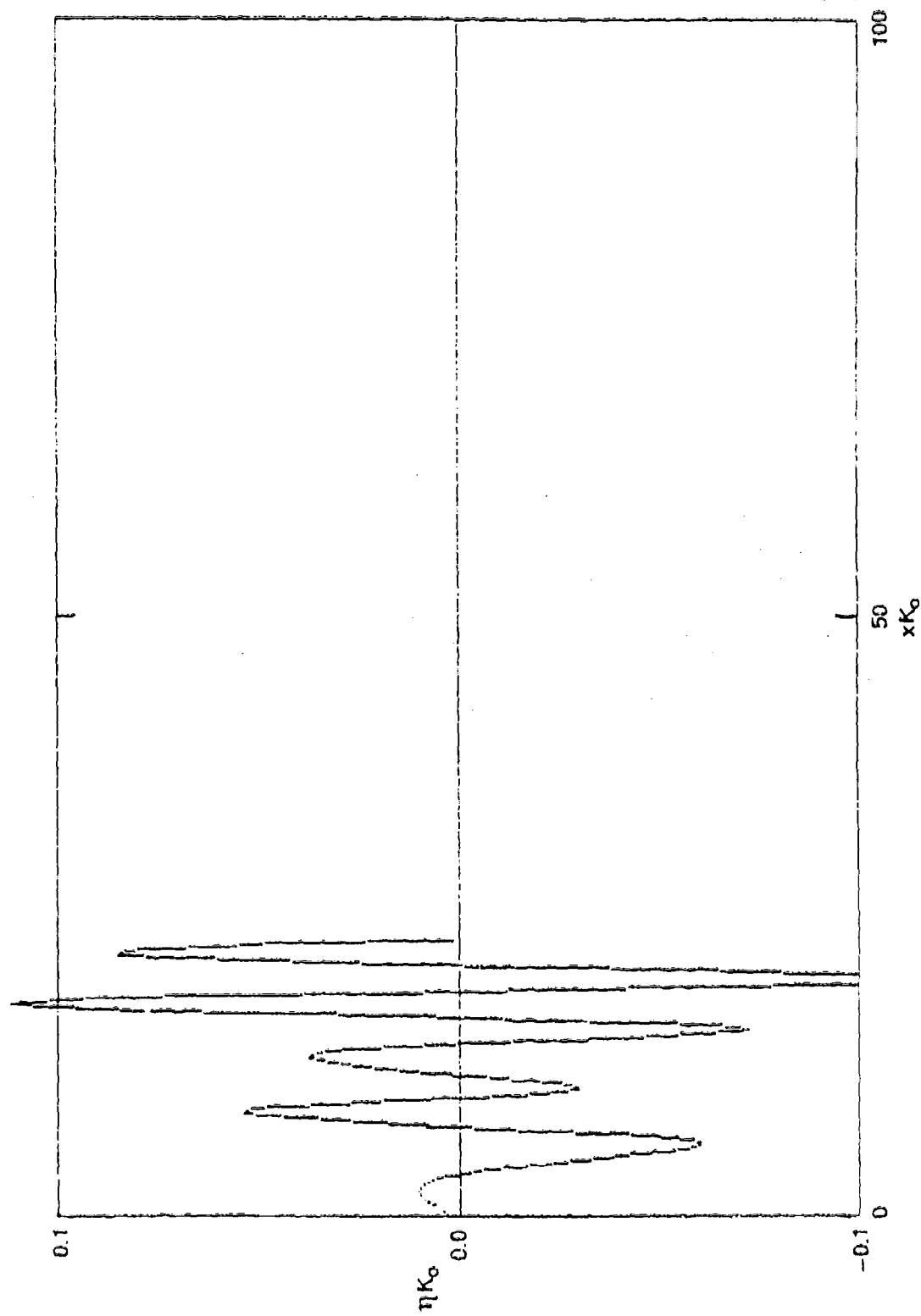


Fig. N.17. Post wake-off XYZFS prediction of wave cut for QUAPAW at $F_n = 0.3197$.

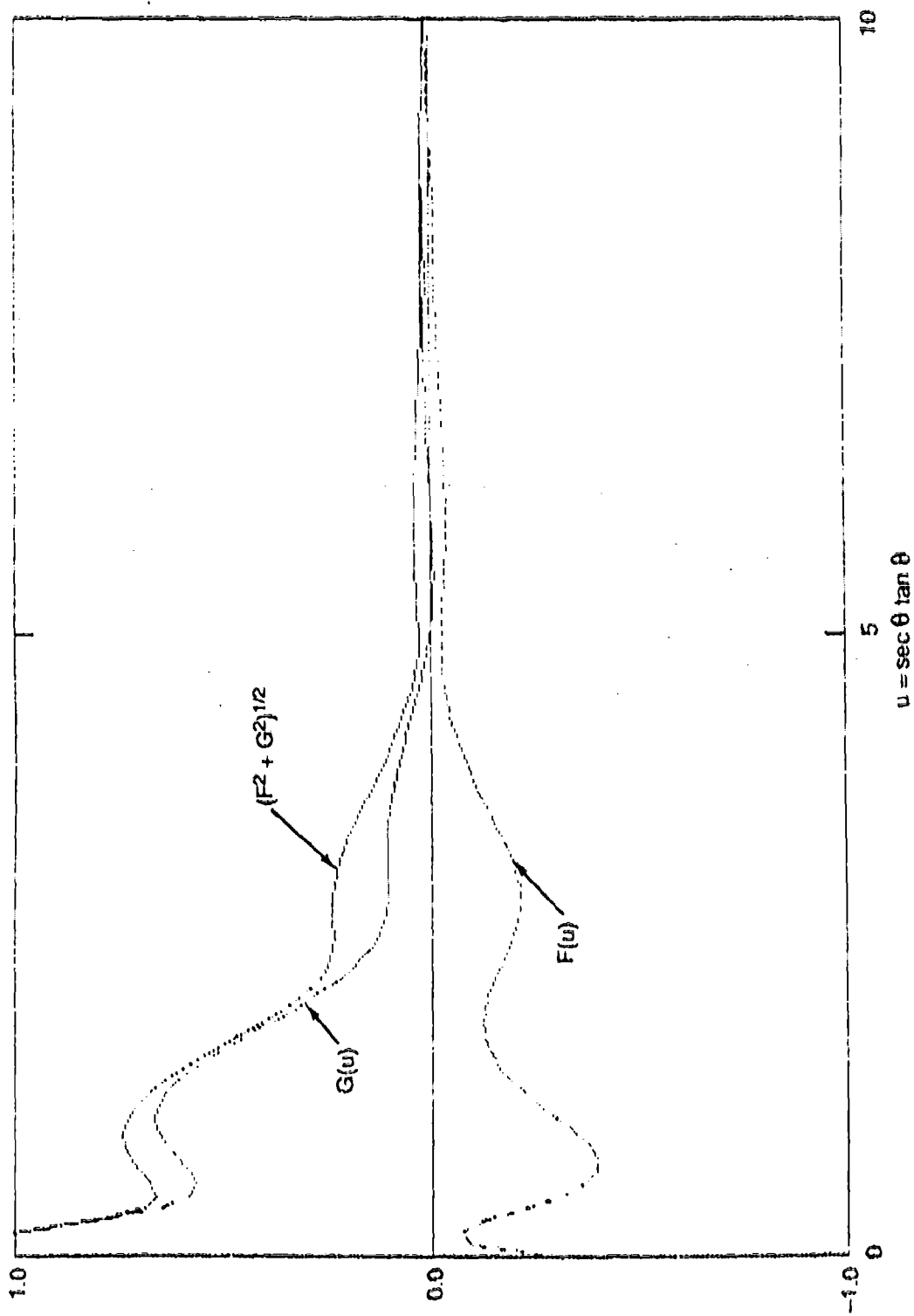


Fig. N.18. Post wake-off XYZFS prediction of wave spectrum for QUAPAW at $F_n = 0.3197$.

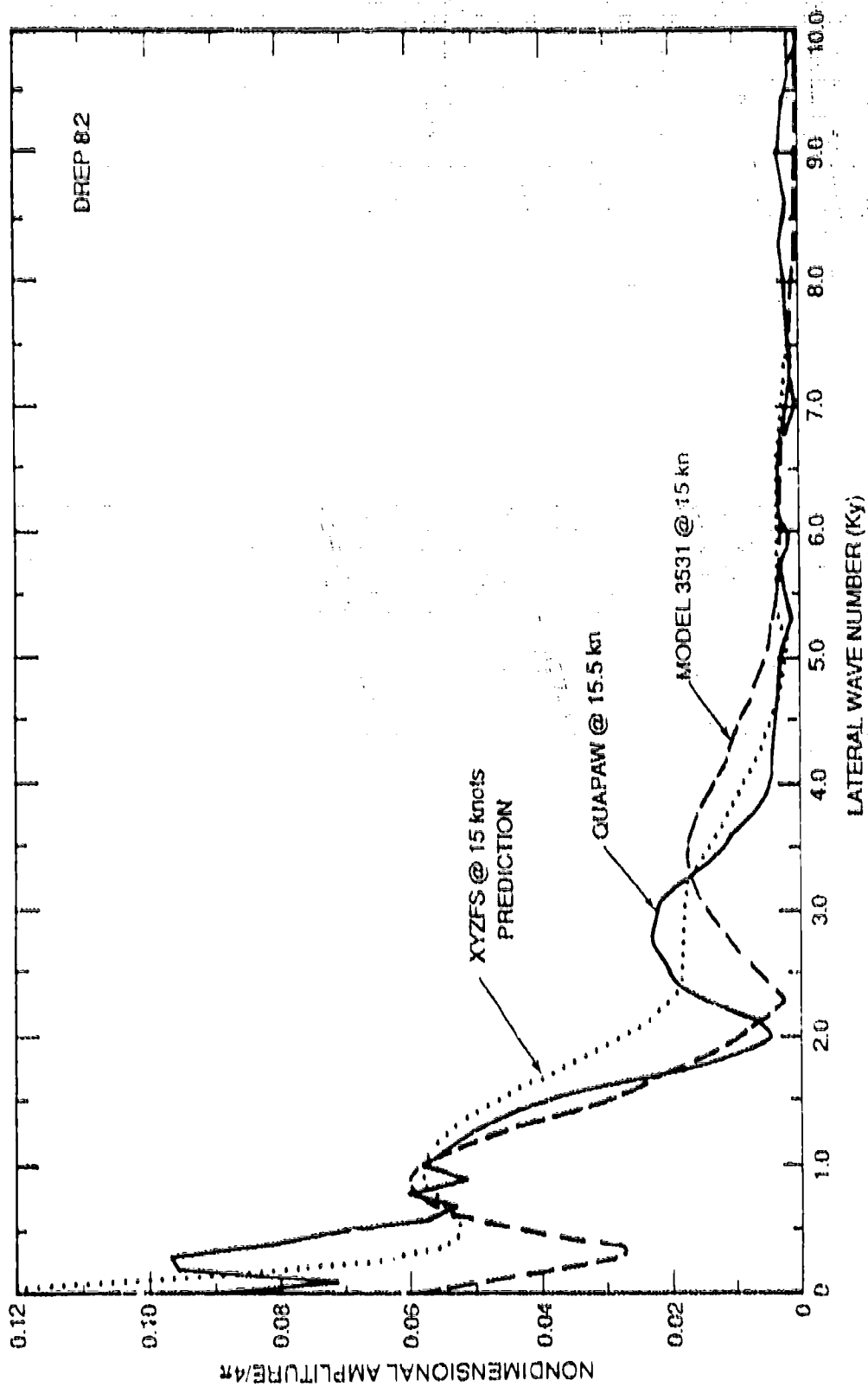


Fig. N.19. XYZFS prediction of QUAPAW wave spectrum compared to full scale and model scale experimental measurements.

REFERENCES

1. Hammond, R.R., R.R. Buntzen, and E.E. Floren, "Using Ship Wake Patterns to evaluate SAR Ocean Wave Imaging Mechanisms," Joint U.S.-Canadian Ocean Wave Investigation Project, Technical Report 978, Naval Ocean Systems Center, San Diego, California (Feb 1985).
2. Dawson, C.W., "A Practical Computer Method for Solving Ship Wave Problems," Second Int. Conf. on Numerical Ship Hydrodynamics, Berkeley, California (Sep 1977).
3. Doctors, L.J. and R.F. Beck, "Numerical Aspects of the Neumann-Kelvin Problem," Journal of Ship Research, Vol. 31, No. 1 (Mar 1987).
4. Doctors, L.J. and R.F. Beck, "Convergence Properties of the Neumann-Kelvin Problem for a Submerged Body," Journal of Ship Research, Vol. 31, No. 4 (Dec 1987).
5. Noblesse, Francis, "A Slender Ship Theory of Wave Resistance," Journal of Ship Research, Vol. 27, No. 1 (Mar 1983).
6. Dommermuth, D.G., C.A. Scragg, and J.C. Talcott, "Computer Codes for Predicting the Kelvin Wakes," Technical Report No. SAIC-88/1796 (Dec 88).
7. Telste, J.G., "Documentation of SWIM and SWIM FS Computer Code," DTRC Report CMLD-87-13 (Jun 1988).
8. Cheng, B.H. and J.S. Dean, "User's Manual for the XYZ Free Surface Program," DTRC Report DTNSRDC 86/029 (Jun 1986).
9. Kim, Y.H. and S.H. Kim, and T. Lucas, "Advanced Panel Method for Ship Wave Inviscid Flow Theory (SWIFT)," DTRC-89/029 (Nov 1989).
10. Boppe, C.W., B.S. Rosen, and J.P. Laiosa, "Stars and Stripes '87, Computational Flow Simulations for Hydrodynamic Design," Proc. the Eighth Chesapeake Sailing Yacht Symposium, Annapolis (Mar 1987).
11. Sclavounos, P., "Stability Analysis of Free Surface Panel Methods for the Wave Resistance Problem," Proc. Third Int. Workshop on Water Waves and Floating Bodies, Woods Hole, Massachusetts (Apr 1988).
12. Ratcliffe, T. J. and M. B. Willson, "Uncertainty in the Measurement of Ship Model Wave Profiles and Wave Pattern Resistance," Proc. of the 22nd American Towing Tank Conference, St. Johns, Newfoundland, Canada (Aug 1989).
13. Wyatt, Donald C. and Robert E. Hall, "Analysis of the Surface Wave Wake of a Ship Using a Method Based Upon the Local Fourier Transform," Science Applications International Corporation, Technical Report SAIC-87/1793 (Jul 1987).

THIS PAGE INTENTIONALLY LEFT BLANK

INITIAL DISTRIBUTION

Copies

3 ONR
 1 1132F (E. Rood)
 1 121 (R.J. Hansen)
 1 1215 (J. Fein)
 1 ONT
 1 211 (Gagorik)
 1 NRL
 1 4420 (O. Griffin)
 1 University of Michigan
 1 Dr. Robert Beck
 2 SAIC / San Diego
 1 Dr. Carl Scragg
 1 Donald Wyatt
 2 SAIC / Annapolis
 1 Clay Oliver
 1 Ken Weems
 1 LMSC
 1 Terry Schmidt
 2 MIT
 1 Dr. Nick Newman
 1 Dr. Jerry Milgram
 1 International Numerics
 1 Charles Boppe
 1 NASA, Langley
 1 Bruce Rosen
 2 Cortana, Falls Church
 1 Ray Grady
 1 K. J. Moore

CENTER DISTRIBUTION

Copies	Code	Name
1	1131	Winegrad
1	1281	Cheng
1	15	Morgan
8	1504	Monacello
1	152	Lin
12	1521	Lindenmuth
1	1522	Wilson
10	1522	Ratcliffe
1	1522	Kim
1	154	McCarthy
1	1542	Noblesse
3	1544	Reed
1	3411	Publications (C)
1	3421	TIC (C)
1	3422	TIC (A)
10	3432	Reports Control